Advances in Clinical and Experimental Medicine

MONTHLY ISSN 1899-5276 (PRINT) ISSN 2451-2680 (ONLINE) www.advances.umed.wroc.pl

2018, Vol. 27, No. 12 (December)

Impact Factor (IF) – 1.262
Ministry of Science and Higher Education – 15 pts.
Index Copernicus (ICV) – 155.19 pts.

Wroclaw Medical University

Advances
in Clinical and Experimental
Medicine

Advances
in Clinical and Experimental Medicine

ISSN 1899-5276 (PRINT) ISSN 2451-2680 (ONLINE) www.advances.umed.wroc.pl

MONTHLY 2018
Vol. 27, No. 12
(December)

Advances in Clinical and Experimental Medicine is a peer-reviewed open access journal published by Wroclaw Medical University. Its abbreviated title is Adv Clin Exp Med. Journal publishes original papers and reviews encompassing all aspects of medicine, including molecular biology, biochemistry, genetics, biotechnology, and other areas. It is published monthly, one volume per year.

Editorial Office
ul. Marcinkowskiego 2–6
50-368 Wrocław, Poland
Tel.: +48 71 784 12 05
E-mail: redakcja@umed.wroc.pl

Publisher
Wroclaw Medical University
Wybrzeże L. Pasteura 1
50-367 Wrocław, Poland

Online edition is the original version of the journal

Editorial Policy

Advances in Clinical and Experimental Medicine (Adv Clin Exp Med) is an independent multidisciplinary forum for exchange of scientific and clinical information, publishing original research and news encompassing all aspects of medicine, including molecular biology, biochemistry, genetics, biotechnology and other areas. During the review process, the Editorial Board conforms to the "Uniform Requirements for Manuscripts Submitted to Biomedical Journals: Writing and Editing for Biomedical Publication" approved by the International Committee of Medical Journal Editors (www.ICMJE.org/). The journal publishes (in English only) original papers and reviews. Short works considered original, novel and significant are given priority. Experimental studies must include a statement that the experimental protocol and informed consent procedure were in compliance with the Helsinki Convention and were approved by an ethics committee.

For all subscription-related queries please contact our Editorial Office:
redakcja@umed.wroc.pl

For more information visit the journal's website:
www.advances.umed.wroc.pl

Pursuant to the ordinance No. 134/XV R/2017 of the Rector of Wroclaw Medical University (as of December 28, 2017) from January 1, 2018 authors are required to pay a fee amounting to 700 euros for each manuscript accepted for publication in the journal Advances in Clinical and Experimental Medicine.

„Podniesienie poziomu naukowego i poziomu umiędzynarodowienia wydawanych czasopism naukowych oraz upowszechniania informacji o wynikach badań naukowych lub prac rozwojowych – zadanie finansowane w ramach umowy 784/p-DUN/2017 ze środków Ministra Nauki i Szkolnictwa Wyższego przeznaczonych na działalność upowszechniającą naukę".

Indexed in: MEDLINE, Science Citation Index Expanded, Journal Citation Reports/Science Edition, Scopus,
EMBASE/Excerpta Medica, Ulrich's™ International Periodicals Directory, Index Copernicus

Typographic design: Monika Kolęda, Piotr Gil
DTP: Wydawnictwo UMW, TYPOGRAF
Cover: Monika Kolęda
Printing and binding: EXDRUK

Advances
in Clinical and Experimental Medicine

MONTHLY 2018, Vol. 27, No. 12 (December)

ISSN 1899-5276 (PRINT)
ISSN 2451-2680 (ONLINE)
www.advances.umed.wroc.pl

Contents

Acknowledgements

We would like to express our gratitude to all reviewers who devoted their time and expertise to evaluate manuscripts in Advances in Clinical and Experimental Medicine. We sincerely appreciate all your hard work and dedication. It is due to your contribution that we can achieve the standard of excellence.

Editors

Reviewers in 2018:

Sami Akbulut, Ersin Aksam, Anna Andrzejewska, Wojciech Apoznański, Lucía Aragonés, Josep Arnabat, Emrah Aslaner, Hanna Augustyniak-Bartosik, Teresa Bachanek, Mirosław Banasik, Julia Bar, Włodzimierz Baranowski, Wojciech Barg, Paweł Basta, Joanna Bauer, Wojciech Bednarz, Monika Bekiesińska-Figatowska, Ihsane Benyahya, Dariusz Biały, Rafał Białynicki-Birula, Jadwiga Biernat, Monika Biernat, Mariusz Blewniewski, Sylwia Bobis-Wozowicz, Andrzej Bohatyrewicz, Anna Bohdanowicz-Pawlak, Agnieszka Bojarska-Junak, Marek Bolanowski, Dariusz Boroń, Anna Brzecka, Da-Zhong Cao, Renata Chałas, Min Chen, Michał Chmielewski, Elżbieta Czkwianianc, Marcin Czyż, Małgorzata Czyżewska, Anna Dąbrowska-Iwanicka, Zofia Danilczuk, Jacek Daroszewski, Dorota Diakowska, Łukasz Dobrek, Katarzyna Drabko, Szymon Dragan, Dorota Drożdż, Magdalena Durlik, Wiesława Duszyńska, Grzegorz Dzida, Piotr Dzięgiel, Jan Długosz, Piotr Eder, Katarzyna Emerich, Gabriella Emri, Jerzy Florjański, Joanna Folwarczna, Ewelina Frejlich, Tomasz Fuchs, Piotr Fudalej, Łukasz Fuławka, Marian Gabryś, Jacek Gajek, Maria Ganeva, Tomasz Gedrange, Justyna Gil, Lidia Gil, Jan Godziński, Agnieszka Gomułkiewicz, Wojciech Górecki, Monika Gos, Waldemar Goździk, Marcin Gruchała, Ewelina Grywalska, Jędrzej Grzegrzółka, Teresa Grzelak, Jakub Hadzik, Friedhelm Heinemann, Lidia Hirnle, Magdalena Hurkacz, Dariusz Janczak, Danuta Jantas, Włodzimierz Jarmundowicz, Monika Jasek, Marek Jasiński, Ewa Jaźwińska-Tarnawska, Sławomir Jeka, Nuerbolati Jialielihan, Elżbieta Jurkiewicz, Urszula Kaczmarek, Tomasz Kaczmarzyk, Krzysztof Kaliszewski, Dorota Kamińska, Wojciech Kamysz, Sabina Kantorowicz, Paweł Karpiński, Andrzej Kiejna, Katarzyna Kiliś-Pstrusińska, Brygida Knysz, Tomasz Kolenda, Krzysztof Kołtowski, Tomasz Konopka, Anna Korycka-Wołowiec, Magdalena Koszewicz, Tomasz Koszutski, Katarzyna Koziak, Krystyna Koziec, Ewa Koziorowska-Gawron, Dariusz Kozłowski, Anna Kołodziej, Paweł Kołodziejski, Anna Kołtowska, Wojciech Krajewski, Barbara Królak-Olejnik, Katarzyna Krzanowska, Paweł Kubasiewicz-Ross, Julita Kulbacka, Tikoo Kulbhushan, Wiktor Kuliczkowski, Mariusz Kusztal, Maria Kłopocka, Silvia Lai, Tomasz Lehmann, Małgorzata Lelonek, Adam Lepczyński, Guiqing Liao, Andrey Lvov, Izabela Łaczmańska, Łukasz Łaczmański, Krystyna Łoboz-Grudzień, Monika Łukomska-Szymańska, Jarek Maciaczyk, Radharao Madhyastha, Katarzyna Madziarska, Joanna Maj, Przemysław Majewski, Agata Majos, Marcin Mikulewicz, Mirosław Markiewicz, Zbigniew Marzec, Rafał Matkowski, Małgorzata Matusiewicz, Marta Mazur, Małgorzata Małodobra-Mazur, Krzysztof Małyszczak, Jolanta Małyszko, Beata Matyjaszek-Matuszek, Krzysztof Michałek, Magdalena Mierzchała-Pasierb, Monika Miklaszewska, Przemysław Mikołajczak, Andrzej Milanowski, Laurent Misery, Błażej Misiak, Marcin Misiek, Marta Misiuk-Hojło, Katarzyna Mizia-Stec, Piotr Morasiewicz, Agata Mulak, Kinga Musiał, Katarzyna Neubauer, Liming Nie, Katarzyna Niepokój, Przemysław Niewiński, Anna Noczyńska, Aleksandra Nowak, Marta Nowakowska-Kotas, Andrzej Oko, Mateusz Olbromski, Paweł Olczyk, Beata Oleszkiewicz, Mustafa Ozen, Małgorzata Paprocka-Borowicz, Artur Pasternak, Dariusz Patkowski, Joanna Pawlak, Edyta Pawlak-Adamska, Cristian Persu, Paweł Petkow-Dimitrow, Elżbieta Piątkowska, Hanna Piotrowska-Kempisty, Agnieszka Piwowar, Andrzej Plewka, Marzenna Podhorska-Okołów, Maria Podolak-Dawidziak, Zygmunt Pojda, Anna Pokryszko-Dragan, Ewa Poleszak, Elżbieta Poniewierka, Tomasz Porażko, Rafał Poręba, Anna Prescha, Magdalena Krajewska, Bernard Panaszek, Beata Sobieszczańska, Andrzej Prokurat, Mariusz Puszczewicz, Bartosz Puła, Andrzej Rapak, Adam Reich, Paweł Reichert, Rafi Romano, Umberto Romeo, Dorota Różańska, Marcin Ruciński, Adam Rzechonek, Hande Sar, Elżbieta Sarnowska, Tomasz Sarnowski, Marek Sąsiadek, Małgorzata Sekuła, Teresa Sierpińska, Dorota Sikorska, Janusz Skalski, Anna Skoczyńska, Andrzej Smętkowski, Magdalena Sobieska, Jiri Sochor, Burak Soner, Jia-yu Song, Anna Sowińska-Seidler, Agata Stanek, Ewelina Stelcer, Agnieszka Stembalska, Tomasz Stompór, Izabela Strużycka, Pan Su, Halis Suleyman, Wojciech Szczeklik, Aleksandra Szczepankiewicz, Jolanta Szelachowska, Monika Szeliga, Jacek Szepietowski, Tomasz Szydełko, Krzysztof Sładek, Agnieszka Sławuta, Robert Śmigiel, Xiaofeng Tan, Juan Tao, Geroges Tawil, Dariusz Timler, Marcin Tkaczyk, Andrzej Tomaszewski, Lech Torliński, Giovana Torrezan, Krzysztof Tupikowski, Anetta Undas, Donata Urbaniak-Kujda, Iwona Urbanowicz, Wiktor Urbański, Marek Ussowicz, Peijun Wang, Dorota Wasko-Czopnik, Anna Wiela-Hojeńska, Jolanta Wierzba, Joanna Wietrzyk, Anna Witkowska, Piotr Wójcicki, Przemysław Wolak, Krzysztof Woźniak, Magdalena Woźniak, Mieczysław Woźniak, Dariusz Wołowiec, Krzysztof Wytrychowski, Jinhua Xu, S. Yusoff, Urszula Zaleska-Dorobisz, Anna Zalewska, Katarzyna Zatońska, Rafał Załuski, Zygmunt Zdrojewicz, Barbara Zdzisińska, Gianpaolo Zerbini, Ai-Hua Zhang, Qingfei Zheng, Magdalena Zielińska, Marek Ziętek, Agnieszka Ziółkowska, Agata Ziomber, Sławomir Zmonarski, Agnieszka Zubkiewicz-Kucharska, Małgorzata Zwolińska-Wcisło, Dorota Zyśko

Simvastatin increases cell viability and suppresses the expression of cytokines and vascular endothelial growth factor in inflamed human dental pulp stem cells in vitro

Dai Xue[1,A–F], Zhongjian Gong[2,B–D,F], Fangyong Zhu[2,C,D,F], Yanjing Qiu[3,B,C,E,F], Xiaodan Li[1,C,F]

[1] Department of Stomatology, Wuxi Children's Hospital, Nanjing Medical University, China
[2] Department of Stomatology, Wuxi People's Hospital, Nanjing Medical University, China
[3] Department of Stomatology, Pudong New Area People's Hospital, Shanghai, China

A – research concept and design; B – collection and/or assembly of data; C – data analysis and interpretation; D – writing the article; E – critical revision of the article; F – final approval of the article

Advances in Clinical and Experimental Medicine, ISSN 1899-5276 (print), ISSN 2451-2680 (online) *Adv Clin Exp Med*. 2018;27(12):1615–1623

Address for correspondence
Dai Xue
E-mail: Z_BJ2014@163

Funding sources
None declared

Conflict of interest
None declared

Received on May 12, 2017
Reviewed on June 16, 2017
Accepted on July 10, 2017

Abstract

Background. In recent years, simvastatin has been demonstrated to be capable of inducing odontogenic differentiation in human dental pulp stem cells (DPSCs), which makes it a promising source for endodontic treatment in pulpitis. However, a comprehensive understanding of how simvastatin affects the behavior of DPSCs and its potential in pulpitis is still lacking.

Objectives. In this study, we investigated the effects of simvastatin on the viability of inflamed DPSCs. The expression of cytokines and vascular endothelial growth factor (VEGF) was also studied in response to simvastatin treatment.

Material and methods. We characterized the cell viability, inflammatory reactions and the production of VEGF in inflamed DPSCs, induced by lipopolysaccharides (LPS). The methylthiazolyldiphenyl-tetrazolium bromide (MTT) assay, cell cycle, apoptosis analysis, quantitative reverse transcription polymerase chain reaction (RT-PCR), enzyme-linked immunosorbent assay (ELISA), and western blot analyses were performed.

Results. We observed that a low dosage of simvastatin accelerated cell proliferation, whereas its high dosage (>15 μg/mL) suppressed propagation. A simvastatin dose of 8 μg/mL was sufficient to promote cell growth and cell cycle progression in DPSCs treated with LPS. Meanwhile, simvastatin induced apoptosis. The expression of multiple cytokines, including interleukins *(IL)-1*, *IL-4* and *IL-1β*, and especially interferon-gamma (*IFN-γ*) and tumor necrosis factor-alpha (*TNF-α*), was significantly suppressed. Moreover, the protein secretion and mRNA transcription of *VEGF* was observed to be markedly inhibited by simvastatin by inactivating mitogen-activated protein kinase (MAPK) signaling.

Conclusions. Taken together, these results suggested that simvastatin might be a potent ingredient to enhance cell proliferation, alleviate inflammation response and attune vasculogenesis in pulpitis.

Key words: cytokines, vascular endothelial growth factor, simvastatin, dental pulp stem cell, pulpitis

DOI
10.17219/acem/75776

Introduction

Pulpitis is a quite commonly occurring inflammation in the dental pulp tissue, which is characterized by increased sensitivity to stimuli, specifically hot and cold stimuli.[1] Following the inflammation, some fundamental alterations have also been reported, such as an increase in blood flow, enhanced capillary permeability, the diffusion of vascular fluid into intercellular spaces, and the immigration of granulocytes and monocytes.[2] Tissue injury caused by trauma, bacterial infection, chemical substances, contusion, etc. is the main cause of pulpitis.[3] The correlation between the invasion of Gram-negative bacteria and their product, lipopolysaccharides (LPS), and the symptoms of pulpitis has been investigated.[4,5]

The dental pulp contains connective tissue, lymphatic tissues, blood vessels, neural fibers, and dental pulp stem cells (DPSCs), and its main functions are to produce dentin and to maintain the biological and physiological vitality of the dentin.[6,7] Within the dental pulp, DPSCs provide a promising source of cells for applications in regenerative medicine. By their nature, DPSCs have the potential through the production of odontoblasts to create reparative dentin in response to injury.[8] Although DPSCs comprise only 1% of the total cell population of the pulp, they play crucial roles in the process of dentin regeneration in both acute and chronic pulpitis.[9,10]

In pulpitis, oral antibiotics having bacteriostatic or bactericidal properties are widely used to control or eliminate the attacking bacteria.[11] However, systematic antibiotics showed poor outcomes in some cases of pulpitis.[12] In regard to regenerative medicine, DPSCs demonstrated strong potential to regenerate the dentin with the aid of recombinant human bone morphogenetic protein 2.[13,14] In recent years, a lipid-lowering medication, simvastatin, has been demonstrated to be capable of inducing odontogenic differentiation of human DPSCs in vitro and in vivo, and of promoting pulp regeneration.[15–17] Until now, studies on how simvastatin affects DPSCs have been limited. In this study, we investigated the effects of simvastatin on the viability of inflamed DPSCs, and the underlying mechanism.

Material and methods

Isolation and culture of dental pulp stem cells

Six impacted 3rd molars were removed by an oral surgeon from 5 teenage subjects with irreversible pulpitis. Dental pulp stem cells were isolated as previously described.[18] Briefly, the dental pulp was harvested and immersed in α-modified minimal essential medium (α-MEM) (Sigma-Aldrich, Burlington, USA) containing 3 mg/mL of type I collagenase and 4 mg/mL of dispase at 37°C for 1 h. After enzymatic disaggregation, the pulp was dissociated and the cell suspension was then plated in a 25 cm^2 flask, and maintained in Iscove modified Dulbecco medium (IMDM) (Thermo Fisher Scientific, Waltham, USA), supplemented with 10% fetal calf serum (FCS) (Gibco, New York, USA), 2 mM of L-glutamine, 100 U/mL of streptomycin, and 100 U/mL of cell colony formed on approx. day 7. Then, it was picked, resuspended and plated in a new flask. Dental pulp stem cells were expanded upon reaching 70% confluency for further study. The study was approved by the Ethics Committee of Wuxi Children's Hospital (China) and written informed consent was obtained from all the enrolled subjects and their parents before admittance to the study.

Cell viability assay

To test the effect of simvastatin on cell proliferation, DPSCs were cultured in 96-well plates, in media containing various concentrations, ranging from 0 to 20 μg/mL (0, 2, 4, 8, 10, 15, and 20 μg/mL). Additionally, cell viability in LPS challenging conditions was also measured by randomly assigning the cells into the control group (not treated), the simvastatin (8 μg/mL) group, an LPS (60 μg/mL) group, and an LPS + simvastatin group. Cell viability was measured by using methylthiazolyldiphenyl-tetrazolium bromide (MTT) purchased from Thermo Fischer Scientific (Waltham, USA). Following exposure to simvastatin or LPS, 10 μL of MTT solution (5 mg/mL) was added to each well, and the plates were incubated for 3 h at 37°C. After removing the medium, the formazan was dissolved in 200 μL of dimethyl sulfoxide (DMSO) (Sigma-Aldrich) in each well. Absorbance was read at 5 nm using a microplate reader (Bio-Rad Laboratories, Hercules, USA).

Cell cycling analysis

The DNA contents of each cell cycle phase was reflected by variations in the propidium iodide (PI) fluorescence intensities, and the distribution of cell cycle phases was analyzed by flow cytometry following PI staining as previously described.[19] In brief, DPSCs were washed with ice-cold phosphate-buffered saline (PBS), suspended in approx. 0.5 mL of 70% cold ethanol and kept at 4°C for 30 min. The cells were subsequently treated with 100 mg/mL of DNase-free RNase (Sigma-Aldrich) and incubated for 30 min at 37°C prior to the addition of PI (50 mg/mL; Sigma-Aldrich) directly into the cell suspension. The suspension was filtered through a 50 mm nylon mesh, and a total of 10,000 stained cells were subjected to flow cytometric analysis (FACSCalibur; BD Biosciences, San Jose, USA).

Assessment of apoptosis

Dental pulp stem cells were stained with an Annexin V-FITC apoptosis detection kit (Sigma-Aldrich) to determine whether the cells underwent apoptosis. Propidium

iodide staining was used as a control to differentiate cells undergoing necrosis. Dental pulp stem cells were seeded in tissue culture slides and allowed to attach for 24 h. Subsequently, the cells were resuspended in 500 µL of binding buffer, 5 µL of Annexin V-FITC and 5 µL of PI were added, and the cells were incubated for 5 min at 37°C in the dark. Flow cytometry analysis was performed to evaluate the apoptosis of DPSCs. Three independent trials were conducted.

Analysis of expression of cytokine genes

Quantitative real-time PCR (qPCR) was performed to quantify the expression of interleukin *(IL)-1*, *IL-4*, *IL-6*, *IL-1β*, interferon-gamma (*IFN-γ*) and tumor necrosis factor-alpha (*TNF-α*). Dental pulp stem cells were lysed with TRIzol reagent (Thermo Fischer Scientific) and the total RNA was extracted. Afterwards, cDNA was synthesized using a PCR kit (Becton-Dickinson, Franklin Lakes, USA). In the quantification of mRNA expression, 1 µL of cDNA was applied on an ABI 7500 real-time machine (ABI, Camarillo, USA), using a SYBR Green reagent (Takara Bio, Kusatsu, Japan). The primer pairs are listed in Table 1. Glyceraldehyde 3-phosphate dehydrogenase (*GAPDH*) was employed as an internal control and used for the normalization of cycle threshold (Ct) values. Experiments were carried out in triplicate.

Enzyme-linked immunosorbent assay for vascular endothelial growth factor secretion

An enzyme-linked immunosorbent assay (ELISA) kit (R&D Systems, Minneapolis, USA) was used to quantify the vascular endothelial growth factor (VEGF) concentration in the medium, strictly following the manufacturer's instructions. Briefly, standards and samples were diluted on 96-well plates, and 50 µL of conjugate solution was added to each well. After incubation at room temperature for 2 h, the wells were washed with PBS solution 3 times. Then, 200 µL of substrate solution was added. The plate was incubated for 10–15 min and the color development was stopped. The absorbance of each well was determined at 450 nm in a microplate reader (BioTeke, Beijing, China). A standard curve was constructed by plotting the absorbance of standards against the known concentration. The VEGF concentration was deduced from the standard curve.

Western blot analysis for mitogen-activated protein kinase signaling

Dental pulp stem cells were lysed and the total protein was extracted using RIPA lysis buffer (Beyotime Biotechnology, Shanghai, China). Electrophoresis was performed on a 12% sodium dodecyl sulfate-polyacrylamide gel loaded with 20 µg of total protein. The proteins were then transferred to a nitrocellulose membrane, followed by blocking with 5% defatted milk at 4°C overnight. Subsequently, the membrane was washed with PBS and incubated with primary antibodies (anti-p38 and anti-phosphorylated p38, 2000× dilution; anti-ERK1/2 and anti-phosphorylated ERK1/2, 1000× dilution; anti-ACTIN, 1000× dilution), and consecutively with peroxidase-conjugated secondary antibodies – goat anti-mouse immunoglobulin G (IgG), diluted 1:5000 (Santa Cruz Biotechnology, Santa Cruz, USA). Chemiluminescence reagents (Thermo Fisher Scientific) were used to visualize the proteins, and the protein bands were exposed onto an X-ray film in a darkroom. Beta-actin served as an endogenous control.

Table 1. Primers used in the study

Gene name	Forward (5′-3′)	Reverse (5′-3′)	Temperature [°C]	Product [bp]
CD73	AGCAGCATTCCTGAAGATCCA	TTCCAGAACATTTCATCCGTGT	59	212
CD90	GATCCTAGCCTCACCCGTCA	TGTTTTTTGCAGCCTTGGCT	60	228
CD166	GATACCATTATCATACCTTGCCG	CTGTCTTCTGAAATGCAGTCACC	60	377
CD14	TCATCAGGACACTGCCAGGA	GCTTCCAGGCTTCACACTTG	60	240
CD34	CTTGGAAGTACCAGCCTGCA	AGGCAGATGCCCTGAGTCAA	60	374
IL-1	TGAGCTCGCCAGTGAAATGA	CATGGCCACAACAACTGACG	59	199
IL-4	GTGCACCGAGTTGACCGTA	CGTACTCTGGTTGGCTTCCT	58	256
IL-6	TCAATATTAGAGTCTCAACCCCCA	AGAAGGCAACTGGACCGAAG	60	161
IL-1β	CCTGAGCTCGCCAGTGAAAT	CATGGCCACAACAACTGACG	60	201
IFN-γ	GCAGCTAAAACAGGGAAGCG	CTTGCTTAGGTTGGCTGCCT	60	349
TNF-α	CTGGGCAGGTCTACTTTGGG	CTGGAGGCCCCAGTTTGAAT	60	272
VEGF	CTCACCAAGGCCAGCACATA	GGCTCCAGGGCATTAGACAG	60	201
GAPDH	TTGTCATCAATGGAAATCCCAT	CCAGTAGAGGCAGGGATGATGT	60	436

IL – interleukin; *IFN-γ* – interferon-gamma; *TNF-α* – tumor necrosis factor-alpha; *VEGF* – vascular endothelial growth factor; *GAPDH* – glyceraldehyde 3-phosphate dehydrogenase.

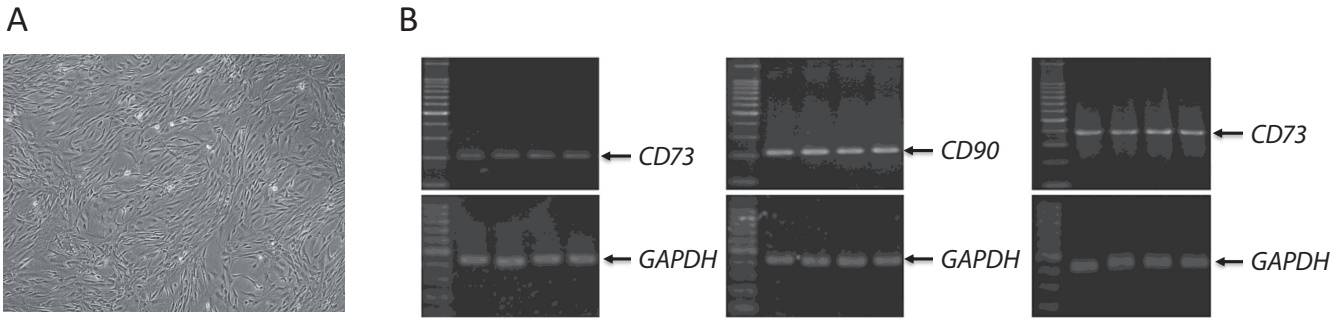

Fig. 1. Characterization of isolated DPSCs

A) morphological analysis of DPSCs; B) expression of mesenchymal markers in DPSCs. DPSCs – dental pulp stem cells; *GAPDH* – glyceraldehyde 3-phosphate dehydrogenase; GAPDH was used as an endogenous control; experiments were carried out in 4 independent trials.

Statistical analysis

SPSS v. 19.0 software (IBM Corp., Armonk, USA) was used for the statistical analysis. After confirming a normal distribution, the data was presented as means ± standard deviation (SD). A 2-tailed t-test was performed to compare the means between the 2 groups. One asterisk (*) indicates a statistical difference complying with $p < 0.05$, and 2 asterisks (**) indicate $p < 0.01$.

Results

Characterization of isolated dental pulp stem cells

The cells from the dental pulp were isolated and cultivated in cell dishes. These cells showed the typical morphology of mesenchymal stem cells (MSCs) (Fig. 1A). To determine whether these cells were mesenchymal, the cell surface markers considered important stemness determinants associated with DPSCs – CD73, CD90 and CD166 – were characterized.[20] In Fig. 1B, these 3 molecules were depicted as highly expressed by using the reverse transcription PCR (RT-PCR) method. Meanwhile, the hematopoietic markers CD14 and CD34 were also examined. A negative expression was observed (data not shown). These results proved that DPSCs were successfully isolated and could be used in further research.

Simvastatin-promoted proliferation of dental pulp stem cells

To explore the effects of simvastatin on the viability of DPSCs, the cells were cultured with gradient concentrations of simvastatin ranging from 0 to 20 μg/mL (0, 2, 4, 8, 10, 15, and 20 μg/mL) and a Cell-Counting Kit-8 (CCK-8) (Sigma-Aldrich) assay was performed. It was observed that cells challenged with a low concentration of simvastatin (2, 4, 8, or 10 μg/mL) propagated faster than untreated ones. High concentrations (15 and 20 μg/mL), however, reduced proliferation. Importantly, 8 μg/mL of simvastatin induced the fastest cell growth (Fig. 2A).

Lipopolysaccharides were considered to be a potent inducer of pulpitis, and they were also reported to inhibit the proliferation of DPSCs.[21,22] Here we investigated whether simvastatin could promote cell proliferation under the conditions of LPS challenging. Compared to the controls, DPSCs treated with 60 μg/mL of LPS showed inhibited proliferation, whereas simvastatin (8 μg/mL) restored a high growth rate in the LPS + simvastatin group (Fig. 2B). These results indicated that simvastatin could stimulate the proliferation of DPSC under both normal and inflammatory conditions.

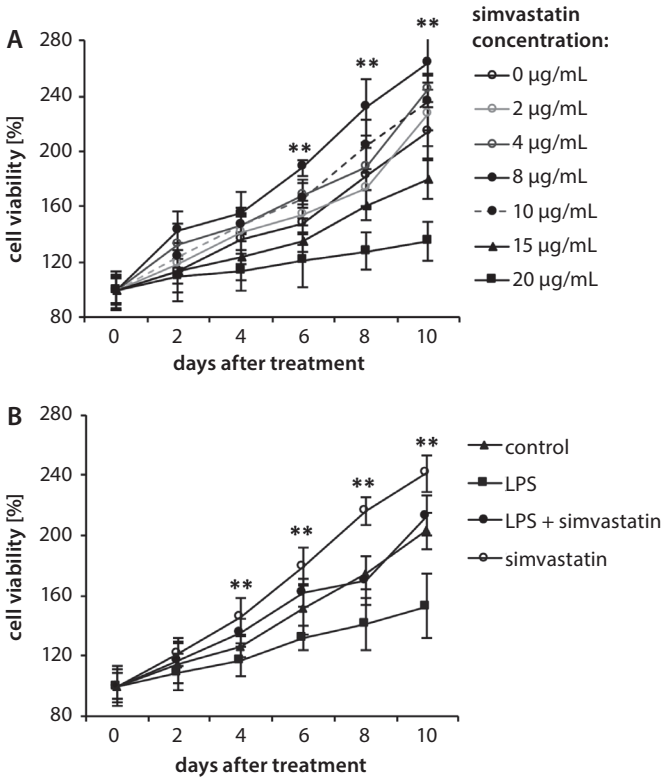

Fig. 2. Analysis of cell viability of DPSCs

A) proliferation of DPSCs treated with different concentrations of simvastatin; ** $p < 0.01$; cell exposure to 8 μg/mL vs 0 μg/mL of simvastatin; B) proliferation of DPSCs treated with LPS or simvastatin; ** $p < 0.01$; LPS + simvastatin group vs LPS group. DPSCs – dental pulp stem cells; LPS – lipopolysaccharides.

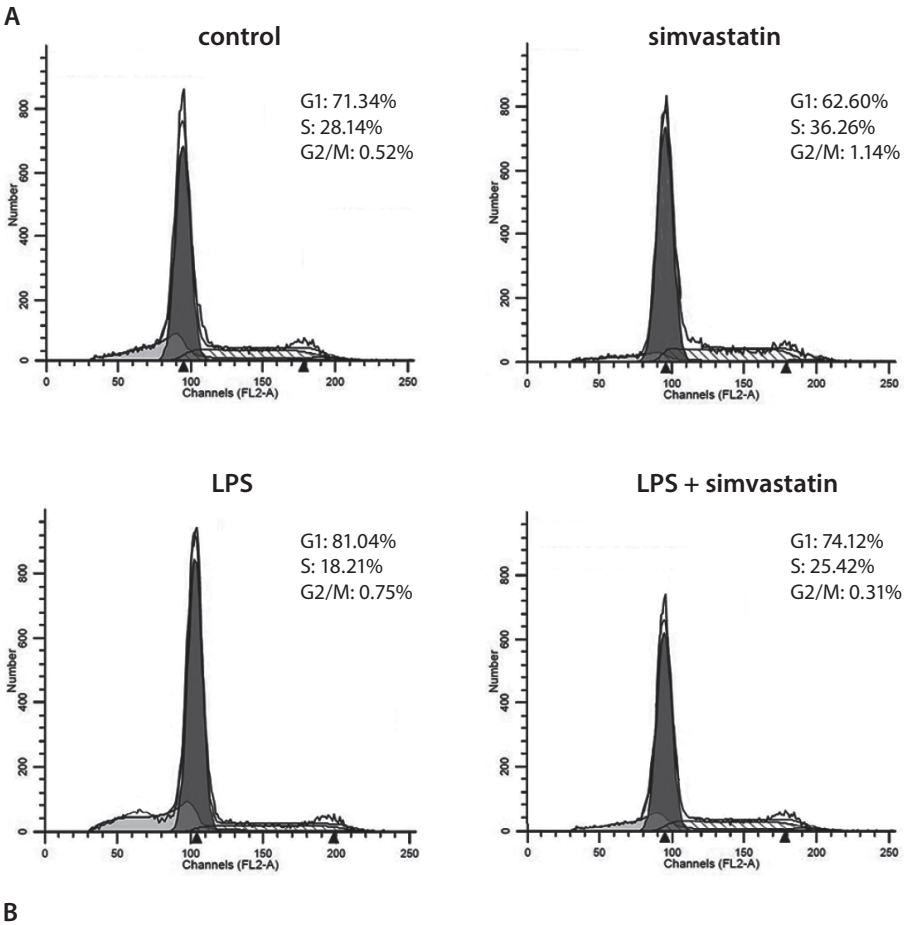

Fig. 3. Effects of simvastatin on cell cycling progression of DPSCs

A) flow cytometry graphs in cells treated with LPS or simvastatin; B) mean values of different cycle phases in untreated cells, cells treated with simvastatin, with LPS, and with LPS + simvastatin; ** $p < 0.01$; LPS + simvastatin group vs LPS group; n = 6. DPSCs – dental pulp stem cells; LPS – lipopolysaccharides.

Simvastatin-promoted cell cycling

In order to investigate the effects of simvastatin on the cell cycling progression of DPSCs, flow cytometry was performed to measure the distributions of each phase. Figure 3B illustrates the mean percentage values of cycling phases in cells treated with LPS or simvastatin. The proportion of the G1 population increased from 71.34 ±1.76% of the control group to 81.04 ±2.43% of the LPS group, while it fell back to 74.12 ±1.12% of the LPS + simvastatin group. These results indicate that LPS arrested DPSCs at the G1 phase, while simvastatin promoted cell cycling progression to the S phase.

Simvastatin-promoted apoptosis

In order to further characterize the effect of simvastatin on the apoptosis of DPSCs, flow cytometry analysis was performed using Annexin V-FITC and PI to differentiate cells undergoing apoptosis or necrosis. As shown in Fig. 4, cells died in response to LPS treatment (8.74 ±2.4% in the LPS group vs 2.49 ±1.3% in the control group). Simvastatin caused a slight increase in the number of apoptotic cells compared to the control group ($p > 0.05$). However, in combination with LPS challenging, there was a significantly elevated rate of apoptosis ($p < 0.01$). This data demonstrates that simvastatin promotes the apoptosis of DPSCs in LPS stimulation.

Simvastatin-suppressed inflammatory response

The inflammatory response in the dental pulp is mediated by various cytokines, including IL-1, IL-4, IL-6, IL-1β, IFN-γ, and TNF-α.[23] The expression of these genes was quantified

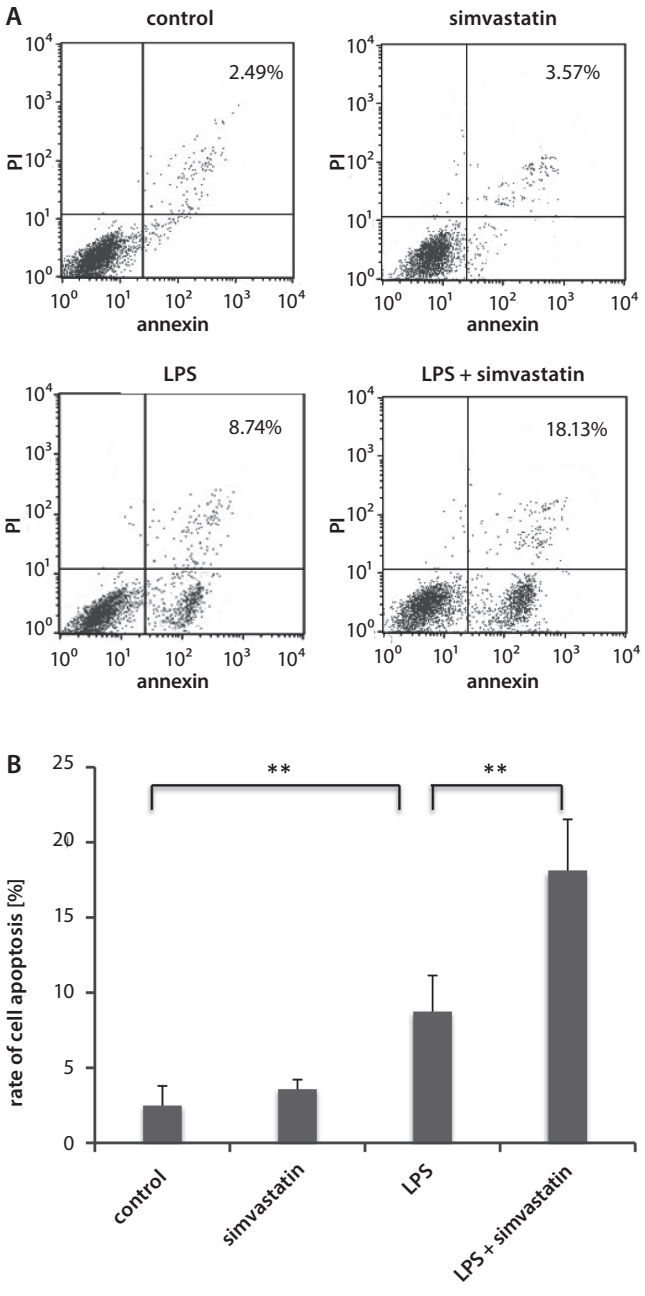

Fig. 4. Effects of simvastatin on cell apoptosis of DPSCs

A) flow cytometry graphs in cells treated with LPS or simvastatin; B) mean values of apoptosis rate in untreated cells, cells treated with simvastatin, with LPS, and with LPS + simvastatin; ** $p < 0.01$; $n = 6$. DPSCs – dental pulp stem cells; LPS – lipopolysaccharides; PI – propidium iodide.

by qPCR and it was found that LPS induced the upregulated expression of *IL-1*, *IL-4*, *IL-6*, *IL-1β*, *IFN-γ*, and *TNF-α*, of which *IL-1β* and *TNF-α* exhibited the highest alterations, with fold changes of 7.84 and 12.17, respectively. By contrast, simvastatin suppressed the genes of increased expression, except for *IL-6*. Compared to the LPS group, the exposure to simvastatin caused a 3.2-fold decrease of *IL-1β* expression and a 3.5-fold decrease of *TNF-α* (Fig. 5). The decreased expression of cytokines indicates that simvastatin suppressed the inflammatory response in inflamed DPSCs.

Simvastatin-downregulated vascular endothelial growth factor expression via inhibiting p38 mitogen-activated protein kinase signaling

During pulpitis, angiogenic growth factor is the crucial element for vasculogenesis, as well as a part of the associated inflammation.[24] Among various factors, the most potent is VEGF, which is responsible for angiogenesis and the development and permeation of new blood vessels.[25] In this study, we evaluated the effects of LPS and simvastatin on VEGF production. The secretion of VEGF was determined by ELISA. Simvastatin dramatically suppressed VEGF secretion, induced by LPS. A reduction was also observed in the expression of the *VEGF* gene (Fig. 6A).

VEGF expression was demonstrated to be induced by LPS, depending on mitogen-activated protein kinase (MAPK) activation.[26] To reveal the pathway on which simvastatin attenuated VEGF expression, we examined the activity of MAPK signaling by western blot. Lipopolysaccharides were found to increase the phosphorylation levels of P38 and ERK1/2, in line with a previous study.[26] Of note, simvastatin markedly decreased P38 and ERK1/2 phosphorylation in both control and LPS-treated cells (Fig. 6B). These results indicate that simvastatin attenuates VEGF expression via blocking p38 MAPK signaling.

Discussion

Dental pulp stem cells are regarded as a subpopulation of MSCs, possessing the property of self-renewal, the expression of multiple MSC surface markers, and differentiation into various cell types, such as odontoblasts, adipocytes, cardiomyocytes, osteoblasts, chondrocytes, liver cells, etc.[27] Their natural capacity for producing odontoblasts to create reparative dentin attracts researchers for applications in the regeneration of tooth structures. In vitro studies showed that DPSCs played important role in the dentin/pulp complex generation and immunoregulation.[28,29] Dental pulp stem cells can be readily isolated from the healthy dental pulp tissue of human impacted 3rd molars, which are naturally lost during childhood or removed during routine dental procedures.[30] Considering the superior property and convenient handling, DPSCs are considered a valuable source of cells utilized in regenerative therapies for various diseases, including dental pulp regeneration, tooth reconstruction, bone tissue engineering, and other applications in cell therapy.[7]

Dental pulp stem cells are able to respond to specific extracellular excitatory signals and play a crucial role in dentin regeneration after injury in acute and chronic pulpitis.[10] Simvastatin, a semisynthetic lipophilic 3-hydroxy-3-methylglutaryl-coenzyme A reductase (HMGCR) inhibitor, was extensively used as a well-established cholesterol-lowering drug, able to inhibit cholesterol synthesis, and showed

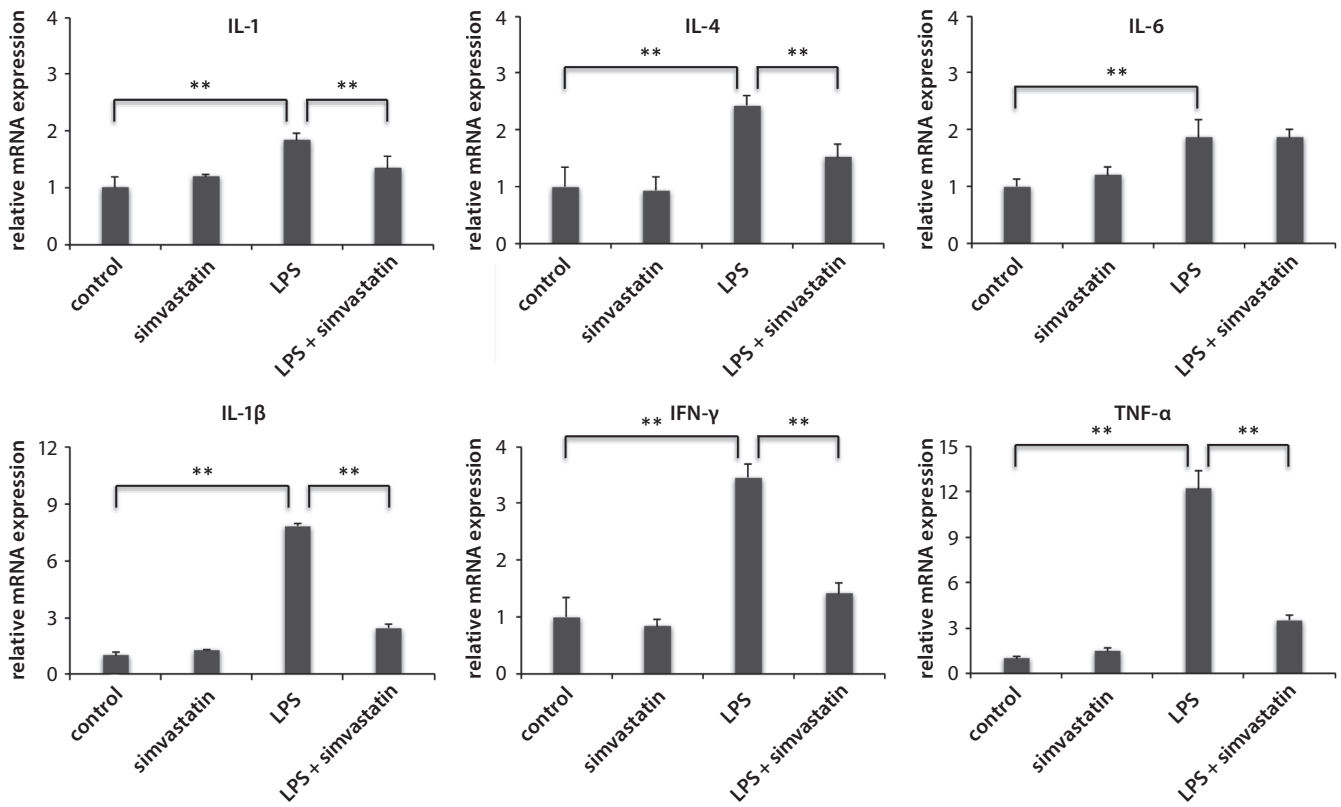

Fig. 5. Expression of cytokines treated with LPS or simvastatin

LPS – lipopolysaccharides; IL – interleukin; IFN-γ – interferon-gamma; TNF-α – tumor necrosis factor-alpha; GAPDH – glyceraldehyde 3-phosphate dehydrogenase; experiments were carried out in triplicate; gene expression was normalized by GAPDH; ** $p < 0.01$.

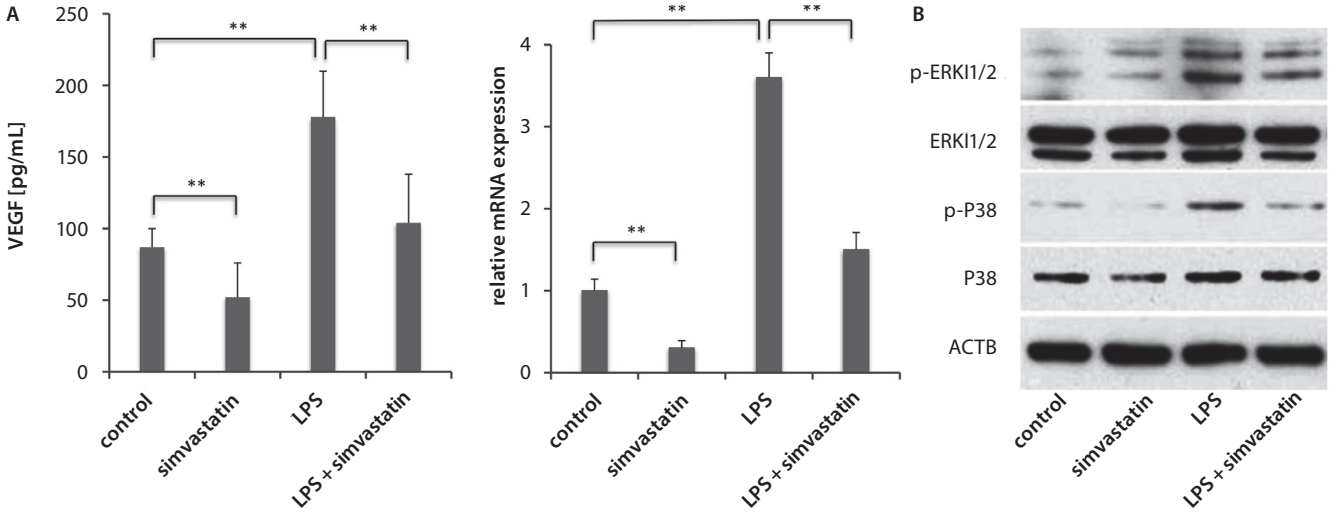

Fig. 6. Effects of simvastatin on VEGF expression

A) simvastatin decreased VEGF secretion (left) and gene expression (right); B) simvastatin-inhibited phosphorylation of p38 and ERK1/2 in MAPK signaling examined by western blot; VEGF – vascular endothelial growth factor; MAPK – mitogen-activated protein kinase; LPS – lipopolysaccharides; p – phosphorylation; ACTB – β-actin; ACTB was used as an internal control; experiments were run in triplicate; ** $p < 0.01$.

potent effects on cell proliferation, cell cycling and apoptosis.[31,32] Besides, simvastatin was demonstrated to be able to induce human DPSCs differentiation into odontoblasts and to promote pulp regeneration.[15,16] This study was aimed at investigating how simvastatin affects DPSCs under the conditions of inflammation caused by LPS. The results showed that low concentrations of simvastatin accelerated the proliferation of DPSCs, while high concentrations of simvastatin (>15 μg/mL) exhibited a suppressive effect. Treatment with LPS also inhibited cell growth, and combinatory stimulation with simvastatin recovered a high proliferation rate. Furthermore, we performed

fluorescence-activated cell sorting (FACS) to characterize the cell cycling and apoptosis in DPSCs treated with simvastatin or LPS, and found that simvastatin promoted cell cycling into phase S, and induced apoptosis as well. These results collectively indicate that simvastatin enhances the proliferation of DPSCs by promoting cell cycling progression and apoptosis (Fig. 2–4).

An inflammatory response is very common during pulpitis caused by carious bacteria and their products, and is mediated by cytokines, such as IL-1, IL-4, IL-6, IL-1β, IFN-γ, and TNF-α.[23] Mesenchymal stem cells, including DPSCs, have the capacity to receive inflammatory signals and to express a large number of cytokines. Conversely, chronic exposure to these cytokines potentially affects the activity of DPSCs, leading to impairment in immunomodulatory and anti-inflammatory roles, and to suppression of the differentiation ability of DPSCs.[33,34] In our study, we observed that simvastatin suppressed the expression of the examined cytokines, with the highest alterations in *IL-1β* and *TNF-α* (Fig. 5), suggesting that simvastatin was capable of relieving the inflammatory response. In a previous study, TNF-α was found to stimulate the proliferation of DPSCs by regulating the Akt/GSK-3β/cyclin D1 signaling pathway.[35] Lipopolysaccharides significantly promoted *TNF-α* expression (Fig. 5), while the growth rate of DPSCs was suppressed (Fig. 2B), inferring that some unknown factors (except for *TNF-α*) affected cell proliferation.

Vascular endothelial growth factor has been found to be strongly expressed in teeth with irreversible pulpitis, and it can increase and extend the severity of the inflammatory processes because of an increased transport of nutrients, oxygen and inflammatory cells to the site of inflammation, and thus it affects dentinogenesis and progresses to necrosis.[24,36] In in vitro cells, the upregulation of VEGF during inflammation was demonstrated to significantly contribute to the pathogenesis associated with the survival and differentiation of DPSCs.[37] Expression of VEGF was previously shown to be induced through MAPK signaling, which was confirmed by the upregulated phosphorylation levels of P38 and ERK1/2 (Fig. 6B).[26] Notably, our results also showed that in inflamed DPSCs, characterized by an elevated expression of various cytokines, augmented VEGF expression and secretion (Fig. 6A) were accompanied by decreased cell viability (Fig. 2). In contrast, simvastatin significantly inhibited VEGF synthesis and promoted cell proliferation. Considering the fact that VEGF was induced by MAPK signaling (Fig. 6B), it is rational to speculate that simvastatin counteracted the effects of LPS on VEGF expression and MAPK signaling, and thus enhanced the proliferation of DPSCs.

In conclusion, we found that simvastatin promoted cell proliferation, cell cycling and apoptosis in inflamed DPSCs induced by LPS. Moreover, the expression of multiple cytokines and VEGF was observed to be significantly inhibited. Vascular endothelial growth factor was demonstrated to be regulated through the blocking of MAPK signaling. Collectively, simvastatin was shown to enhance cell viability, perhaps via the MAPK/VEGF axis, and to relieve inflammation response as well. This study provided some evidence to support the hypothesis that simvastatin might be a potent therapy for pulpitis.

References

1. Michaelson PL, Holland GR. Is pulpitis painful? *Int Endod J*. 2002;35(10):829–832.
2. Ahlquist ML, Franzen OG. Inflammation and dental pain in man. *Endod Dent Traumatol*. 1994;10(5):201–209.
3. Hahn CL, Liewehr FR. Relationships between caries bacteria, host responses, and clinical signs and symptoms of pulpitis. *J Endod*. 2007;33(3):213–219.
4. Khabbaz MG, Anastasiadis PL, Sykaras SN. Determination of endotoxins in caries: Association with pulpal pain. *Int Endod J*. 2000;33(2):132–137.
5. Jacinto RC, Gomes BP, Shah HN, Ferraz CC, Zaia AA, Souza-Filho FJ. Quantification of endotoxins in necrotic root canals from symptomatic and asymptomatic teeth. *J Med Microbiol*. 2005;54(Pt 8):777–783.
6. Liu H, Gronthos S, Shi S. Dental pulp stem cells. *Methods Enzymol*. 2006;419:99–113.
7. Tatullo M, Marrelli M, Shakesheff KM, White LJ. Dental pulp stem cells: Function, isolation and applications in regenerative medicine. *J Tissue Eng Regen Med*. 2015;9(11):1205–1216.
8. Na S, Zhang H, Huang F, et al. Regeneration of dental pulp/dentine complex with a three-dimensional and scaffold-free stem-cell sheet-derived pellet. *J Tissue Eng Regen Med*. 2016;10(3):261–270.
9. Paino F, Ricci G, De Rosa A, et al. Ecto-mesenchymal stem cells from dental pulp are committed to differentiate into active melanocytes. *Eur Cell Mater*. 2010;20:295–305.
10. Ustiashvili M, Kordzaia D, Mamaladze M, Jangavadze M, Sanodze L. Investigation of functional activity human dental pulp stem cells at acute and chronic pulpitis. *Georgian Med News*.2014;234:19–24.
11. Fedorowicz Z, van Zuuren EJ, Farman AG, Agnihotry A, Al-Langawi JH. Antibiotic use for irreversible pulpitis. *Cochrane Database Syst Rev*. 2013;2:CD004969. doi: 10.1002/14651858.CD004969.pub4
12. Hoskin E, Veitz-Keenan A. Antibiotics are not useful to reduce pain associated with irreversible pulpitis. *Evid Based Dent*. 2016;17(3):81–82.
13. Iohara K, Nakashima M, Ito M, Ishikawa M, Nakasima A, Akamine A. Dentin regeneration by dental pulp stem cell therapy with recombinant human bone morphogenetic protein 2. *J Dent Res*. 2004;83(8):590–595.
14. Saito T, Ogawa M, Hata Y, Bessho K. Acceleration effect of human recombinant bone morphogenetic protein-2 on differentiation of human pulp cells into odontoblasts. *J Endod*. 2004;30(4):205–208.
15. Karanxha L, Park SJ, Son WJ, Nor JE, Min KS. Combined effects of simvastatin and enamel matrix derivative on odontoblastic differentiation of human dental pulp cells. *J Endod*. 2013;39(1):76–82.
16. Okamoto Y, Sonoyama W, Ono M, et al. Simvastatin induces the odontogenic differentiation of human dental pulp stem cells in vitro and in vivo. *J Endod*. 2009;35(3):367–372.
17. Jia W, Zhao Y, Yang J, et al. Simvastatin promotes dental pulp stem cell-induced coronal pulp regeneration in pulpotomized teeth. *J Endod*. 2016;42(7):1049–1054.
18. Raoof M, Yaghoobi MM, Derakhshani A, et al. A modified efficient method for dental pulp stem cell isolation. *Dent Res J (Isfahan)*. 2014;11(2):244–250.
19. Shi X, Gipp J, Dries M, Bushman W. Prostate progenitor cells proliferate in response to castration. *Stem Cell Res*. 2014;13(1):154–163.
20. Lee SY, Huang GW, Shiung JN, et al. Magnetic cryopreservation for dental pulp stem cells. *Cells Tissues Organs*. 2012;196(1):23–33.
21. Warfvinge J, Dahlen G, Bergenholtz G. Dental pulp response to bacterial cell wall material. *J Dent Res*. 1985;64(8):1046–1050.
22. Liu Y, Gao Y, Zhan X, et al. TLR4 activation by lipopolysaccharide and *Streptococcus mutans* induces differential regulation of proliferation and migration in human dental pulp stem cells. *J Endod*. 2014;40(9):1375–1381.
23. Hozhabri NS, Benson MD, Vu MD, et al. Decreasing NF-kappaB expression enhances odontoblastic differentiation and collagen expression in dental pulp stem cells exposed to inflammatory cytokines. *PLoS One*. 2015;10(1):e0113334. doi: 10.1371/journal.pone.0113334

24. Guven G, Altun C, Gunhan O, et al. Co-expression of cyclooxygenase-2 and vascular endothelial growth factor in inflamed human pulp: An immunohistochemical study. *J Endod*. 2007;33(1):18–20.
25. Dvorak HF, Nagy JA, Feng D, Brown LF, Dvorak AM. Vascular permeability factor/vascular endothelial growth factor and the significance of microvascular hyperpermeability in angiogenesis. *Curr Top Microbiol Immunol*. 1999;237:97–132.
26. Botero TM, Son JS, Vodopyanov D, Hasegawa M, Shelburne CE, Nör JE. MAPK signaling is required for LPS-induced VEGF in pulp stem cells. *J Dent Res*. 2010;89(3):264–269.
27. Potdar PD, Jethmalani YD. Human dental pulp stem cells: Applications in future regenerative medicine. *World J Stem Cells*. 2015;7(5):839–851.
28. Batouli S, Miura M, Brahim J, et al. Comparison of stem-cell-mediated osteogenesis and dentinogenesis. *J Dent Res*. 2003;82(12):976–981.
29. Wada N, Menicanin D, Shi S, Bartold PM, Gronthos S. Immunomodulatory properties of human periodontal ligament stem cells. *J Cell Physiol*. 2009;219(3):667–676.
30. Gronthos S, Mankani M, Brahim J, Robey PG, Shi S. Postnatal human dental pulp stem cells (DPSCs) in vitro and in vivo. *Proc Natl Acad Sci U S A*. 2000;97(25):13625–13630.
31. Afzali M, Vatankhah M, Ostad SN. Investigation of simvastatin-induced apoptosis and cell cycle arrest in cancer stem cells of MCF-7. *J Cancer Res Ther*. 2016;12(2):725–730.
32. Wang G, Cao R, Wang Y, et al. Simvastatin induces cell cycle arrest and inhibits proliferation of bladder cancer cells via PPARγ signalling pathway. *Sci Rep*. 2016;6:35783. doi: 10.1038/srep35783
33. Le Blanc K. Mesenchymal stromal cells: Tissue repair and immune modulation. *Cytotherapy*. 2006;8(6):559–561.
34. Sonoda S, Yamaza H, Ma L, et al. Interferon-gamma improves impaired dentinogenic and immunosuppressive functions of irreversible pulpitis-derived human dental pulp stem cells. *Sci Rep*. 2016;6:19286. doi: 10.1038/srep19286
35. Qin Z, Li Y, Li Y, Liu G. Tumor necrosis factor alpha stimulates proliferation of dental pulp stem cells via Akt/glycogen synthase kinase-3beta/cyclin D1 signaling pathway. *J Endod*. 2015;41(7):1066–1072.
36. Chu SC, Tsai CH, Yang SF, et al. Induction of vascular endothelial growth factor gene expression by proinflammatory cytokines in human pulp and gingival fibroblasts. *J Endod*. 2004;30(10):704–707.
37. Matsushita K, Motani R, Sakuta T, et al. The role of vascular endothelial growth factor in human dental pulp cells: Induction of chemotaxis, proliferation, and differentiation and activation of the AP-1-dependent signaling pathway. *J Dent Res*. 2000;79(8):1596–1603.

Effects of young extracellular matrix on the biological characteristics of aged tendon stem cells

Dapeng Jiang[1,A,C,D,F], Bo Xu[2,B,C,E], Peng Gao[2,C–F]

[1] Department of Urology, Shanghai Children's Medical Center, Shanghai Jiao Tong University School of Medicine, China
[2] Department of Pediatric Surgery, Second Affiliated Hospital of Harbin Medical University, China

A – research concept and design; B – collection and/or assembly of data; C – data analysis and interpretation;
D – writing the article; E – critical revision of the article; F – final approval of the article

Advances in Clinical and Experimental Medicine, ISSN 1899-5276 (print), ISSN 2451-2680 (online) *Adv Clin Exp Med*. 2018;27(12):1625–1630

Address for correspondence
Dapeng Jiang
E-mail: jdp509@163.com

Funding sources
This work was supported by grants from the National Natural Sciences Foundation of China (No. 30901516, 81472085).

Conflict of interest
None declared

Received on March 19, 2016
Reviewed on May 30, 2016
Accepted on June 26, 2017

Abstract

Background. Age-related changes in the properties of tendon stem cells (TSCs) may play a role in the progressive degeneration and increased risk of injury to tendon tissue. Recent reports have demonstrated that a decellularized extracellular matrix (DECM) can provide an appropriate niche to maintain the proliferation and differentiation capacity of adult stem cells.

Objectives. We investigated the biological effects of DECM obtained from young TSCs on the proliferation, stemness, senescence, and differentiation of the aged TSCs.

Material and methods. Tendon stem cells were isolated from rat patellar tendons and the DECM was collected. The proliferative capacity, β-galactosidase activity, stem cell marker expression, and tenogenic differentiation potential of TSCs were assessed.

Results. Our results showed that DECM from young TSCs enhanced the proliferation and tenogenic differentiation of aged TSCs. Moreover, the senescence-associated β-galactosidase activity of aged TSCs was decreased by young DECM. After being cultured on the young DECM, the expression of stem cell markers by aged TSCs was more extensive. The young DECM preserved stem cell properties of aged TSCs.

Conclusions. Taken together, the impaired capacity of aged TSCs can be rejuvenated by exposure to young DECM. The positive results in our study suggest that young TSC-derived DECM may provide a novel approach for the prevention and treatment of age-dependent tendon disorders.

Key words: proliferation, aging, extracellular matrix, differentiation, tendon

DOI
10.17219/acem/75503

Tendon disorders, such as injury and tendinopathy, pose a critical challenge for sports medicine. It was suggested that the rupture of a tendon often occurs in aged tendons which are weakened by overuse or degeneration.[1] Age-related changes in the structural and functional properties of tendon tissue contribute to the progressive degeneration and an increased risk of injury.[2,3] Tendon injuries and tendinopathy cause physical frailty in old age with a general reduction in quality of life. There are changes in the number and activity of tendon cells observed with aging.[4,5] Moreover, aging has been postulated to exert a negative effect on the proliferation and synthesis of tenocytes.[6] Thus, tendon injuries in a geriatric patient are believed to regenerate more slowly.

The ultimate goal of treating tendon injury is to regenerate tissues. Cells in tendon tissue that produce and organize extracellular matrix (ECM) are very important in maintaining the homeostasis of tendons. More recently, it was reported that tendon tissues contain a minor population of cells with stem cell properties, called tendon stem cells (TSCs).[7,8] Moreover, the application of these stem cells has been considered a promising approach for the restoration of structure and function after tendon injury.[9,10] However, the negative effects of increased age on the properties of TSCs and tenocytes have also been reported.[5] These age-related changes in TSCs would seriously affect the regeneration of tendons.

Studies have demonstrated that TSCs need a specific microenvironment, the so-called stem cell niche, in order to keep their stemness or to orient tenogenic differentiation.[10,11] It has been reported that the structure and ECM protein expression levels in aged tendons are different from those found in young ones.[2] Recent studies have also demonstrated that the decellularized stem cell matrix can provide an appropriate niche in which adult stem cells can greatly expand, delay replicative senescence and restore their differentiation capacity.[12,13] We hypothesize that decellularized extracellular matrix (DECM) derived from young TSCs can modulate the properties of aged TSCs. Based on this hypothesis, the present study was designed to investigate the biological effect of DECM of young TSCs on the proliferation, stemness, senescence, and differentiation of aged TSCs.

Material and methods

Isolation and culture of rat

All experiments in this study were performed in accordance with the guidelines for animal research from the National Institutes of Health (Bethesda, USA) and were carried out under the Rules and Regulations of the Animal Care and Use Committee at Shanghai Jiao Tong University School of Medicine, China. Ten young (2-month-old) and 10 old (24-month-old) Sprague-Dawley male rats were used for the isolation of TSCs. Tendon stem cells were isolated from rat patellar tendons. The procedures for the isolation and culture of TSCs have been established.[8] The mid-substance of the patellar tendon was removed, cut into small sections and minced. The tissues were digested with type I collagenase (3 mg/mL; Sigma-Aldrich, St. Louis, USA) and dispase (4 mg/mL; Stem Cell Technologies, Vancouver, Canada) at 37°C for 1 h. The fragments were then passed through a 70-mm cell strainer (Becton Dickinson, Tokyo, Japan) to yield a single-cell suspension. The isolated cells were resuspended in Dulbecco's Modified Eagle Medium (DMEM), 10% fetal bovine serum (FBS), and 1% penicillin and streptomycin. After 8–10 days in culture, TSCs formed colonies on the culture plates and were collected through the local application of trypsin and mixed together as passage 0. The stem cell identities of TSCs were routinely confirmed by the expression of stem-cell-related surface markers, clonogenicity and multilineage differentiation potentials before being used in this study.

Preparation of decellularized extracellular matrix generated by young or aged tendon stem cells

Decellularized extracellular matrix was obtained using the previously described method.[14] Six-well plates were precoated with 0.2% gelatin (Sigma-Aldrich) at 37°C for 1 h and young or old TSCs at passage 2 were plated at a density of 4000 cells/cm^2. L-ascorbic acid phosphate (50 mg/mL) (Sigma-Aldrich) was added to the medium for 8 days after the cells reached 90% confluence. The deposited ECM by TSCs was incubated with 0.5% Triton X-100 (Sigma-Aldrich) containing 20 mM of ammonium hydroxide for 5 min at 37°C followed by treatment with 100 U/mL of DNase at room temperature for 1 h. Then, the matrix was stored in phosphate-buffered saline (PBS) containing antibiotics at 4°C for subsequent cell culture experiments.

Tendon stem cells grown on decellularized extracellular matrix

Aged and young TSCs at passage 2 were plated at a density of 3000 cells/cm^2 in 6-well plates coated with or without DECM. There were 4 groups, including a young TSC group, an aged TSC group, an aged TSC + aged DECM group, and an aged TSC + young DECM group. The TSCs were cultured in DMEM containing 10% FBS and antibiotics for 7 days at 37°C under 5% CO_2. The medium was changed every 3 days.

Cell proliferation assay

To assess the effect of DECM on the proliferation of aged TSCs, cell numbers were counted and the population doubling time (PDT) of each group was estimated as previously described.[8]

Senescence-associated β-galactosidase activity assay

The senescence-associated β-galactosidase activity was determined as described previously.[15] A sample of 50 mg of protein from TSCs in each group (HT) and TDSCs (CI) at P5 was used to assess the senescence-associated β-galactosidase activity by using a Pierce Mammalian β-Galactosidase Assay Kit (Thermo Scientific, Inc., Rockford, USA). Absorbances were measured at 405 nm using a plate-reading spectrophotometer.

Immunostaining of stem cell markers

Immunocytochemistry was used to examine the following stem cell markers: octamer-binding transcription factor 4 (Oct-4) and stage-specific embryonic antigen-4 (SSEA-4). The TSCs were fixed with freshly prepared 4% paraformaldehyde for 30 min and then permeabilized with 0.1% Triton X-100 (Sigma-Aldrich) for 20 min at room temperature. After being washed with PBS 3 times, they were incubated with the primary antibody monoclonal mouse anti-Oct-4 (1:350). After the cells were washed with PBS, Cy3-conjugated secondary antibody (1:500) was applied for 1 h at room temperature in the dark. For the staining of SSEA-4, the cells were fixed with 4% paraformaldehyde. Cells were then incubated with mouse anti-SSEA-4 antibody (1:350) for 2 h at room temperature. After washing, a secondary antibody (1:500) conjugated with fluorescein isothiocyanate (FITC) was applied for 1 h at room temperature in a darkened humidified chamber. Finally, the samples were washed with PBS and mounted in nuclear staining reagent Hoechst fluorochrome 33342 (1 mg/mL; Sigma-Aldrich). Each tissue section was observed under a fluorescence microscope. Twenty-five views from all 6 samples per group were obtained. Fifty cells were counted in 1 view and the percentage of stem cell marker-positive cells was analyzed for each staining.

Expression of tenogenic markers

At day 7, the cells were harvested and the expression of tenogenic markers, including tenomodulin (Tnmd) and scleraxis (Scx), were evaluated using quantitative reverse transcription polymerase chain reaction (qRT-PCR). The mRNA was reverse transcribed to cDNA using a First Strand Kit (Invitrogen, Carlsbad, USA). The qRT-PCR was carried out with a QuantiTect SYBR Green RT-PCR kit (Qiagen, Hilden, Germany). Two microliters of total cDNA from each sample were amplified in a 25-μL reaction mixture. The cycling conditions were as follows: denaturation at 65°C for 5 min, snap cooling at 4°C for 1 min, 42°C for 50 min, and finally at 72°C for 15 min. The expression of the target gene was normalized to that of the glyceraldehyde-3-phosphate dehydrogenase (GAPDH). The relative gene expression was calculated using the $2^{\Delta CT}$ formula.

Rat-specific primers were used for *Tnmd*, *Scx* and *GAPDH* as follows: 5'-CCATGCTGGATGAGAGAGGTTAC-3' (forward) and 5'CACAGACCCTGCGGCAGTA-3' (reverse) for *Tnmd*; 5'-AACACGGCCTTCACTGCGCTG-3' (forward) and 5'-CAGTAGCACGTTGCCCAGGTG-3' (reverse) for *Scx*; 5'-TGACTCTACCCACGGCAAGTTCAA-3' (forward) and 5'-ACGACATACTCAGCACCAGCATCA-3' (reverse) for *GAPDH*.

Statistical analysis

The data is presented as mean ± standard deviation (SD). One-way analysis of variance (ANOVA) with the Student-Newman-Keuls test was used for multiple comparisons. Statistical analyses were carried out with SPSS v. 11.0 statistical package (IBM Corp., Armonk. USA). All p-values <0.05 were accepted as statistically significant.

Results

Proliferative capacity of tendon stem cells

The proliferation of TSCs was determined by PDT. The young TSCs grew faster than the aged TSCs when cultured on a plastic surface. Decellularized extracellular matrix from young and aged donors enhanced the proliferation of aged TSCs. It was observed that the PDT of TSCs was significantly lower in the aged TSC + young DECM and aged TSC + aged DECM groups compared to the aged TSC group (Fig. 1; $p < 0.05$). These findings indicated that aging can decrease the proliferation of TSCs and that this feature could be altered by exposure to DECM. Unexpectedly, we found that there was no significant difference in the PDT of aged TSCs after culturing on young DECM and aged DECM.

Senescence-associated β-galactosidase activity assay

There was significantly higher β-galactosidase activity in aged TSCs compared to young TSCs when cultured on plastic (Fig. 2; $p < 0.05$), indicating that the β-galactosidase activity increased with age. Aged TSCs cultured on young DECM exhibited significantly lower levels of β-galactosidase activity when compared to those cultured on aged DECM or on plastic (Fig. 2; $p < 0.05$).

Stem cell marker expression

Immunofluorescence staining for Oct-4 and SSEA-1 showed that the fluorescent density of stem cell markers was more extensive in young TSCs (Fig. 3,4). There were significant differences in the percentage of positive cells among the 2 groups (Fig. 5; $p < 0.05$). These findings

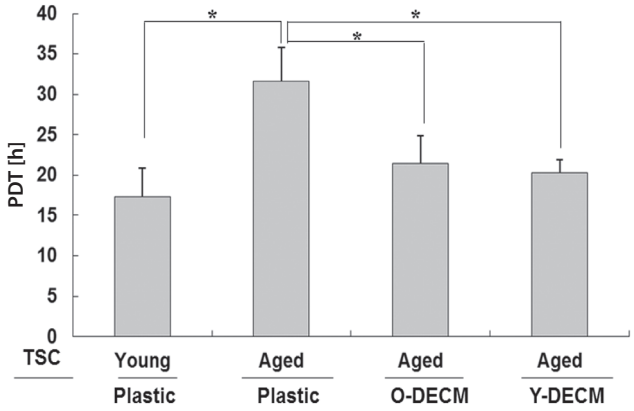

Fig. 1. The population doubling time (PDT) of TSCs on plastic, Y-DECM and O-DECM. The PDT of aged TSCs on plastic was significantly higher when compared to other groups

* p < 0.05; Y-DECM – young decellularized extracellular matrix; O-DECM – old decellularized extracellular matrix; TSCs – tendon stem cells.

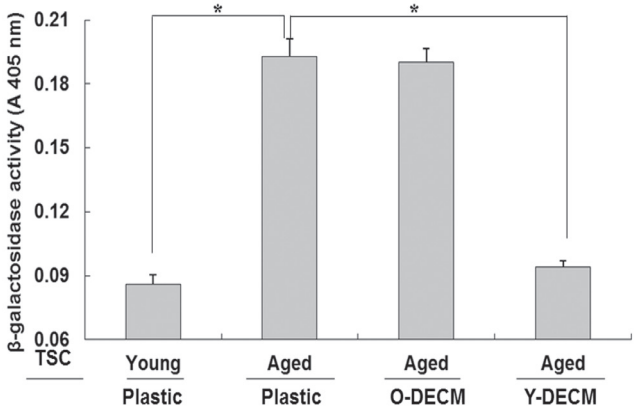

Fig. 2. The senescence-associated β-galactosidase activities of TSCs in different groups. The Y-DECM significantly decreased the β-galactosidase activity of aged TSCs

* p < 0.05; Y-DECM – young decellularized extracellular matrix; O-DECM – old decellularized extracellular matrix; TSCs – tendon stem cells.

suggest that the decreased stem cell marker expression in aged TSCs may contribute to reduced stemness with age. After being cultured on young DECM, the expressions of Oct-4 and SSEA-1 by aged TSCs were more extensive than those expressed by aged TSCs cultured on aged DECM or on plastic.

Tendon-related marker expression

The results indicated that the expression of tendon lineage-specific genes, *Tnmd* and *Scx*, were lower in aged TSCs than in young cells (Fig. 6; $p < 0.05$). It was also found that expressions of *Tnmd* and *Scx* were significantly enhanced in the aged TSC + young DECM group when compared to that of the aged TSCs cultured on aged DECM or on plastic (Fig. 6; $p < 0.05$).

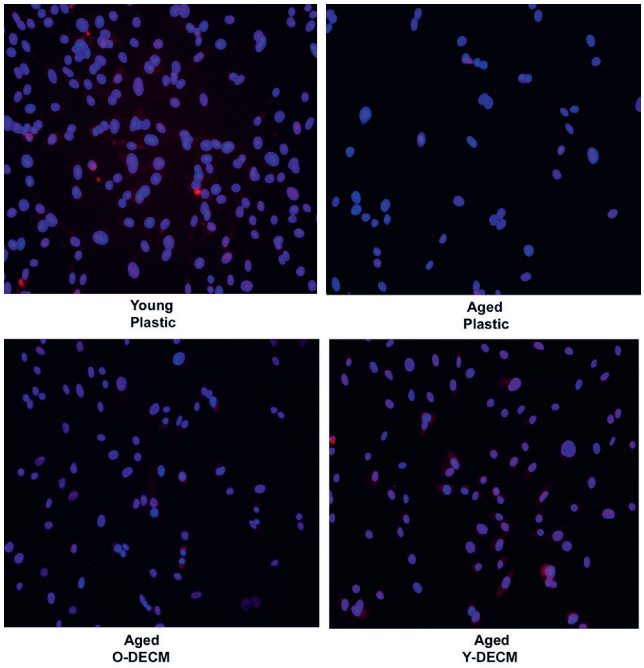

Fig. 3. The expression of octamer-binding transcription factor 4 (Oct-4) was evaluated by immunofluorescence assay. The density of Oct-4 in young TSCs was higher than in aged TSCs. After being cultured on the Y-DECM, the expression of Oct-4 by aged TSCs was upregulated. Original magnification is ×200

Y-DECM – young decellularized extracellular matrix; O-DECM – old decellularized extracellular matrix; TSCs – tendon stem cells.

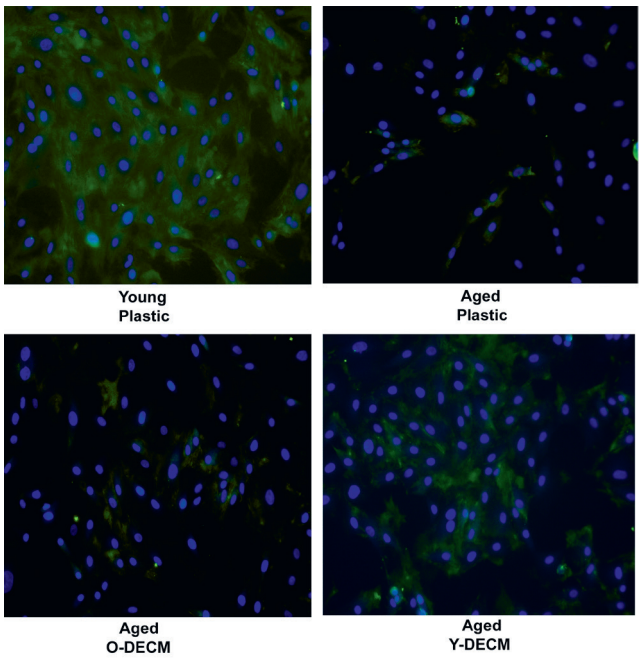

Fig. 4. The expression of stage-specific embryonic antigen-4 (SSEA-4) was evaluated by immunofluorescence assay. The density of SSEA-1 in young TSCs was higher than in aged TSCs. After being cultured on the Y-DECM, the expression of SSEA-1 by aged TSCs was upregulated. Original magnification is ×200

Y-DECM – young decellularized extracellular matrix; O-DECM – old decellularized extracellular matrix; TSCs – tendon stem cells.

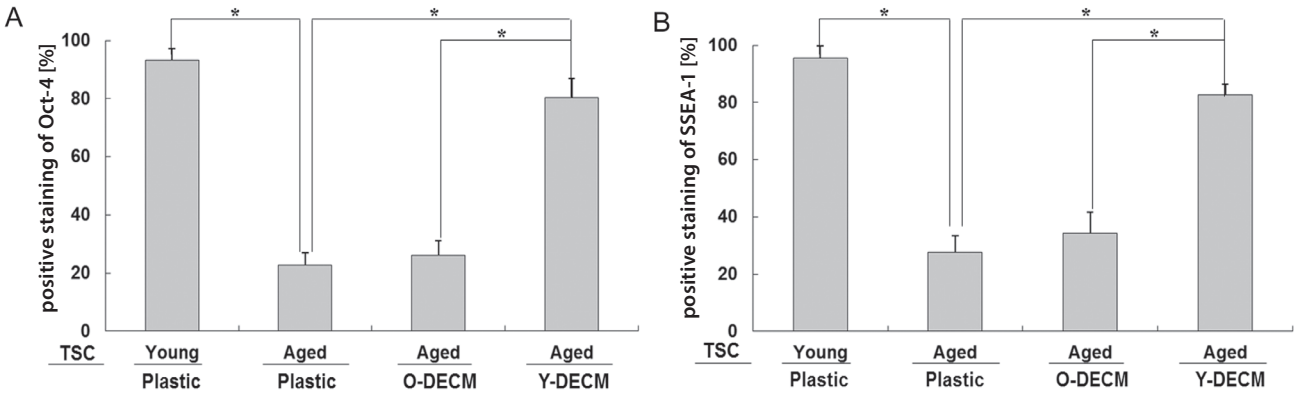

Fig. 5. The percentage of stem cell marker-positive cells. There were significant differences in the percentage of stem cell marker-positive cells among young and aged TSCs. After being cultured on the Y-DECM, the percentages of octamer-binding transcription factor 4 (Oct-4) (A) and stage-specific embryonic antigen-4 (SSEA-4) (B) in aged TSCs were increased

* $p < 0.05$; Y-DECM – young decellularized extracellular matrix; O-DECM – old decellularized extracellular matrix; TSCs – tendon stem cells.

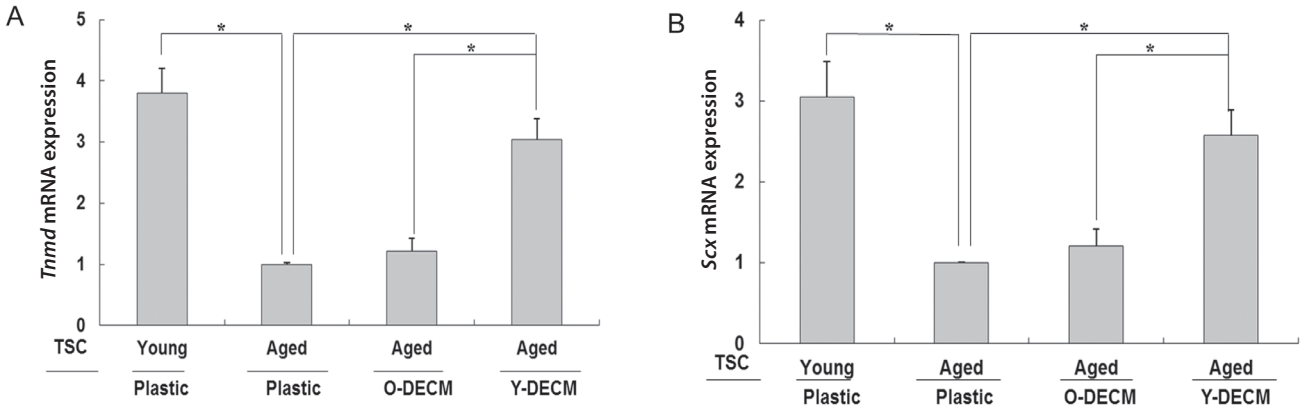

Fig. 6. The expression of tenocyte-related genes was evaluated by quantitative reverse transcription polymerase chain reaction (qRT-PCR). The mRNA of *Tnmd* (A) and *Scx* (B) were significantly upregulated in TSCs after treatment with Y-DECM. The expression level was normalized to that of glyceraldehyde-3-phosphate dehydrogenase (GAPDH).

* $p < 0.05$; Y-DECM – young decellularized extracellular matrix; O-DECM – old decellularized extracellular matrix; TSCs – tendon stem cells.

Discussion

Tendon stem cells can form a colony, self-renew and differentiate into multiple cell lineages.[7,8] Moreover, as tendon-specific stem cells, they can differentiate into tenocytes by default.[16] As a result of these capabilities, TSCs play an important role in the continuous maintenance and regeneration of injured tendons.[9,10] Recently, it was reported that the number and function of TSCs decrease with advancing age, which may affect the structure and function of tendon tissue.[5] It remains to be determined whether these age-related changes can be reversed. Thus, we examined whether properties of aged TSCs would be altered by exposure to ECM produced by young TSCs.

In this study, we showed that the deleterious effect of aging on the TSCs was remarkable when the cells were cultured on plastic. As previously reported, a higher proliferation potential of TSCs from young donors was observed when compared to that of aged donors.[5] It also corroborated the results obtained from periodontal ligament stem cells and tenocytes.[6,17] These results suggest a significant impact of aging on TSCs, ligament stem cells and tenocytes in terms of proliferative activity and differentiation potential. In addition to the effect of donor age on the proliferation of TSCs, we investigated its effects on the senescence-associated β-galactosidase activity. As a marker of aging, increased β-galactosidase activity was observed in aged TSCs. However, the surface expressions of Oct-4 and SSEA-4 in aged TSCs were downregulated in our study. These may reduce the pool of TSCs for the regeneration of aged tendons after injury. It was also observed that tenogenic activity was reduced in aged donors. This result was supported by the tendon lineage-specific gene expression, which revealed age-related declines in the expression of *Tnmd* and *Scx*. The loss of tenogenic differentiation potential with aging was also reported in a previous study.[5] This implies that there are fewer stem cells with tenogenic potential in aged donors than in younger donors.

Tendon stem cells are surrounded by ECM in tendon tissue, which form a microenvironment or niche. Recent studies have demonstrated the importance of extrinsic ECM

on the rejuvenation of stem cells.[13,18] For example, aged mesenchymal stem cells can continue to function without any decline in function when cultured on a young ECM.[18] These findings made us question whether aged TSCs can be influenced by the ECM obtained from young donors. In this study, we successfully developed DECM scaffold using TSCs in vitro. It was found that DECM prepared from young and aged TSCs significantly promoted the proliferation of aged TSCs. It indicated that DECM of TSCs might provide a proper microenvironment that can mimic the niche that TSCs reside in. This feature of ECM obtained from TSCs is similar to a recent finding that ECM deposited by human bone marrow stromal cells (BMSCs) facilitates the proliferation of BMSCs.[19]

Our study also provided evidence that young DECM preserved the stem cell properties of aged TSCs. We measured several stem cell markers such as Oct-4 and SSEA-4; Oct-4 is essential for maintaining undifferentiated pluripotent stem cells, while SSEA-4, originally identified as an early embryonic glycolipid antigen, is a molecule characteristic of undifferentiated pluripotent human stem cells.[20,21] Our data revealed that the proportion of those positive cells was significantly higher in aged TSCs when treated with young DECM. Moreover, the senescence-associated β-galactosidase activity of aged TSCs was decreased by young DECM. It was suggested that high quality of stem cells from aged TSCs was enriched by exposure to a young DECM.

In parallel with determining the effects of young DECM on cell proliferation and stemness, we also examined the effect of young DECM on the tenogenic differentiation potential of aged TSCs. Young DECM had significantly increased the mRNA expression of tenogenic markers, such as *Tnmd* and *Scx*. Our data provided evidence that young DECM enhanced the tenogenic differentiation potential of aged TSCs. Together, this data demonstrates that young DECM is capable of rejuvenating the altered biological activities of aged TSCs.

It was reported that compositions of ECM deposited by young and old cells are different.[18] Another study also suggested that tissue-specific stem cells could retain their intrinsic capacity even when old, but the aged niche in which stem cells reside inhibit the signal pathway activation of these cells.[22] Thus, aged TSCs, as a surrounding environment, may be the major determinant causing aging of cells.[18] The composition of DECM from young or aged TSCs should be different. However, we did not compare the composition of these 2 ECMs in this study. Moreover, a signal mechanism might contribute to the rejuvenation of aged TSCs by young DECM. Further studies are required to investigate these problems.

Conclusions

We have shown that the aging process induces senescence and a decline in the proliferation, stemness and tenogenic differentiation of TSCs. Moreover, the impaired capacity of aged TSCs can be improved by exposure to young DECM, thereby improving the effectiveness of aged TSCs. The positive results of our study suggest that the use of young DECM could be promising in the prevention and treatment of age-dependent tendon disorders.

References

1. Couppé C, Hansen P, Kongsgaard M, et al. Mechanical properties and collagen cross-linking of the patellar tendon in old and young men. *J Appl Physiol (1985).* 2009;107(3):880–886.
2. Kostrominova TY, Brooks SV. Age-related changes in structure and extracellular matrix protein expression levels in rat tendons. *Age (Dordr).* 2013;35(6):2203–2214.
3. Klatte-Schulz F, Pauly S, Scheibel M, et al. Influence of age on the cell biological characteristics and the stimulation potential of male human tenocyte-like cells. *Eur Cell Mater.* 2012;24:74–89.
4. Dudhia J, Scott CM, Draper ER, Heinegård D, Pitsillides AA, Smith RK. Aging enhances a mechanically-induced reduction in tendon strength by an active process involving matrix metalloproteinase activity. *Aging Cell.* 2007;6(4):547–556.
5. Zhou Z, Akinbiyi T, Xu L, et al. Tendon-derived stem/progenitor cell aging: Defective self-renewal and altered fate. *Aging Cell.* 2010;9(5):911–915.
6. Tsai WC, Chang HN, Yu TY, et al. Decreased senescence-inhibited gene and up-regulation of p27. *J Orthop Res.* 2011;29(10):1598–1603.
7. Tan Q, Lui PP, Rui YF. Effect of in vitro passaging on the stem cell-related properties of tendon-derived stem cells-implications in tissue engineering. *Stem Cells Dev.* 2012;21(5):790–800.
8. Bi Y, Ehirchiou D, Kilts TM, et al. Identification of tendon stem/progenitor cells and the role of the extracellular matrix in their niche. *Nat Med.* 2007;13(10):1219–1227.
9. Chen L, Dong SW, Liu JP, Tao X, Tang KL, Xu JZ. Synergy of tendon stem cells and platelet-rich plasma in tendon healing. *J Orthop Res.* 2012;30(6):991–997.
10. Ni M, Rui YF, Tan Q, et al. Engineered scaffold-free tendon tissue produced by tendon-derived stem cells. *Biomaterials.* 2013;34(8):2024–2037.
11. Zhang J, Li B, Wang JH. The role of engineered tendon matrix in the stemness of tendon stem cells in vitro and the promotion of tendon-like tissue formation in vivo. *Biomaterials.* 2011;32(29):6972–6981.
12. Pei M, He F. Extracellular matrix deposited by synovium-derived stem cells delays replicative senescent chondrocyte dedifferentiation and enhances redifferentiation. *J Cell Physiol.* 2012;227(5):2163–2174.
13. He F, Pei M. Rejuvenation of nucleus pulposus cells using extracellular matrix deposited by synovium-derived stem cells. *Spine.* 2012;15(37):459–469.
14. Li J, Pei M. Optimization of an in vitro three-dimensional microenvironment to reprogram synovium-derived stem cells for cartilage tissue engineering. *Tissue Eng Part A.* 2011;17(5–6):703–712.
15. Rui YF, Lui PP, Wong YM, Tan Q, Chan KM. Altered fate of tendon-derived stem cells isolated from a failed tendon-healing animal model of tendinopathy. *Stem Cells Dev.* 2013;22(7):1076–1085.
16. Zhang J, Wang JH. Characterization of differential properties of rabbit tendon stem cells and tenocytes. *BMC Musculoskelet Disord.* 2010;11:10. doi: 10.1186/1471-2474-11-10
17. Zheng W, Wang S, Ma D, Tang L, Duan Y, Jin Y. Loss of proliferation and differentiation capacity of aged human periodontal ligament stem cells and rejuvenation by exposure to the young extrinsic environment. *Tissue Eng Part A.* 2009;15(9):2363–2371.
18. Sun Y, Li W, Lu Z, et al. Rescuing replication and osteogenesis of aged mesenchymal stem cells by exposure to a young extracellular matrix. *FASEB J.* 2011;25(5):1474–1485.
19. Pei M, He F, Kish VL. Expansion on extracellular matrix deposited by human bone marrow stromal cells facilitates stem cell proliferation and tissue-specific lineage potential. *Tissue Eng Part A.* 2011;17(23–24):3067–3076.
20. Pesce M, Scholer HR. Oct-4: Gatekeeper in the beginnings of mammalian development. *Stem Cells.* 2001;19(4):271–278.
21. Gang EJ, Bosnakovski D, Figueiredo CA, Visser JW, Perlingeiro RC. SSEA-4 identifies mesenchymal stem cells from bone marrow. *Blood.* 2007;109(4):1743–1751.
22. Conboy IM, Conboy MJ, Wagers AJ, Girma ER, Weissman IL, Rando TA. Rejuvenation of aged progenitor cells by exposure to a young systemic environment. *Nature.* 2005;433(7027):760–764.

All-trans retinoic acid effectively reduces atheroma plaque size in a rabbit model of high-fat-induced atherosclerosis

Leila Zarei[1,A,B,D,F], Mehran Bahrami[2,B–D], Negin Farhad[2,B,D], Seyyed Meysam Abtahi Froushani[3,B,D], Ata Abbasi[4,A,C–F]

[1] Solid Tumor Research Center, Urmia University of Medical Sciences, Iran
[2] Student Research Committee, Urmia University of Medical Sciences, Iran
[3] Department of Microbiology, Veterinary Faculty, Urmia University, Iran
[4] Department of Pathology, Faculty of Medicine, Urmia University of Medical Sciences, Iran

A – research concept and design; B – collection and/or assembly of data; C – data analysis and interpretation;
D – writing the article; E – critical revision of the article; F – final approval of the article

Advances in Clinical and Experimental Medicine, ISSN 1899-5276 (print), ISSN 2451-2680 (online) *Adv Clin Exp Med*. 2018;27(12):1631–1636

Address for correspondence
Ata Abbasi
E-mail: aabbasi@alumnus.tums.ac.ir

Funding sources
Research grant No. 1886 from Urmia University of Medical Sciences, Iran

Conflict of interest
None declared

Received on December 9, 2016
Reviewed on May 5, 2017
Accepted on June 7, 2017

Abstract

Background. Atherosclerosis (AS) is one of the most prevalent causes of death around the world. Since there are different types of risk factors, different types of medications focus on preventing atheromas and plaques from establishing or on preventing established plaques from growing.

Objectives. The aim of this study was to evaluate the effect of all-trans retinoic acid (atRA) on AS in a rabbit model of fat-induced AS.

Material and methods. Atherosclerosis was induced by a high-fat diet (HFD) for 75 days. Thirty rabbits were randomly divided into 5 groups. Group 1 was the negative control group and received a normal diet. The animals in the other groups were fed a HFD. Group 2 (the AS positive control group) received no drugs, Group 3 received atorvastatin orally (20 mg/kg/day), Group 4 received atRA (5 mg/kg/day, orally), and Group 5 received both drugs. All medications were started on day 45 and continued until the end of the study. Fasting blood samples were obtained for lipid profile evaluation. The aorta sections were evaluated for maximum wall and intima thickness.

Results. Oral administration of atRA, atorvastatin or their combination significantly improved serum lipid profile ($p < 0.001$). Atorvastatin and atRA significantly decreased serum total cholesterol and LDL-cholesterol levels in HFD ($p < 0.001$). No difference was found in serum HDL-cholesterol levels among the studied groups. The HFD group (Group 2 – positive control) showed significant intima irregularities with fat deposition and foamy macrophage accumulation (atheroma). Administration of atRA and atorvastatin significantly decreased the size of atherosclerotic plaques (intima thickness). The maximum vessel wall and intima thickness were significantly decreased after atRA and atorvastatin administration ($p < 0.001$). No difference was found between atRA and atorvastatin effectiveness, but combination therapy significantly decreased AS size in comparison to using either of the drugs alone ($p < 0.001$).

Conclusions. In reducing AS plaque size, atRA is as effective as atorvastatin. Additionally, the combination therapy of atRA and atorvastatin decreased AS size much more effectively, showing their synergistic effect. atRA can also improve the serum lipid profile.

Key words: atherosclerosis, high-fat diet, all-trans retinoic acid

DOI
10.17219/acem/74552

Introduction

Atherosclerosis (AS) is one of the most prevalent causes of death around the world.[1] The formation and progression of atherosclerosis is a long-term process which begins with an accumulation of fat within the vessel walls. The fat accumulation triggers an inflammatory process as well as platelet activation and accumulation, which subsequently leads to the formation of an atherosclerotic plaque.[2,3] There are some traditional risk factors involved in the initiation or progression of plaques. Hypertension, smoking, diabetes mellitus (DM), obesity, hyperlipidemia, and infections are some well-known risk factors.[1,4] Since there are different types of risk factors, different types of medications are used, but most of therapy methods have focused on preventing atheromas and plaques from establishing and on preventing established plaques from growing.

All-trans retinoic acid (atRA) is derived from vitamin A through an enzymatic process.[5] It has antioxidant activity and is involved in cellular development, growth and differentiation.[6–8] It is also known that atRA acts as an anti-inflammatory agent and can inhibit platelet function.[2] Recent studies have uncovered some protective effects of atRA on the cardiovascular system.[9,10] It has also been shown that atRA and its derivatives can inhibit DM development, and decrease body weight and lipid production by regulating fat metabolism in various organs.[5,9–12] Considering the effects of atRA on DM and lipid metabolism, as well as its anti-inflammatory and anti-platelet activation effect, we hypothesized that atRA can be useful in the treatment of AS.

The aim of this study was to evaluate the effect of atRA on AS in a rabbit model of fat-induced AS and to compare the results with atorvastatin as a control drug.

Material and methods

Animals

Thirty male New Zealand rabbits were included in the present study. All animals were housed for 1 week in a temperature- and humidity-controlled vivarium (22 ±2°C, 30–60%) with a light/dark cycle of 10 h/14 h and access to a standard diet and water.

All animal procedures were performed in accordance with the Guide for the Care and Use of Laboratory Animals (National Institutes of Health (NIH) US publication No. 85–23, revised 1985). All experiments were performed in agreement with the ethical considerations recommended by the Pasteur Institute of Iran in Tehran, and the study protocol was reviewed and approved by the Ethical Committee of the Urmia University of Medical Sciences, Iran.

Drug administration

The rabbits were randomly divided into 5 groups. Each group contained 6 rabbits. Group 1 was treated as a negative control group and was fed a normal diet for 75 days. The animals in Groups 2–5 were fed a high-cholesterol (fat) diet (HFD; 1% of body weight) for 75 days. Group 2 served as the AS positive control group and was not treated with any drugs, Group 3 received atorvastatin orally (20 mg/kg/day) starting on day 45 for 30 days (until the end of the study), Group 4 received atRA (5 mg/kg/day, orally) starting on day 45 for 30 days (until the end of the study), and Group 5 received both atorvastatin (10 mg/kg/day) and atRA (2.5 mg/kg/day) starting on day 45 for 30 days (until the end of the study).

At the end of the experiment, the rabbits fasted for 12 h prior to anesthesia and peripheral blood samples were obtained from the marginal vein of their ear. Then, serum samples were separated and analyzed for total cholesterol (TC), triglyceride (TG), high-density lipoprotein (HDL), and low-density lipoprotein (LDL) counts. Finally, the rabbits were sacrificed and the aorta of each rabbit was carefully resected as previously described. [13]

Biochemical measurement

Blood samples were centrifuged at 3000 rpm for 10 min and serum samples were separated. Serum levels of TC, TG, LDL, and HDL were measured using an autoanalyzer (BT 4500; Biotecnica Instruments, Rome, Italy).

Tissue preparation

The aorta, including the ascending and descending parts, was excised and totally immersed in phosphate buffered formalin (PBF) for at least 24 h for fixation. After

Table 1. Serum lipid levels in the studied groups [mg/dL]

Serum	Group 1 (negative control)	Group 2 (positive control)	Group 3 (atorvastatin)	Group 4 (atRA*)	Group 5 (atRA + atorvastatin)	p-value**
TC	36.5 ±20	1,966.2 ±330*	147.5 ±102	621 ±259	153.8 ±61	<0.001
TG	136 ±44	68.5 ±45	75.5 ±47	145.2 ±73	54.3 ±30	>0.05
HDL	15 ±1.5	32 ±5	39.2 ±20	65 ±34	30.6 ±5	>0.05
LDL	13 ±5	916 ±42	102.7 ±100	462.5 ±99	119 ±32	<0.001

TC – total cholesterol; TG – triglyceride; HDL – high-density lipoprotein; LDL – low-density lipoprotein; * atRA – all-trans retinoic acid; ** p-value <0.05 is significant.

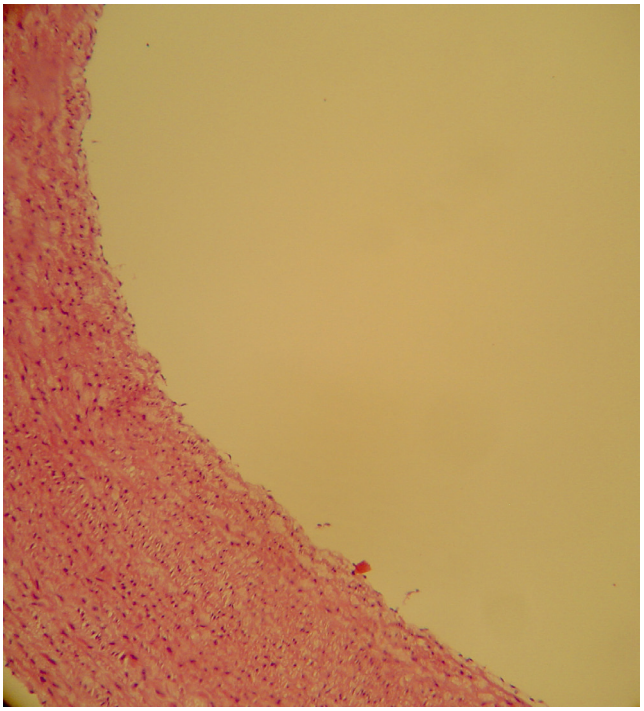

Fig. 1A. Aortic tissue (muscular wall) of a rabbit not receiving a high-fat diet (HFD) (negative control – Group 1) (hematoxylin and eosin (H&E) staining, ×10 magnification)

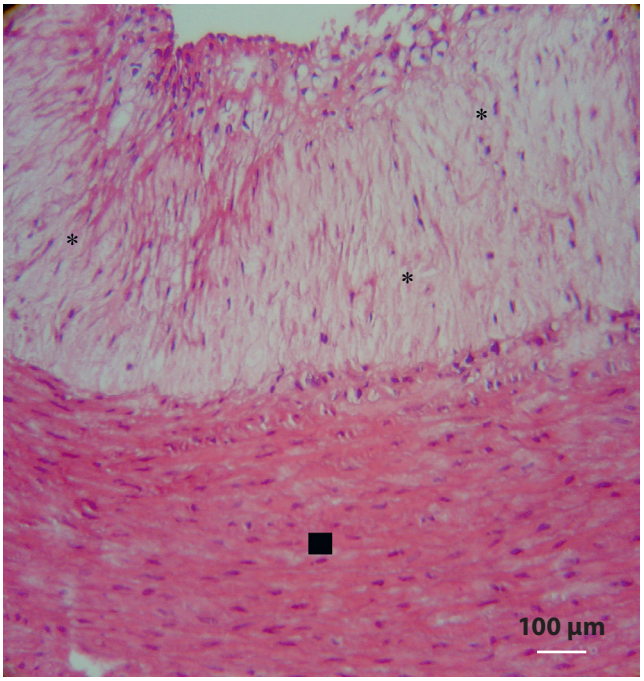

Fig. 1B. Aortic tissue of a rabbit receiving a high-fat diet (HFD) without any drug administration (positive control – Group 2). A large atherosclerotic plaque composed of foamy macrophages (clearly stained area marked with *) is seen attached to the vessel wall (marked with a black square), (hematoxylin and eosin (H&E) staining, ×40 magnification)

fixation, the samples were embedded in paraffin. Then, 5 µm sections were obtained from each paraffin block and stained with hematoxylin and eosin (H&E). The maximum wall thickness of the aorta and the intima thickness

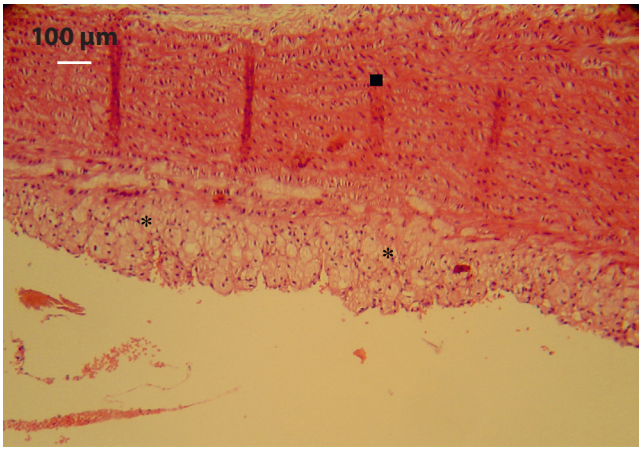

Fig. 1C. Aortic tissue of a rabbit treated with atorvastatin (Group 3), with smaller atherosclerotic plaque (area marked with *) compared to the positive control (Group 2) in Fig. 2. The vessel wall is marked with a black square (hematoxylin and eosin (H&E) staining, ×20 magnification)

Fig. 1D. Aortic tissue of a rabbit receiving atRA (Group 4), with smaller atherosclerotic plaque (area marked with *), compared to the positive control (Group 2) in Fig. 2. The vessel wall is marked with a black square. The black circle shows the vessel serosa (hematoxylin and eosin (H&E) staining, ×20 magnification)

(plaque size) of each sample were measured using an image evaluation program (Optika, Vittorio Veneto, Italy) and were compared with other samples.

Statistical analysis

The results are expressed as mean ± standard error of the mean (SEM). Statistical analysis was performed using SPSS v. 16.0 (SPSS Inc., Chicago, USA). Statistical evaluation of the data was performed using an analysis of variance (ANOVA). The normality of data was evaluated with the Kolmogorov-Smirnov test; p-values <0.05 were considered statistically significant.

Results

Serum lipid profile

Levels of LDL, HDL, TG, and TC were significantly higher in the HFD positive control group (Group 2) compared to the negative control group (Group 1) ($p < 0.001$). Our data showed that oral administration of atRA or atorvastatin, or their combination, significantly decreased TC and LDL serum levels ($p < 0.001$). Additionally, we found that atorvastatin reduced serum TC and LDL levels more effectively than atRA ($p < 0.001$), but their combination therapy showed no significant difference in effectiveness compared to atorvastatin alone ($p = 0.21$). No statistical difference was found in serum HDL levels among the studied groups. The details of the serum lipid profiles are included in Table 1.

Histopathological evaluation

The sample from each rabbit's aorta was evaluated using a light microscope (Olympus BH-21; Olympus, Tokyo, Japan). In the negative control group no atheromas were identified, but the HFD group (Group 2 – positive control) showed significant irregularities on the inner surface of the aorta (intima), with fat deposition and foamy macrophage accumulation (atheroma). Oral administration of atRA and atorvastatin significantly decreased the size of the atherosclerotic plaques and intima thickness (Fig. 1A–D, 2). The maximum vessel wall and intima thickness were measured in each group and showed a significant decrease after atRA, atorvastatin or their combined administration ($p < 0.001$). No difference was found between atRA and atorvastatin in reducing AS size, but the combination therapy of atRA and atorvastatin significantly decreased AS size in comparison to using either drug alone ($p < 0.001$), (Fig. 3A, 3B).

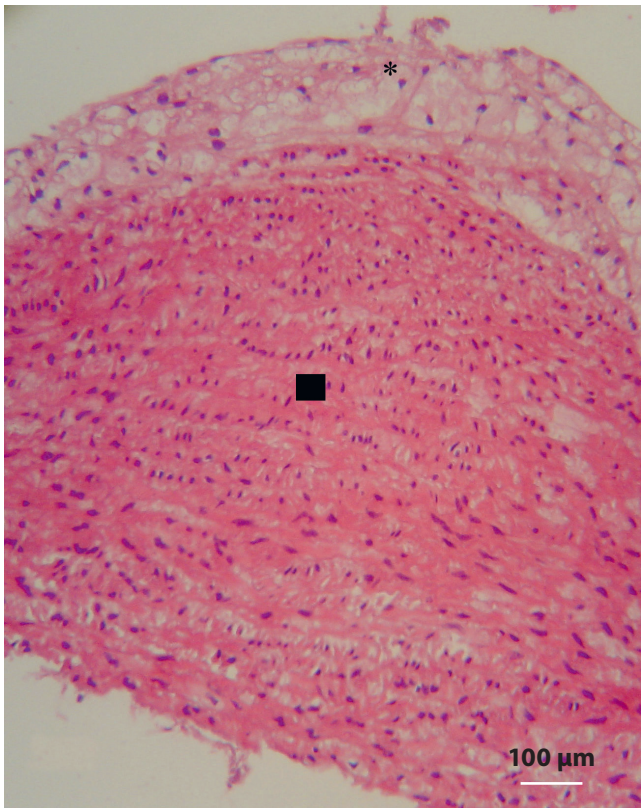

Fig. 2. Aortic tissue of a rabbit receiving both atorvastatin and atRA (Group 5). There is a small plaque (area marked with *) attached to the vessel wall (area marked with a black square) (hematoxylin and eosin (H&E) staining, ×40 magnification)

Discussion

Derived from vitamin A, atRA is involved in some cell regulatory processes, including cell migration, healing and differentiation.[2,13] Recent studies have revealed the effects of atRA on the cardiovascular system. It was shown that atRA can inhibit restenosis of a coronary artery after angioplasty.[14] In this study, we demonstrated that oral administration of atRA in a rabbit model of fat-induced AS improved the serum lipid profile and also decreased the size of atherosclerotic plaques. We observed similar results with atorvastatin, which was used in our study as a control drug. Atorvastatin is one of the main drugs widely used to lower serum lipids levels in clinical practice.[9,15–17]

In this study, we found atRA very effective in decreasing the size of AS. Although we found no superiority for atRA over atorvastatin in reducing AS, there are some studies which have shown that atRA is much more effective than atorvastatin.[2] The benefits of atRA can be related to the following mechanisms: reducing lipotoxicity-induced oxidative stress, inhibiting the production of reactive oxygen species (ROS), enhancing fatty acid oxidation, activating macrophages, reducing inflammation, and inhibiting coagulatory factors.[2,18–22] As a novel finding, we found that combination therapy of atRA and atorvastatin decreased AS size more effectively than administering either one alone. These findings suggest that atRA and atorvastatin act through different mechanisms and that their combination therapy has a synergistic effect on AS treatment.

We also found that atRA can reduce serum TC and LDL-cholesterol levels, although we found atorvastatin to be more effective in reducing serum TC and LDL-cholesterol levels than atRA. We also found no difference between atorvastatin and its combination therapy with atRA in lowering serum TC and LDL-cholesterol levels. These findings are in line with other studies on this topic.[2] We also found no differences in serum HDL-cholesterol levels in the compared groups.

Our study had some limitations. We did not explore the underlying mechanisms through which atRA could reduced atheroma size or serum lipid levels. Some studies have explored the role of inflammation and stated that atherosclerosis is an inflammatory process.[23] Others have shown that macrophage activation by retinoic acid

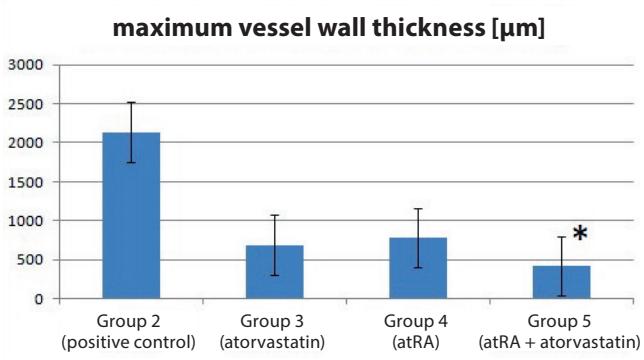

Fig. 3A. Aortic maximal wall thickness in rabbits. The wall thickness analysis showed that all-trans retinoic acid (atRA) and atorvastatin can both reduce the wall thickness and that their combination therapy had the most effective results ($p < 0.001$). There was no difference in effectiveness between atRA and atorvastatin, but as this figure shows ($p = 0.3$), combination therapy showed a significant difference in effectiveness with both atRA and atorvastatin (* $p < 0.001$)

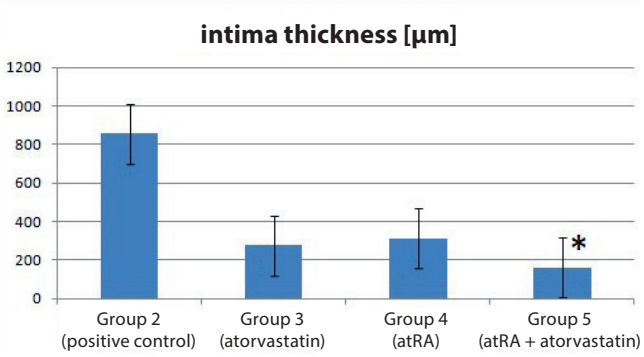

Fig. 3B. Aortic intimal thickness. The results were similar to wall thickness analysis as both all-trans retinoic acid (atRA) and atorvastatin significantly decreased the intima thickness ($p < 0.001$). Combination therapy decreased the intima thickness more effectively than either of the drugs alone (* $p < 0.001$). No difference in effectiveness was found between atRA and atorvastatin ($p = 0.24$)

receptors, which leads to improved antiapoptotic activity of the macrophages, can increase removal of apoptotic cells in AS plaques.[20] In another study by Bilbija et al., an overexpression of retinoic acid target genes was shown in coronary artery disease (CAD).[24] Bilbija et al. also reported that atRA has antiproliferative effects on cardiomyocytes and cardiofibroblasts and concluded that the antiproliferative effects of atRA may be beneficial because it may be used to delay cardiomyocyte remodeling, reduce restenosis and preserve the functions of the cardiovascular system.[24] But in none of the related studies are the underlying signal transduction pathways, which lead to AS reduction and inhibition, clearly defined.

We found that atRA can reduce AS plaque size as effectively as atorvastatin. Additionally, their combination therapy improved their power and decreased AS size much more effectively. Our study is a novel experiment which studied the combination effect of atRA and atorvastatin on both AS and serum lipid profile. This combination effect has not been evaluated in any other study. We found that combined administration of atRA and atorvastatin had a synergistic effect only in reducing AS plaque size, but not in lowering serum lipids levels. This finding may suggest a mechanism other than lowering serum lipids levels in reducing AS plaque size. We also showed a lipid-lowering effect for atRA, although it was less effective than atorvastatin. Our results nominate atRA as a potential therapeutic agent in the treatment of AS and subsequent CAD. We suggest performing further studies to find out other therapeutic and adverse effects of atRA, as well as its mechanism of action, the optimal dosage and the route of administration. This may lead to its use in a combination therapy with statins in patients with CAD to better control the disease and reduce ischemic attacks in future.

References

1. Rezaee-Zavareh MS, Tohidi M, Sabouri A, Ramezani-Binabaj M, Sadeghi-Ghahrodi M, Einollahi B. Infectious and coronary artery disease. *ARYA Atheroscler.* 2016;12(1):41–49.
2. Zhou B, Pan Y, Hu Z, et al. All-trans-retinoic acid ameliorated high fat diet-induced atherosclerosis in rabbits by inhibiting platelet activation and inflammation. *J Biomed Biotechnol.* 2012;2012:259693.
3. Lusis AJ. Atherosclerosis. *Nature.* 2000;407(6801):233–241.
4. Talavera-Garcia E, Delgado-Lista J, Garcia-Rios A, et al. Influence of obesity and metabolic disease on carotid atherosclerosis in patients with coronary artery disease (CordioPrev Study). *PLoS One.* 2016;11(4):e0153096.
5. Pellegrini C, Columbaro M, Capanni C, et al. All-trans retinoic acid and rapamycin normalize Hutchinson Gilford progeria fibroblast phenotype. *Oncotarget.* 2015;6(30):29914–29928.
6. Swift J, Ivanovska IL, Buxboim A, et al. Nuclear lamin-A scales with tissue stiffness and enhances matrix-directed differentiation. *Science.* 2013;341(6149):1240104.
7. Jiang SJ, Campbell LA, Berry MW, Rosenfeld ME, Kuo CC. Retinoic acid prevents *Chlamydia pneumoniae*-induced foam cell development in a mouse model of atherosclerosis. *Microbes Infect.* 2008;10(12–13):1393–1397.
8. Chambon P. A decade of molecular biology of retinoic acid receptors. *FASEB J.* 1996;10(9):940–954.
9. Guleria RS, Singh AB, Nizamutdinova IT, et al. Activation of retinoid receptor-mediated signaling ameliorates diabetes-induced cardiac dysfunction in Zucker diabetic rats. *J Mol Cell Cardiol.* 2013;57:106–118.
10. Van YH, Lee WH, Ortiz S, Lee MH, Qin HJ, Liu CP. All-trans retinoic acid inhibits type-1 diabetes by T regulatory (Treg)-dependent suppression of interferon-gamma-producing T-cells without affecting Th17 cells. *Diabetes.* 2009;58(1):146–155.
11. Amengual J, Ribot J, Bonet ML, Palou A. Retinoic acid treatment increases lipid oxidation capacity in skeletal muscle of mice. *Obesity.* 2008;16(3):585–591.
12. Berry DC, Noy N. All-trans-retinoic acid represses obesity and insulin resistance by activating both peroxisome proliferation-activated receptor beta/delta and retinoic acid receptor. *Mol Cell Biol.* 2009;29(12):3286–3296.
13. Benson MJ, Pino-Lagos K, Rosemblatt M, Noelle RJ. All-trans retinoic acid mediates enhanced T reg cell growth, differentiation, and gut homing in the face of high levels of co-stimulation. *J Exp Med.* 2007;204(8):1765–1774.
14. Herdeg C, Oberhoff M, Baumbach A, et al. Effects of local all-trans-retinoic acid delivery on experimental atherosclerosis in the rabbit carotid artery. *Cardiovasc Res.* 2003;57(2):544–553.
15. Tehrani S, Mobarrez F, Antovic A, et al. Atorvastatin has antithrombotic effects in patients with type 1 diabetes and dyslipidemia. *Thromb Res.* 2010;126(3):e225–231.
16. Chockalingam P, Vinayagam NS, Chockalingam V, Chockalingam A. Remarkable regression of coronary atherosclerosis: An interplay of pharmacotherapeutic and lifestyle factors. *Ind Heart J.* 2016;68(2):188–189.
17. Puri R, Nissen SE, Ballantyne CM, et al. Factors underlying regression of coronary atheroma with potent statin therapy. *Eur Heart J.* 2013;34(24):1818–1825.

18. Nissen SE, Nicholls SJ, Sipahi I, et al; ASTEROID Investigators. Effect of very high-intensity statin therapy on regression of coronary atherosclerosis: The ASTEROID trial. *JAMA*. 2006;295(13):1556–1565.
19. Amengual J, Ribot J, Bonet ML, Palou A. Retinoic acid treatment increases lipid oxidation capacity in skeletal muscle of mice. *Obesity (Silver Spring).* 2008;16(3):585–591.
20. Rebe C, Raveneau M, Chevriaux A, et al. Induction of transglutaminase 2 by a liver X receptor/retinoic acid receptor alpha pathway increases the clearance of apoptotic cells by human macrophages. *Circ Res*. 2009;105(4):393–401.
21. Imaizumi T, Yagihashi N, Kubota K, et al. Expression of retinoic acid-inducible gene-I (RIG-I) in macrophages: Possible involvement of RIG-I in atherosclerosis. *J Atheroscler Thromb*. 2007;14(2):51–55.
22. Kim YM, Kim JH, Park SW, Kim HJ, Chang KC. Retinoic acid inhibits tissue factor and HMGB1 via modulation of AMPK activity in TNF-α activated endothelial cells and LPS-injected mice. *Atherosclerosis*. 2015;241(2):615–623.
23. Ross R. Atherosclerosis – an inflammatory disease. *N Engl J Med*. 1999;340(2):115–126.
24. Bilbija D, Elmabsout AA, Sagave J, et al. Expression of retinoic acid target genes in coronary artery disease. *Int J Mol Med*. 2014;33(3):677–686.

ENHO gene expression and serum adropin level in rheumatoid arthritis and systemic lupus erythematosus

Servet Yolbas[1,A,D], Murat Kara[2,C], Mehmet Kalayci[3,C], Ahmet Yildirim[1,B], Baris Gundogdu[1,B], Suleyman Aydin[3,C], Suleyman Serdar Koca[1,A,D–F]

[1] Department of Rheumatology, Faculty of Medicine, Firat University, Elazig, Turkey
[2] Department of Medical Genetics, Faculty of Medicine, Mugla Sitki Kocman University, Turkey
[3] Department of Biochemistry, Faculty of Medicine, Firat University, Elazig, Turkey

A – research concept and design; B – collection and/or assembly of data; C – data analysis and interpretation;
D – writing the article; E – critical revision of the article; F – final approval of the article

Advances in Clinical and Experimental Medicine, ISSN 1899-5276 (print), ISSN 2451-2680 (online) *Adv Clin Exp Med*. 2018;27(12):1637–1641

Address for correspondence
Suleyman Serdar Koca
E-mail: kocassk@yahoo.com

Funding sources
None declared

Conflict of interest
None declared

Received on October 28, 2015
Reviewed on December 9, 2015
Accepted on July 18, 2017

Abstract

Background. Adropin, a secreted protein, is encoded by the energy homeostasis-associated gene (*ENHO*). It is expressed by a variety of tissues and cells. It has been implicated in several physiological and pathological processes, such as angiogenesis and apoptosis.

Objectives. The aim of the present study was to investigate the *ENHO* gene expression and serum adropin levels in patients with rheumatoid arthritis (RA) and systemic lupus erythematosus (SLE).

Material and methods. The study included 36 patients with RA, 22 patients with SLE and 20 healthy controls (HC). Patients with a disease activity score-28-erythrocyte sedimentation rate (DAS28-ESR) >2.6 in the RA group and an SLE disease activity index (SLEDAI) >6 in the SLE group were accepted as active. Serum adropin levels were analyzed with the enzyme-linked immunosorbent assay (ELISA) method. The *ENHO* gene and glyceraldehyde 3-phosphate dehydrogenase (*GAPDH*) gene expressions in peripheral blood mononuclear cells were analyzed with real-time polymerase chain reaction (PCR).

Results. The *ENHO* gene mRNA expression was significantly higher in the RA group than in the HC group ($p = 0.024$), although it was similar between the SLE and HC groups ($p = 0.920$). On the other hand, there were no significant differences among the study groups in terms of serum adropin levels ($p > 0.05$ for all). Moreover, there was no significant difference in terms of the *ENHO* expression and serum adropin levels between active and inactive RA and SLE patients.

Conclusions. Although the *ENHO* gene expression is increased, serum adropin level is not altered in RA. Similarly, adropin seems not to be associated with SLE. However, the potential link between adropin and inflammatory diseases need to be tested in further studies.

Key words: rheumatoid arthritis, systemic lupus erythematosus, adropin, energy homeostasis-associated gene

DOI
10.17219/acem/75944

Introduction

Rheumatoid arthritis (RA) is a chronic inflammatory disease characterized by synovitis and damage to the joints. Its prevalence in the general population is around 1%.[1] Although the pathological immunological process of the disease is uncertain, many immune cells, such as lymphocytes, macrophages, and leukocytes, and many other molecules, such as cytokines and chemokines, have been shown to play a role in this process.[1] Angiogenesis also plays a prominent role in pannus tissue formation in RA.[1] It has been shown that adipocytokines in the peptide structure are associated with many signaling pathways and that pro-inflammatory cytokine release is involved in the pathogenesis of RA.[2–4] Moreover, they may influence disease phenotype and the course of the disease.[2–4]

Adropin, encoded by the energy homeostasis-associated (*ENHO*) gene, is a secretory protein playing an active role in energy homeostasis.[5] The *ENHO* gene has been determined to be expressed in many organs besides endothelial cells, such as the liver, the brain, the pancreas, and the kidneys.[6,7] Adropin affects the regulation of glucose and lipid metabolism, energy homeostasis and the modulation of insulin sensitivity.[5–7]

In addition to the metabolic effects, adropin has been shown to have many non-metabolic effect potentials related to angiogenesis, apoptosis and inflammation.[5,6,8] Adropin has been demonstrated to have an effect on vascular endothelial growth factor receptor (VEGFR), intracellular pathways like PI3K-Akt and ERK1/2, and local and systemic mediators like interleukin 6 (IL-6), which are also effective in RA pathogenesis.[5,6,9] In addition, while adropin stimulates the critical stages of angiogenesis, such as proliferation, migration and tube formation, it reduces the apoptosis of endothelial cells and vascular permeability. Furthermore, adropin therapy has been shown to ameliorate endothelial function.[6]

These effects of adropin suggest that it may play an active role in the pathophysiology of inflammatory rheumatic diseases. The aim of this study was to evaluate serum adropin levels and the *ENHO* gene expression in RA and systemic lupus erythematosus (SLE).

Material and methods

The study included 36 patients with RA, 22 patients with SLE, and 20 healthy controls (HC). The patients fulfilled the established classification criteria.[10,11] Participants under the age of 18 years or above the age of 80 years, those with signs of infection, and pregnant women were excluded from the study. The protocol of this study was approved by the institutional Ethics Committee, and all the participants gave informed consent before being enrolled in the study. Detailed histories of all the participants were obtained, and systemic and rheumatological examinations were performed. The clinical process and treatments for all participants were also recorded.

Disease activity and/or severity scores were determined by the disease activity score (DAS)-28-erythrocyte sedimentation rate (ESR) in the RA group (patients with a DAS28-ESR score >2.6 were considered active); the SLE disease activity index (SLEDAI) and the Systemic Lupus International Collaborating Clinics/American College of Rheumatology damage index (SLICC/ACR) were used in the SLE group (patients with an SLEDAI score >6 were considered active).[12–14]

Blood samples were drawn from all the participants, after fasting overnight. Erythrocyte sedimentation rate and C-reactive protein (CRP) levels were assessed by the classic Westergren and immunoturbidimetric methods, respectively. Routine laboratory evaluations of complete blood count, creatinine and total creatinine kinase levels were assessed in all the participants, using standard laboratory methods. Rheumatoid factor (RF) and anti-cyclic citrullinated peptide (anti-CCP) antibody levels were analyzed in the RA group, and RF and anti-CCP titers higher than 15 IU/mL were considered positive. In addition, autoantibody work-ups (antinuclear antibody – ANA, anti-double stranded DNA (anti-dsDNA) and anti-Sm antibodies) were studied with standard methods in the SLE group on the same day. Antinuclear antibody was detected by the indirect immunofluorescence antibody (IFA) test. Anti-dsDNA and anti-Sm antibodies were measured by the enzyme-linked immunosorbent assay (ELISA), using suitable commercial kits (Euroimmun, Lübeck, Germany).

Serum adropin levels were analyzed by the ELISA method, using an appropriate commercial kit (Cusabio Biotech Co., Wuhan, China).

Total RNA was prepared from peripheral blood cells by the use of a QIAamp RNA Blood Mini kit (Qiagen, Hilden, Germany). Equal amounts of RNA from these samples were reverse transcribed to cDNA, using a Superscript First-Strand cDNA Synthesis Kit (Invitrogen, San Diego, USA). The mRNA expression of *ENHO* (Qiagen) was quantified and normalized against glyceraldehyde-3-phosphate dehydrogenase (*GAPDH*). The levels of *ENHO* and *GAPDH* were measured by the Rotor-Gene SYBR green-based real-time polymerase chain reaction (PCR), using a real-time PCR system (Rotor-Gene Q; Qiagen). Gene expression was determined by the 2-ΔΔCt methodology, normalized against the reference gene *GAPDH*. Changes in gene expression are represented as a fold change relative to 1, where the control equals 1.

Statistical analysis was performed using the Statistical Package for the Social Sciences (SPSS) v. 21.0 (IBM, Chicago, USA). Results were given as mean ± standard deviation (SD). The normal distribution of the variables was evaluated by the Kolmogorov-Smirnov test, and logarithmic transformations were performed to normalize data with a skewed distribution before statistical analysis.

Statistical differences among the groups were identified with one-way analysis of variance (ANOVA), followed by Tukey's post hoc test for parametric data and the Mann-Whitney U test for nonparametric data. The χ^2 test was done to compare the categorical variables. Correlation analysis was performed using Pearson's correlation coefficient. Analysis of covariance (ANCOVA) was also used to adjust the variables for age, body mass index (BMI) and current drug usage. The p-values <0.05 were considered significant.

Results

The demographic and clinical data of the study group are summarized in Table 1. The mean DAS28-ESR score was 3.1 ±1.6 in the RA group. The mean SLEDAI and SLICC/ACR indices in the SLE group were 11.3 ±10.6 and 1.7 ±1.5, respectively. There were 17 and 13 active patients in the RA and SLE groups, respectively. In the RA group, the mean swollen, tender and deformed joint counts were 2.5 ±4.7, 3.8 ±6.7, and 1.1 ±2.7, respectively, and the mean morning stiffness duration was 60.1 ±76.2 min. In addition, the mean titers of RF and anti-CCP in the RA group were 73.2 ±93.3 U/mL and 363 ±50.8 U/mL, respectively, and 19 and 26 RA patients were positive for RF and anti-CCP, respectively. In the SLE group, anti-dsDNA was 78.8 ±5.3 IU/mL, and 14 and 6 patients were positive for dsDNA and anti-Sm antibody, respectively.

Table 1. The demographics in all the study groups

Variables	RA (n = 36)	SLE (n = 22)	HC (n = 20)	p-value
Age [years]	49.6 ±15.9†††	31.1 ±8.8**	44.2 ±12.9	<0.001[a]
Sex (F/M)	8/28	1/21	3/17	0.193[b]
BMI [kg/m^2]	27.4 ±6.2†	23.7 ±4.8	27.1 ±4.8	0.025[a]
Disease duration [years]	10.6 ±9.4	4.7 ±5.9	–	0.008[c]
Smoking (n)	3	4	2	0.506[b]
GC usage (n)	29	18	–	0.821[c]
GC dose [mg/day]*	4.5 ±3.7	6.0 ±5.2	–	0.261[c]

Data expressed as mean ± standard deviation (SD). RA – rheumatoid arthritis; SLE – systemic lupus erythematosus; HC – healthy control; F – female; M – male; BMI – body mass index; GC – glucocorticoid. * The dose of glucocorticoid is equivalent to prednisolone. The p-values of [a] ANOVA, [b] χ^2, and [c] Student's t-tests are given. When compared to the HC group: ** p < 0.01. When compared to the SLE group: † p < 0.05 and †††p < 0.001.

Table 2. Laboratory parameters in all the study groups

Variables	RA (n = 36)	SLE (n = 22)	HC (n = 20)	p-value
ESR [mm/h]	32.7 ±25.0*	38.3 ±29.5**	17.2 ±11.6	0.007[a]
CRP [mg/dL]	1.7 ±3.1	0.6 ±1.4	0.3 ±0.2	0.040[a]
WBC [10^3/μL]	7.3 ±2.1††	5.3 ±2.1	6.3 ±1.4	0.001[a]
PLT [10^3/μL]	280.6 ±77.8	244.7 ±102.1	271.1 ±79.5	0.271[a]
Hb [g/dL]	12.5 ±1.5*†	11.3 ±1.7***	13.5 ±1.2	<0.001[a]
TG [mg/dL]	92.6 ±48.5**	112.6 ±65.9	150.3 ±79.6	0.003[a]
TC [mg/dL]	163.3 ±38.5*	151.5 ±32.8**	191.1 ±50.5	0.002[a]
LDL-C [mg/dL]	104.2 ±32.6*	96.9 ±24.3**	129.4 ±43.8	0.002[a]
HDL-C [mg/dL]	48.6 ±13.2	48.1 ±17.7	47.6 ±11.6	0.964[a]
Serum adropin [ng/mL]	1.1 ±0.9	1.1 ±0.6	0.8 ±0.5	0.190[b]
ENHO gene expression [AU]	1.25 ±0.11*	1.19 ±0.12	1.18 ±0.10	0.036[b]

Data expressed as mean ± standard deviation (SD). RA – rheumatoid arthritis; SLE – systemic lupus erythematosus; HC – healthy controls; ESR – erythrocyte sedimentation rate; CRP – C-reactive protein; WBC – white blood cell count; PLT – platelet count; Hb – hemoglobin; TG – triglyceride; TC – total cholesterol; LDL-C – low-density lipoprotein cholesterol; HDL-C – high-density lipoprotein cholesterol. The p-values of [a] ANOVA and [b] Kruskal-Wallis tests are given. When compared to the HC group: * p < 0.05, ** p < 0.01 and *** p < 0.001. When compared to the SLE group: † p < 0.05 and †† p < 0.01.

There was no significant difference among the groups in terms of serum adropin level (p > 0.05 for all). The *ENHO* gene expression was significantly higher in the RA group when compared to the HC group (1.25 ±0.11 AU vs 1.18 ±0.10 AU; p = 0.024). There was no significant difference between the HC and SLE groups in terms of the *ENHO* gene expression (p = 0.921) (Table 2).

There was no significant difference between active and inactive RA groups in terms of serum adropin and the *ENHO* gene expression levels (p > 0.05 for all, data not shown). There was no significant difference between RA patients using and not using glucocorticoid (GC), methotrexate, sulfasalazine, hydroxychloroquine (HCQ), and leflunomide in terms of serum adropin levels or the *ENHO* gene expression. In addition, serum adropin levels and the *ENHO* gene expression were similar in the patients positive and negative for RF and anti-CCP (p > 0.05). Furthermore, serum adropin levels and the *ENHO* gene expression were not significantly correlated with DAS28-ESR, ESR, and CRP levels, or RF and anti-CCP titers in the RA group (p > 0.05).

There was no significant difference between the active and inactive SLE subgroups in terms of serum adropin levels and the *ENHO* gene expression (p > 0.05 for all, data not shown). In the SLE group, there was no significant difference between the patients with and without renal involvement and ANA positivity in terms of serum adropin levels and the *ENHO* gene expression. Moreover, there was no significant difference between patients using and not using GC, azathioprine and HCQ in terms of serum adropin levels or the *ENHO* gene expression (p > 0.05 for all, data not shown). However, in the SLE group, the *ENHO* gene expression was negatively correlated with hemoglobin (r = −0.430; p = 0.046) and low-density lipoprotein (LDL) cholesterol levels (r = −0.465; p = 0.029).

Discussion

The current study evaluated serum adropin levels and the *ENHO* gene expression in RA and SLE, which are chronic inflammatory diseases. There was no significant difference among the groups in terms of serum adropin levels. However, significantly higher *ENHO* gene expression was observed in RA. On the other hand, the *ENHO* gene expression was similar between the SLE and HC groups.

Adropin is a molecule in the structure of the peptide and has been shown to act on many chronic pathological processes. Plasma adropin levels increase in patients with heart failure, characterized by chronic, low-grade inflammation.[9] Furthermore, plasma adropin level shows a positive correlation with IL-6.[9] On the other hand, Lovren et al. reported that in vitro adropin administration increased Akt and ERK1/2 phosphorylation.[6] Akt was also shown to interact with several intracellular pathways like GSK3, p21/p27, EDG-1, and FOXO, which were increased as a result of the inflammatory process.[6] We found increased *ENHO* gene expression in RA, but not in SLE in our study. Serum adropin levels were not significantly altered in RA and SLE, although they are chronic inflammatory diseases.

Adropin stimulates critical neovascularization processes, including proliferation, migration and capillary-like tube formation. Lovren et al. reported that in vitro adropin administration increased the level of VEGFR2 protein.[6] Also, an increase in capillary density was observed in the adropin-administered group in a mouse hind limp ischemia model.[6] Moreover, a low adropin level was shown to be associated with a decrease in vascular microcirculation.[15,16] In the present study, high levels of the *ENHO* gene expression in the RA group may suggest that adropin could be associated with pannus formation in RA. In contrast to RA, similar *ENHO* gene expression between SLE patients and healthy volunteers may be caused by a lack of pannus formation in SLE.

Cardiovascular morbidity and mortality are higher in RA and SLE.[17–19] The pathogenesis of increased atherosclerosis cannot be explained by common cardiovascular risk factors, such as age, sex, obesity, smoking, hyperlipidemia, hypertension, and diabetes. Inflammation is one of the important non-conventional reasons of increased cardiovascular risk in these inflammatory diseases. In addition, insulin resistance is one of the most important triggering risk factors in the development and progression of atherosclerotic cardiovascular diseases. Adropin is related to metabolic diseases and atherosclerosis.[5] Increased adipocytes, dyslipidemia, impaired glucose tolerance, and insulin resistance were demonstrated in adropin knockout mice.[20] Conversely, systemic treatment or transgenic overexpression of adropin were shown to improve obesity, hepatosteatosis and insulin resistance.[6,21,22] It were shown that a low serum adropin level is associated with endothelial dysfunction and that this dysfunction improves with adropin treatment.[6,21,22] Increased adropin levels are expected in RA and SLE due to their inflammatory nature. However, in our study, this level was not higher in RA and SLE. It suggests that the adropin level which is not increased may be one cause of the increased metabolic and atherosclerotic complications of RA and SLE.

Liver *ENHO* gene expression was documented to be affected by changes in one's energy balance, the content of one's diet and the presence of obesity.[5] While a short-term diet with a high fat content increases the *ENHO* gene expression, chronic exposure, through obesity, for example, decreases its expression.[5] Serum adropin level is high in the case of chow diets and decreases in hunger and diet-induced obesity. While the adropin level is high when fed with a high-fat and low-carbohydrate diet, the adropin level is lower when fed with a low-fat and high-carbohydrate diet.[20] Additionally, liver *ENHO* mRNA expression is regulated by liver X receptors α (LXRα) and peroxisome proliferator activated receptor-γ (PPAR-γ), which is an insulin sensitizer, playing a role in cholesterol and triglyceride metabolism.[5] The nuclear receptor families, LXRα and PPAR-γ, playing a role in energy homeostasis, were shown to be higher in RA fibroblast-like synoviocytes and synovial fluid. Also, an increase in LXRα and PPAR-γ was demonstrated to be related with a decrease in the *ENHO* gene expression and the adropin level.[5,23–26] Thus, it can be concluded that one cause of the adropin level that is not increased may be the possible suppressive effect of LXRα and PPAR-γ on adropin production.

Similarly, leptin may suppress adropin production in RA and SLE. A decreased adropin level was observed to be associated with an increased leptin level.[5,27] The leptin level significantly increases RA and SLE.[28,29]

There are some limitations of this study. Foremost, the sample size is relatively small. The analysis of the *ENHO* gene expression by peripheral blood mononuclear cells may be another limitation of the present study. It could be analyzed by liver tissue or any affected tissue. Thirdly, another limitation may be that the mean ages of the study groups are significantly different in our study. However, this is difficult to correct, since RA and SLE affect and start at different ages. The differences for data were also analyzed with ANCOVA to adjust.

In conclusion, the *ENHO* gene expression is increased in RA but not in SLE. However, the adropin level does not change in RA and SLE, which are chronic inflammatory diseases. Consequently, adropin may not be directly related to these diseases. However, further studies are needed to draw a more precise conclusion.

References

1. McInnes IB, Schett G. The pathogenesis of rheumatoid arthritis. *N Engl J Med.* 2011;365:2205–2219.
2. Scotece M, Conde J, Gómez R, et al. Beyond fat mass: Exploring the role of adipokines in rheumatic diseases. *Sci World J.* 2011;11:1932–1947.
3. Krysiak R, Handzlik-Orlik G, Okopien B. The role of adipokines in connective tissue diseases. *Eur J Nutr.* 2012;51:513–528.

4. Conde J, Scotece M, López VJ, et al. Adipokines: Novel players in rheumatic diseases. *Discov Med.* 2013;15:73–83.
5. Kumar KG, Trevaskis JL, Lam DD, et al. Identification of adropin as a secreted factor linking dietary macronutrient intake with energy homeostasis and lipid metabolism. *Cell Metab.* 2008;8:468–481.
6. Lovren F, Pan Y, Quan A, et al. Adropin is a novel regulator of endothelial function. *Circulation.* 2010;122:185–192.
7. Aydin S, Kuloglu T, Aydin S, et al. Expression of adropin in rat brain, cerebellum, kidneys, heart, liver, and pancreas in streptozotocin-induced diabetes. *Mol Cell Biochem.* 2013;380:73–81.
8. Aydin S, Kuloglu T, Aydin S. Copeptin, adropin and irisin concentrations in breast milk and plasma of healthy women and those with gestational diabetes mellitus. *Peptides.* 2013;47:66–70.
9. Lian W, Gu X, Qin Y, Zheng X. Elevated plasma levels of adropin in heart failure patients. *Intern Med.* 2011;50:1523–1527.
10. Aletaha D, Neogi T, Silman AJ, et al. 2010 rheumatoid arthritis classification criteria: An American College of Rheumatology/European League Against Rheumatism collaborative initiative. *Ann Rheum Dis.* 2010;69:1580–1588.
11. Petri M, Orbai AM, Alarcón GS, et al. Derivation and validation of the Systemic Lupus International Collaborating Clinics classification criteria for systemic lupus erythematosus. *Arthritis Rheum.* 2012;64:2677–2686.
12. Prevoo ML, van't Hof MA, Kuper HH, et al. Modified disease activity scores that include twenty-eight-joint counts. Development and validation in a prospective longitudinal study of patients with rheumatoid arthritis. *Arthritis Rheum.* 1995;38:44–48.
13. Bombardier C, Gladman DD, Urowitz MB, et al. Derivation of the SLEDAI. A disease activity index for lupus patients. The Committee on Prognosis Studies in SLE. *Arthritis Rheum.* 1992;35:630–640.
14. Gladman D, Ginzler E, Goldsmith C, et al. The development and initial validation of the Systemic Lupus International Collaborating Clinics/American College of Rheumatology damage index for systemic lupus erythematosus. *Arthritis Rheum.* 1996;39:363–369.
15. Ahn J, Kim J. Mechanisms and consequences of inflammatory signaling in the myocardium. *Curr Hypertens Rep.* 2012;14(6):510–516.
16. Celik A, Balin M, Kobat MA, et al. Deficiency of a new protein associated with cardiac syndrome X; called adropin. *Cardiovasc Ther.* 2013;31:174–178.
17. Mason JC, Libby P. Cardiovascular disease in patients with chronic inflammation: Mechanisms underlying premature cardiovascular events in rheumatologic conditions. *Eur Heart J.* 2015;36(8):482–489c.
18. Ku IA, Imboden JB, Hsue PY, Ganz P. Rheumatoid arthritis: Model of systemic inflammation driving atherosclerosis. *Circ J.* 2009;73:977–985.
19. McMahon M, Skaggs B. Pathogenesis and treatment of atherosclerosis in lupus. *Rheum Dis Clin North Am.* 2014;40(3):475–495.
20. Ganesh Kumar K, Zhang J, Gao S, et al. Adropin deficiency is associated with increased adiposity and insulin resistance. *Obesity (Silver Spring).* 2012;20:1394–1402.
21. Gozal D, Kheirandish-Gozal L, Bhattacharjee R, et al. Circulating adropin concentrations in pediatric obstructive sleep apnea: Potential relevance to endothelial function. *J Pediatr.* 2013;163:1122–1126.
22. Topuz M, Celik A, Aslantas T, et al. Plasma adropin levels predict endothelial dysfunction like flow-mediated dilatation in patients with type 2 diabetes mellitus. *J Investig Med.* 2013;61:1161–1164.
23. Palma A, Sainaghi PP, Amoruso A, et al. Peroxisome proliferator-activated receptor-gamma expression in monocytes/macrophages from rheumatoid arthritis patients: Relation to disease activity and therapy efficacy – a pilot study. *Rheumatology (Oxford).* 2012;51:1942–1952.
24. Zhou JJ, Ma JD, Mo YQ, et al. Down-regulating peroxisome proliferator-activated receptor-gamma coactivator-1beta alleviates the pro-inflammatory effect of rheumatoid arthritis fibroblast-like synoviocytes through inhibiting extracellular signal-regulated kinase, p38 and nuclear factor-kappa B activation. *Arthritis Res Ther.* 2014;16:472. https://doi.org/10.1186/s13075-014-0472-6
25. Marder W, Khalatbari S, Myles JD, et al. The peroxisome proliferator activated receptor-γ pioglitazone improves vascular function and decreases disease activity in patients with rheumatoid arthritis. *J Am Heart Assoc.* 2013;2:e000441. doi: 10.1161/JAHA.113.000441
26. Laragione T, Gulko PS. Liver X receptor regulates rheumatoid arthritis fibroblast-like synoviocyte invasiveness, matrix metalloproteinase 2 activation, interleukin-6 and CXCL10. *Mol Med.* 2012;18:1009–1017.
27. Sayin O, Tokgöz Y, Arslan N. Investigation of adropin and leptin levels in pediatric obesity-related nonalcoholic fatty liver disease. *J Pediatr Endocrinol Metab.* 2014;27:479–484.
28. Tian G, Liang JN, Wang ZY, Zhou D. Emerging role of leptin in rheumatoid arthritis. *Clin Exp Immunol.* 2014;177(3):557–570.
29. Vadacca M, Zardi EM, Margiotta D, et al. Leptin, adiponectin and vascular stiffness parameters in women with systemic lupus erythematosus. *Intern Emerg Med.* 2013;8(8):705–712.

The effect of anakinra to nephrotoxicity with cisplatin induced in rats: Biochemical, gene expression and histopathological evaluation

Adalet Ozcicek[1,A,B,D,F], Fatih Ozcicek[1,B,E,F], Ferda Keskin Cimen[2,C,F], Renad Mammadov[3,B,F], Murat Cankaya[4,C,F], Talat Ezmeci[5,E,F], Durdu Altuner[3,A,D,F]

[1] Department of Internal Medicine, Faculty of Medicine, Erzincan University, Turkey
[2] Department of Pathology, Faculty of Medicine, Erzincan University, Turkey
[3] Department of Pharmacology, Faculty of Medicine, Erzincan University, Turkey
[4] Department of Biology, Arts and Sciences, Erzincan University, Turkey
[5] Department of Public Health, Faculty of Medicine, Erzincan University, Turkey

A – research concept and design; B – collection and/or assembly of data; C – data analysis and interpretation;
D – writing the article; E – critical revision of the article; F – final approval of the article

Advances in Clinical and Experimental Medicine, ISSN 1899-5276 (print), ISSN 2451-2680 (online) *Adv Clin Exp Med*. 2018;27(12):1643–1650

Address for correspondence
Durdu Altuner
E-mail: durdualtuner@hotmail.com

Funding sources
None declared

Conflict of interest
None declared

Received on February 17, 2017
Reviewed on June 12, 2017
Accepted on July 10, 2017

Abstract

Background. Oxidative stress and interleukin-1 beta (IL-1β) have been reported to play a role in the pathogenesis of nephrotoxicity induced by cisplatin.

Objectives. The objective of this study was to investigate the effect of anakinra, which is an IL-1β receptor antagonist, on cisplatin-induced nephrotoxicity in rats, through biochemical, gene expression and histopathological analyses.

Material and methods. The study was designed with 4 groups. For 1 week, the control group (C) and the cisplatin (Cis) group received distilled water, while the cisplatin + anakinra 50 (Cis + ANA50) group and the cisplatin + anakinra 100 (Cis + ANA100) group were intraperitoneally administered 50 mg/kg and 100 mg/kg of anakinra, respectively. The Cis, Cis + ANA50 and Cis + ANA100 groups were intraperitoneally injected with a 2.5 mg/kg dose of cisplatin for 7 days. After sacrifice, the kidney tissue of each rat was extracted for the assessment of the malondialdehyde (MDA) and total glutathione (tGSH) levels, and for gene expression analyses of *IL-1β*. The kidney tissues were histopathologically evaluated. Statistical analyses of the data were performed using one-way analysis of variance (ANOVA).

Results. The administration of cisplatin (the Cis group) yielded a higher level of MDA (4.75 ±0.25 nmol/mL; $p < 0.001$) and lower levels of tGSH (1.80 ±0.35 mg/L; $p < 0.001$) compared to other groups. Cisplatin also increased *IL-1β* gene expression (6.33 ±0.27 gene expression levels; $p < 0.001$) compared to other groups. The impact of anakinra on the MDA and tGSH levels, and on *IL-1β* gene expression induced by cisplatin was observed as a reversal of these findings ($p < 0.05$). Anakinra better prevented an increase of the levels of MDA and IL-1β at a dose of 100 mg/kg compared to a 50 mg/kg dose.

Conclusions. Anakinra prevents oxidative kidney damage induced by cisplatin in a dose-dependent manner. This result suggests that anakinra may be useful in the treatment of cisplatin-induced kidney damage.

Key words: rats, cisplatin-nephrotoxicity, anakinra

DOI
10.17219/acem/75775

Introduction

Cisplatin is a platinum-derived anticancer drug which is widely used in chemotherapy. Since cisplatin is a non-cell-cycle specific chemotherapeutic agent, it is a broad-spectrum drug, commonly used in the treatment of various solid cancer types (stomach, testicular, ovarian, bladder, kidney, uterocervical, head and neck).[1] However, nephrotoxicity during cisplatin chemotherapy makes it necessary to use cisplatin in limited doses, and sometimes even to discontinue the treatment.[2] While the administration of cisplatin at low doses causes necrosis in the tubule cells of the kidney, high doses lead to apoptosis.[3] Cisplatin has been reported to cause severe damage, especially in the epithelial cells of the proximal tubule of the kidney.[4] Free oxygen radicals have been demonstrated to play a role in cellular death due to the use of cisplatin.[5] On the other hand, interleukin-1 beta (IL-1β) has been reported to play a crucial role in the pathogenesis of nephrotoxicity induced by cisplatin.[6] These results suggest that antioxidants and IL-1β antagonists may be beneficial in the prevention of cisplatin nephrotoxicity. Anakinra, which we tested against cisplatin nephrotoxicity in the present study, is a recombinant human IL-1β receptor antagonist and the first biological agent which has been demonstrated to block pro-inflammatory effects in patients with rheumatoid arthritis.[7] Hasturk et al. reported on the antioxidant activity of anakinra in animals.[8] There are studies which associate the protective effect of anakinra with antioxidant activity resulting from the blockage of IL-β receptors.[9] Anakinra has also been reported to protect the ovarian tissue from ischemia-reperfusion injury by anti-inflammatory and antioxidant activity.[10] It was found that anakinra suppressed hyperalgesia by preventing an increase in the malondialdehyde (MDA), myeloperoxidase and IL-1β levels, and a decrease in the total glutathione (tGSH) levels.[11] In the literature, there have been no studies on the use of anakinra, taking into consideration both its antioxidant and IL-1β-antagonist properties against cisplatin nephrotoxicity. Therefore, the objective of this study was to investigate the effect of anakinra against cisplatin-induced nephrotoxicity in rats, through biochemical, gene expression and histopathological analyses.

Material and methods

Animals

A total of 40 male albino Wistar rats, each weighing 220–230 g, were randomly chosen. Prior to the experiment, the rats were divided into 4 groups, with 10 rats per group. The rats were kept and fed in the pharmacology laboratory at normal room temperature (22°C). The animal experiments were performed in accordance with the National Guidelines for the Use and Care of Laboratory Animals, and approved by the local animal ethics committee (No. 179, November 27, 2015).

Chemical substances

Cisplatin, ketamine hydrochloride and anakinra were purchased from Koçak Farma Drug Industry (Istanbul, Turkey), Pfizer Drugs, Ltd. (Istanbul, Turkey) and Swedish Orphan Biovitrum AB (Stockholm, Sweden), respectively.

Experimental groups

The experimental animals were divided into control (C), cisplatin (Cis), cisplatin + anakinra 50 (Cis + ANA50), and cisplatin + anakinra 100 (Cis + ANA100) groups.

Experimental procedure

The Cis + ANA50 and Cis + ANA100 groups were intraperitoneally administered 50 mg/kg and 100 mg/kg of anakinra, respectively. As in the previous studies, anakinra was given intraperitoneally. In addition, the effects of anakinra on antioxidants and cytokines had been investigated previously at these dosages.[10] Distilled water was given to the Cis and C groups as a solvent in the same way. Since anakinra is a solution dissolved in distilled water, we also used distilled water as a solvent. One hour after anakinra was administered, the Cis, Cis + ANA50 and Cis + ANA100 groups were injected with a 2.5 mg/kg dose of cisplatin intraperitoneally. In the literature, drugs that have been investigated for protective effects against cisplatin toxicity are generally given to experimental animals 1 h before cisplatin.[12] In our preliminary study, administering cisplatin at a dose of 2.5 mg/kg for 1 week resulted in significant nephrotoxicity in the animals. These procedures were repeated once a day for 7 days. At the end of this period, all the rats were sacrificed with high-dose ketamine hydrochloride anesthesia and their kidney tissues were removed. Following the macroscopic evaluation of the kidney tissues, the MDA, tGSH and *IL-1β* gene expression levels were determined. In addition, the kidney tissues were histopathologically evaluated. The results obtained from the Cis + ANA50, Cis + ANA100 and C groups were evaluated in comparison with the Cis group.

Biochemical analysis

Malondialdehyde analysis

According to the method defined by Ohkawa et al., MDA forms a pink complex with thiobarbituric acid (TBA) at 95°C, which can be measured using spectrophotometry at a wavelength of 532 nm.[13] A sample of 25 mg of tissue was homogenized using a solution of 1.15% KCl. Homogenates were centrifuged at 5000 g for 20 min, and the supernatants were used to determine the amount of MDA; 250 µL of homogenate, 100 µL of 8% sodium dodecyl sulfate (SDS), 750 µL of 20% acetic acid, 750 µL of 0.08% TBA, and 150 µL of purified water were pipetted into capped test tubes and

vortexed. The mixture was left for incubation at 100°C for 60 min before 2.5 mL of n-butanol was added to it, and then spectrophotometric measurement was conducted. The amounts of red color formed were read at 532 nm, using cuvettes of 3 mL, and, taking into account dilution coefficients, the MDA amounts in the samples were determined, using the standard chart. The standard chart created using MDA stock solution was prepared before.

Total glutathione analysis

The amount of GSH in the total homogenate was measured according to the method of Sedlak and Lindsay with some modifications.[14] The sample was weighed and homogenized in 2 mL of 50 mmol/L Tris–HCl buffer, containing 20 mmol/L of ethylenediaminetetraacetic acid (EDTA) and 0.2 mmol/L of sucrose at pH 7.5. The homogenate was immediately precipitated with 0.1 mL of 25% trichloroacetic acid (TCAA), the precipitate was removed after centrifugation at 4200 rpm for 40 min at 4°C, and the supernatant was used to determine the GSH level. A total of 1500 µL of measurement buffer (200 mmol/L of Tris–HCl buffer, containing 0.2 mmol/L of EDTA at pH 7.5), 500 µL of the supernatant, 100 µL of 5,5'-Dithiobis (2-nitrobenzoic acid) (DTNB), and 7900 µL of methanol were added to a tube and vortexed, and incubated for 30 min at 37°C. DTNB was used as a chromogen and it formed a yellow-colored complex with sulfhydryl groups. The absorbance was measured at 412 nm, using a spectrophotometer (Beckman DU 500; Beckman Coulter, Inc., Brea, USA). The standard curve was obtained by using reduced glutathione.

Superoxide dismutase analysis

The superoxide dismutase (SOD) activity was based on the generation of superoxide radicals, produced by xanthine and xanthine oxidase, which reacts with nitro blue tetrazolium to form formazan dye. The SOD activity was then measured at 560 nm by the degree of inhibition of this reaction.[15]

Interleukin-1 beta quantity measurement

The tissue homogenate IL-1β concentrations were measured using a rat-specific sandwich enzyme-linked immunosorbent assay Rat Interleukin-1β ELISA Kit (Cat. No. YHB0616Ra; Shanghai LZ Biotech Co., Ltd., Shanghai, China). The analyses were performed according to the manufacturers' instructions. Briefly, a monoclonal antibody specific for rat IL-1β was coated onto the wells of microplates. The tissue homogenate, standard solutions, biotinylated spesific monoclonal antibody and streptavidin-HRP were pipetted into these wells, and then incubated at 37°C for 60 min. After washing, chromogen reagent A and chromogen reagent B were added, which were acted upon by the bound enzyme to produce a color. The mixture was incubated at 37°C for 10 min. Then, a stop solution was added. The intensity of this colored product was directly proportional to the concentration of rat IL-1β present in the original specimen. At the end of the course, the well plates were read at 450 nm via a microplate reader (BioTek, Winooski, USA). The absorbance of the samples was estimated with formulas that used standard graphics.

Gene expression of *IL-1β*

RNA isolation

RNA was isolated from the homogenized kidney tissue samples using a Roche Magna Pure Compact LC device with a MagNA Pure LC RNA Kit (Roche Diagnostics GmbH, Mannheim, Germany). The quantity and quality of the isolated RNA was assessed with a nucleic acid measurement device (MaestroNano; Nucleotest Bio Ltd., Budapest, Hungary). The 50 µL RNA samples were stored at –80°C.

Complementary DNA synthesis

Complementary DNA (cDNA) was synthesized from the isolated RNA samples using a Transcriptor First Strand cDNA Synthesis Kit (Roche Diagnostics GmbH). For each subject, 1 µL of ddH_2O, 10 µL of RNA and 2 µL of random primer were combined and incubated in a thermal cycler for 10 min at 65°C. After incubation, 4 µL of reaction buffer, 0.5 µL of RNAase, 2 µL of deoxynucleotide mix, and 0.5 µL of reverse transcriptase were added. The reactions were incubated for 10 min at 25°C, for 30 min at 55°C, for 5 min at 85°C, and then they were held at 4°C. At the end of incubation, 1 µL of RNase H was added. The reaction was stopped by allowing the polymerase chain rection (PCR) device to stand for 20 min at 37°C. The prepared product was stored at –80°C.

Quantitative gene expression evaluation with real-time polymerase chain reaction

For each cDNA sample, the gene expression of *IL-1β* and the reference gene (*G6PD*) was analyzed, using a Roche LightCycler 480 II Real-Time PCR instrument (Roche Diagnostics GmbH). The PCR reactions were recorded in a final volume of 20 µL, including 5 µL of cDNA, 3 µL of distilled water, 10 µL of LightCycler 480 Probes Master (Roche Diagnostics GmbH), and 2 µL of primer-probe set (Real-Time Ready single assay; Roche Diagnostics GmbH). The cycle conditions of the relative quantitative PCR (qPCR) were preincubation at 95°C for 10 min, followed by 45 amplification cycles of 95°C for 10 s, at 6°C for 30 s and at 72°C for 1 s, followed by cooling at 40°C for 30 s. The qPCR analysis and the calculation of quantification cycle (Cq) values for relative quantification were performed with the LightCycler 480 Software, v. 1.5 (Roche

Diagnostics GmbH). Relative quantitative amounts were calculated by dividing the target genes by the expression level of the reference gene. The reference gene was used for the normalization of the target gene expression.

Histopathological examination

The renal tissues taken from the rats were fixed in 10% formalin for 24 h. Following the routine processing of tissue-embedded paraffin sections, 4 µm slices were obtained from the paraffin blocks. After deparaffinization and rehydration, the slices were stained with hematoxylin and eosin (H&E). The stained slices were evaluated under a light microscope (Olympus BX 52; Olympus, Tokyo, Japan) by a pathologist who did not know the applied treatment protocol. To assess inflammation and histopathological damage, some symptoms were examined, such as glomerular and tubular necrosis, dilatation and congestion in the blood vessels, and edema and hemorrhage in the interstitial area.

Statistical analysis

Statistical analyses were performed using the Statistical Package for Social Sciences, Windows v. 19.0 (SPSS Inc., Chicago, USA). Descriptive statistics for each variable were determined. The normality of data distribution was assessed by the Kolmogorov-Smirnov test. The results for continuous variables were demonstrated as mean ± standard error of the mean (mean ±SEM). The significance of differences between the groups was determined using the one-way analysis of variance (ANOVA) test followed by Tukey's analysis. The results obtained from the drug-treated groups were evaluated in comparison with the Cis and C groups. A p-value <0.05 was considered significant.

Results

Biochemical results

The MDA level was significantly higher ($p < 0.001$) in the Cis group (4.75 ±0.25 nmol/mL) than that of the Cis + ANA50, Cis + ANA100 and C groups (2.93 ±0.08 nmol/mL, 1.93 ±0.14 nmol/mL and 2.03 ±0.39 nmol/mL, respectively). As seen in Fig. 1, the amount of MDA was significantly higher in the kidney tissue of the Cis group rats than in the C group ($p < 0.001$). The level of MDA was significantly lower in the kidney tissue of the Cis + ANA50 and Cis + ANA100 groups compared to the Cis group ($p < 0.001$). There was a significant difference in the MDA levels between the Cis + ANA50 and C groups ($p < 0.01$), while the levels of MDA were almost the same between the Cis + ANA100 and C groups ($p > 0.05$).

The tGSH level in the Cis group (1.80 ±0.14 mg/L) was significantly lower than that of the Cis + ANA50, Cis + ANA100 and C groups (3.15 ±0.18 mg/L; $p < 0.005$, 5.03 ±0.29 mg/L; $p < 0.001$ and 5.47 ±0.27 mg/L; $p < 0.001$, respectively). The level of tGSH was significantly higher in the kidney tissue of the Cis + ANA50 and Cis + ANA100 groups than in the Cis group ($p < 0.001$). There was a significant difference between the tGSH levels in the Cis + ANA50 and C groups, while the levels of tGSH were almost the same between the Cis + ANA100 and C groups (Fig. 2).

The SOD activity measured in the kidney tissue of the Cis group rats was 8.57 ±0.26 U/g protein, and the SOD activity in the Cis + ANA50, Cis + ANA100 and C groups were 5.55 ±0.34 U/g protein, 3.8 ±0.3 U/g protein and 3.4 ±0.22 U/g protein, respectively (Fig. 3).

The quantity of IL-1β was measured as 5.3 ±0.19 pg/mL in the kidney tissue of the Cis group. However, the amount of IL-1β was calculated as 3.1 ±0.16 pg/mL, 1.9 ±0.09 pg/mL and 1.6 ±0.13 pg/mL in the Cis + ANA50, Cis + ANA100 and C groups, respectively (Fig. 4).

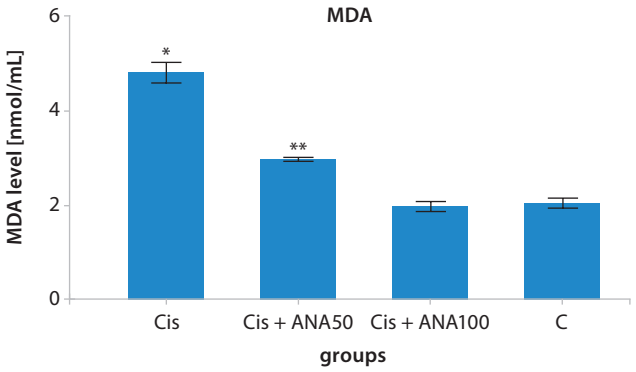

Fig. 1. The MDA levels in the study groups

MDA – malondialdehyde; Cis – group receiving cisplatin only; Cis + ANA50 – group receiving cisplatin and 50 mg/kg of anakinra; Cis + ANA100 – group receiving cisplatin and 100 mg/kg of anakinra; C – control group, receiving no drugs; * $p < 0.001$ compared with the C group; ** $p < 0.01$ compared with the C group.

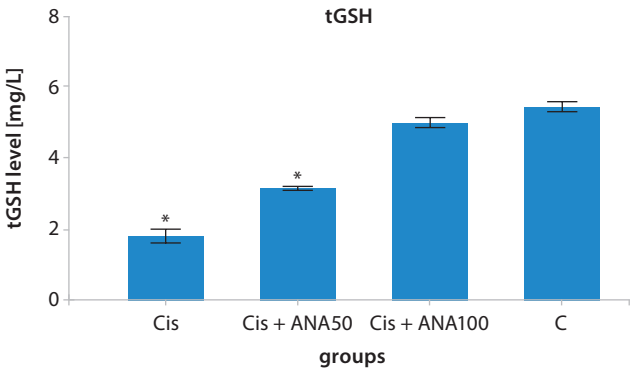

Fig. 2. The tGSH levels in the study groups

tGSH – total glutathione; Cis – group receiving cisplatin only; Cis + ANA50 – group receiving cisplatin and 50 mg/kg of anakinra; Cis + ANA100 – group receiving cisplatin and 100 mg/kg of anakinra; C – control group, receiving no drugs; * $p < 0.001$ compared with the C group.

Interleukin-1 beta gene expression results

The *IL-1β* gene expression level was significantly higher ($p < 0.001$) in the Cis group (6.33 ±0.27) than in the Cis + ANA50, Cis + ANA100 and C groups (3.63 ±0.20, 2.62 ±0.18, and 2.22 ±0.21, respectively). As seen in Fig. 5, the gene expression level of *IL-1β* was significantly higher in the kidney tissue of the Cis group rats compared to other groups ($p < 0.001$). There was no statistically significant difference between the Cis + ANA100 and C groups regarding the *IL-1β* gene expression levels ($p > 0.05$).

Histopathological results

Histopathological examination of the renal tissue of the C group showed normal glomerular structure, Bowman's capsule and Bowman's space (Fig. 6A). However, a wide hemorrhagic area, dilated and congested blood vessels, and interstitial inflammation were observed in the Cis group (Fig. 6B). Moreover, in the renal tissue of the Cis group, hemorrhage was accompanied by glomerular and tubular damage, edema (circle arrow), and interstitial hemorrhage areas (Fig. 6C). Tubular necrosis, interstitial infiltration, and dilated and congested blood vessels were observed in the renal tissue of the Cis group (Fig. 6D). A near-normal appearance, mildly persistent tubule irregularities, and hemorrhage were found in the kidney glomeruli of the Cis + ANA50 group rats (Fig. 6E), whereas protected near-normal glomerulus, proximal and distal tubules were observed in the renal tissue of the group administered 100 mg/kg of anakinra (Fig. 6F).

Discussion

In this study, the effect of anakinra on cisplatin-induced nephrotoxicity in rats was investigated through biochemical and histopathological findings, and through gene expression analysis. Cisplatin increased the levels of MDA and IL-1β, and decreased the levels of tGSH in the renal tissue of rats. Anakinra prevented an increase of MDA and IL-1 β, and a decrease of tGSH due to cisplatin. Additionally, the histopathological examination of anakinra used at a dosage of 100 mg/kg was found to improve renal damage which occurred due to cisplatin.

The pathogenesis of the nephrotoxic effect of cisplatin has not been fully elucidated; however, it has been argued in previous studies that the increase in the production of reactive oxygen species (ROS) leads to nephrotoxicity.[16] As is known, ROS play a key role in the pathogenesis of cellular damage. As it is understood from the results of our biochemical experiment, the amount of MDA was increased and the amount of tGSH was decreased in the renal tissue of the rats administered cisplatin. It has also been reported that cisplatin causes oxidative damage to the kidneys by increasing the amount of MDA.[17] The increase in the MDA level, the end product of lipid peroxidation

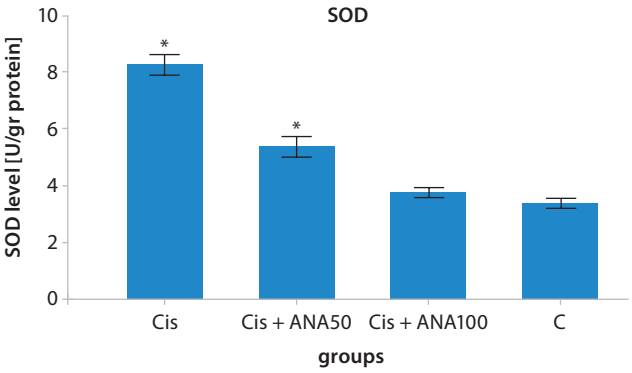

Fig. 3. The SOD levels in the study groups

SOD – superoxide dismutase; Cis – group receiving cisplatin only; Cis + ANA50 – group receiving cisplatin and 50 mg/kg of anakinra; Cis + ANA100 – group receiving cisplatin and 100 mg/kg of anakinra; C – control group, receiving no drugs; * $p < 0.001$ compared with the C group.

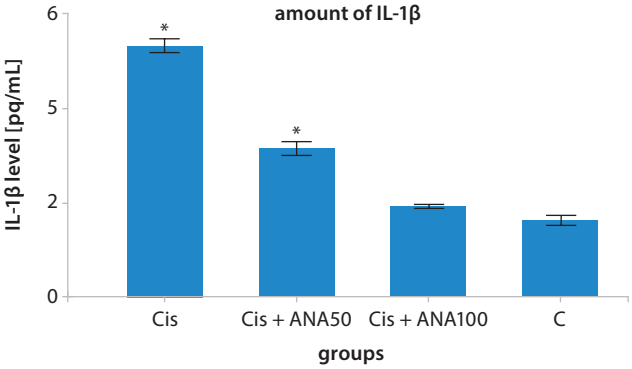

Fig. 4. The IL-1β levels in the study groups

IL-1β – interleukin-1β; Cis – group receiving cisplatin only; Cis + ANA50 – group receiving cisplatin and 50 mg/kg of anakinra; Cis + ANA100 – group receiving cisplatin and 100 mg/kg of anakinra; C – control group, receiving no drugs; * $p < 0.001$ compared with the C group.

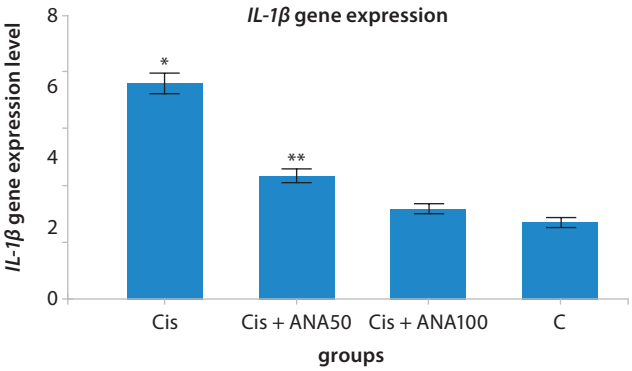

Fig. 5. The *IL-1β* gene expression levels in the study groups

IL-1β – interleukin-1β; Cis – group receiving cisplatin only; Cis + ANA50 – group receiving cisplatin and 50 mg/kg of anakinra; Cis + ANA100 – group receiving cisplatin and 100 mg/kg of anakinra; C – control group, receiving no drugs; * $p < 0.001$ compared with the C group; ** $p < 0.005$ compared with the C group.

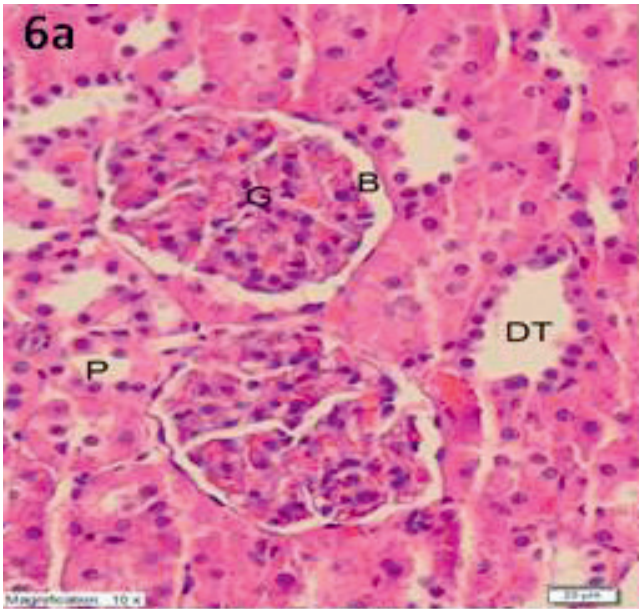

Fig. 6A. A section showing normal glomerular structure, Bowman's capsule and space, and proximal and distal tubules in the renal tissue of the control group (H&E, ×200 magnification)

G – glomerulus; B – Bowman's capsule; P – proximal tubule; D – distal tubules; H&E – hematoxylin and eosin staining.

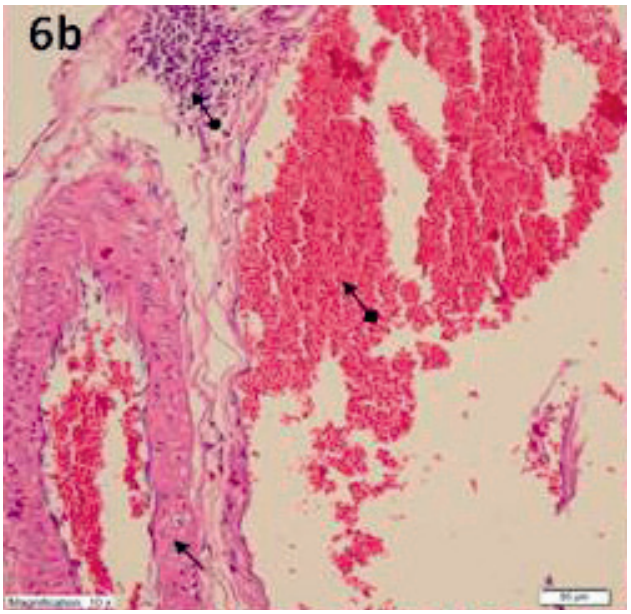

Fig. 6B. A section involving a wide hemorrhage area (square arrow), a dilated, congested blood vessel (straight arrow) and interstitial inflammation in the Cis group (H&E, ×200 magnification)

Cis – group receiving cisplatin only; H&E – hematoxylin and eosin staining.

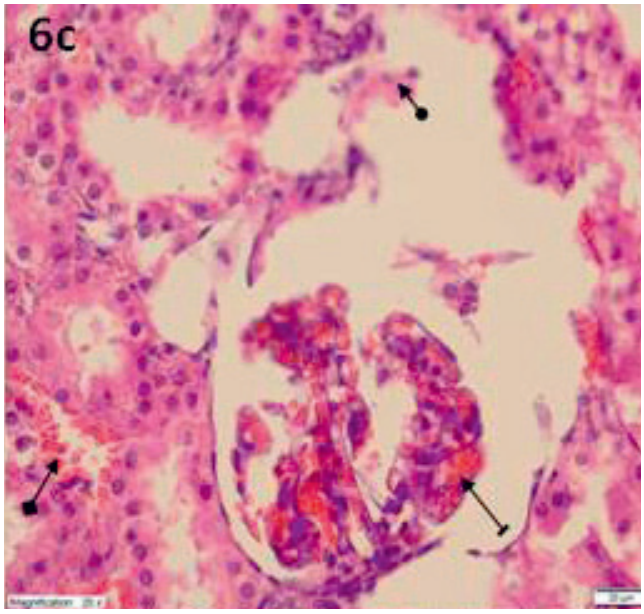

Fig. 6C. A section showing hemorrhage accompanied by glomerular damage (line arrow), diffuse tubular damage, edema (circle arrow), and an interstitial hemorrhage area (square arrow) in the Cis group (H&E, ×400 magnification)

Cis – group receiving cisplatin only; H&E – hematoxylin and eosin staining.

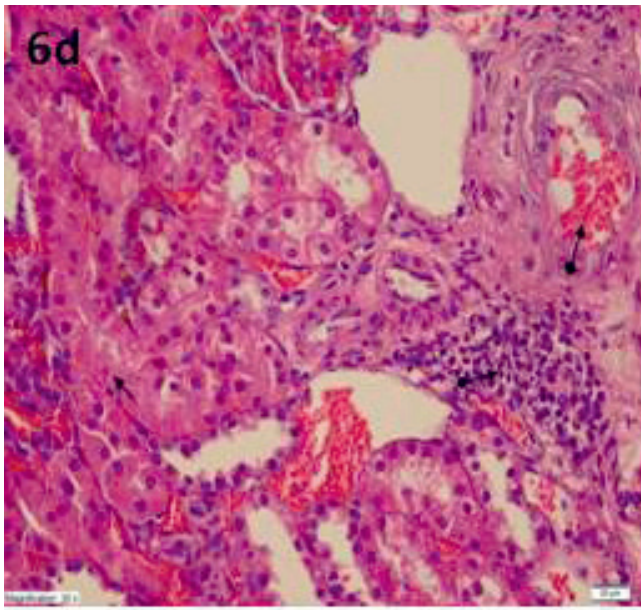

Fig. 6D. A section involving tubular necrosis (straight arrow), interstitial infiltration (circle arrow) and dilated, congested blood vessels (square arrow) in the renal tissue of the Cis group (H&E, ×400 magnification)

Cis – group receiving cisplatin only; H&E – hematoxylin and eosin staining.

in the tissues, is indicative of the increased ROS.[18] It has also been documented that oxidative stress and inflammation are important factors in the development of cisplatin-induced nephrotoxicity.[19] In our study, significant increases in the amount of MDA, as well as in the pro-inflammatory *IL-1β* gene expression and amounts, were noted in the kidneys of animals receiving cisplatin.

Interleukin-1 beta has a number of functions, including the oxidative burst of neutrophils via the signaling molecules of inflammation and the release of free radicals.[20] The increased expression and amount of IL-1β we found supports the direct association between IL-1β and oxidative stress in the renal tissue with high MDA and low tGSH and SOD levels. Additionally, it has been stated

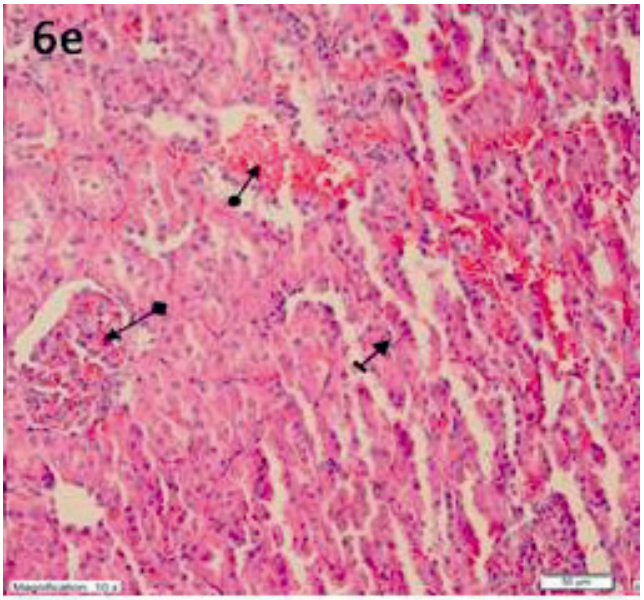

Fig. 6E. A section involving a near-normal appearance (square arrow), mildly persistent tubular irregularities (line arrow) and hemorrhage areas (circle arrow) in the kidney glomeruli of the Cis + ANA50 group (H&E, ×200 magnification)

Cis + ANA50 – group receiving cisplatin and 50 mg/kg of anakinra; H&E – hematoxylin and eosin staining.

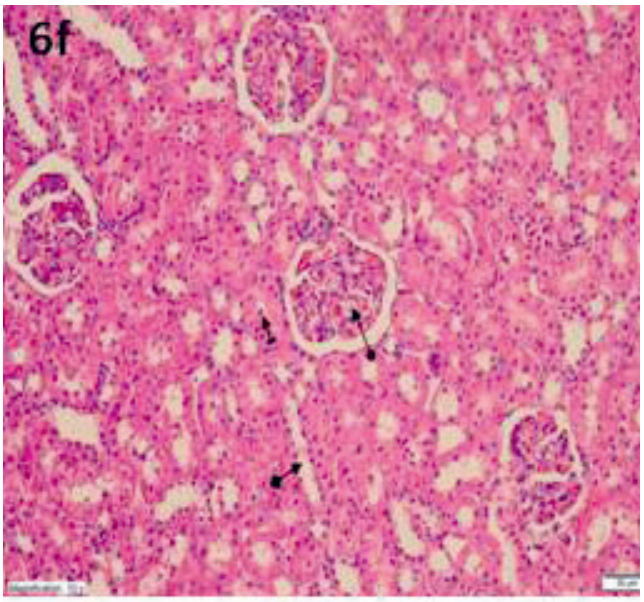

Fig. 6F. A section showing a near-normal glomerulus (circle arrow), proximal tubule (line arrow), and distal tubule (square arrow) in the renal tissue of the Cis + ANA100 group (H&E, ×200 magnification)

Cis + ANA100 – group receiving cisplatin and 100 mg/kg of anakinra; H&E – hematoxylin and eosin staining.

with histopathological examinations that cisplatin leads to renal damage by increasing the levels of oxidants and of IL-1β. Cisplatin is known to cause interstitial inflammation, dilated and congested blood vessels, hemorrhage, and edema in the kidneys.[21–23] Furthermore, it has been argued that the serious side effects of cisplatin, such as tubular necrosis, are caused by the induction of cytokine production.[24] In our experimental results, we also found that there was evidence of inflammatory markers (hemorrhage, dilated and congested blood vessels, interstitial inflammation, and edema), glomerular damage and tubular necrosis in the kidney tissues of the cisplatin group, whose MDA and IL-1β gene expression levels increased significantly. These biochemical and histopathological findings suggest that oxidative stress develops in the kidney tissue when we administer cisplatin.

There are endogenous antioxidant defense systems against ROS in living tissues. However, an overproduction of ROS leads to the consumption of the antioxidant defense system and also to oxidative stress.[25] In our current study, the levels of non-enzymatic and enzymatic antioxidants, such as tGSH and SOD, in the kidney tissue of the cisplatin group (in which the above-mentioned histopathological damage was observed) was decreased. There are studies showing that a significant reduction in the amount of tGSH is associated with oxidative stress in cisplatin nephrotoxicity.[26] It has also been reported that the SOD activity decreases in the kidney tissue with tubular damage, apoptosis and inflammation due to cisplatin treatment.[27] These results support the hypothesis that cisplatin nephrotoxicity is associated with oxidative stress.

This information has led to the testing of anti-inflammatory and antioxidant drugs against cisplatin nephrotoxicity. The IL-1β receptor antagonist anakinra, which is used against the nephrotoxicity of cisplatin, has been found to prevent the increase in MDA and IL-1β, caused by cisplatin, and also to decrease the tGSH and SOD levels in the kidney tissue. The antioxidant and anti-inflammatory features of anakinra are believed to protect the renal tissue against the oxidative damage of cisplatin.[7,8] In addition, there are studies associating the protective effect of anakinra with the antioxidant activity resulting from the blockage of IL-β receptors.[9] Severe pathological findings were observed in the renal tissue of the Cis group with significantly increased levels of oxidants and IL-1β, such as wide hemorrhage areas, dilated and congested blood vessels, interstitial inflammation, glomerular and tubular damage, edema, and tubular necrosis. However, while mildly persistent tubule irregularities and hemorrhage were seen in the Cis + ANA50 group with high amounts of tGSH identified, the glomerulus, proximal tubule and distal tubule were evaluated as healthy in the Cis + ANA100 group, in which the amount of tGSH was found to be higher. There are studies in the literature which histopathologically demonstrate that hemorrhage areas were developed in the renal tissues of animals treated with cisplatin.[21]

The formation of congested blood vessels due to cisplatin has also been shown in previous studies.[22] In addition, cisplatin leads to interstitial inflammation and edema in the kidneys.[21,23] It has been stated that cisplatin causes more severe damage in the kidney tubules, such as necrosis.[22] The role of free oxygen radicals has also been demonstrated in cellular death due to cisplatin.[5]

As a result, severe histopathological damage was developed in the kidney tissue of the cisplatin group, which had high levels of the oxidant MDA and of gene expression, and high amount of pro-inflammatory IL-1β, but also had a low amount of the antioxidant tGSH. It was found that the increase in MDA and *IL-1β* gene expression and amount as well as the decrease in tGSH due to cisplatin in the kidney tissue were significantly inhibited by anakinra at a dose of 100 mg/kg compared to a dose of 50 mg/kg. It was observed that histopathologically, anakinra at a dose of 100 mg/kg better protects the renal tissue against the oxidative damage of cisplatin and more efficiently suppresses the production of MDA and IL-1β. This information suggests that anakinra may be useful in clinically reducing the toxic effect of cisplatin on the kidneys.

References

1. Lebwohl D, Canetta R. Clinical development of platinum complexes in cancer therapy: A historical perspective and an update. *Eur J Cancer*. 1998;34(10):1522–1534.
2. Hartshorn EA, Anand AJ, Bashey B. Newer insights into cisplatin nephrotoxicity. *Ann Pharmacother*. 1993;27(12):1519–1525.
3. Baek SM, Kwon CH, Kim JH, Woo JS, Jung JS, Kim YK. Differential roles of hydrogen peroxide and hydroxyl radical in cisplatin-induced cell death in renal proximal tubular epithelial cells. *J Lab Clin Med*. 2003;142(3):178–186.
4. Fouad AA, Morsy MA, Gomaa W. Protective effect of carnosine against cisplatin-induced nephrotoxicity in mice. *Environ Toxicol Pharmacol*. 2008;25(3):292–297.
5. Özen S, Akyol Ö, Iraz M, et al. Role of caffeic acid phenethyl ester, an active component of propolis, against cisplatin-induced nephrotoxicity in rats. *J Appl Toxicol*. 2004;24(1):27–35.
6. Zirak MR, Rahimian R, Ghazi-Khansari M, et al. Tropisetron attenuates cisplatin-induced nephrotoxicity in mice. *Eur J Pharmacol*. 2014;738:222–229.
7. Cvetkovic RS, Keating G. Anakinra. *BioDrugs*. 2002;16(4):303–311.
8. Hasturk AE, Yilmaz ER, Turkoglu E, et al. Potential neuroprotective effect of Anakinra in spinal cord injury in an in vivo experimental animal model. *Neuroscience*. 2015;20(2):124.
9. Askin Esen Hasturk M, Yilmaz ER, Turkoglu E, et al. Therapeutic evaluation of interleukin-1 beta antagonist Anakinra against traumatic brain injury in rats. *Ulus Travma Acil Cerrahi Derg*. 2015;21(1):1–8.
10. Nayki UA, Nayki C, Cetin N, et al. Effect of Kineret® on ovarian ischemia reperfusion injury in a rat model. *J Obstet Gynaecol Res*. 2016;42(11):1525–1533.
11. Kuyrukluyıldız U, Küpeli İ, Bedir Z, et al. The effect of anakinra on paclitaxel-induced peripheral neuropathic pain in rats. *Turk J Anaesthesiol Reanim*. 2016;44(6):287.
12. Coskun R, Turan MI, Turan IS, Gulapoglu M. The protective effect of thiamine pyrophosphate, but not thiamine, against cardiotoxicity induced with cisplatin in rats. *Drug Chem Toxicol*. 2014;37(3):290–294.
13. Ohkawa H, Ohishi N, Yagi K. Assay for lipid peroxides in animal tissues by thiobarbituric acid reaction. *Anal Biochem*. 1979;95(2):351–358.
14. Sedlak J, Lindsay RH. Estimation of total, protein-bound and nonprotein sulfhydryl groups in tissue with Ellman's reagent. *Anal Biochem*. 1968;25:192–205.
15. Sun Y, Oberley LW, Li Y. A simple method for clinical assay of superoxide dismutase. *Clin Chem*. 1988;34(3):497–500.
16. Peres LAB, Cunha AD Jr. Acute nephrotoxicity of cisplatin: Molecular mechanisms. *J Bras Nefrol*. 2013;35(4):332–340.
17. Parlakpinar H, Sahna E, Ozer M, Ozugurlu F, Vardi N, Acet A. Physiological and pharmacological concentrations of melatonin protect against cisplatin-induced acute renal injury. *J Pineal Res*. 2002;33(3):161–166.
18. Girotti AW. Lipid hydroperoxide generation, turnover and effector action in biological systems. *J Lipid Res*. 1998;39(8):1529–1542.
19. Kilic U, Kilic E, Tuzcu Z, et al. Melatonin suppresses cisplatin-induced nephrotoxicity via activation of Nrf-2/HO-1 pathway. *Nutr Metab*. 2013;10(1):7.
20. Dinarello CA. Proinflammatory cytokines. *Chest*. 2000;118(2):503–508.
21. Youssef Nasr A, Al Shahat Ibrahim A. Aged garlic extract ameliorates the oxidative stress, histomorphological and ultrastructural changes of cisplatin-induced nephrotoxicity in adult male rats. *Microsc Res Tech*. 2015;78(6):452–461.
22. Boroushaki MT, Rajabian A, Farzadnia M, et al. Protective effect of pomegranate seed oil against cisplatin-induced nephrotoxicity in rat. *Ren Fail*. 2015;37(8):1338–1343.
23. Alfieri AB, Cubeddu LX. Role of NK1 receptors on cisplatin-induced nephrotoxicity in the rat. *Naunyn Schmiedebergs Arch Pharmacol*. 2000;361(3):334–338.
24. Pabla N, Dong Z. Cisplatin nephrotoxicity: Mechanisms and renoprotective strategies. *Kidney Int*. 2008;73(9):994–1007.
25. Kisaoglu A, Borekci B, Yapca OE, Bilen H, Suleyman H. Tissue damage and oxidant/antioxidant balance. *Eurasian J Med*. 2013;45(1):47.
26. Noori S, Mahboob T. Antioxidant effect of carnosine pretreatment on cisplatin-induced renal oxidative stress in rats. *Indian J Clin Biochem*. 2010;25(1):86–91.
27. Karakoc H, Altintas R, Parlakpinar H, et al. Protective effects of molsidomine against cisplatin-induced nephrotoxicity. *Adv Clin Exp Med*. 2014;24(4):585–593.

Health needs in local government policies in Poland in the context of anti-smoking health policy programs

Anna Augustynowicz[1,A,B,D,F], Aleksandra I. Czerw[1,C,D,F], Andrzej Deptała[2,3,E,F]

[1] Department of Public Health, Faculty of Health Sciences, Medical University of Warsaw, Poland
[2] Department of Cancer Prevention, Faculty of Health Sciences, Medical University of Warsaw, Poland
[3] Department of Oncology and Hematology, Central Clinical Hospital of the Ministry of Interior, Warszawa, Poland

A – research concept and design; B – collection and/or assembly of data; C – data analysis and interpretation;
D – writing the article; E – critical revision of the article; F – final approval of the article

Advances in Clinical and Experimental Medicine, ISSN 1899-5276 (print), ISSN 2451-2680 (online) *Adv Clin Exp Med*. 2018;27(12):1651–1659

Address for correspondence
Aleksandra Czerw
E-mail: ola_czerw@wp.pl

Funding sources
None declared

Conflict of interest
None declared

Received on June 21, 2016
Revised on July 26, 2016
Accepted on June 13, 2017

Abstract

Background. According to the World Health Organization (WHO), every year tobacco smoking kills around 5.4 million people worldwide. Tobacco smoking is a major risk factor for cardiovascular diseases, respiratory diseases and cancer. In Poland, an average of 67,000 people die every year on account of smoking.

Objectives. The aim of the study was to evaluate the health security guaranteed by local governments based on an analysis of health policy programs associated with tobacco consumption, which were conducted in Poland from 2009 to 2014 by local governments.

Material and methods. The study was based on desk research. The data was sourced from the annual reports submitted to the Minister of Health, concerning the health policy programs which were carried out. The analysis covered programs whose name, objective or description of tasks indicated that they concerned tobacco smoking.

Results. The largest number of programs was completed in the West Pomeranian, Warmian-Masurian and Masovian voivodeships. The smallest number of programs were completed in Kuyavian-Pomeranian, Łódź and Opole voivodeships. The greatest number of programs were carried out by municipalities, followed by counties and county towns, and finally by self-governments of the voivodeships. The number of preventive programs was significantly greater than the number of other types of programs. The majority of programs were aimed at children; there were fewer programs dedicated to adults. The expenditure on the programs was the highest in self-governments of the voivodeships, while the lowest was in municipalities.

Conclusions. The steady growth in the number of anti-smoking programs completed in 2009–2014 was one of the factors that reduced tobacco smoking. In view of the mortality rates due to cardiovascular diseases, the inhabitants of Lublin and Warmian-Masurian voivodeships had their health needs addressed most efficiently. In the case of mortality rates due to tracheal, bronchial and lung cancer, the health needs of the inhabitants of Warmian-Masurian and West Pomeranian voivodeships were addressed most efficiently.

Key words: health promotion, tobacco smoking, local government, health policy program

DOI
10.17219/acem/74756

Background

Tobacco smoking is one of the most serious contemporary threats to civilization. According to the World Health Organization (WHO), tobacco smoking kills around 5.4 million people every year.[1] Without any action, by 2030 the number of deaths caused by tobacco smoking will exceed 8 million per year. More than 80% of those deaths will occur in developing regions.[1]

Tobacco smoking is a major risk factor for cardiovascular and respiratory diseases, as well as for cancer.[1]

Tobacco consumption is believed to be a risk factor for 6 out of the 8 most common causes of death in the world, i.e., ischemic heart disease, cerebrovascular disease, lower respiratory infection, chronic obstructive pulmonary disease (COPD), tuberculosis, as well as tracheal, bronchial and lung cancer. Smokers usually die of tracheal, bronchial or lung cancer, COPD, and ischemic heart disease.[1]

Despite regular preventive actions, an average of 67,000 people per year dies in Poland on account of smoking (51,000 men and 16,000 women).[2] The dominant causes of death among Poles are cardiovascular diseases and cancers.

In 2010, cardiovascular diseases claimed the lives of 174,003 people in Poland; they caused 456 deaths per 100,000 people.[3] Cardiovascular diseases accounted for around 46% of deaths in 2010 and 45.5% in 2011. They are also the main cause of premature death (before the age of 65).[4] It is estimated that with current incidence trends and the rate of aging of the Polish population, the number of deaths due to cardiovascular diseases will exceed 200,000 in 2020.[5]

The most common life-threatening types of malignant tumors among the Polish population are tracheal, bronchial and lung cancer, which claimed the lives of 22,374 people in 2010, i.e., 24% of all deaths due to malignant tumors.[3] In 2010, lung cancer accounted for 31.2% of deaths due to cancer among men and 15% of deaths among women.[6] In 2013, similarly, the largest percentage of cancer deaths among men and women were due to lung cancer – 30.6% and 15.9%, respectively.[7]

According to an analysis conducted by the WHO, there would be around 80% fewer cases of cardiovascular diseases, strokes and type 2 diabetes, and around 40% fewer cancer cases if we managed to eliminate the major risk factors, including tobacco smoking.[8]

In light of the data presented above, an assessment of the implementation of health policy programs aimed at reducing tobacco smoking in the Polish population seems appropriate.

Objectives

The aim of the study was to evaluate how local governments addressed the health needs of their citizens by analyzing the health policy programs concerning tobacco product consumption completed in Poland between 2009 and 2014.

Methods

The study was based on desk research. The data was sourced from the annual reports submitted by voivodes to the Minister of Health on the health policy programs implemented by local governments. The analysis covered all anti-smoking health policy programs completed from 2009 to 2014 – 1,482 programs in total.

The analysis covered programs whose name, objective or description of tasks indicated that they had concerned tobacco smoking. The programs were classified into one of 3 groups: preventive programs, diagnostic and therapeutic programs, and preventive, diagnostic and therapeutic programs. The classification into particular groups was based on the objective specified by the given local government, the type of program and the description of actions taken within the program. The analysis of the differences in the number of programs between voivodeships and the number of programs completed in particular years was based on a one-sample χ^2 test. The differences in terms of the number of programs completed between 2009 and 2014 by municipalities, counties and voivodeships were analyzed with Cochran's Q test, just as the differences in terms of specific programs completed in particular years. The differences in terms of the costs of programs realized depending on the type of program and the type of local government that implemented the program were analyzed by two-way analysis of variance (ANOVA). One-way ANOVA was applied for the evaluation of differences in the average values of expenditure on the programs in voivodeships in particular years.

Results

Based on a χ^2 test for 1 sample, statistically significant differences concerning the number of programs implemented in particular voivodeships were found (χ^2 [15] = 791.68, $p < 0.001$).

The largest number of programs was implemented in West Pomeranian, Warmian-Masurian and Masovian voivodeships. The smallest number of programs was carried out in Kuyavian-Pomeranian, Łódź and Opole voivodeships (Fig. 1).

Based on a χ^2 test for 1 sample, statistically significant differences in terms of the number of programs implemented in the subsequent years were found (χ^2[5] = 24.34, $p < 0.001$).

The number of programs implemented between 2013 and 2014 was higher than the number of programs implemented between 2009 and 2012 (Fig. 2).

Statistically significant dynamics of change were found in the number of programs implemented in subsequent years in Lower Silesian, Lublin, Lesser Poland, Masovian, Subcarpathian, Pomeranian, Silesian, Warmian-Masurian, Greater Poland, West Pomeranian, and Lubusz voivodeships. Such statistically significant dynamics of change

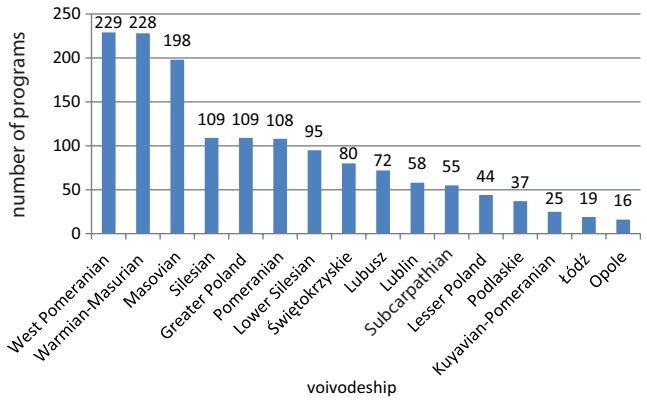

Fig. 1. Frequency distribution – the number of programs implemented in particular voivodeships between 2009 and 2014

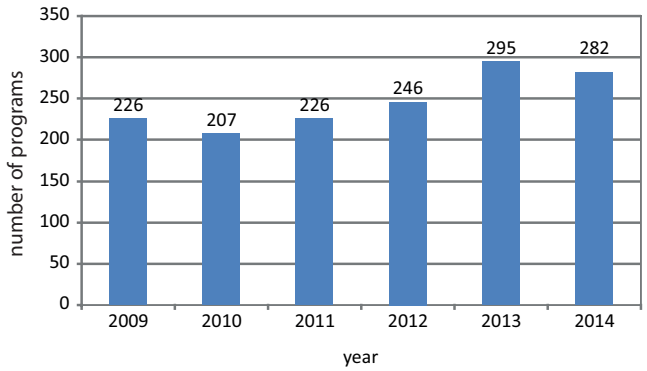

Fig. 2. Frequency distribution – the number of programs implemented between 2009 and 2014

were not found in the number of programs implemented in Kuyavian-Pomeranian, Łódź, Opole, Podlaskie, and Świętokrzyskie voivodeships (Table 1).

The number of programs implemented in subsequent years grew in Lower Silesian, Masovian, Warmian-Masurian, West Pomeranian, Greater Poland, and Lubusz voivodeships. The number of programs implemented in Łódź, Opole, Silesian, and Świętokrzyskie voivodeships dropped. The number of programs implemented in Lublin, Podlaskie, Pomeranian, and Subcarpathian voivodeships was found to have dropped, but then it increased (Table 1).

Based on Cochran's Q test, statistically significant differences in the number of programs implemented by particular local government units were found ($Q(2) = 670.07$, $p < 0.001$).

The largest number of programs were implemented by municipalities, followed by counties. The smallest number of programs was conducted by voivodeships (Fig. 3).

A statistically significant increase in the number of programs implemented by municipalities in subsequent years was found. No statistically significant changes were found in the number of programs implemented by counties and self-governments of the voivodeships (Table 2).

The analysis covered the variation of programs in terms of the type: preventive programs, diagnostic and therapeutic programs, or preventive, diagnostic and therapeutic programs (Fig. 4).

Based on Cochran's Q test, statistically significant differences in the number of programs implemented by particular local governments were found ($Q(2) = 1{,}964.98$, $p < 0.001$).

The number of preventive programs was significantly higher compared to diagnostic and therapeutic programs, and to preventive, diagnostic and therapeutic programs.

A statistically significant increase in the number of preventive programs implemented in subsequent years, and

Table 1. Frequency distribution – programs implemented in subsequent years in particular voivodeships

Variables	Year						Test		
Voivodeship	2009	2010	2011	2012	2013	2014	χ^2	df	p-value
Lower Silesian	5	15	10	21	23	21	16.22**	5	0.006
Kuyavian-Pomeranian	7	7	3	3	3	2	5.96	5	0.310
Lublin	15	2	7	14	10	10	11.72*	5	0.039
Łódź	7	5	1	1	4	1	10.37	5	0.065
Lesser Poland	17	13	7	1	3	3	27.73***	5	0.000
Masovian	25	24	35	27	49	38	14.12*	5	0.015
Opole	3	5	2	3	2	1	3.50	5	0.623
Subcarpathian	2	5	13	23	8	4	33.04***	5	0.000
Podlaskie	7	5	3	6	4	12	8.24	5	0.143
Pomeranian	19	22	17	1	24	25	21.75**	5	0.001
Silesian	44	10	24	19	8	4	59.05***	5	0.000
Świętokrzyskie	20	15	15	13	10	7	7.60	5	0.180
Warmian-Masurian	21	26	26	43	56	56	32.89***	5	0.000
Greater Poland	8	19	28	10	18	26	18.10**	5	0.003
West Pomeranian	23	29	27	39	60	51	28.32***	5	0.000
Lubusz	3	5	8	22	13	21	27.33***	5	0.000

χ^2 – chi-squared test; df – degree of freedom; p – statistical significance; *p < 0.05; **p < 0.01; ***p < 0.001.

Table 2. Frequency distribution – programs implemented in subsequent years by local governments, with χ^2 test values for 1 sample

Local government unit	Year						Test		
	2009	2010	2011	2012	2013	2014	χ^2	df	p-value
Municipality	117	103	129	153	176	173	32.10**	5	0.001
County	97	92	79	82	112	104	8.54	5	0.129
Self-governments of the voivodeships	14	12	5	9	7	5	8.00	5	0.156

χ^2 – chi-squared test; df – degree of freedom; p – statistical significance; **p < 0.01.

Table 3. Frequency distribution – preventive programs, diagnostic and therapeutic programs, and preventive, diagnostic and therapeutic programs implemented in subsequent years by local governments, with χ^2 test values for 1 sample

Program type	Year						Test		
	2009	2010	2011	2012	2013	2014	χ^2	df	p-value
Preventive	166	161	185	231	275	263	57.91***	5	0.000
Diagnostic and therapeutic	19	14	15	10	16	9	5.12	5	0.401
Preventive, diagnostic and therapeutic	39	32	11	3	4	10	70.15***	5	0.000

χ^2 – chi-squared test; df – degree of freedom; p – statistical significance; ***p < 0.001.

Table 4. The number of preventive programs, diagnostic and therapeutic programs, and preventive, diagnostic and therapeutic programs implemented by municipalities, counties and voivodeships

Program type	Local government unit			Test		
	municipality	county	voivodeship	Q	df	p-value
Preventive	759	499	22	654.92***	2	0.000
Diagnostic and therapeutic	42	29	11	17.73***	2	0.000
Preventive, diagnostic and therapeutic	48	35	19	12.79**	2	0.002

Q – Cochran's Q test value; df – degree of freedom; p – statistical significance; **p < 0.01; ***p < 0.001.

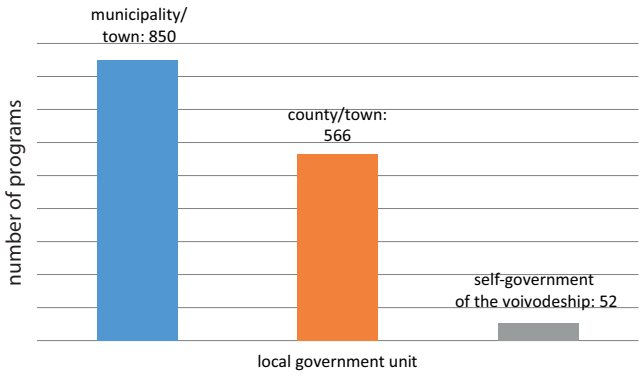

Fig. 3. Frequency distribution – the number of programs implemented between 2009 and 2014 by local governments

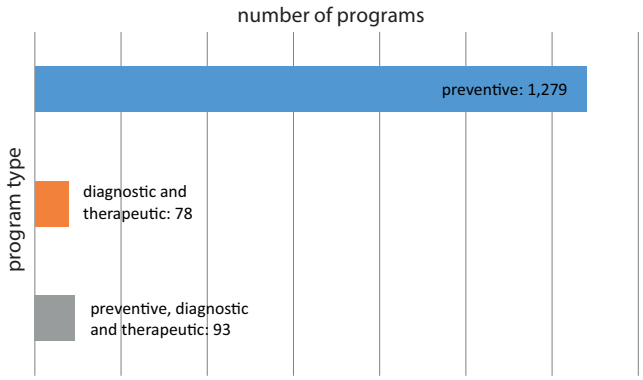

Fig. 4. Frequency distribution – the number of preventive programs, diagnostic and therapeutic programs, and preventive, diagnostic and therapeutic programs implemented between 2009 and 2014

a statistically significant decrease in the number of preventive, diagnostic and therapeutic programs were found (Table 3).

The associations between the types of programs (preventive programs, diagnostic and therapeutic programs, and preventive, diagnostic and therapeutic programs) and the type of local government (municipality, county and voivodeship) were also analyzed (Table 4).

It was found that the greatest number of programs, regardless of the type, were implemented by municipalities, while the smallest number of them were implemented by self-governments of the voivodeships.

The analysis also covered the variation of programs in terms of the population covered by a given program. The authors checked how many programs were aimed at children and teenagers, and how many at adults, as well as how many programs were dedicated to women, and how many to men (Fig. 5).

Based on Cochran's Q test, statistically significant differences in the number of programs aimed at adults, children, women, and men were found ($Q(3) = 2{,}527.56$, $p < 0.001$).

The largest number of programs were aimed at children.

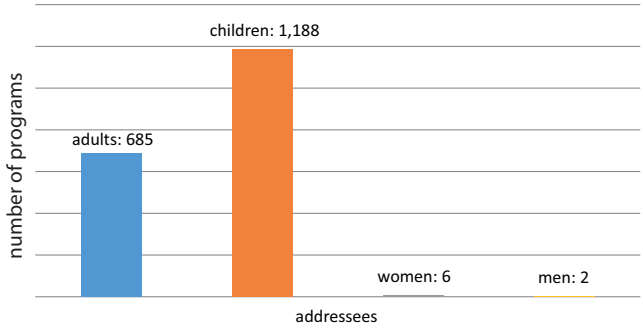

Fig. 5. Frequency distribution – the number of programs addressed to adults, children, women, and men implemented between 2009 and 2014

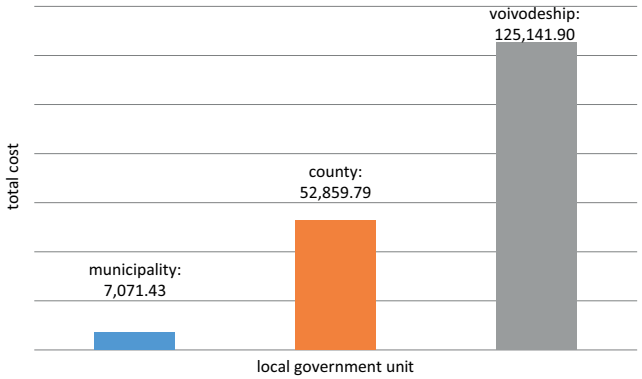

Fig. 6. Mean value of costs (in PLN) of programs implemented by municipalities, counties and voivodeships

Table 5. Mean value of overall costs (in PLN) of preventive programs, diagnostic and therapeutic programs, and preventive, diagnostic and therapeutic programs in municipalities, counties and voivodeships

Variables	Local government unit		
Program type	municipality	county	voivodeship
Preventive	6,982.47	51,653.32	28,332.94
Diagnostic and therapeutic	2,885.02	89,157.12	216,189.17
Preventive, diagnostic and therapeutic	10,758.69	28,329.78	168,732.58

There were fewer programs dedicated to adults. Only 6 programs were aimed specifically at women, and 2 were dedicated to men. Some programs were dedicated both to children and adults, which is why they were classified into both groups.

The analysis also covered the total costs of preventive programs, diagnostic and therapeutic programs, and preventive, diagnostic and therapeutic programs in municipalities, counties and voivodeships (Table 5).

Based on the analyses conducted under two-way ANOVA, statistically significant differences in terms of the costs of programs implemented by particular local governments were found ($F(2.587) = 3.16$, $p < 0.05$, $\eta^2 = 0.01$). No statistically significant differences were found in terms of the costs depending on the type of program ($F(2.587) = 1.28$, $p > 0.05$), nor in terms of the costs depending on the type of program implemented by a municipality, county or voivodeship ($F(4.587) = 0.78$, $p > 0.05$).

The programs implemented by voivodeships entailed the highest costs. The programs implemented by counties cost less, while the programs implemented by municipalities cost the least (Fig. 6).

Based on the results of a one-way ANOVA, no statistically significant differences in the mean values of expenditure on anti-smoking programs in particular years were found ($F(1.592) = 0.70$, $p > 0.05$) (Table 6).

Based on the results of one-way ANOVA, statistically significant differences were found in the mean values of expenditure on anti-smoking programs in the Lublin were to implemented in particular years ($F(5.38) = 3.23$, $p < 0.05$, $\eta^2 = 0.30$) (Table 7).

Table 6. Mean value of expenditure (in PLN) on anti-smoking programs in particular years

Year	M	SD	n
2009	46,488.30	405,518.95	187
2010	33,414.05	173,804.10	105
2011	90,754.79	529,147.92	68
2012	5,499.41	17,326.73	84
2013	24,135.07	104,926.08	82
2014	25,507.68	107,811.46	72
Total	37,877.41	302,283.12	598

M – mean value; SD – standard deviation; n – number of programs.

The expenditure in 2010 was statistically higher than the expenditure incurred in the other years.

There were statistically significant differences in the mean values of expenditure on anti-smoking programs in Łódź Voivodeship implemented in particular years ($F(4.11) = 25.02$, $p < 0.001$, $\eta^2 = 0.90$) (Table 8).

The expenditure in 2014 was statistically higher than the expenditure incurred in the other years.

There were statistically significant differences in the mean values of expenditure on anti-smoking programs in Subcarpathian Voivodeship implemented in particular years ($F(4.20) = 16.80$, $p < 0.001$, $\eta^2 = 0.77$) (Table 9).

Table 7. Mean value of expenditure (in PLN) on anti-smoking programs in Lublin Voivodeship in particular years

Year	M	SD	n
2009	10,869.93	23,710.77	14
2010	113,900.00	158,533.34	2
2011	770.00	625.81	7
2012	903.35	1,109.70	8
2013	25,319.69	65,039.83	7
2014	794.14	1,094.89	6
Total	13,059.06	43,785.53	44

M – mean value; SD – standard deviation; n – number of programs.

Table 8. Mean value of expenditure (in PLN) on anti-smoking programs in Łódź Voivodeship in particular years

Year	M	SD	n
2009	21,636.31	48,202.18	6
2010	1,710.30	730.63	4
2011	65,000.00	.	1
2012	–	–	–
2013	12,789.50	15,614.60	4
2014	357,750.00	.	1
Total	38,160.44	91,190.50	16

M – mean value; SD – standard deviation; n – number of programs.

Table 9. Mean value of expenditure (in PLN) on anti-smoking programs in Subcarpathian Voivodeship in particular years

Year	M	SD	n
2009	105,219.90	35,666.32	2
2010	66,839.43	80,383.09	2
2011	–	–	–
2012	571.38	1,149.19	16
2013	570.00	.	1
2014	152.50	153.05	4
Total	14,177.63	37,534.09	25

M – mean value; SD – standard deviation; n – number of programs.

The expenditure in 2009–2010 was statistically higher than the expenditure incurred in the other years.

Discussion

The results of research conducted in recent years point to a reduction in the spread of tobacco smoking in Poland. In 2004, the percentage of smokers was 30.1%, while in 2009 it was 29.2%.[9,10] Over the next 5 years, the percentage of smokers dropped by more than 3% and reached 26.1% in 2014.[11] The reduction in the consumption of tobacco is a consequence of legislative actions and all kinds of activities carried out at the national, regional and local levels. This positive trend should be continued in the future.

For cardiovascular diseases, there was the National Program of Prevention and Treatment of Cardiovascular Diseases for 2003–2005, 2006–2008, 2009, and 2010–2012, as well as the National Program of Equal Access to Prevention and Treatment of Cardiovascular Diseases for 2013–2016.[12–16] The programs provided education aimed at the entire society and focused on raising the awareness of risk factors for cardiovascular diseases, including tobacco smoking. For cancers, there was the National Cancer Control Programme, in effect from 2005 to 2015.[17] This program continues as the National Cancer Control Programme for 2016–2024.[18] Those programs provide for actions aimed at health promotion and cancer prevention, including actions focused on the reduction of tobacco smoking. According to the assumptions of the programs, they should be supported by regional and local initiatives, scientific associations, and non-government organizations.

The implementation of local government health policy programs concerning tobacco smoking is an example of regional and local actions. In the period covered by this analysis, the most health policy programs were implemented by municipalities and the fewest by voivodeships. The greatest expenditure on the implementation of anti-smoking programs was incurred by voivodeships, while municipalities spent the least. The structure of expenditure incurred by particular local governments may suggest that the funds are first of all allocated for fulfilling the obligatory health protection tasks defined by law.[19–21]

Most of the programs implemented by local governments from 2009 to 2014 were preventive programs. In 2002, the WHO estimated the proportional contribution of particular risk factors in the overall number of deaths in European countries. Tobacco smoking proved to be a major risk factor in Poland.[22–24] According to the estimates made by the WHO, risk factors accounted for around 55% of deaths in Poland and nearly 40% of years that could have otherwise been lived in health.[23] In this context, the implementation of preventive programs by local governments, and the statistically significant annual increase in the number of preventive programs implemented in subsequent years, should be viewed as positive. The implementation of preventive programs remains in line with the guidelines for effectively fighting tobacco smoking listed in the World WHO's MPOWER policy. The policy aims to protect people from tobacco smoke and to warn them about the dangers of tobacco smoke.[1] The implementation of preventive programs by local governments is in line with the guidelines set forth in the Strategy for Fighting Cancer in Poland for 2015–2024 and the White Book report.[25,26] One of the objectives of the strategy is to prevent cancers caused by tobacco smoking by disseminating information on the negative effects of smoking, specifically among minors.

In the period covered by this analysis, the greatest number of anti-smoking health policy programs were implemented in West Pomeranian, Warmian-Masurian and Masovian voivodeships, while the smallest number of such programs were implemented in Kuyavian-Pomeranian, Łódź and Opole voivodeships. Taking into account the territorial variation, one can conclude that the fewest regular smokers live in Subcarpathian and Lesser Poland voivodeships – around 18% of the adult population. The greatest number of smokers live in Lower Silesian, Kuyavian-Pomeranian, Lubusz, and West Pomeranian voivodeships, where the percentage of regular smokers is 10% higher.[10] Among the voivodeships with the highest percentage of smokers, only West Pomeranian Voivodeship properly addressed the health needs of its inhabitants arising from tobacco consumption. In the period covered by this analysis, the voivodeship implemented

the most anti-smoking health policy programs: 229. From 2009 to 2014, Lower Silesian Voivodeship implemented 95 programs, Lubusz 58, and Kuyavian-Pomeranian only 25. In those voivodeships, the health needs of the inhabitants were not addressed properly.

The analysis also covered the implementation of health policy programs in terms of satisfying the health needs of the inhabitants arising from diseases caused by tobacco smoking.

In 2009 and 2010, the mortality rates due to cardiovascular diseases were the highest in Świętokrzyskie (over 397/100,000), Łódź (over 374/100,000) and Lublin voivodeships. The lowest mortality rates were recorded in Pomeranian (over 281/100,000), Podlaskie (over 304/100,000) and Greater Poland (323/100,000) voivodeships. From 2000 to 2010, the mortality rates due to cardiovascular diseases in Poland dropped by 21%, and the decrease was the most significant in Pomeranian (by 30%) and Silesian (by 29%) voivodeships. The least significant improvement was recorded in Warmian-Masurian (by only 2%) and in Świętokrzyskie (by 6%) voivodeships.[3] In 2012, the highest mortality rates due to cardiovascular diseases were recorded in Silesian, Świętokrzyskie and Lublin voivodeships (over 490/100,000), and the rate was around 25% higher than in Podlaskie Voivodeship, where the lowest rates were recorded (394/100,000).[5] Although the mortality rates in Świętokrzyskie and Łódź voivodeships ranked among the highest, local governments did not increase the number of anti-smoking health policy programs in subsequent years. A downward trend was observed in Świętokrzyskie and Łódź voivodeships from 2009 to 2014. Those voivodeships failed to properly address the health needs of their inhabitants. The actions taken by the local governments of Lublin and Warmian-Masurian voivodeships must be viewed as positive.

The greatest incidence of lung cancer in 2009 was recorded in Warmian-Masurian, Pomeranian and Kuyavian-Pomeranian voivodeships for men, and in Pomeranian, Warmian-Masurian and Kuyavian-Pomeranian voivodeships for women (63/100,000 and 20/100,000, respectively).[27] In 2012, the highest incidence among men was recorded in Warmian-Masurian, Kuyavian-Pomeranian (over 65/100,000) and Pomeranian (over 58/100,000) voivodeships; the highest incidence among women was found in Warmian-Masurian (over 24/100,000) and Kuyavian-Pomeranian voivodeships (over 23/100,000).[9,28] Local governments in West Pomeranian and Warmian-Masurian voivodeships addressed the health needs of the inhabitants most effectively. The activity of local governments in Kuyavian-Pomeranian Voivodeship, who implemented only 25 programs despite high incidence rates, should be viewed as negative. One could also expect a higher number of anti-smoking health policy programs in Pomeranian Voivodeship.

The highest mortality rates due to tracheal, bronchial and lung cancer in 2009–2010 were recorded in Warmian-Masurian, Lubusz (over 195/100,000), Łódź (over 204/100,000), and Kuyavian-Pomeranian (209/100,000) voivodeships. The most favorable situations were recorded in Subcarpathian (over 160/100,000), Opole, Świętokrzyskie, and Lesser Poland (over 168/100,000) voivodeships. In Podkarpackie Voivodeship, where the recorded mortality rates due to tracheal, bronchial and lung cancer in 2000–2001 and 2009–2010 were the lowest in the country, the mortality was 25% lower than the national average, and 42% lower than in Warmian-Masurian Voivodeship.[3] In 2012, the highest standardized mortality ratios due to lung cancer among men were recorded in Warmian-Masurian (over 68/100,000), Kuyavian-Pomeranian (over 62/100,000) and Masovian (over 58/100,000) voivodeships, whereas among women the highest standardized mortality ratios due to lung cancer were recorded in Warmian-Masurian, West Pomeranian and Kuyavian-Pomeranian voivodeships (over 20/100,000).[28] The greatest mortality among the general population due to respiratory diseases, including chronic lower respiratory diseases, from 2000 to 2010, was recorded in Warmian-Masurian Voivodeship. The significant increase in mortality rates between 2000 and 2010 recorded in this voivodeship – which reached 40% of the general population – was alarming. In this context, Warmian-Masurian, West Pomeranian and Masovian voivodeships, which from 2009 to 2014 implemented the most anti-smoking health policy programs, addressed the health needs of inhabitants most effectively. It was quite the contrary in Kuyavian-Pomeranian Voivodeship. This was one of the 3 voivodeships that implemented the fewest anti-smoking health policy programs between 2009 and 2014.

The analysis also covered the mean value of expenditure on anti-smoking programs in particular voivodeships. It was found that there were significant differences in this respect in Lublin, Łódź and Subcarpathian voivodeships in the period covered by our analysis. The lowest force of mortality in Poland due to tracheal, bronchial and lung cancer in 2009–2010 was recorded in Subcarpathian voivodeship. A reasonably favorable situation in this respect was also observed in Lublin Voivodeship: the mortality rates in 2009–2010 were lower than the national average. The significantly higher expenditure from 2009 to 2014 in Lublin and Subcarpathian voivodeships – in the context of attempting to further decrease mortality rates due to cardiovascular diseases – should be viewed as positive. The highest expenditure on anti-smoking health policy programs in Łódź Voivodeship was incurred in 2014. The increase in the expenditure in Lublin Voivodeship in 2010 and in Łódź Voivodeship in 2014 seems justified in view of the high mortality rates due to cardiovascular diseases. In 2009–2010, the highest mortality rates due to cardiovascular diseases were recorded in Świętokrzyskie, Łódź and Lublin voivodeships.

The analysis also covered the number of health policy programs dedicated to children and teenagers. The most

serious aspects of tobacco smoking in Poland include the decreasing age of children who experiment with cigarettes, some of whom become regular smokers, the steady number of female smokers, including pregnant women and young mothers, and passive smoking, specifically among children. That final aspect becomes even more serious when one considers that, according to recent data, inhaling tobacco smoke is just as dangerous – or even more dangerous – than active smoking.[29] The scale of passive exposure of children to tobacco smoke in Poland is massive: every day around 4 million Polish children inhale tobacco smoke at home or in public places.[29] According to 2009 data, nearly 1/4 of children aged 0–14 were exposed to tobacco smoke. One third of young people aged 15–29 were exposed to passive smoking.[30] The results of a study of 2003 indicate that 64% of boys and 53% of girls aged 13–15 have smoked at least once in their life, while 30% of boys and 21% of girls had tried smoking before they reached the age of 10.[29] In 2009, 11.8% of people aged 15–19 admitted that they smoked, and 7.3% of them smoked every day.[30] In the period covered by the analysis, the number of anti-smoking health policy programs aimed at children reached 1,188. There were 685 programs aimed at adults. This structure seems reasonable, taking into consideration the growing problem of tobacco smoking among children and teenagers and the exposure of this group to tobacco smoke.

The experience of other EU member states demonstrates that the best effects are obtained by a long-term policy implemented on many levels. It covers legislative, preventive and controlling actions, as well as addiction therapy.[31] These actions require the interaction of many entities – central authorities, local governments and non-government organizations. The highest smoking cessation success rates (>45%) were recorded in Sweden, UK, the Netherlands, Belgium, and France. Those are the countries that have a well-developed smoking restriction policy. The smoking cessation success rates were relatively low (<30%) in Lithuania and Latvia. The smoking restriction policies that most frequently led to smoking cessation included a pricing policy and a ban on the advertising of tobacco products.[32] On the other hand, as a result of the long-term prevention of cancer in some EU member states, there is a high incidence of smoking-related diseases arising from high cancer detection rates, low or medium mortality, high 5-year survival rates, and high prevalence. This applies to France, Germany, Norway, Italy, Switzerland, and the UK. In Finland and Sweden, the low risk of lung cancer results from successful long-term anti-smoking campaigns.[31] Europe's experience demonstrates that anti-smoking programs of a preventive nature should be implemented on a micro-, macro- and meso-level. In the first step, factors which encourage young girls and boys or men and women to smoke must be identified. Preventive health policy programs, potentially dedicated to a specific sex, should then be aimed at eliminating that factors.[33]

Conclusions

The growing number of anti-smoking programs implemented from 2009 to 2013 is one of the factors that led to a decrease in tobacco smoking in Poland. In terms of mortality rates due to cardiovascular diseases, local governments in Lublin and Warmian-Masurian voivodeships addressed the health needs of the local population most effectively. In terms of mortality rates due to tracheal, bronchial and lung cancer, the health needs of the inhabitants of Warmian-Masurian and West Pomeranian voivodeships were addressed most effectively. The anti-smoking programs addressed the problem of the growing incidence of tobacco smoking mainly among children and teenagers.

References

1. WHO Global Tobacco Epidemic – WHO report. MPOWER package. Report summary. www.who.int/tobacco/mpower/2008/en; Accessed March 15, 2016.
2. Peto R, Lopez AD, Boreham J, Thun M, Heath Jr C. *Mortality From Smoking In Developed Countries 1950–2000*. Oxford, UK: Oxford University Press; 2012.
3. Wojtyniak B, Stokwiszewski J, Goryński P, Poznańska A. Długość życia i umieralność ludności Polski (w:) Sytuacja zdrowotna ludności Polski i jej uwarunkowania [Life expectancy and mortality of the Polish population. In: Wojtyniak B, Goryński P, Moskalewicz B, eds. *Health Situation Of The Polish Population and Its Determinants*]. National Institute of Public Health – National Institute of Hygiene: Warszawa, Poland; 2012: 38–122.
4. National Program for Equalization of Accessibility to Prevention and Treatment of Cardiovascular Diseases POLKARD for 2013–2016. Warsaw, Poland; 2015. https://www.gov.pl/zdrowie/program-profilaktyki-i-leczenia-chorob-ukladu-sercowo-naczyniowego-polkard; Accessed March 15, 2016.
5. Zachorowania i umieralność na choroby układu krążenia a sytuacja demograficzna Polski [Morbidity and mortality from cardiovascular disease and the demographic situation of Poland]. Government Population Council: Warszawa, Poland; 2015.
6. Didkowska J, Wojciechowska U, Zatoński W. Nowotwory złośliwe w Polsce w 2010 roku [Cancer in Poland in 2010]. Publication issued under the task "Registration of cancer conducted by the National Cancer Control Programme". Warszawa, Poland; 2012. http://onkologia.org.pl/wp-content/uploads/Nowotwory_2010.pdf. Accessed March 12, 2016.
7. Didkowska J, Wojciechowska U. Nowotwory złośliwe w Polsce w 2013 roku [Cancer in Poland in 2013]. Publication issued under the task "Registration of cancer conducted by the National Cancer Control Programme". Warszawa, Poland; 2015. http://onkologia.org.pl/wp-content/uploads/BIUL2013.pdf. Accessed March 12, 2016.
8. WHO report. Gaining Health. The European Strategy for the Prevention and Control of Non-communicable Diseases 2006 http://www.euro.who.int/en/publications/abstracts/gaining-health.-the-european-strategy-for-the-prevention-and-control-of-noncommunicable-diseases; Accessed March 15, 2016.
9. Stan zdrowia ludności Polski w przekroju terytorialnym w 2004 r. [The health status of the Polish population by territorial division in 2004]. Statistics Poland: Warszawa, Poland; 2007. http://stat.gov.pl/cps/rde/xbcr/gus/stan_zdrowia_2004_teryt.pdf. Accessed March 12, 2016.
10. Piekarzewska M. Styl życia (w:) Stan zdrowia ludności Polski w 2009 r. [Lifestyle. In: Koehne N, Lednicki B, Piekarzewska M, Wieczorkowski R, Zajenkowska-Kozłowska A, eds. *The Health Status of the Polish Population in 2009*. Statistics Poland: Warszawa 2011: 62–68.
11. Zdrowie i zachowania zdrowotne mieszkańców Polski w świetle Europejskiego Ankietowego Badania Zdrowia (EHIS) 2014 [Health and health behaviors of Polish citizens in the light of the European Health Interview Survey (EHIS) 2014]. Statistics Poland: Warszawa, Poland; 2016. http://stat.gov.pl. Accessed March 12, 2016.

12. National Program for Prevention and Treatment of Cardiovascular Diseases for 2003–2005 POLKARD. Warszawa, Poland; 2003. http://www.archiwum.mz.gov.pl/zdrowie-i-profilaktyka/programy-zdrowotne/wykaz-programow/narodowy-program-wyrownywania-dostpnoci-do-profilaktyki-i-leczenia-chorob-ukadu-sercowo-naczyniowego-polkard; Accessed March 15, 2016.
13. National Program for Prevention and Treatment of Cardiovascular Diseases for 2006–2008 POLKARD. Warsaw 2005. http://www.archiwum.mz.gov.pl/zdrowie-i-profilaktyka/programy-zdrowotne/wykaz-programow/narodowy-program-wyrownywania-dostpnoci-do-profilaktyki-i-leczenia-chorob-ukadu-sercowo-naczyniowego-polkard; Accessed March 15, 2016.
14. National Program for Prevention and Treatment of Cardiovascular Diseases for 2009 POLKARD. Warszawa, Poland; 2009. http://www.archiwum.mz.gov.pl/zdrowie-i-profilaktyka/programy-zdrowotne/wykaz-programow/narodowy-program-wyrownywania-dostpnoci-do-profilaktyki-i-leczenia-chorob-ukadu-sercowo-naczyniowego-polkard; Accessed March 15, 2016.
15. National Program for Prevention and Treatment of Cardiovascular Diseases for 2010–2012 POLKARD. Warszawa, Poland; 2010. http://www.archiwum.mz.gov.pl/zdrowie-i-profilaktyka/programy-zdrowotne/wykaz-programow/narodowy-program-wyrownywania-dostpnoci-do-profilaktyki-i-leczenia-chorob-ukadu-sercowo-naczyniowego-polkard; Accessed March 15, 2016.
16. National Program for Equalization of Accessibility to Prevention and Treatment of Cardiovascular Diseases POLKARD for 2013–2016. Warszawa, Poland; 2015. https://www.gov.pl/zdrowie/program-profilaktyki-i-leczenia-chorob-ukladu-sercowo-naczyniowego-polkard; Accessed March 15, 2016.
17. 17 Act of July 1, 2005 on Establishing a Multiannual Program "National Program for Fighting Cancer" (Dz.U.05.143.1200) text in Polish.
18. Resolution of the Cabinet No. 208 as of November 3, 2015 on Establishing a Multiannual Program for 2016–2024 entitled "National Program for Fighting Cancer", (M.P. 2015. 1165). text in Polish.
19. Zdrowie i Ochrona Zdrowia w 2011 r. [Health and Health Care in 2011]. Central Statistical Office of Poland: Warszawa, Poland; 2012. http://stat.gov.pl/cps/rde/xbcr/gus/zo_zdrowie_i_ochrona_zdrowia_w_2011.pdf. Accessed March 12, 2016.
20. Zdrowie i Ochrona Zdrowia w 2013 r. [Health and Health Care in 2013]. Central Statistical Office of Poland: Warszawa, Poland; 2014. http://stat.gov.pl/obszary-tematyczne/zdrowie/zdrowie/zdrowie-i-ochrona-zdrowia-w-2013-r-,1,4.html. Accessed March 12, 2016.
21. Zdrowie i Ochrona Zdrowia w 2014 r. [Health and Health Care in 2014]. Central Statistical Office of Poland: Warszawa, Poland; 2015. http://stat.gov.pl/obszary-tematyczne/zdrowie/zdrowie/zdrowie-i-ochrona-zdrowia-w-2013-r-,1,4.html. Accessed March 12, 2016.
22. Badura B. What is and what determines health. In: Laaser U, de Leeuw E, Stock Ch, eds. *Scientific Foundations for Public Health Policy in Europe*. Juventa Verlag: Munich, Germany;1995.
23. WHO Europe. The European Health Report 2005: Public health action for healthier children and populations. http://www.euro.who.int/__data/assets/pdf_file/0004/82435/E87325.pdf. Accessed March 12, 2016.
24. WHO. Global Strategy on Diet, Physical Activity and Health. Geneva, Switzerland; 2004. http://www.who.int/gb/ebwha/pdf_files/WHA57/A57_R17-en.pdf. Accessed March 12, 2016.
25. Strategy for Fighting Cancer in Poland 2015–2024. PWC. Warsaw, Poland; 2014 http://www.walkazrakiem.pl; Accessed March 15, 2016.
26. Biała Księga. Zwalczanie raka jelita grubego i raka piersi w Polsce na tle wybranych krajów europejskich. Analiza zasobów systemu opieki onkologicznej i czynników warunkujących sukces [White Book. Fighting colorectal cancer and breast cancer in Poland in comparison to selected European countries. Resource analysis of the oncological care system and success factors]. Center for University Research: Warszawa–Kraków, Poland; 2011.
27. Didkowska J, Wojciechowska U, Zatoński W. Nowotwory złośliwe w Polsce w 2009 roku [Cancer in Poland in 2009]. Publication issued under the task "Registration of cancer conducted by the National Cancer Control Programme". Warszawa, Poland; 2011. http://onkologia.org.pl/wp-content/uploads/Nowotwory_2009.pdf. Accessed March 12, 2016.
28. Didkowska J, Wojciechowska U, Zatoński W. Nowotwory złośliwe w Polsce w 2012 roku [Cancer in Poland in 2012]. Publication issued under the task "Registration of cancer conducted by the National Cancer Control Programme". Warszawa, Poland; 2014 http://onkologia.org.pl/wp-content/uploads/Biul2012net.pdf. Accessed March 12, 2016.
29. Present danger of tobacco epidemic in Poland. WHO Regional Office for Europehttp://www2.mz.gov.pl/wwwfiles/ma_struktura/docs/raport_epidemia_16082010.pdf. Accessed March 12, 2016.
30. Zdrowie dzieci i młodzieży w Polsce w 2009 r. [Health of children and adolescents in Poland in 2009]. Statistics Poland, Statistical Office in Kraków: Kraków, Poland; 2011. http://stat.gov.pl/cps/rde/xbcr/gus/zo_zdrowie_dzieci_mlodziezy_w_polsce_2009.pdf. Accessed March 12, 2016.
31. Bielska-Lasota M, Car J, Rzepczak-Zacharek E. Obciążenie nowotworami złośliwymi w Polsce na tle krajów Unii Europejskiej (w:) Sytuacja zdrowotna ludności Polski i jej uwarunkowania. [Burden of cancer in Poland in comparison to other Member States. In: Wojtyniak B, Goryński P, Moskalewicz B, eds. *Health Situation Of The Polish Population and Its Determinants*]. National Institute of Public Health – National Institute of Hygiene: Warszawa, Poland; 2012:38–122.
32. Schaap MM, Kunst AE, Leinsalu M, et al. Effect of nationwide tobacco control policies on smoking cessation in high and low educated groups in 18 European countries. *Tobacco Control*. 2008;17:248–255.
33. de Vries H, Mudde A, Leijs I, et al. The European Smoking Prevention Framework Approach (EFSA): an example of integral prevention. *Health Educ Res*. 2003;18(5):611–626.

Design and control of system for elbow rehabilitation: Preliminary findings

Tadeusz Mikołajczyk[1,A–F], Adam Kłodowski[2,A–F], Emilia Mikołajewska[3,B–F], Paweł Walkowiak[1,B–F], Pedro Berjano[4,A–F], Jorge Hugo Villafañe[5,A–F], Francesco Aggogeri[6,B–F], Alberto Borboni[6,B–F], Davide Fausti[7,B–F], Gianluigi Petrogalli[7,B–F]

[1] Department of Production Technology, Faculty of Mechanical Engineering, University of Science and Technology, Bydgoszcz, Poland
[2] Laboratory of Machine Design, School of Energy Systems, Lappeenranta University of Technology, Finland
[3] Department of Physiotherapy, Faculty of Health Sciences, Ludwik Rydygier Collegium Medicum in Bydgoszcz, Nicolaus Copernicus University in Toruń, Poland
[4] GSpine4 Spine Surgery Division, Institute for Recovery and Care of Scientific Characteristics – Galeazzi Orthopedic Institute, Milan, Italy
[5] Institute for Recovery and Care of Scientific Characteristics – Don Gnocchi Foundation, Milan, Italy
[6] Applied Mechanics Research Group, Faculty of Engineering, University of Brescia, Italy
[7] Research and Development Department, Polibrixia Innovation Engineering, Brescia, Italy

A – research concept and design; B – collection and/or assembly of data; C – data analysis and interpretation;
D – writing the article; E – critical revision of the article; F – final approval of the article

Advances in Clinical and Experimental Medicine, ISSN 1899-5276 (print), ISSN 2451-2680 (online) *Adv Clin Exp Med*. 2018;27(12):1661–1669

Address for correspondence
Emilia Mikołajewska
E-mail: e.mikolajewska@wp.pl

Funding sources
None declared

Conflict of interest
None declared

Received on October 31, 2016
Reviewed on March 13, 2017
Accepted on June 8, 2017

Abstract

Background. The use of an exoskeleton elbow is considered an effective treatment in several pathologies, including post-stroke complications, traumatic brain injury (TBI) and spinal cord injury (SCI), as well as in patients with neurodegenerative disorders. The effectiveness of rehabilitation is closely linked to a suitably chosen therapy. The treatment can be performed only by specialized personnel, significantly supported with the use of automated devices.

Objectives. The aim of this study was to present a novel exoskeleton for elbow rehabilitation without a complicated control system.

Material and methods. Single-degree-of-freedom (SDOF) solution in constructing the prototype of an elbow exoskeleton for rehabilitation purposes has been applied. The simplicity of the actuation mechanism was set as one of the priorities in the design; thus, a single-axis stepper motor with a controller was found to be adequate for providing a reliable and precise source of motion for the exoskeleton.

Results. Technological development may provide novel solutions, such as an exoskeleton – a wearable, external structure which supports or (in selected applications) even replaces the muscle actuation in the patient. The reported advantages of the proposed exoskeleton reflect current state-of-the-art. The proposed control strategy relies on closed-loop position control, performance, low manufacturing cost, and predicted performance in a rehabilitation scenario. All these factors play an important role in establishing the directions for further research, e.g., an integrated force sensor in the device, measurements of torque interactions on the elbow joint, and assessment and response to an overload of articulation.

Conclusions. This study suggests not only the clinical but also the possible economic and logistical advantages offered by the portability of the system, and its effective support for therapists applying an elbow exoskeleton.

Key words: rehabilitation, assistive technology, elbow, exoskeleton, upper limb exoskeleton

DOI
10.17219/acem/74556

Introduction

In Western countries, elderly people will suffer from a growing number of neuromotor disorders each year, and this age group is at greatest risk for disability. In that population, it is important that physically weak people are able to take care of themselves.[1] The question of the superiority of robot training of the upper limbs over classical therapies in neuromotor disorder patients remains controversial.[2–4] During the subacute stage, upper limbs training is likely to be the most useful.

Advances in technology have led to the development of a variety of robotic devices for the use in rehabilitation. Robotic devices have been progressively included in neurorehabilitation programs.[5–8] Exoskeletons are wearable robots which exhibit a close cognitive and physical interaction with the human user. They are robotic exoskeletal structures that typically operate alongside human limbs.[9] Scientific and technological work on exoskeletons began in the early 1960s, but only recently they have been applied to rehabilitation and functional substitution in patients suffering from motor disorders.[10,11] The effectiveness of rehabilitation is closely linked with the suitability of the chosen therapy.[12,13] Robotic techniques allow the precise recording of movements and the application of forces to the affected limb using visual cues; they convert repetitive movement practice into a useful task within everyday activity.[14] Current state-of-the-art of robotic systems and their prospective function in the post-stroke rehabilitation of the upper limbs is presented in the studies conducted by Fausti et al.,[12] Bishop and Stein,[15] Hochstenbach-Waelen et al.,[16] Loureiro et al.,[17] Lu et al.,[18] Maciejasz et al.,[19] and Morales et al.[20] The application of robotics in neurorehabilitation is promising, but is still not widely used in clinical settings.

The aim of this study was to present a novel exoskeleton for elbow rehabilitation without a complicated control system.

Challenges and requirements

We took into consideration the needs and preferences of patients, their families and caregivers, and therapists when designing a robot supporting upper limb rehabilitation. A study by Lu et al. showed the main requirements for an upper limb rehabilitation device, including the following:

- facilitating a variety of arm movements;
- being usable in a seated position;
- giving feedback to clients;
- including virtual activities specific to daily living;
- being useful at home;
- having adjustable resistance, and
- costing less than 6000 USD.[18,21]

To sum up, based on the classification proposed by Maciejasz et al.,[19] we proposed a novel exoskeleton for upper limb rehabilitation purposes in low- and middle-income countries, with the following features:

- application field: supporting basic activities of daily living (ADL), neurological rehabilitation and orthopedic rehabilitation;
- target group: patients with severe neurological deficits, including post-stroke patients, those with traumatic brain injury (TBI) or spinal cord injury (SCI), geriatric patients with neurodegenerative disorders, and people who need similar solutions for functional support during recovery only (e.g., for avoiding physical effort after cardiopulmonary diseases);
- type of assistance: active device and elbow strength assistance;
- mechanical design: exoskeleton-based arm with a single one-degree-of-freedom (SDOF) stepper motor and control system;
- control strategy: a mix of kinematic and dynamic; and
- clinical evaluation: experimental study, further research and a randomized controlled trial.

The most common symptoms in elbow functional deficits are weakness, loss of joint control, excessive muscle contraction, spastic co-contraction, and pathological synergies.[22–27] The most recent, state-of-the-art advances in the area of the elbow exoskeletons has been presented by Vitiello et al.[28]

An elbow exoskeleton combines motor (re)learning principles. It should provide repetition of task-related movements, tailored to the patient and the patient's goals, in a meaningful context, with associated variability and increasing levels of difficulty in exercises. The hardware and software should allow for easy use (including preparation for the exercises), and easy adjustment to individual patients' health status, needs and change over time (recovery or relapse). The important features are safety, price, proven efficacy, and motivation to exercise.

Safety precautions

An elbow exoskeleton supports physiological movements, taking into consideration the current health status of the patients, the goals of the therapy, etc. The most important factors which influence patient and therapist safety that we took into consideration during the development of the elbow exoskeleton were as follows:

- the method of wearing and repeatedly fixing the exoskeleton to the arm and elbow joint in order to avoid injuries;
- limitations of the personal range of motion (ROM);
- regulation and limitation of personal speed of movement;
- an emergency switch;
- protection against unauthorized use;
- safety alerts, low-battery and error signals; and
- online help desk and availability of service.

The potential for robots constraining the natural movement of the shoulder joint to cause subluxation at the shoulder was described by Jeong-Ho et al., but this does not apply in the case of an elbow exoskeleton.[27]

An important issue, especially in elderly patients, is the acceptance of advanced devices by the patients, their families and caregivers. It should be facilitated by reasonable and patient-adjusted learning of novel technologies.

Material and methods

Design of elbow exoskeleton

It has been decided that it will be sufficient to use a SDOF solution in constructing the prototype of an elbow exoskeleton for rehabilitation purposes. The simplicity of the actuation mechanism was set as one of the priorities in the design; thus, a single-axis stepper motor with a controller was found to be adequate for providing a reliable and precise source of motion for the exoskeleton, in contrast to the bionic model of the human arm, which requires an antagonistic actuator control, resulting in a much more complex control system and possibly also a heavier device.

This paper presents 2 solutions for an elbow exoskeleton for rehabilitation:

– asymmetrical with a 1-side drive system (Fig. 1,2)[29];

– symmetrical with a 2-side drive system (Fig. 3,4).

The asymmetrical design of the upper limb exoskeleton (ULE) was presented as a virtual prototype (Fig. 1) and a functional prototype of ULE (Fig. 2). In order to ensure a strong and lightweight support structure, the exoskeleton frame was manufactured from aluminum.

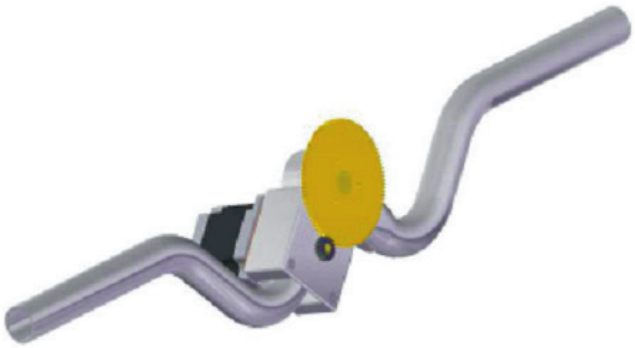

Fig. 1. Asymmetric upper limb exoskeleton (ULE) with a 1-side drive system: the virtual model made in Solid Edge (Siemens PLM Software, Plano, USA)

Fig. 2. Prototype of an asymmetrical upper limb exoskeleton (ULE) with a 1-side drive system

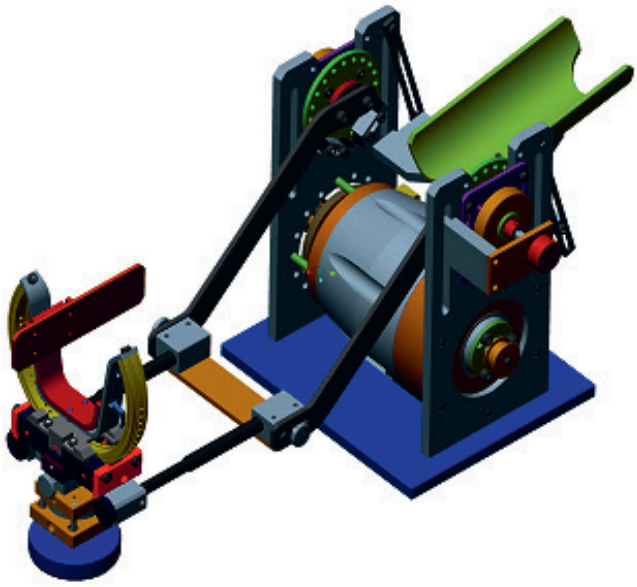

Fig. 3. Virtual model of a symmetrical upper limb exoskeleton (ULE) with 2-side drive system: upper arm (1) and wrist (2) supports

Design work showed that locating the motor close to the elbow should provide the optimal functionality of the exoskeleton. A standard NEMA 23 stepper motor (MOONS', Shanghai, China) with a 1.8° step size and a nominal torque of 1 Nm was chosen for this project. To increase the torque, the motor was equipped with a helical gearbox with a 1:5 gear ratio, which effectively increased the available torque to 5 Nm. This provided for low weight and sufficient torque for joint actuation. The maximum peak torque output of 5 Nm needs to be improved because it does not seem high enough to mobilize patients with no residual mobility. Spasticity can generate articulation torque higher than 5 Nm, preventing passive mobilization from the robot.

A virtual model of a symmetrical device is presented in Fig. 3. Its architecture consisted of 2 vertical side plates fixed to a base support, between which, in the lower part, a rotary motor is located. In the upper part of the plates, 2 parallel rods are hinged, which are able to link with the appendix to support the wrist.

As shown in Fig. 3, the patient puts his/her upper arm into the support positioned at the rear of the device and, using a special orthopedic glove, engages the wrist to the support positioned in front of the device. The wrist support has a semicircular guide and can rotate around its own axis, so as to allow the pronation–supination movement of the hand.

Integration (Fig. 4) of the symmetrical device was done by adopting 3D-printed polymeric materials to create an ergonomic interface with the patients and by transferring the exoskeleton architecture around the arm of the patient to align the rotary joint of the device with the biomechanical rotary joint associated with the elbow of the patient.

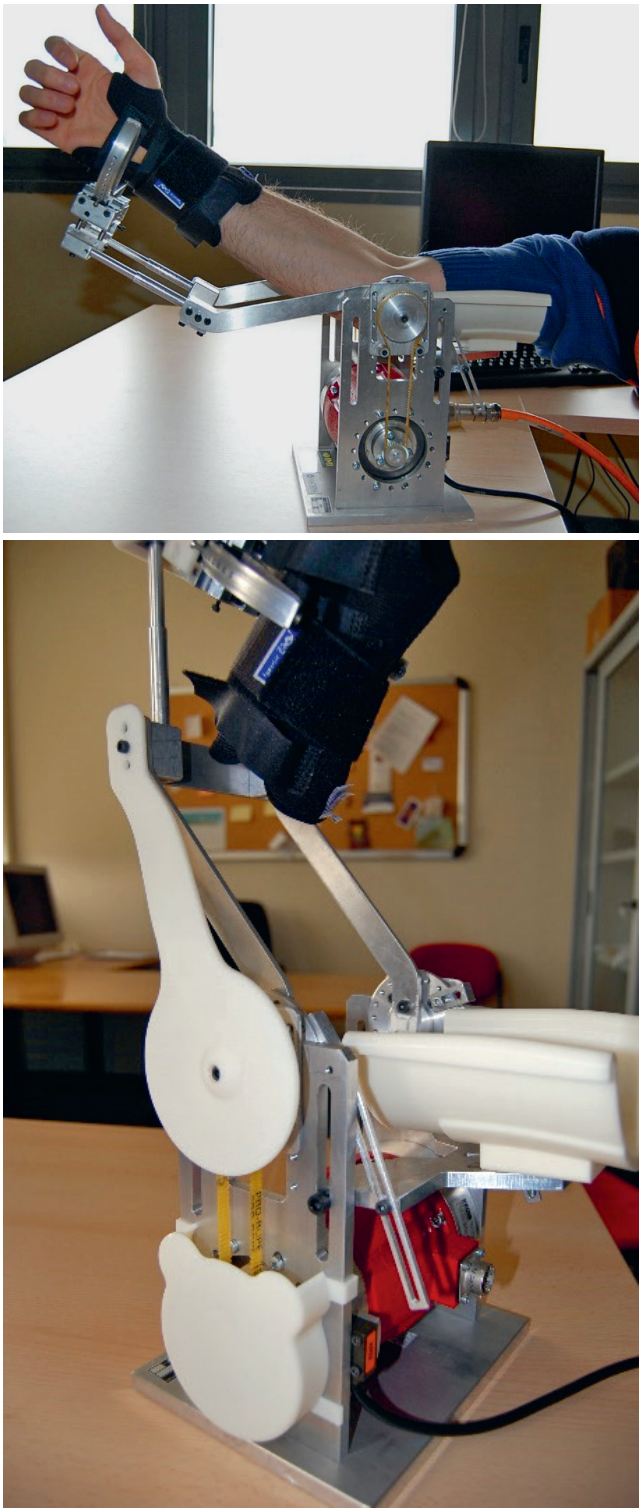

Fig. 4. Prototype of a symmetrical device with 2-side drive system: a) view of the device, b) view of 3D-printed ergonomic elements

Exoskeleton control system

The idea of the ULE control system is an asymmetrical design (Fig. 1,2). The exoskeleton control was created using a TB6560, a single-axis stepper motor driver control unit (Toshiba, Minata, Tokyo, Japan) (Fig. 5,6A) connected to the computer through an LPT port (Fig. 6B). A limit

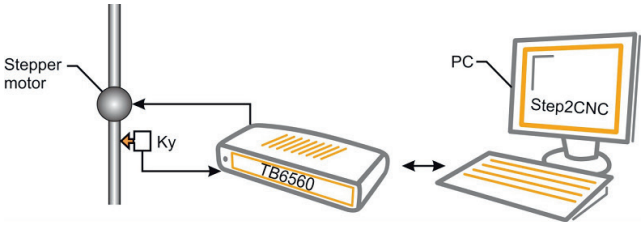

Fig. 5. Upper limb exoskeleton (ULE) control system with a single-axis stepper motor

Ky – rotary encoder for stepper motor; Step2CNC – software for the controller; TB6560 – single-axis stepper motor driver control unit.

switch was used for reliable system start-up with a known position (Ky).

The system is powered with an industrial 600 W power supply (Power Control Systems, Veneto, Italy) providing a regulated output voltage up to 36 V and an output current of 16 A. A Dell GM 520 computer (Dell Computer Corporation, Round Rock, USA) (Fig. 6B) was used for control because of its available LPT port. In addition, this computer model has many USB ports, which makes it suitable for interfacing with other hardware. A touch LED screen (Fig. 6C) was used for easy interfacing with ULE.

The software interface for the controller was provided by Step2CNC v. 2.51 (Akcesoria CNC Elżbieta Taraszkiewicz, Augustów, Poland).[30] It is mainly designed for numerical controlling of machining stations utilizing stepper motors. The main screen of the application is presented in Fig. 7. This software allows for both manual and automatic control using G-code. G-code can be imported from an external file or it can be edited directly in the Step2CNC software.[31,32] The software was calibrated to use angular position as input. The position and the speed of movement can be controlled. G-code simplifies the creation of even complex motion patterns for training.

Using Step2CNC software enables complex control of the position and velocity of the motion path throughout the whole range. Motion can be prescribed as a function of *f*, which can later be converted to G-code. Positioning accuracy is dependent on the stepper motor step size. For a standard 1.8° step size, 200 steps per revolution allow for more than sufficient control accuracy for a human–machine interaction. The gearbox used in the design with a 1:5 gear ratio allowed the positioning accuracy to be increased to 0.36° in full-step mode. The controller we used also allows operation in micro-stepping modes up to 1/16 of a step. Step division can be selected using jumper switches available inside the casing. Figure 8 illustrates the positioning accuracy which can be obtained using different step size settings with and without an external gearbox.

Results

This study presents the original concept of an automatic control system based on Step2CNC software for the ULE (Fig. 7). The system consists of a limited number of commands

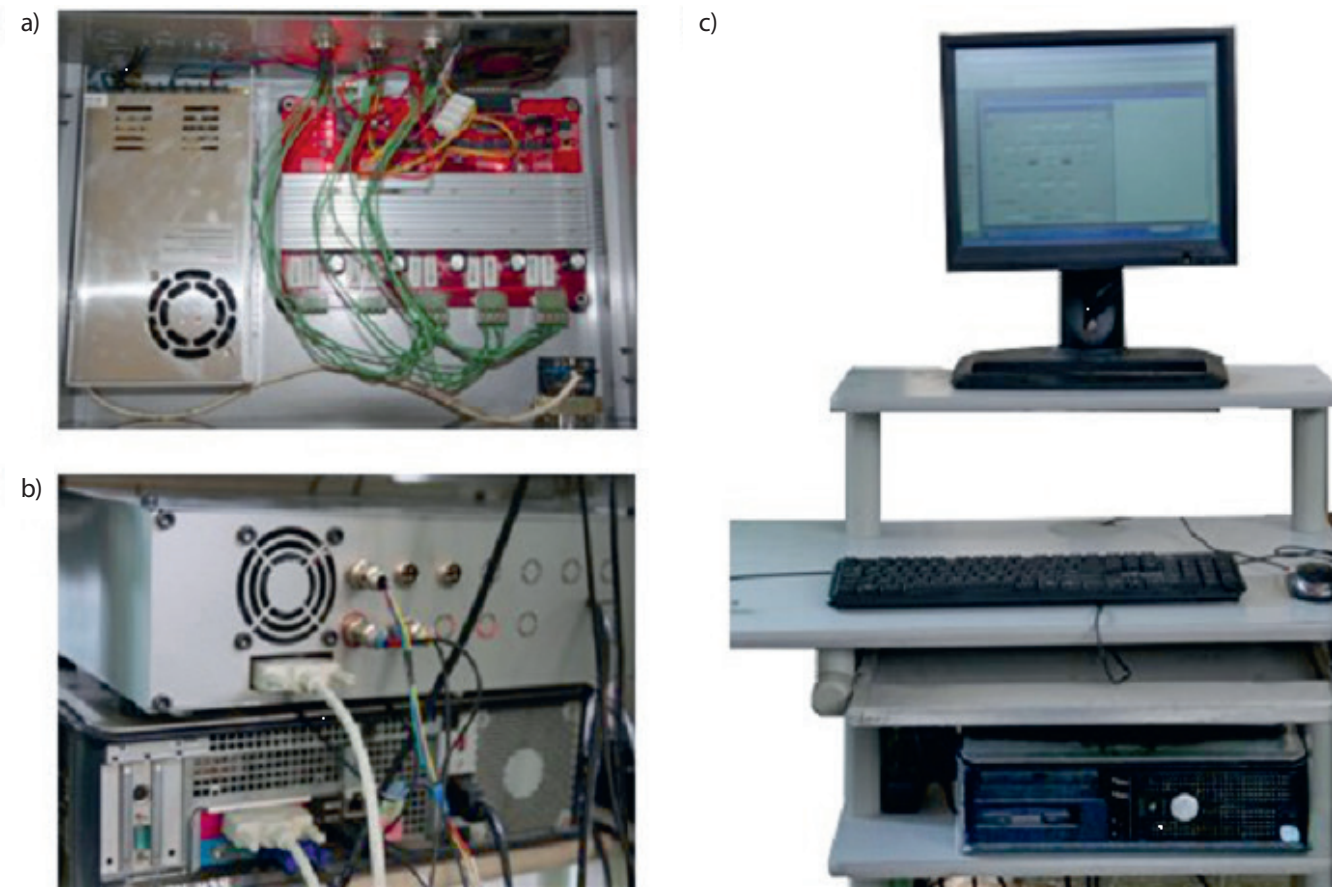

Fig. 6. Mobile control system

a – interior of the stepper motor controller; b – stepper motor controller and PC connection; c – complete station.

used to describe the movement trajectory and speed in an absolute coordinate system. The software includes visualization of the movement as a function of time. The limit switch position is also visualized. Despite the limitations of the visualization, the software is useful for the ULE control.

The following actions are possible for the ULE:

– clockwise motion of the motor (arm flexion);
– counterclockwise rotation of the motor (arm extension);
– stoppage of the motor for a specified time.

Figure 9 presents a definition of the control parameters of arm rotation.

Forearm motion speed can be individually predefined for each motion segment, which can be defined as fast movement speed or exercise speed. In case of exercise speed, it can be adjusted freely. Fast movement is performed at 1 predefined speed.

The following G-codes are used for the proposed system:

– G00 – fast motion with 1 predefined speed;
– G01 – exercise motion – the speed of motion can be freely defined on the control panel;
– G04 Hpar – a break in motion for a defined length of time, for instance, G04 H200 stops motion for 200 ms;
– M04 – works analogically to G04, using 0 as a delay parameter: the program is stopped until the "continue" key is pressed on the software interface;

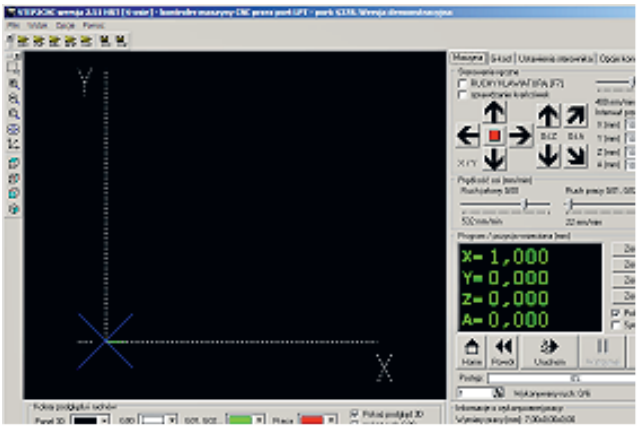

Fig. 7. Step2CNC user interface

– commands G00 and G01 can accept the following parameters:
  • Xpar – 1st axis coordinate;
  • Ypar – 2nd axis coordinate;
  • Fpar – speed setting in mm/min.
– M30 – ends the program;
– G90 – enables absolute positioning;
– G91 – switches to relative positioning;
– G28 – returns to the home switch position.

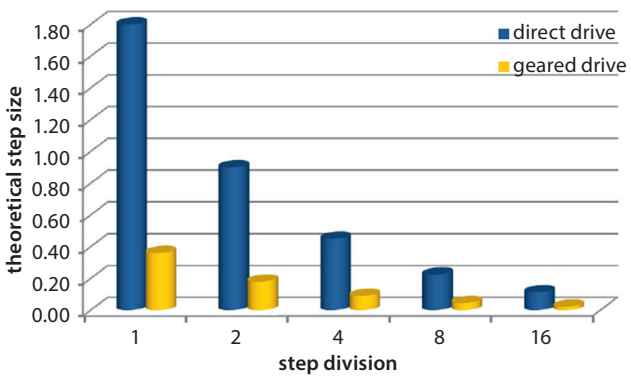

Fig. 8. Influence of step size on theoretical positioning accuracy with and without a gearbox

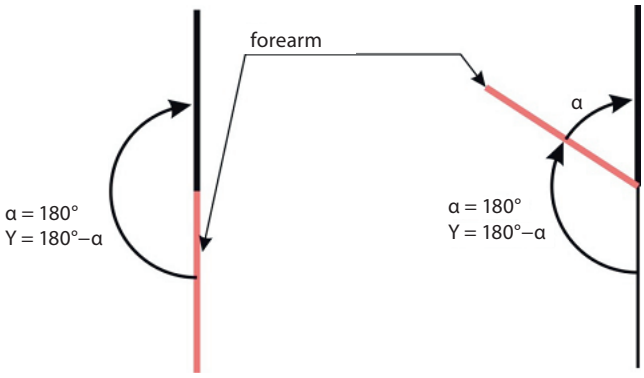

Fig. 9. Angle computation for the Step2CNC

Y – the angle parameter.

Even though only a single axis is controlled, the X parameter is used for visualization of the movement on the software interface. The G04 command can be used to pause the motion to let the patient rest between exercise sequences.

The velocity of the motion, *fy*, can be defined using the following relationship:

$$fy = \frac{Dy}{T} \times 60,$$

where *Dy* is the rotation angle of the forearm and *T* is the rotation time in seconds. Break time, T_b, which is a parameter of the G04 and M04 commands, needs to be expressed in miliseconds, thus:

$$T_b = T \times 1000,$$

where *T* is the break time expressed in seconds.

Exemplary G-code is presented in Table 1. The sample code does not include the X parameter used only for visualization of the movement.

The presented code has been tested with the forearm exoskeleton. The formation of motion loops requires the same code fragment to be copied multiple times. Based on the example G-code and available commands, an automatic G-code generator was created according to the algorithm presented in Fig. 10.

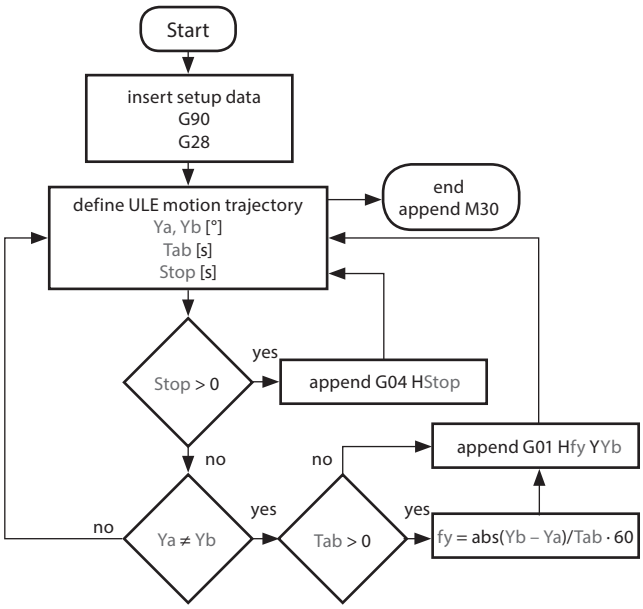

Fig. 10. Simplified algorithm of G-code generation

Ya, Yb – initial and final angles, Stop – pause time, Tab – motion time, fy – motion speed; ULE – upper limb exoskeleton.

The algorithm has been implemented in the custom Visual Basic 6 (Microsoft Corp., Redmond, USA) code CodeMake software (Fig. 11). The tool allows for simple G-code generation based on an input motion pattern. The software visualizes computation results and G-code output during operation. The text field in the software allows for easy copy-pasting of the code into Step2CNC. In addition, the generated code can be saved in a file. The CodeMake software contains a preview from a USB camera. It also has the "on top" feature, which locks the window in front of other windows, including Step2CNC. Such a configuration is convenient while using the remote control of Step2CNC, for instance, TeamViewer or Remote Desktop.[33]

Table 1. Example of G-code

G-code	Description
ULE control file	file header – lines preceded with a semicolon are treated as comments
G90	switches on absolute positioning mode
G28 Y	homing the arm unit limit switch is reached to initialize the system with the arm position
G01 F100 Y150	rotates the forearm 100°/min until reaching an absolute position of 150°
G04 H0	pauses the program execution until the "continue" button is pressed
G01 F20 Y60	slow motion with a velocity of 20°/min until an angular position of 60° is reached
G04 H2000	pauses program for 2 s and then continues automatically
G01 F50 Y0	sets motion at a velocity of 50°/min until initial position (0°) is reached
M30	ends program

ULE – upper limb exoskeleton.

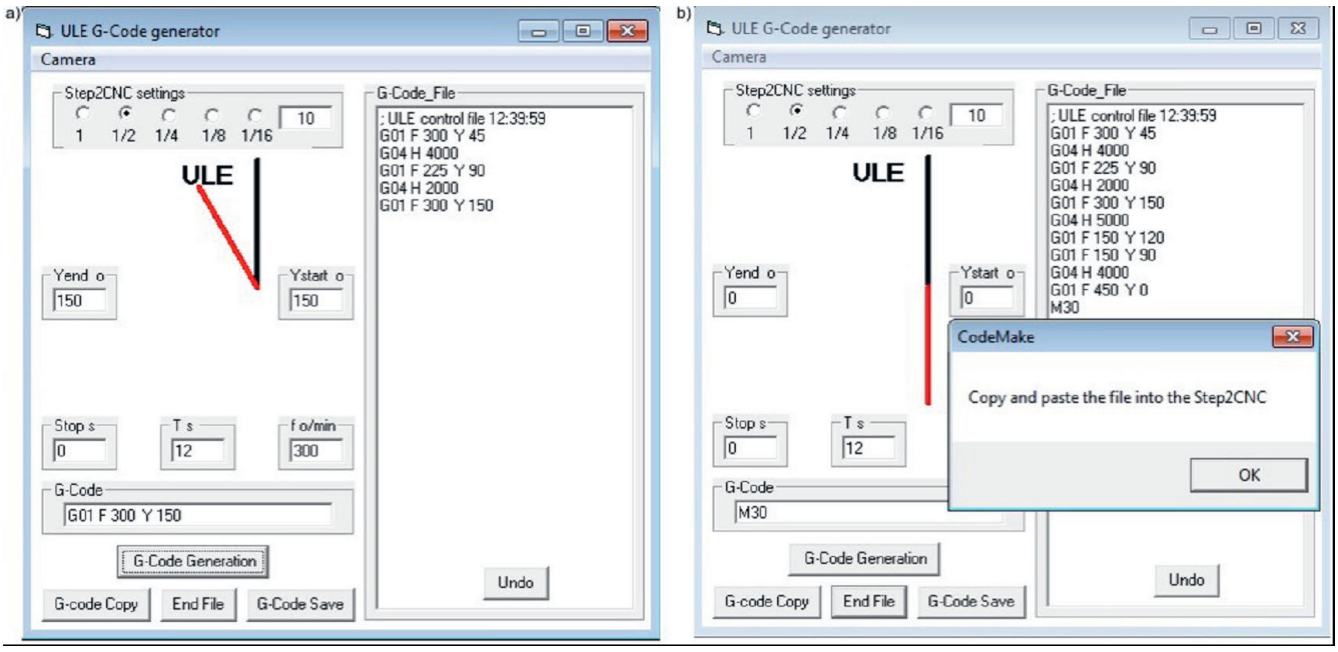

Fig. 11. Main window of the CodeMake tool: a) during control code generation; b) when the G-code is ready

During remote operation (Fig. 12,13), there is an option of adjusting the camera resolution to provide smooth image transmission even in the case of slow Internet connection. Remote operation mode allows the user to create exercise programs and to supervise exercise performance even if the patient and the operator are at distant locations.

Quantitative analysis showed significant benefits from an economic point of view (lower price and wider accessibility) and from a logistical one (easier manufacturing, 3D-printing potential and reverse engineering for customized solutions).

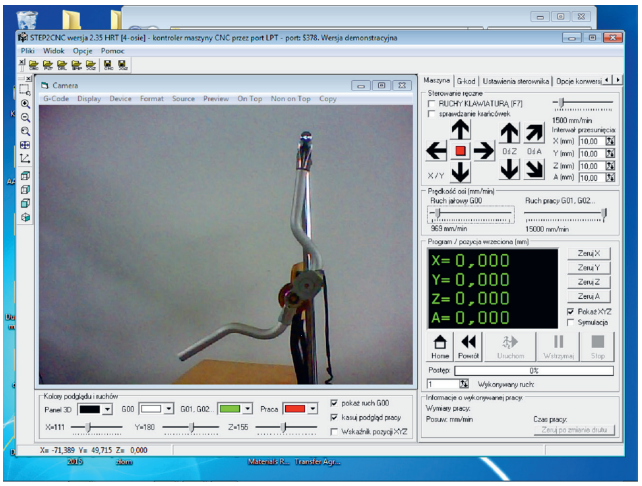

Fig. 12. Remote view of the Step2CNC and CodeMake window on top with a live preview of upper limb exoskeleton (ULE)

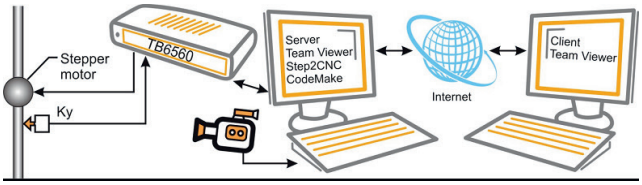

Fig. 13. System setup for upper limb exoskeleton (ULE) remote control

Ky – Ky encoder for motor control purposes.

Discussion

Despite several decades of work on exoskeletons, significant scientific contributions in the applications of rehabilitation and functional compensation and substitution have only begun to appear in the last 10 years. As exoskeletons are characterized by close cognitive and physical interaction with the human user, the requirements applied to the cognitive interaction are strict. As technological advances are made, there is much potential for growth in this field.

The evidence supporting the upper limb rehabilitation using robotics to facilitate therapeutic process makes robotic control systems a significant emerging field in robotics, biocybernetics, rehabilitation engineering, and clinical medicine. It becomes more complex and integral, taking into consideration the International Classification of Functioning (ICF) perspective to correctly evaluate the disabling effect of neuromotor disorders. Prior to the year 2000, there was a paucity of high-quality evidence regarding the management of neuromotor disorders with elbow exoskeletons. At one time, practitioners might have believed that elbow neurorehabilitation with such an exoskeleton was not effective because of the lack of empirical evidence. Robot-aided rehabilitation of the upper limbs is still a complementary therapy method, even as a home-based

rehabilitation treatment. There is still a lack of evidence that robotic therapy is more effective than traditional face-to-face treatment. Strong evidence can be obtained using randomized controlled trials, large patient samples and a control group for comparison. However, shortages in the area of specialized personnel (including physicians, physiotherapists, nurses, etc.) make the robotic solution cheaper and more accessible. Easily transportable, wearable devices could improve rehabilitation after discharge as well, in outpatient or home-based settings. Efforts are being made to establish the ideal type of treatment, length of training and patient's characteristics for a successful treatment of this type. Cost-effective solutions, reduced effective hospitalization, early discharge, and home-based, long-term rehabilitation make robotic systems a new, basic and cheaper modality.[34,35]

The advantages of the proposed exoskeleton reported here reflect current state-of-the-art. A proposed control strategy relies on a closed-loop position control, performance, low manufacturing costs, and predictable performance in a rehabilitation setting. All these factors play an important role in establishing the directions for further research, e.g., integrated force sensors in the device, measurements of torque interactions on the elbow joint, and assessment and response to an overload of articulation.

The aforementioned issues describe the main limitations of the current study.

Based on a literature review and our own experience during working on the proposed system, we can formulate the following conclusions.

The designed actuation system utilizing a stepper motor and a special gearbox provides precise positioning and repeatability of movement (angular accuracy within 0.18–0.36°), a wide range of speeds, and full torque availability even at 0 speed (as long as there is power in the windings).

Step2CNC software offers a simple software–hardware interface, providing G-code interpretation and control strategy; it also allows the user to edit G-code, thus providing an option for code sequence generation. The aluminum construction of the exoskeleton yields a strong and lightweight system (2 kg).

The prototype consisted of easily obtainable components, with a simple and off-the-shelf control system.

The prepared Code-Make software allows for camera image previews, useful for remote operation, as well as for straightforward G-code generation concerning desired positions and delays in the exercise program.

Remote operation of the system is possible and easy to implement using Remote Desktop or Team Viewer.

The control system presented above uses a standard G-code implementation as well as a typical Computer Numerical Control (CNC). Therefore, it is possible to expand this system by adding additional degrees of freedom.

The limitations of the study are the imperfections observed in the construction of the exoskeleton and its shortcomings in terms of mapping all the movements of the elbow and forearm. In this respect, the exoskeleton must be improved. Another limitation is the fact that this is only a theoretical paper with no clinical studies. Further research should include deeper clinical studies on large samples of patients. Such an approach allows for further compartmental studies and better fulfillment of the needs of the patients, their families and caregivers, as well as therapists.

Conclusions

The current study suggests that choosing an elbow exoskeleton may have not only clinical but also possible economic and logistical advantages. In the future, exoskeleton-based rehabilitation of upper limb function may constitute the most promising therapeutic tool which can meet the increasing demand for therapy.

The design of ULE presented here is a good solution for the rehabilitation of the patient. The components of the control system are easy obtainable and can be used for control of a ULE by the available application, Step2CNC. CodeMake software allows for a camera image preview, is useful for remote operation and can generate G-code straightforwardly.

References

1. Kiguchi K, Kariya S, Watanabe K, Izumi K, Fukuda T. An exoskeletal robot for human elbow motion support-sensor fusion, adaptation, and control. *IEEE Trans Syst Man Cybern B Cybern.* 2001;31(3):353–361.
2. Lo AC, Guarino PD, Richards LG, et al. Robot-assisted therapy for long-term upper-limb impairment after stroke. *N Engl J Med.* 2010;362(19):1772–1783.
3. Lum P, Reinkensmeyer D, Mahoney R, Rymer WZ, Burgar C. Robotic devices for movement therapy after stroke: Current status and challenges to clinical acceptance. *Top Stroke Rehabil.* 2002;8(4):40–53.
4. Marchal-Crespo L, Reinkensmeyer DJ. Review of control strategies for robotic movement training after neurologic injury. *J Neuroeng Rehabil.* 2009;6:20.
5. Takahashi CD, Der-Yeghiaian L, Le V, Motiwala RR, Cramer SC. Robot-based hand motor therapy after stroke. *Brain.* 2008;131(Pt 2):425–437.
6. Howard A, Brooks D, Brown E, Gebregiorgis A, Chen YP. Non-contact versus contact-based sensing methodologies for in-home upper arm robotic rehabilitation. *IEEE Int Conf Rehabil Robot.* 2013;2013: 6650487.
7. Brochard S, Robertson J, Médée B, Rémy-Néris O. What's new in new technologies for upper extremity rehabilitation? *Curr Opin Neurol.* 2010;23(6):683–687.
8. Li C, Rusák Z, Horváth I, Ji L. Influence of complementing a robotic upper limb rehabilitation system with video games on the engagement of the participants: A study focusing on muscle activities. *Int J Rehabil Res.* 2014;37(4):334–342.
9. Tsagarakis NG, Caldwell DG. Development and control of a "soft-actuated" exoskeleton for use in physiotherapy and training. *Auton Robots.* 2003;15(1):21–33.
10. Pons JL. Rehabilitation exoskeletal robotics. The promise of an emerging field. *IEEE Eng Med Biol Mag.* 2010;29(3):57–63.
11. Taveggia G, Villafañe JH, Vavassori F, Lecchi C, Borboni A, Negrini S. Multimodal treatment of distal sensorimotor polyneuropathy in diabetic patients: A randomized clinical trial. *J Manipulative Physiol Ther.* 2014;37(4):242–252.
12. Fausti D, Petrogalli G, Villafañe JH, Faglia R. Study, design and preliminary tests of an automatic device for elbow rehabilitation. *Appl Mech Mater.* 2015;783:1–15.
13. Nycz CJ, Delph MA, Fischer GS. Modeling and design of a tendon actuated soft robotic exoskeleton for hemiparetic upper limb rehabilitation. *Conf Proc IEEE Eng Med Biol Soc.* 2015:3889–3892.

14. Taveggia G, Borboni A, Mule C, Villafañe JH, Negrini S. Conflicting results of robot-assisted versus usual gait training during postacute rehabilitation of stroke patients: A randomized clinical trial. *Int J Rehabil Res*. 2016;39(1):29–35.
15. Bishop L, Stein J. Three upper limb robotic devices for stroke rehabilitation: A review and clinical perspective. *NeuroRehabilitation*. 2013;33(1):3–11.
16. Hochstenbach-Waelen A, Seelen HA. Embracing change: Practical and theoretical considerations for successful implementation of technology assisting upper limb training in stroke. *J Neuroeng Rehabil*. 2012;9:52.
17. Loureiro RC, Harwin WS, Nagai K, Johnson M. Advances in upper limb stroke rehabilitation: A technology push. *Med Biol Eng Comput*. 2011;49(10):1103–1118.
18. Lu EC, Wang RH, Hebert D, Boger J, Galea MP, Mihailidis A. The development of an upper limb stroke rehabilitation robot: Identification of clinical practices and design requirements through a survey of therapists. *Disabil Rehabil Assist Technol*. 2011;6(5):420–431.
19. Maciejasz P, Eschweiler J, Gerlach-Hahn K, Jansen-Troy A, Leonhardt S. A survey on robotic devices for upper limb rehabilitation. *J Neuroeng Rehabil*. 2014;11:3.
20. Morales R, Badesa FJ, Garcia-Aracil N, Sabater JM, Perez-Vidal C. Pneumatic robotic systems for upper limb rehabilitation. *Med Biol Eng Comput*. 2011;49(10):1145–1156.
21. Huang LL, Lee CF, Hsieh CL, Chen MH. Upper extremity rehabilitation equipment for stroke patients in Taiwan: Usage problems and improvement needs. *Occup Ther Int*. 2013;20(4):205–214.
22. Sukal-Moulton T, Krosschell KJ, Gaebler-Spira DJ. Dewald JP. Motor impairment factors related to brain injury timing in early hemiparesis. Part I: Expression of upper-extremity weakness. *Neurorehabil Neural Repair*. 2014;28(1):13–23.
23. Zackowski KM, Dromerick AW, Sahrmann SA, Thach WT, Bastian AJ. How do strength, sensation, spasticity and joint individuation relate to the reaching deficits of people with chronic hemiparesis? *Brain*. 2004;127(Pt 5):1035–1046.
24. Mottram CJ, Suresh NL, Heckman CJ, Gorassini MA, Rymer WZ. Origins of abnormal excitability in biceps brachii motoneurons of spastic-paretic stroke survivors. *J Neurophysiol*. 2009;102(4):2026–2038.
25. Gracies JM. Pathophysiology of spastic paresis. II: Emergence of muscle overactivity. *Muscle Nerve*. 2005;31(5):552–571.
26. Brunnstrom S. *Movement Therapy in Hemiplegia: A Neurophysiological Approach*. New York, NY: Harper & Row; 1970.
27. Jeong-Ho P, Kyoung-Soub L, Kyeong-Hun J, Dong-Hyun K, Hyung-Soon P. Low cost and light-weight multi-DOF exoskeleton for comprehensive upper limb rehabilitation. Proceedings of 11th Conference on Ubiquitous Robots and Ambient Intelligence (URAI). 2014:138–139.
28. Vitiello N, Lenzi T, Roccello S, et al. NEUROExos: A powered elbow exoskeleton for physical rehabilitation. *IEEE Trans. Robot*. 2013;29(1):220–235.
29. Mikołajczyk T, Olaru A, Walkowiak P. Upper limb exoskeleton controlled by stepper motor. *Applied Mechanics and Materials*. 2015;811:305–310.
30. Step2CNC. https://www.ebmia.pl/step2cnc-p-11637.html. Updated January 5, 2015. Accessed January 5, 2015.
31. Mikołajczyk T, Borboni A, Mackowski D, Matuszewski M. Example of tool with two numerical controlled axes. *Applied Mechanics and Materials*. 2015;772:224–229.
32. Mikołajczyk T, Dorsz D, Romanowski L. Design and control system of parallel kinematics manipulator. *Applied Mechanics and Materials*. 2013;436:390–339.
33. TeamViewer. https://www.teamviewer.com/pl/download/windows/. Updated January 5, 2015. Accessed January 5, 2015.
34. Poli P, Morone G, Rosati G, Masiero S. Robotic technologies and rehabilitation: New tools for stroke patients' therapy. *Biomed Res Int*. 2013:153872.
35. Masiero S, Poli P, Rosati G, et al. The value of robotic systems in stroke rehabilitation. *Expert Rev Med Devices*. 2014;11(2):187–198.

Iron excretion in urine in patients with acute kidney injury after cardiac surgery

Jowita Biernawska[1,A–F], Joanna Bober[2,C], Katarzyna Kotfis[3,A,B,D], Iwona Noceń[2,B], Anna Bogacka[4,B], Edyta Barnik[3,D], Dariusz Chlubek[5,C], Maciej Żukowski[3,A,C,E,F]

[1] Department of Anesthesiology and Intensive Therapy, Pomeranian Medical University, Szczecin, Poland
[2] Department of Medical Chemistry, Pomeranian Medical University, Szczecin, Poland
[3] Department of Anesthesiology, Intensive Therapy and Acute Intoxications, Pomeranian Medical University, Szczecin, Poland
[4] Department of Human Nutrition, West Pomeranian University of Technology, Szczecin, Poland
[5] Department of Biochemistry and Chemistry, Pomeranian Medical University, Szczecin, Poland

A – research concept and design; B – collection and/or assembly of data; C – data analysis and interpretation;
D – writing the article; E – critical revision of the article; F – final approval of the article

Advances in Clinical and Experimental Medicine, ISSN 1899-5276 (print), ISSN 2451-2680 (online) *Adv Clin Exp Med*. 2018;27(12):1671–1676

Address for correspondence
Edyta Barnik
E-mail: edytabarnik@op.pl

Funding sources
None declared

Conflict of interest
None declared

Received on December 8, 2016
Reviewed on January 5, 2017
Accepted on June 26, 2017

Abstract

Background. Hemolysis during cardiopulmonary bypass may lead to acute kidney injury caused by an excessive amount of iron. The clinical usefulness of the measurement of total iron concentration in the urine with the use of the atomic absorption spectrometry method for early identification of patients with postoperative acute kidney injury is not well-established.

Objectives. An observational, prospective study was conducted on a group of 88 pre-selected adult patients undergoing a planned coronary artery bypass grafting (CABG) procedure.

Material and methods. The amount and concentrations of total iron, creatinine and neutrophil gelatinase-associated lipocalin (NGAL) were evaluated in urine samples. A comparative analysis of the evaluated biochemical parameters was performed in regard to the occurrence of acute kidney injury 48 h postoperatively.

Results. Patients in the acute kidney injury group presented more advanced age ($p = 0.01$), preoperative myocardial infarction ($p = 0.02$), diuresis reduction ($p = 0.04$), and lower total iron levels in the 48-hour urine sample ($p = 0.01$). There was no difference when considering iron concentration in single urine samples in the study group.

Conclusions. The sole result of total iron concentration in single urine samples is unreliable for the diagnosis of acute kidney injury after cardiac surgery. Decreased excretion of iron in the urine seems to be an important additional element in the multifactorial pathogenesis of acute postoperative kidney failure.

Key words: iron, acute kidney injury, atomic absorption spectrometry

DOI
10.17219/acem/75504

Cardiac surgery-associated acute kidney injury (CSA-AKI) is an important clinical problem. Kidney injury usually occurs following a cardiac surgery procedure.[1–3] The pathomechanism of acute kidney injury (AKI) after cardiac surgery procedures performed with cardiopulmonary bypass (CPB) is complex and multifactorial. It involves several injury pathways: endogenous and exogenous toxins, ischemia and reperfusion, metabolic factors, inflammation, and oxidative stress.[4,5]

Undoubtedly, an important and frequently underlined factor increasing the negative effect of cardiopulmonary bypass on kidney function is oxidative stress.[6–9] The generation of free oxygen species is catalyzed by free iron ions (Haber-Weiss and Fenton reactions), which are especially active in acidic environments.[10] It has been shown in experimental studies that strategies targeting iron toxicity and renal protection using iron-chelating agents have a positive effect on pigment nephropathy and acute myocardial infarction.[11,12] Until recently, there has been no official recommendations toward their routine use.

It is a fact that nephron overload due to an excessive amount of iron released during hemolysis initiates a vicious cycle, where progressive oliguria makes it impossible to excrete excess iron, thus leading to a prolongation of the toxic effect of iron. On the other hand, there is some data indicating that urine iron is bound by urine neutrophil gelatinase-associated lipocalin (NGAL), or if unbound, could be reabsorbed at the Henle's loop.[13] Akrawinthawong et al. reported the clinical usefulness of urine (not plasma) iron concentration in a pilot study. They suggested that there is an overspill mechanism from hemolysis combined with overwhelming iron reabsorption at the tubules and collecting ducts and decreased reabsorption of iron in the tubules as AKI develops. The authors concluded that baseline and postoperative serial urine catalytic iron measurements are valuable indicators of AKI after open heart surgery.[13] A question arises of whether perioperative determination of total iron level in the urine could serve as a good marker for the diagnosis of CSA-AKI. To date, there has been no definitive answer to that question. Therefore, any additional element helpful in the understanding of reasons for postoperative kidney failure enables the establishment of proper therapeutic procedures.

This research paper assessed the clinical utility of the determination of total iron level in the urine, using atomic absorption spectrometry for the identification of patients with postoperative AKI. Our study was concentrated on assessing the utility of urine iron at 1 h postoperatively in the early AKI detection. We also analyzed the dynamism of urine iron level changes within the first 24 h after a cardiac procedure.

Material and methods

This observational, prospective study was conducted in a group of 88 Caucasian patients over the age of 18 years after signing an informed consent form.

All patients underwent a planned procedure of cardiac artery bypass grafting (CABG) with the use of CPB in the Department of Cardiac Surgery of the Pomeranian Medical University in Szczecin (Poland). The study protocol was approved by the local Ethical Committee of the Pomeranian Medical University in Szczecin, Poland (KB – 0012/146/10).

The inclusion criteria of the study covered a planned operation of CABG with the use of CPB. Exclusion criteria regarding the preoperative period were defined as:

- emergency operations or re-operations;
- a known pathology of the urinary tract or renal failure;
- chronic use of the following medications: iron, non-steroidal anti-inflammatory drugs (NSAIDs), immunosuppression, or steroids in the preoperative period;
- polycythemia, porphyria or pathological hemoglobin species in anamnesis;
- preoperative signs of hepatic failure;
- active autoimmune or neoplastic diseases, active infection;
- anticipated significant bleeding (anti-platelet agents), suggesting the use of blood-derived products during the operation and afterward.

The study population was divided into 2 groups regarding postoperative AKI: group "non-AKI" (n = 75), aged 62 ±7 years, 61 men (81%) and group "AKI" (n = 13), aged 70 ±6 years, 9 men (69%).

Acute kidney injury was defined according to Acute Kidney Injury Network (AKIN) criteria.[3]

Before the cardiac operation, full physical examinations were performed to assess the patients' clinical status and to qualify them for the study. In the operating room, standard patient monitoring was initiated and general anesthesia was induced using fentanyl, etomidat, pancuronium (doses calculated according to body weight), and sevoflurane. Electrocardiography (ECG), invasive blood pressure monitoring, central venous pressure, deep body temperature, and mechanical ventilation parameters were monitored continuously; diuresis and fluid balance were evaluated on an hourly basis, during the operation and for the first 24 h postoperatively, after that time, every 12 h. Metabolic monitoring was performed with a blood gas and electrolyte analysis in arterial blood using a GEM 3000 machine (Instrumentation Laboratory, Bedford, USA). Plasma iron concentration was measured on the day of the operation. Iron was determined with an atomic absorption spectrometer which had been calibrated using standard solutions. Measurements were made in an air-acetylene flame against the corresponding lamps at a wavelength of 248.3 nm.

Serum creatinine levels and other standard laboratory parameters were evaluated on the day of the operation and 24 h and 48 h postoperatively.

Additionally, we measured NGAL level in the urine using a commercially available enzyme-linked immunosorbent assay (ELISA) kit (Human Lipocalin-2/NGAL Quantikine

ELISA Kit; R&D Systems, Minneapolis, USA) with a microplate reader ELx808 (BIO-TEK Instruments, Inc., Winooski, USA), according to the manufacturer's instructions. The time-points for NGAL measurement were 1 h after CPB (post-op sample) and 24 h from the beginning of the operation (postoperative day 1, POD 1 sample).

Moreover, an analysis of total iron concentration in single urine samples was performed. The method for performing the biochemical studies is presented below. After collection, the urine was centrifuged (1850 g, 10 min, 4°C). The supernatant was immediately frozen to –80°C until the analysis was performed. Iron level in the urine was evaluated using mass atomic absorption spectrometry by means of an absorption meter (PU 9100X; Philips, Cambridge, England). The applied wavelength was 248.3 nm. Without any intervention, the normal value for total iron in the 24-hour urine was set at 40–150 μg (0.71–2.68 μmol). The normal value for total iron in the 24-hour urine of cardiac surgery patients (after CPB as an intervention) is unknown. The time-points for urine total iron concentration measurement were preoperative (zero sample), 1 h after CPB (post-op sample), and over 24 h from the beginning of the operation (POD 1 sample). Plasma-free hemoglobin concentration was measured in a reaction with Drabkin's reagent. The change of absorbance was noticed at wavelengths of 540 nm and 680 nm. The normal value is 5–40 mg/dL.

Cardiopulmonary bypass was performed using a non-pulsatile pump (Maquet, Hirrlingen, Germany) and a membrane oxygenator (Terumo Cardiovascular Systems, Ann Arbor, USA) primed with 1000 mL of Ringer's lactate, 500 mL of Gelofusine, 60 mEq of sodium bicarbonate, and 4 mg/kg of heparin. An individual CPB flow was calculated on the basis of 2.5 L/min/m^2 and systemic arterial blood pressure was maintained between 50 and 70 mm Hg. If the systemic perfusion pressure decreased, CPB flow was increased up to a maximum of 130% of the calculated flow. If the systemic pressure decrease could not be compensated for by increasing CPB flow, a norepinephrine infusion was used. The operation was performed in normothermia.

Statistical analysis included evaluating the changes of serum creatinine concentration and the biochemical parameters in the urine (total iron and creatinine) in relation to the occurrence of AKI according to the AKIN criteria up to 48 h postoperatively.

Statistical analysis

All results are presented as mean ± standard deviation (SD). The Shapiro-Wilk test was used to check for normality of the sample data. To determine the differences between the AKI group and the non-AKI group, the Mann-Whitney U test was used for quantitative variables and Pearson's χ^2 test was used for qualitative variables. A logistic regression model was performed to predict whether urine iron concentration at defined time-points is a postoperative AKI risk factor based on the patient's age (covariate). The independent variables were urine iron concentration and age. The analysis was done using STATISTICA v. 10 software (StatSoft, Kraków, Poland). Statistical significance was set at $p < 0.05$.

Results

Early postoperative kidney failure based on the AKIN criteria was diagnosed in 13 patients (14%) during the first 48 h postoperatively. In all of the cases, the AKIN diuresis criteria were equivalent to the AKIN creatinine criteria. Cardiac surgery-associated acute kidney injury was diagnosed in 6 patients within the first 6 h postoperatively (AKIN stage 1, next progression to stage 2 based on oliguria) and in 7 patients within the 48-hour period after the procedure based on oliguria and serum creatinine level (AKIN stage 2). The characteristics of the patient population are shown in Table 1.

When comparing the time of CPB, minimal mean arterial pressure, the need for vasopressors or inotropes, and minimal body temperature, there were no differences between the 2 subgroups in the intraoperative period. In the study group, none of the patients needed perioperative transfusion of blood products. Selected data from the intraoperative period and the first 24 h postoperatively are presented in Table 2.

There were no statistically significant differences in the concentration of plasma iron or serum and urine creatinine, nor in the urinary iron concentration in the preoperative period (zero sample) or directly after the CPB (POD 1 sample). There were differences in diuresis in the intraoperative and postoperative periods, though. Therefore, the excretion of total iron was not only shown

Table 1. Demographic data and comorbidities of the study population

Characteristics	Non-AKI n = 75	AKI n = 13	p-value
Age [years], mean ±SD	62 ±7	70 ±6	<0.01
BMI [kg/m^2], mean ±SD	28.02 ±3.71	31.20 ±3.98	0.01
LV EF [%], mean ±SD	53.52 ±9.57	46.85 ±12.79	0.08
EuroScore [points], mean ±SD	2.36 ±1.91	3.77 ±2.62	0.07
Gender [male], n [%]	61 (81)	9 (69)	0.32
Left ventricular dysfunction NYHA ≥II, n [%]	48 (64)	11 (84)	0.53
Myocardial infarction, n [%]	31 (41)	10 (76)	0.02
Arterial hypertension, n [%]	64 (85)	11 (84)	0.46
Diabetes mellitus, n [%]	23 (30)	8 (61)	0.07
Peripheral vascular disease, n [%]	74 (98)	13 (100)	0.33
Atrial fibrillation, n [%]	4 (5)	1 (7)	0.75

AKI – acute kidney injury; BMI – body mass index; LV EF – left ventricle ejection fraction before procedure; EuroScore – European System for Cardiac Operative Risk Evaluation; NYHA – New York Heart Association.

Table 2. Interventions and clinical outcomes of the study population

Characteristics (mean ±SD) Interventions	Non-AKI n = 75	AKI n = 13	p-value
Cardiopulmonary bypass time [min]	48 ±13	48 ±15	0.78
Aorta cross-clamp time [min]	29 ±7	29 ±8	0.71
Surgical procedure time [min]	167 ±28	165 ±24	0.82
Minimal value of MAP (CPB) [mm Hg]	68 ±8	64 ±6	0.24
Urine output during a surgical procedure [mL]	659 ±389	453 ±368	0.04
Fluid balance during a surgical procedure [mL]	715 ±569	530 ±765	0.33
Urine output [mL]*	3215 ±799	2607 ±460	<0.01
Fluid balance [mL]*	−627 ±1204	−584 ±780	0.87

AKI – acute kidney injury; MAP – mean arterial pressure; CPB – cardiopulmonary bypass; SD – standard deviation; * from the beginning of the operation to 24 h thereafter.

as the concentration in a single sample, but also as the total amount of iron in the urine collected 24 h postoperatively. A comparison of creatinine, total iron and NGAL excretion in the urine in pre-defined time-points is shown in Table 3.

We compared the changes of free hemoglobin (plasma) concentration in 65 patients (no-AKI group) and 13 patients (AKI group) at defined time-points. There were no significant differences.

The logistic regression model showed that the patient's age (covariate) is not a factor determining postoperative AKI. This result was observed in all variables in the study.

Table 3. Perioperative values of serum and urine parameters in the study population

Characteristics (mean ±SD)	Non-AKI n = 75	AKI n = 13	p-value
Preoperative (zero sample)			
Iron concentration [mg/L^{-1}] (urine)	0.12 ±0.06 OR = 4.5 × 10^{-5} 95% CI: 8.15 × 10^{-10}–2.5	0.14 ±0.07 0.07	0.07
Iron concentration [mg/dL^{-1}] (plasma)	130.8 ±27.21	123.9 ±6.1	0.92
Creatinine [mg/dL^{-1}] (serum)	0.88 ±0.19	0.96 ±0.28	0.47
1 h after the end of CPB (post-op sample)			
Iron concentration [mg/L^{-1}] (urine)	0.08 ±0.05 OR = 9.3 × 10^{-4} 95% CI: 6.28 × 10^{-9}–138.9	0.10 ±0.06 0.24	0.29
NGAL [ng/mL^{-1}] (urine)	3.12 ±7.20	9.30 ±13.78	<0.01
24 h after the beginning of the operation (POD 1 sample)			
Iron concentration [mg/L^{-1}] (urine)	0.12 ±0.05 OR = 320.74 95% CI: 5.58 × 10^{-4}–1.8 × 10^{4}	0.09 ±0.06 0.38	0.09
Total iron (urine)*	407 ±191.01	268 ±120.74	<0.01
Creatinine [mg/dL^{-1}] (serum)	0.86 ±0.22	1.29 ±0.38	<0.01
NGAL [ng/mL^{-1}] (urine)	12.19 ±11.76	25.02 ±11.89	<0.01
48 h after the beginning of the operation (POD 2 sample)			
Creatinine [mg/dL^{-1}] (serum)	0.84 ±0.25	1.67 ±0.55	<0.01

AKI – acute kidney injury; CPB – cardiopulmonary bypass; POD – postoperative day; NGAL – neutrophil gelatinase-associated lipocalin; OR – odds ratio; CI – confidence interval; SD – standard deviation; * the mean ±SD of total iron (µg/day) excreted in the urine during the 1st postoperative day (urine collected for 24 h).

Discussion

The pathomechanism of pigment nephropathy after cardiac surgery is based on kidney injury secondary to the influence of free hemoglobin released from erythrocytes during CPB.[7] Active free iron ions are generated during erythrocyte damage and hemolysis by the CPB set. A sudden increase in the amount of iron can exceed the iron binding capacity. As a result, it can be observed that many changes occur within the epithelium of the tubular cells. Previous studies confirmed iron toxicity in the case of acute and chronic kidney failure, acute cardiac ischemic injury and neurodegenerative diseases.[8–10,14,15] There is evidence from animal studies that iron is involved in a variety of models of AKI. However, there is limited data from human studies to support our study.

An important human defense mechanism in the case of iron overload is iron excretion in the urine. One can imagine that the assessment of iron excretion in the urine would be an ideal marker of this pathomechanism. However, one must take into account the fact that a reduction of diuresis and increased NGAL concentration (an important iron-translocating compound) can modify final iron excretion. The result of our study was that patients with AKI showed significant differences in total iron levels in the urine collected 24 h postoperatively, as assessed by atomic absorption spectrometry. Urine iron level was assessed in the first 24 h only because we defined this as an early marker. In our opinion, a decrease of urine output as a clinical manifestation of AKI might cause a decrease in the iron-excreting ability in the AKI group. This fact underlines the importance of actual diuresis and fluid balance when the purifying function of the kidneys is analyzed.

In our study, total iron excreted with the urine was elevated in all patients in the study group. However, to date no validated "normal values" for cardiac surgery patients have been determined. The most important conclusion of this study is that the single result of total iron concentration in a single urine sample is unreliable for AKI diagnosis after cardiac

surgery. This result is opposite to the findings of the sole human pilot study.[13] The authors of that trial noticed increased levels of urine catalytic iron at the same time as urine NGAL. In our opinion, this difference is caused by the very small sample size. In our unpublished data, we observed a similar trend in the first few results. In the current study, we observed a rise of urine NGAL at 1 h and 24 h postoperatively. However, when we considered the values of serum creatinine levels and urine NGAL levels in individual patients, we detected some differences. Regarding serum creatinine, we diagnosed 13 AKI cases within the first 48 h after operation. However, an elevated NGAL level was observed in 5 of 13 patients and in 4 cases without AKI. To date, NGAL is not a criterion in the recognizing and staging of AKI. Akrawinthawong et al. showed the results of serial urine catalytic iron measurements, but urine catalytic iron and NGAL were first measured 8 h postoperatively. We cannot compare our results because in our study the time-point was different (1 h after the end of CPB).[13]

A decrease in diuresis is a clinical manifestation of renal tubule insufficiency. This fact underlines the need for the purifying function of the kidneys in the context of actual diuresis and fluid balance, as the changes in the amount of iron are usually minimal and the clinical implications are very important. Acute kidney injury occurred more frequently in patients with a past medical history of myocardial infarction. This fact could be explained as follows: oxygen free radicals are generated as a consequence of oxidative stress related to myocardial infarction and this process is catalyzed by iron ions. These free radicals cause organ damage, including the kidneys. The presence of another damaging factor, i.e., CPB, leads to an increase of the previously subclinical kidney damage.

Iron measurement methods

The question is: what should we measure – plasma or urine iron? Leaf et al. showed that increased plasma catalytic iron in patients might mediate AKI and death following cardiac surgery.[16] However, plasma catalytic iron concentration may increase due to reduced filtration. In the study by Leaf et al., urine output was not assessed. They did not use oliguria as an AKI criterion. In the available literature, the measurement of urine output regarding its purifying role is crucial. The amount of urine output during CPB can be a simple method to predict the development of AKI after cardiac surgery.[17] The population analyzed by Leaf et al. was heterogenic (the majority of patients had valve or mixed procedures). More than 30% of the procedures were urgent or re-operations. The mean CPB time was 3-fold longer than in our study. All these factors are important regarding hemolysis, load of iron, the staging of cardiac surgery-related AKI, and the need for renal replacement therapy in the case of postoperative AKI. However, the authors did not show a comparison among the group regarding these factors, so we cannot compare results to our "isolated CABG group." In our study, the population is homogenic. The variation in urine iron excretion is also noticeable, but statistically insignificant among the study group.

The role of iron as a mediator of CSA-AKI is still not fully appreciated; therefore, the methods of iron measurement are not widely used in clinical practice. The chemical identification of the labile iron pool is difficult due to the variety of iron ligands present in cells.[10] Atomic absorption spectrometry is an analysis technique which enables iron determination in liquid, solid and gas samples. The analysis is based on the absorption of radiation at a specific wavelength by free iron atoms, evaluation of its absorbency, and therefore its ion concentration. This method enables the detection of even minimal quantities of the metal in a sample. This is especially important in patients after CABG, because perioperative hemodilution leads to a situation where the amount of iron in the analyzed sample is minimal. The clinical utility of this method and the indications for its routine use require further studies.

One source of iron is hemolysis. Hemolysis is a recognized consequence of CPB. It has been shown to increase with complex procedures (CABG + valve surgery) because of longer perfusion times.[18] Hemolysis during cardiac surgery may be diagnosed and monitored by plasma extracellular (free) hemoglobin and plasma haptoglobin (the physiological intravascular free hemoglobin scavenger) concentration, assessed at regular time-points. However, there were no significant differences in our results.

One limitation of the current study is the lack of plasma iron concentrations at 1 h and 24 h postoperatively. Another limitation is the lack of plasma and urinary iron measurements 48 h postoperatively.

In conclusion, the presented study confirms that the sole result of total iron concentration in a single urine sample is unreliable in the diagnosis of AKI after cardiac surgery. This study indicates that decreased iron excretion with decreased urine volume seems to be an important additional element in the multifactorial pathogenesis of acute postoperative kidney failure. It is possible that in the future, iron-chelating compounds or elective intraoperative hemofiltration will be used as a method of targeted preventive therapy. In the early postoperative period, the interpretation of biochemical parameters in the context of current diuresis and fluid balance seems to be of critical importance.

References

1. Bellomo R, Auriemma S, Fabbri A, et al. The pathophysiology of cardiac surgery-associated acute kidney injury (CSA-AKI). *Int J Artif Organs*. 2008;31:166–178.
2. McCullough PA, Kellum JA, Haase M, et al. Pathophysiology of the cardiorenal syndromes: Executive summary from the eleventh consensus conference of the Acute Dialysis Quality Initiative (ADQI). *Contrib Nephrol*. 2013;182:82–98.
3. Mehta RL, Kellum JA, Shah SV, et al. Acute Kidney Injury Network: report of an initiative to improve outcomes in acute kidney injury. *Crit Care*. 2007;11:R31. doi: 10.1186/cc5713

4. O'Neal J, Shaw A, Billings F. Acute kidney injury following cardiac surgery: Current understanding and future directions. *Crit Care*. 2016;20:187. doi: 10.1186/s13054-016-1352-z
5. Haase-Fielitz A, Bellomo R, Devarajan P, et al. Novel and conventional serum biomarkers predicting acute kidney injury in adult cardiac surgery – a prospective cohort study. *Crit Care Med.* 2009;37:553–560.
6. Mao H, Katz N, Ariyanon W. Cardiac surgery-associated acute kidney injury. *Cardiorenal Med*. 2013;3:178–199. doi: 10.1159/000353134
7. Haase M, Haase-Fielitz A, Bagshaw SM, Ronco C, Bellomo R. Cardiopulmonary bypass-associated acute kidney injury: A pigment nephropathy? *Contrib Nephrol*. 2007;156:340–353.
8. Shah S, Rajapurkar M, Baliga R. The role of catalytic iron in acute kidney injury. *Clin J Am Soc Nephrol*. 2011;6:2329–2331.
9. Haase M, Bellomo R, Haase-Fielitz A. Novel biomarkers, oxidative stress, and the role of labile iron toxicity in cardiopulmonary bypass-associated acute kidney injury. *J Am Coll Cardiol*. 2010;55:2024–2033.
10. Kakhlon O, Cabantchik ZI. The labile iron pool: Characterization, measurement, and participation in cellular processes. *Free Radic Biol Med*. 2002;33:1037–1046.
11. Ambrus CM, Stadler I, Toumbis CA, et al. Removal of non-transferrin-bound iron from blood with iron overload using a device with immobilized desferrioxamine. *J Med*. 1999;30:211–224.
12. Paraskevaidis IA, Iliodromitis EK, Vlahakos D, et al. Deferoxamine infusion during coronary artery bypass grafting ameliorates lipid peroxidation and protects the myocardium against reperfusion injury: Immediate and long-term significance. *Eur Heart J*. 2005;26:263–270.
13. Akrawinthawong K, Shaw M, Kachner J, et al. Urine catalytic iron and neutrophil gelatinase-associated lipocalin as companion early markers of acute kidney injury after cardiac surgery: A prospective pilot study. *Cardiorenal Med*. 2013;3(1):7–16.
14. Korsak J. Posttransfusion iron overload. *Pol Merk Lek*. 2011;30:177.
15. Martines AM, Masereeuw R, Tjalsma H, Hoenderop JG, Wetzels JF, Swinkels DW. Iron metabolism in the pathogenesis of iron-induced kidney injury. *Nat Rev Nephrol*. 2013;9(7):385–398. doi: 10.1038/nrneph.2013.98
16. Leaf DE, Rajapurkar M, Lele SS, et al. Increased plasma catalytic iron in patients may mediate acute kidney injury and death following cardiac surgery. *Kidney Int*. 2015;87(5):1046-1054. doi: 10.1038/ki.2014.374
17. Song Y, Kim DW, Kwak YL. Urine output during cardiopulmonary bypass predicts acute kidney injury after cardiac surgery: A single center retrospective analysis. *Medicine (Baltimore)*. 2016;95(22):e3757.
18. Vermeulen Windsant IC, de Wit NC, Sertorio JT, et al. Hemolysis during cardiac surgery is associated with increased intravascular nitric oxide consumption and perioperative kidney and intestinal tissue damage. *Front Physiol*. 2014;8(5):340. doi: 10.3389/fphys.2014.00340

The peripheral neutrophils in subjects with COPD-OSA overlap syndrome and severe comorbidities: A feasible inflammatory biomarker?

Madalina Macrea[1,2,A–F], Sabrina Campbell[1,3,B], Thomas Martin[1,2,E,F], Kris Ann Oursler[1,3,A,C,E,F]

[1] Salem Veterans Affairs Medical Center, USA
[2] Department of Medicine, University of Virginia School of Medicine, Charlottesville, USA
[3] Virginia Tech Carilion School of Medicine, Roanoke, USA

A – research concept and design; B – collection and/or assembly of data; C – data analysis and interpretation;
D – writing the article; E – critical revision of the article; F – final approval of the article

Advances in Clinical and Experimental Medicine, ISSN 1899-5276 (print), ISSN 2451-2680 (online) *Adv Clin Exp Med*. 2018;27(12):1677–1682

Address for correspondence
Madalina Macrea
E-mail: madalina.macrea@va.gov

Funding sources
This research was supported by the Department of Veteran Affairs, Veterans Health Administration, Rehabilitation Research and Development Service through the VA Career Development Award given to Dr. Macrea.

Conflict of interest
None declared

Received on August 25, 2016
Reviewed on December 25, 2016
Accepted on July 14, 2017

Abstract

Background. Overlap syndrome (OS) describes the association of obstructive sleep apnea (OSA) and chronic obstructive pulmonary disease (COPD) in a single individual. Subjects with OS have increased cardiovascular mortality which is presumed to be inflammation-mediated. As a clinical biomarker, an increased neutrophil count correlates with the severity of coronary artery stenosis.

Objectives. As little is known about the role of neutrophils in the underlying inflammatory mechanisms in OS, we aimed to assess the percentage of peripheral neutrophils (PPN) in OS vs in COPD alone.

Material and methods. A cross-sectional study of patients with COPD and severe comorbidities, as defined by a Care Assessment Need score over 95, were seen in the Pulmonary Tele-Health Clinic at the Salem Veteran Affairs Medical Center, USA, over a 1-year period. Demographic and polysomnographic data, FEV1 and the Charlson Comorbidity Index (CCI) were extracted from the Electronic Medical Records. Obstructive sleep apnea was defined according to the American Academy of Sleep Medicine (AASM) guidelines. Serum inflammatory markers (PPN, CRP, fibrinogen and procalcitonin) were obtained after the Tele-Health appointment.

Results. Out of the 38 subjects with COPD, 17 (44%) had OS. Compliance with continuous positive airway pressure therapy (CPAP) was excellent in 7 OS subjects (41%). There was a significant difference in the PPN of subjects with OS vs COPD alone, regardless of whether they were compliant ($p = 0.03$) with the CPAP therapy or not ($p = 0.005$). No differences in the severity of COPD, baseline comorbidity, smoking, or inflammatory markers were found between the OS and COPD-only subjects. Body mass index (BMI), COPD severity, smoking, and home oxygen therapy (HOT) use were not associated with PPN ($p > 0.2$).

Conclusions. Overlap syndrome subjects have higher PPN than those with COPD alone, regardless of their CPAP compliance. Our results could be used to motivate OS subjects to improve their lifestyles and to comply with drug therapies aimed at reducing cardiovascular disease (CVD).

Key words: obstructive sleep apnea, chronic obstructive pulmonary disease, cardiovascular, systemic inflammation, neutrophils

DOI
10.17219/acem/75904

Introduction

Chronic obstructive pulmonary disease (COPD), a disease characterized by irreversible airflow limitation, and obstructive sleep apnea disease (OSA), a disease characterized by intermittent collapse of the upper airway, are each responsible for major morbidity, mortality and economic burden.[1] The term "overlap syndrome" (OS) was introduced to describe the association of both conditions in a single patient. Given the high prevalence of both COPD and OSA, it is expected that up to 29% of OSA subjects could be affected by OS.[2] Although the evidence suggests that the increased mortality in OS subjects is primarily cardiovascular, the exact mechanisms remain unclear.[1] It is likely, though, that cell-mediated inflammation plays an important role given the shared systemic inflammation pathways in COPD, OSA and atherosclerosis.[3] The possible biological pathways by which neutrophils might influence the development of cardiovascular disease (CVD) are protean and include an increased adherence of platelets to subendothelial collagen and the release of leukotriene, superoxide and inflammatory mediators.[4–6] As a clinical biomarker, increased neutrophil count correlates with the severity of coronary artery stenosis and survival in subjects with stable coronary artery disease and demonstrates good specificity as a prognostic marker for acute coronary syndrome when the electrocardiogram was nonspecific.[7,8] McNicholas suggested that COPD and OSA are systemic disorders that can cause or worsen CVD, one of the mechanisms related to the chronic intermittent hypoxia that stimulates the inflammatory cytokines in which neutrophils participate.[3] Despite these findings, the abovedescribed findings were not demonstrated in OS and little is known about the role of neutrophils in the underlying mechanisms of increased mortality in these subjects. We therefore aimed to assess peripheral neutrophils in OS subjects compared to COPD-only subjects with a similar degree of comorbidity. In addition, as it is has been suggested that the current standard therapy for OSA, i.e., continuous positive airway pressure (CPAP), could alter the inflammatory markers in OSA, we evaluated the inflammatory response in both CPAP-compliant and noncompliant OS subjects as compared to COPD-only subjects.

Material and methods

The study is a cross-sectional retrospective evaluation of subjects with COPD and severe comorbidities selected from subjects followed for routine primary care at the community-based outpatient clinics (CBOC) satellite to the Salem Veterans Affairs Medical Center (VAMC), USA, over 1 year. The severity of comorbidity was assessed by the Care Assessment Need Score (CAN), which indicates how a given patient compares to other individuals in terms of the likelihood of hospitalization or death. Higher CAN scores reflect an increased number of healthcare providers, medications and mental health diagnoses.[9] Subjects with a CAN score greater than 95 were eligible for the study and their charts were screened for a pulmonary function test (PFT) that showed COPD according to American Thoracic Society (ATS) guidelines. Three hundred and fifty-three subjects with a CAN score over 95 were identified in the CBOC; 150 of these subjects were diagnosed with COPD. Thirty-eight of the COPD subjects were evaluated in the Pulmonary Tele-Health Clinic, out of which 17 had a diagnosis of OSA prior to this study and were defined as cases of OS. Demographic, clinical and medication data (inhaled and oral corticosteroid) were extracted from the Electronic Medical Records (EMR). The Charlson Comorbidity Index (CCI) and the Framingham (FH) 10-year cardiovascular risk score were calculated based on EMR data.[10,11] Dyspnea severity was assessed using the Medical Research Council Scale.[12] The study was approved by the Salem VAMC Review Board as quality improvement data.

Among the COPD participants, a chart review was performed for a diagnosis of OSA. The inclusion of OSA subjects was done based on a diagnostic polysomnogram completed prior to our study (SensorMedics, Sunnyvale, USA). The stages of sleep were identified using 2-channel electroencephalogram (C4–A1, C3–A2), chin electromyogram, and left and right electrooculograms. Thoracoabdominal movements were monitored with thoracic and abdominal strain gauges. Airflow was monitored with an oronasal thermistor per the clinical protocol. Arterial oxyhemoglobin saturation was recorded with the use of a pulse oximeter. Electrocardiogram, snoring and body position were also recorded. Recordings were manually scored according to the standard criteria.[13] An episode of obstructive apnea was defined as an absence of airflow for at least 10 s, in the presence of rib cage and abdominal excursions. Hypopnea was defined as a discernible reduction in airflow lasting 10 s or longer and associated with at least a 4% decrease in arterial oxyhemoglobin saturation, an electroencephalographic arousal, or both. The number of episodes of apnea and hypopnea per hour was referred to as the apnea hypopnea index (AHI). The mean and minimal oxygen saturation for the entire night was estimated, along with the duration of stages 1, 2, 3, and rapid eye movement (REM) of sleep; sleep fragmentation was assessed using the arousal index (AI). The sleep parameters were scored and OSA was defined according to the criteria established by the American Academy of Sleep Medicine Manual for Scoring Sleep and Associated Events.[13]

Morning blood samples were collected for white blood cell count (WBC) with the percentage of peripheral neutrophils (PPN), C-reactive protein (CRP), fibrinogen, and procalcitonin, from subjects who attended the Tele-Health appointment. Assays were performed in a single run by the Salem VAMC laboratory.

The normality of continuous variables was evaluated by the Shapiro-Wilk test. Comparison of continuous data between the OS and COPD-only groups was performed using a t-test for data with normal distribution. Peripheral neutrophils, systolic blood pressure and serum procalcitonin had a skewed distribution and the difference between groups was tested by the Wilcoxon-Mann-Whitney test. Since BMI has a known association with OS and chronic inflammation, stratified analysis by obesity (BMI >30 kg/m^2) was performed to assess for potential confounding. A 2-sided p-value <0.05 was considered statistically significant. All analyses were performed using STATA v. 11.0 software (Stata Corporation, College Station, USA).

Results

Thirty-eight subjects with confirmed COPD were included in the study and 17 (44%) of these were classified as OS. Seven out of the 17 subjects with OS had an excellent CPAP compliance as defined by Medicare guidelines, i.e., the use of CPAP devices for 4 or more hours per night on 70% of nights.[14] The subjects' baseline characteristics are detailed in Table 1. The 112 subjects who were eligible for the study (CAN score >95 and a diagnosis of COPD) but could not be reached by phone or who declined participation in the Tele-Health appointments were not demographically different from those included in the analysis.

All OS subjects had an AHI greater than 5, except 1 patient whose AHI was 4.7. This patient was diagnosed with OSA and therefore classified as OS as well, due to the evidence of snoring with arousals during REM sleep, desaturations (at least 4%) and symptoms suggestive of OSA, such as excessive daytime sleepiness. The AI, as well as mean and lowest oxygen saturations during the sleep study are described in Table 2. There was a significant difference (p = 0.002) in PPN values in OS patients (73 ±9.3) vs COPD-only patients (60 ±14.9), regardless of whether OS subjects were compliant with the CPAP therapy (p = 0.03) or not (p = 0.005). There was no difference in the PPN values between CPAP-compliant and noncompliant OS subjects (p = 0.91). The association of PPN and OS remained significant for obese subjects (p = 0.04) and non-obese subjects (p = 0.03). The serum inflammatory markers, WBC, CRP, fibrinogen, and procalcitonin were similar between the OS subjects and COPD-only subjects (Table 3), regardless of their compliance (p > 0.11) or noncompliance (p > 0.17) with the CPAP therapy. No differences in the severity of COPD, baseline comorbidities, smoking, or home oxygen therapy (HOT) use (at night, during the day or continuously) were found between OS subjects and COPD-only subjects (Table 1). Body mass index was higher in the OS group (Table 2). Body mass index, COPD severity, smoking, and HOT use (diurnal, nocturnal or continuous) were not associated with PPN (p-values >0.2).

Table 1. Subjects' baseline characteristics

Variable	OS group (mean ±SEM)	COPD-only group (mean ±SEM)	p-value
Number	17	21	NS
Demographics			
age [years]	69 ±1.3	74 ±1.9	NS
active smoking [%]	23	33	NS
BMI [kg/m^2]	32 ±1.9	27 ±1.3	0.02
Hemodynamics			
systolic blood pressure [mm Hg]	131 ±4.9	128 ±7.1	NS
diastolic blood pressure [mm Hg]	74 ±2	69 ±3	NS
heart rate [beats/min]	77 ±3	811e	NS
CCI Score	6 ±0.31	5 ±0.53	NS
Framingham Score	23 ±1.4	26 ±1.7	NS

OS – overlap syndrome; CCI – Charlson Comorbidity Index; COPD – chronic obstructive pulmonary disease; BMI – body mass index; SEM – standard error of the mean; NS – not significant.

Table 2. Description of the severity of COPD and OSA disease

Variable	OS group (mean ±SD)	COPD-only group (mean ±SD)	p-value
COPD			
FEV1 [L]	1.6 ±0.6	1.6 ±0.5	NS
FEV1 [%]	48 ±17	52 ±13	NS
mild [%]	43	60	NS
moderate [%]	43	30	NS
severe [%]	12	10	NS
OSA			
AHI	17 ±6	NA	
CPAP compliant, n	7	NA	
arousal index [events/h]	28.6 ±16	NA	NA
mean oxygen saturation [%]	81 ±6.3	NA	
lowest oxygen saturation [%]	91 ±1.7	NA	
MRC Dyspnea Score	2.8 ±1.2	2.9 ±1	NS
BMI	32 ±8.1	27 ±6.4	NA
HOT			
diurnal [%]	35	38	NS
nocturnal [%]	35	38	NS
continuous [%]	0	0	NS
Steroid use			
inhaled, n	10	9	NS
oral steroid, n	2	0	NS

COPD – chronic obstructive pulmonary disease; FEV1 (L) – forced expiratory volume in 1 min in liters; FEV1 (%) – forced expiratory volume in 1 min as a percentage compared to controls; OSA – obstructive sleep apnea; AHI – apnea-hypopnea index; CPAP – positive airway pressure therapy; MRC Dyspnea Score – Medical Research Council Dyspnea Score; BMI – body mass index; HOT – home oxygen therapy; SD – standard deviation; NS – not significant; NA – not applicable.

Discussion

In a clinic-based sample of community-dwelling subjects with a high level of overall comorbidity, we found that PPN is higher in OS subjects compared to COPD-only subjects, regardless of their compliance with the CPAP therapy.

Table 3. Description of the inflammatory markers

Inflammatory marker	OS group (mean ±SD)		COPD-only (mean ±SD)	p-value
	CPAP compliant	CPAP noncompliant		
White blood cells [cells/mm^3]	8.8 ±4.1	8.7 ±2.3	7.8 ±1.8	NS
PPN [%]	72 ±1.7*	73 ±9.5**	60 ±14.9	<0.03
C-reactive protein [mg/L]	9.6 ±4.9	5.7 ±3.8	9.2 ±12.4	NS
Fibrinogen [mg/dL]	403 ±58	442 ±114	397 ±70.6	NS
Procalcitonin [mg/mL]	0.06 ±0.03	0.07 ±0.04	0.05 ±0.007	NS

* PPN in CPAP compliant vs COPD subjects, p = 0.03; ** PPN in CPAP noncompliant vs COPD subjects, p = 0.005); OS – overlap syndrome; COPD – chronic obstructive pulmonary disease; PPN – peripheral neutrophils; CPAP – positive airway pressure therapy; SD – standard deviation.

The severity of COPD was similar between groups and, moreover, was not associated with PPN. These results suggest that the additive adverse effect of OSA is associated with increased PPN in OS and they support further research on neutrophil-related inflammation and cardiovascular disease (CVD) in these subjects.

The role of increased inflammation in sleep disordered breathing (SDB) has been receiving increased attention recently. Systemic inflammation measured by standard inflammatory markers such as CRP and interleukin-6 (IL-6) has been studied in both COPD and OSA and supports causation between inflammation and early atherosclerosis and association between inflammation and worse outcomes.[15–17] Data on the inflammatory response in OS is currently limited to only a few studies to date. Nural et al. demonstrated that the serum CRP level was higher in the OS group than the COPD-only or OSA-only groups.[18] Mansour et al. showed that nasal CPAP decreased levels of TNF-α, CRP and IL-6 in these subjects.[19] While no direct link has yet been demonstrated between inflammation and CVD in OS subjects, Marin et al. reported a higher number of cardiovascular deaths in subjects with untreated OS compared to treated OS, and a higher number of deaths than in those with COPD only.[1] Although the concept of inflammation-related CVD in SDB is largely accepted,the evidence supporting it is difficult to find as the typical inflammatory markers, such as CRP and IL-6, are heavily confounded by obesity and smoking status.[20] Therefore, other serum markers, such as neutrophils, are worth exploring given their lack of a strong connection with BMI (less than 10% of the variance of change).[21] Moreover, the neutrophil count is inexpensive, reliable, easy to interpret, and ordered routinely in inpatient and outpatient settings. Whether neutrophils are different in obesity or not is controversial, as both increased percentages in African-American children and unchanged numbers in men have been reported.[22,23] In addition, Dixon et al. showed that even when neutrophils change with BMI in adults, this change was small and accounted for less than 10% of the variance of baseline counts.[21] In our study, OS subjects had a significantly higher BMI than the COPD-only subjects, but BMI was not associated with PPN.

The detailed mechanism by which neutrophils contribute to inflammation-mediated CVD is yet unknown, but possibly related to an abnormal antiapoptotic response as a response to hypoxia, with increased neutrophil survival, migration towards endothelial injury and augmentation of the atherosclerotic nidus.[24] Recent evidence suggests that hypoxia is associated with delayed apoptosis of neutrophils in COPD and decreases apoptosis in OSA subjects, a process that may induce vascular damage through the previously mentioned biochemical and hematological mechanisms.[24,25] Overall, the apoptosis of neutrophils represents a fundamental and intricate process of intracellular death/survival signaling pathways whose overall balance aims at containing the inflammatory response.[26] In OSA and COPD subjects, antiapoptotic myeloid cell leukemia 1 (Mcl-1) is upregulated and the proapoptotic Bax or Bak molecules are downregulated.[24,27] This concept becomes especially important for OS subjects who have both COPD and OSA. In addition to these quantitative changes, in both OSA and COPD, the neutrophils undergo qualitative changes being "primed" for an enhanced respiratory burst and ROS production, thus activating the inflammatory cascade and leading to the development of impaired endothelial function.[28–30] These findings suggest congruently

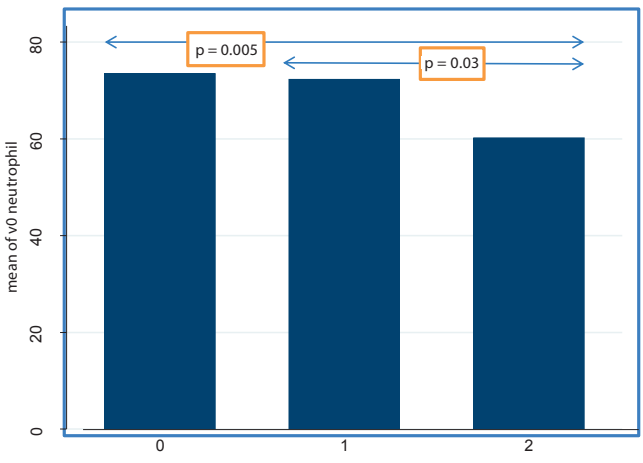

Fig. 1. Peripheral neutrophils (PPN) in subjects with OS vs COPD-only

OS – overlap syndrome; CPAP – positive airway pressure therapy; COPD – chronic obstructive pulmonary disease; group 0 – OS subjects noncompliant with CPAP; group 1 – OS subjects compliant with CPAP; group 2 – COPD-only subjects; PPN was higher in subjects with OS than COPD regardless of CPAP compliance.

that the study of neutrophils in OS is clinically significant given their participation in the pathophysiology of CVD and the minimal confounding effects of obesity.

To the best of our knowledge, our study is the first to compare PPN in OS subjects to COPD-only subjects, thus providing important clinical results that invite larger studies on neutrophil-related inflammation in these subjects. One benefit of the study is that both groups of subjects were followed in the same outpatient clinic and had a similar degree of comorbidity (CCI and FH score), smoking and corticosteroid use (inhaled and oral). The severity of COPD was not different between the groups and was not associated with PPN.

To date, the only 2 randomized, controlled studies that explored the effect of CPAP therapy on systemic inflammation disagreed on their conclusions.[31–33] Drager et al. showed that the systemic inflammation in moderate to severe OSA was not influenced by short-term CPAP therapy.[32] Although our study did not show a difference in PPN between CPAP-compliant and noncompliant OS subjects, it also had the same limitations as the other previous studies, i.e., a small sample size and variation in CPAP therapy duration and compliance.

Our study has a few other limitations. Firstly, we included subjects who were on HOT for chronic hypoxia or CPAP therapy for OSA. However, treatment with oxygen would bias the results against an association with PPN between the OS and COPD-only subjects. Secondly, since we used the CAN score as a screening tool, our study included a population that had other complex chronic illnesses and, as such, our results might not be applicable to all OS subjects. However, as the CAN score refers to the likelihood of hospitalization or death of a patient within a 1-year period, our results are applicable to the large population of high-risk OS subjects. In addition, our subjects were evenly distributed between the severity levels of COPD disease, with a majority of those having mild to moderately severe OSA, thus matching a large cohort of subjects with OS. Because we limited participants to those with COPD and a high CAN score, our study resulted in a small sample size. For this reason, these findings cannot be generalized to the broader community-based sleep subjects. Comparison to CRP was limited due to the lack of a high-sensitivity CRP (hs-CRP) assay.

In conclusion, our study of a small sample of subjects with COPD and severe comorbidities suggests that those with OS have higher PPN than those with COPD alone, regardless of their compliance status with the CPAP therapy. Future research in neutrophil-related inflammation and CVD in a larger and more diverse group of OS subjects is needed. If our results are confirmed in a larger study, they could be used to motivate OS subjects to improve their lifestyles (e.g., smoking cessation, dietary modification, exercise, and weight loss) or to comply with drug therapies aimed at reducing CVD.

References

1. Marin J, Soriano J, Carrizo SJ, Boldova A, Celli BR. Outcomes in patients with COPD and OSA. *Am J Respir Crit Care Med.* 2010;182(3):325–331.
2. Lopez-Acevedo M, Torres-Palacios A, Elena Ocasio-Tascón M, Campos-Santiago Z, Rodríguez-Cintrón W. Overlap syndrome: An indication for sleep studies? *Sleep Breath.* 2009;13(4):409–413.
3. McNicholas WT. Chronic obstructive pulmonary disease and obstructive sleep apnoea: The overlap syndrome. *J Thorac Dis.* 2016;8(2): 236–242.
4. Madjid M, Awan I, Willerson JT, Casscells SW. Leukocyte count and coronary heart disease: Implications for risk assessment. *J Am Coll Cardiol*. 2004;44(10):1945–1956.
5. Harlan JM, Killen PD, Harker LA, Striker GE, Wright DG. Neutrophil-mediated endothelial injury in vitro mechanisms of cell detachment. *J Clin Invest.* 1981;68(6):1394–1403.
6. Mehta J, Dinerman J, Mehta P, et al. Neutrophil function in ischemic heart disease. *Circulation.* 1989;79(3):549–556.
7. Chen J, Chen MH, Li S, et al. Usefulness of the neutrophil-to-lymphocyte ratio in predicting the severity of coronary artery disease: A Gensini score assessment. *J Atheroscler Thromb.* 2014;21(12):1271–1282.
8. Green SM, Vowels J, Waterman B, Rothrock SG, Kuniyoshi G. Leukocytosis: A new look at an old marker for acute myocardial infarction. *Acad Emerg Med.* 1996;3(11):1034–1041.
9. Office of Informatics and Analytics Veterans Health Administration. Care Assessment Need (CAN) Score and the Patient Care Assessment System (PCAS): Tools for Care Management. http://www.hsrd.research.va.gov/for_researchers/cyber_seminars/archives/713-notes.pdf. Accessed June 8, 2018.
10. Hall WH, Ramachandran R, Narayan S, Jani AB, Vijayakumar S. An electronic application for rapidly calculating Charlson comorbidity score. *BMC Cancer.* 2004;94. doi: 10.1186/1471-2407-4-94
11. National Heart Lung and Blood Institute. Assessing Cardiovascular Risk: Systematic Evidence Review from the Risk Assessment Work Group. http://cvdrisk.nhlbi.nih.gov/calculator.asp. Accessed June 18, 2018.
12. Stenton C. The MRC breathlessness scale. *Occup Med (Lond).* 2008;58(3):226–227.
13. Kales A, Rechtschaffen A, eds. *13A Manual of Standardized Terminology and Techniques and Scoring System for Sleep Stages of Human Subjects*. Bethesda, MD: National Institute of Neurological Diseases and Blindness, Neurological Information Network; 1968.
14. Department of Health and Human Services, Centers for Medicare and Medicaid Services. Continuous and Bi-level Positive Airway Pressure(CPAP/BPAP) Devices: Complying with Documentation and Coverage Requirements. https://www.cms.gov/Outreach-and-Education/Medicare-Learning-Network-MLN/MLNProducts/downloads/PAP_DocCvg_FactSheet_ICN905064.pdf. Accessed June 18, 2018.
15. Nadeem R, Molnar J, Madbouly EM, et al. Serum inflammatory markers in obstructive sleep apnea: A meta-analysis. *J Clin Sleep Med.* 2013;9(10):1003–1012.
16. Agustí A, Edwards LD, Rennard SI, et al.; Evaluation of COPD Longitudinally to Identify Predictive Surrogate Endpoints (ECLIPSE) Investigators. Persistent systemic inflammation is associated with poor clinical outcomes in COPD: A novel phenotype. *PLoS One*. 2012;7(5):e37483. doi: 10.1371/journal.pone.0037483
17. Guven SF, Turkkani MH, Ciftci B, Ciftci TU, Erdogan Y. The relationship between high-sensitivity C-reactive protein levels and the severity of obstructive sleep apnea. *Sleep Breath.* 2012;16(1):217–221.
18. Nural S, Günay E, Halici B, Celik S, Ünlü M. Inflammatory processes and effects of continuous positive airway pressure (CPAP) in overlap syndrome. *Inflammation*. 2013;36(1):66–74.
19. Mansour H, Fathy A, Aref H. Effect of nasal continuous positive airway pressure on inflammatory mediators inpatients with overlap syndrome. *Egyptian Journal of Ear, Nose, Throat and Allied Sciences*. 2011;12:99–104.
20. Quan SF, Gersh BJ. Cardiovascular consequences of sleep-disordered breathing: Past, present and future report of a workshop from the National Center on Sleep Disorders Research and the National Heart, Lung, and Blood Institute. *Circulation.* 2004;109(8):951–957.
21. Dixon JB, O'Brien PE. Obesity and the white blood cell count: Changes with sustained weight loss. *Obes Surg.* 2006;16(3):251–257.
22. Xu X, Su S, Wang X, et al. Obesity is associated with more activated neutrophils in African American male youth. *Int J Obes (Lond).* 2015;39(1):26–32.

23. Ilavská S, Horváthová M, Szabová M, et al. Association between the human immune response and body mass index. *Hum Immunol*. 2012;73(5):480–485.
24. Zhang J, He J, Xia J, Chen Z, Chen X. Delayed apoptosis by neutrophils from COPD patients is associated with altered bak, bcl-xl, and mcl-1 mRNA expression. *Diagn Pathol*. 2012;7:65. doi: 10.1186/1746-1596-7-65
25. Dyugovskaya L, Polyakov A, Lavie P, Lavie L. Delayed neutrophil apoptosis in patients with sleep apnea. *Am J Respir Crit Care Med*. 2008;177(5):544–554.
26. Dyugovskaya L, Polyakov A, Ginsberg D, Lavie P, Lavie L. Molecular pathways of spontaneous and TNF-α-mediated neutrophil apoptosis under intermittent hypoxia. *Am J Respir Cell Mol Biol*. 2011;45(1):154–162.
27. Dyugovskaya L, Polyakov A, Cohen-Kaplan V, Lavie P, Lavie L. Bax/Mcl-1 balance affects neutrophil survival in intermittent hypoxia and obstructive sleep apnea: Effects of p38MAPK and ERK1/2 signalling. *J Transl Med*. 2012;10:211. doi: 10.1186/1479-5876-10-211
28. Schulz R, Mahmoudi S, Hattar K, et al. Enhanced release of superoxide from polymorphonuclear neutrophils in obstructive sleep apnea. Impact of continuous positive airway pressure therapy. *Am J Respir Crit Care Med*. 2000;162(2 Pt 1):566–570.
29. Stockley JA, Walton GM, Lord JM, Sapey E. Aberrant neutrophil functions in stable chronic obstructive pulmonary disease: The neutrophil as an immunotherapeutic target. *Int Immunopharmacol*. 2013;17(4):1211–1217.
30. Pilkauskaite G, Miliauskas S, Sakalauskas R. Reactive oxygen species production in peripheral blood neutrophils of obstructive sleep apnea patients. *ScientificWorldJournal*. 2013;12:421763. doi: 10.1155/2013/421763
31. Xie X, Pan L, Ren D, et al. Effects of continuous positive airway pressure therapy on systemic inflammation in obstructive sleep apnea: A meta-analysis. *Sleep Med*. 2013;14(11):1139–1150.
32. Drager LF, Bortolotto LA, Figueiredo AC, et al. Effects of continuous positive airway pressure on early signs of atherosclerosis in obstructive sleep apnea. *Am J Respir Crit Care Med*. 2007;176(7):706–712.
33. Kohler M, Ayers L, Pepperell J, et al. Effects of continuous positive airway pressure on systemic inflammation in patients with moderate to severe obstructive sleep apnoea: A randomized controlled trial. *Thorax*. 2009;64(1):67–73.

Richter syndrome: A rare complication of chronic lymphocytic leukemia or small lymphocytic lymphoma

Ewa Wąsik-Szczepanek[1,A–F], Agnieszka Szymczyk[1,2,A–D,F], Dariusz Szczepanek[3,A–F], Joanna Wszoła-Kleinrok[4,B–D,F], Sylwia Chocholska[1,B,C,F], Andrzej Pluta[5,B–F], Marek Hus[1,A–F]

[1] Chair and Department of Hematooncology and Bone Marrow Transplantation, Medical University of Lublin, Poland
[2] Independent Clinical Transplantology Unit, Medical University of Lublin, Poland
[3] Chair and Department of Neurosurgery and Pediatric Neurosurgery, Medical University of Lublin, Poland
[4] Department of Nephrology, Endocrinology, Hypertension and Internal Diseases of Independent Public Hospital in Zamość, Poland
[5] Department of Hematooncology, Oncology Centre, Brzozów, Poland

A – research concept and design; B – collection and/or assembly of data; C – data analysis and interpretation;
D – writing the article; E – critical revision of the article; F – final approval of the article

Advances in Clinical and Experimental Medicine, ISSN 1899-5276 (print), ISSN 2451-2680 (online) *Adv Clin Exp Med*. 2018;27(12):1683–1689

Address for correspondence
Agnieszka Szymczyk
E-mail: agnieszka.szymczyk.med@wp.pl

Funding sources
None declared

Conflict of interest
None declared

Received on October 29, 2016
Reviewed on January 28, 2017
Accepted on July 14, 2017

Abstract

Background. Richter's syndrome (RS) is a rare complication with an unfavorable prognosis, in which chronic lymphocytic leukemia (CLL) or small lymphocytic lymphoma (SLL) transform into a more aggressive type of lymphoma, most commonly into diffuse large B cell lymphoma (DLBCL) or less often into Hodgkin's lymphoma (HL).

Objectives. The objective of this research paper was to present a retrospective analysis of patients with CLL/SLL whose disease transformed into RS.

Material and methods. The study included 217 patients (100 women and 107 men) with CLL/SLL diagnosed in the years 2006–2015 at the Department of Hematooncology and Bone Marrow Transplantation of the Medical University of Lublin, which transformed into RS. We analyzed clinical, laboratory, immunophenotypic (ZAP-70 and CD38 expression), histopathological, and genetic data (del(17p), del(11q)), which was collected at the time of CLL/SLL diagnosis, and some which was collected at the time of transformation.

Results. Richter's syndrome was diagnosed in 4.6% of all CLL and SLL patients. The group of patients with RS consisted of 9 patients with primary CLL and 1 patient with a diagnosis of SLL (8 patients with transformation into DLBCL and 2 patients with transformation into HL). Leukemic lymphocytes showed evidence of peripheral blood lymphocyte membrane expression of ZAP70^{+}/CD38^{+} (1 patient), of ZAP-70^{+}/CD38^{-} (3 patients), of ZAP-70^{-}/CD38^{-} (1 patient), and of ZAP-70^{-}/CD38^{+} (5 patients). The deletion of 11q (del(11q)) was documented in 2 patients. In 4 cases, the location of RS was extremely rare (the thyroid gland, liver, skin, bladder, and central nervous system).

Conclusions. Richter's syndrome is a rare, but probable complication of CLL/SLL with an unfavorable prognosis, and it should be taken into account at every stage of the disease, particularly when the course of the disease is aggressive.

Key words: chronic lymphocytic leukemia, Richter's syndrome, small lymphocytic lymphoma

DOI
10.17219/acem/75903

Introduction

Chronic lymphocytic leukemia (CLL) is the most common type of leukemia in adults in the Western Hemisphere. The clinical course is heterogenic in nature. In many patients, the disease follows an indolent course and it does not require cytostatic treatment.[1]

Richter's syndrome (RS) has been defined as a separate clinical condition, which may occur following the transformation from chronic lymphocytic leukemia/small lymphocytic lymphoma (CLL/SLL) into an aggressive form of non-Hodgkin lymphoma (NHL), most commonly into diffuse large B cell lymphoma (DLBCL), particularly into the ABC subtype (DLBCL-RS) or less commonly into Hodgkin's lymphoma (HL) – a Hodgkin variant of RS, HvRS.[2] Research carried out over the last few years has shown that in the majority of cases (80%), a more aggressive subtype of DLBCL is clonally related to DLBCL. In the remaining group of patients, it is clonally independent of the DLBCL clone.[3] At the same time, patients with CLL and SLL are at a higher risk of developing secondary malignancies, arising outside of the hematopoietic system.[4]

The term RS also refers to the transformation of indolent NHL outside of CLL/SLL; hence, it has been observed in 11–30% of patients with follicular lymphoma (FL), in 13% of patients with lymphoplasmacytic lymphoma (LPL) and in 11% of patients with marginal zone lymphoma (MZL).[5–7]

Objectives

The objective of this research paper was to present a retrospective analysis of patients with CLL/SLL whose disease underwent RS and who were treated at the Department of Hematooncology and Bone Marrow Transplantation of the Medical University of Lublin (Poland) between 2006 and 2015.

Material and methods

The analysis included patients with CLL/SLL diagnosed in the years 2006–2015, which transformed into RS.

In this timeframe, 217 CLL/SLL patients were hospitalized at the Department of Hematooncology and Bone Marrow Transplantation of the Medical University of Lublin (Poland). Apart from the patients with RS, 100 women and 107 men at a median age of 64.2 years (34–86 years), Rai stage 0–4 and Ann Arbor clinical stage II–IV were observed or treated.

Clinical, laboratory, immunophenotypic (ZAP-70 and CD38 expression), histopathological, and genetic data (deletion of 17p – del(17p) and deletion of 11q – del(11q)) was collected at the time of CLL/SLL diagnosis, and some was collected at the time of transformation (genetic testing was repeated in 8 patients). Due to logistical reasons, the IgVH mutational status was not assessed.

The expression of ZAP-70 and CD38 was considered positive if it was present in more than 20% of leukemic cells. The diagnosis of RS was confirmed in every patient on the basis of a lymph node biopsy, bone marrow trephine or histopathology assessment of the extralymphatic system organs. Survival time was defined as the time from RS diagnosis until death or until the last follow-up of the patient. Tables 1 and 2 present the clinical characteristics, and the immunological and genetic parameters of all patients with CLL/SLL and patients with RS at the time of CLL/SLL diagnosis.

The current study was approved by the Ethics Committee of the Medical University of Lublin (Poland).

Results

The study group included 9 patients with primary CLL and 1 patient with a diagnosis of SLL. The patients' cohort included 6 women and 4 men with a median age of 65.4 years (54–81 years), Rai stage 0–4 and Ann Arbor stage II. Leukemic lymphocytes showed evidence of peripheral blood lymphocyte membrane expression of $ZAP70^{+}/CD38^{+}$ (1 patient), of $ZAP\text{-}70^{+}/CD38^{-}$ (3 patients), of $ZAP\text{-}70^{-}/CD38^{-}$ (1 patient), and of $ZAP\text{-}70^{-}/CD38^{+}$ (5 patients). The del(11q) was documented in 2 patients. Richter's syndrome was diagnosed in all patients on the basis of the lymph node biopsy of and/or a histologically proven biopsy of infiltrated tissue (8 patients with DLBCL and 2 patients with HL) involved in the pathology. The analyzed group represented 4.6% of all CLL and SLL patients treated at the Department of Hematooncology and Bone Marrow Transplantation of the Medical University of Lublin (Poland) in the years 2006–2015.

In most cases (9 patients), RS occurred during progression in the CLL/SLL phase, while in 1 patient, the disease developed at the moment of leukemia diagnosis. Systemic symptoms and increased activity of lactate dehydrogenase (LDH) were found in 9 patients.

The time from the diagnosis of CLL/SLL to the transformation ranged from 0 to 111 months (median: 42 months). Usually, 1–5 cycles of chemotherapy were administered before Richter's transformation occurred. The drugs used in chemoimmunotherapy consisted of purine analogs, alkylating agents, rituximab, ibrutinib, and idelalisib.

Five patients died during the study. Three of them did not receive cytostatic treatment due to their very poor clinical state. They survived from 2 weeks to 2 months.

The following 2 patients did not respond to chemoimmunotherapy (the disease remained active and the survival time was 1–2 months). The survival time of the remaining patients who were observed until the end of the study was 5–18 months (median: 13 months).

The treatment resulted in complete remission (CR) in 1 patient, partial remission (PR) in 2 patients and stable disease (SD) in 2 patients. The clinical characteristics of patients at the time of RS diagnosis and during transformation is presented in Tables 3 and 4.

Table 1. Clinical characteristics, and immunological and genetic parameters of patients with CLL/SLL and RS transformation at the time of CLL/SLL diagnosis

Patients	F/M ratio	Median age [years]	Rai clinical stage	Ann Arbor stage	Immunophenotyping of leukemic lymphocyte (ZAP70/CD38) [%]	del(11q) [%]	del TP53 [%]
CLL/SLL (207)	0.93	64.2	0–4	II–IV	$ZAP70^+/CD38^+$ 33.8 $ZAP70^+/CD38^-$ 15.5 $ZAP70^-/CD38^+$ 17.4 $ZAP70^-/CD38^-$ 33.3	3.4	7.2
RS (10)	1.5	65.4	0–4	II	$ZAP70^+/CD38^+$ 10 $ZAP70^+/CD38^-$ 30 $ZAP70^-/CD38^+$ 50 $ZAP70^-/CD38^-$ 10	2	0

CLL – chronic lymphocytic leukemia; SLL – small lymphocytic lymphoma; RS – Richter's syndrome; del – deletion; F – female; M – male.

Table 2. Clinical characteristics and immunological and genetic parameters of patients with RS at the time of CLL/SLL diagnosis

Patient	Sex	Age [years]	Rai clinical stage	Immunophenotyping of leukemic lymphocyte (ZAP70/CD38)	Genetic abnormalities	Lymph nodes >3 cm
No. 1	F	70	0	$ZAP70^-/CD38^-$	del(11q)	no
No. 2	F	67	2	$ZAP70^+/CD38^-$	no	yes
No. 3	F	58	II*	$ZAP70^+/CD38^-$	no	yes
No. 4	M	71	3	$ZAP70^-/CD38^+$	no	yes
No. 5	M	70	2	$ZAP70^-/CD38^+$	no	yes
No. 6	F	60	1	$ZAP70^+/CD38^+$	no	yes
No. 7	M	63	2	$ZAP70^-/CD38^+$	del(11q)	yes
No. 8	M	54	2	$ZAP70^-/CD38^+$	no	yes
No. 9	F	60	4	$ZAP70^-/CD38^+$	no	yes
No. 10	F	81	3	$ZAP70^-/CD38^-$	no	yes

RS – Richter's syndrome; CLL – chronic lymphocytic leukemia; SLL – small lymphocytic lymphoma; F – female; M – male; del – deletion; * Ann Arbor staging.

Table 3. Clinical characteristics of patients at the time of RS diagnosis

Patient	Rai clinical stage	B-symptoms	LDH [U/L]	Phase of CLL	CLL duration [months]	Treatment of CLL	Genetic abnormalities
No. 1	2	yes	↑	progression	26	B, BR	del(11q)
No. 2	2	no	↑	progression	12	without treatment	no
No. 3	IV*	yes	↑	progression	88	FC, CHOP, BR, ibrutynib	no
No. 4	3	yes	↑	progression	48	FC	no
No. 5	4	yes	↑	progression	36	R-CHOP	no
No. 6	2	yes	↑	progression	111	FC, B, CHOP, ibrutynib	no
No. 7	4	yes	↑	progression	22	R-CHOP, F, FC, BR	ND
No. 8	2	yes	N	progression	71	COP, CHOP, FC, F, ofatumumab + idelalisib	ND
No. 9	2	yes	↑	progression	92	ChlP	no
No. 10	3	yes	↑	at the time of diagnosis	0	without treatment	no

RS – Richter's syndrome; LDH – lactate dehydrogenase; CLL – chronic lymphocytic leukemia; ↑ – increases; N – normal; B – bendamustine; R – rituximab; F – fludarabine; C – cyclophosphamide; H – doxorubicin; O – vincristine; P – prednisone; Chl – chlorambucil; del – deletion; ND – not done; * Ann Arbor staging.

In 6 patients, the disease involved extranodal sites (the bone marrow, skin, pleura, urinary bladder, thyroid gland, liver, and central nervous system). In patient No. 9, abdominal computed tomography (CT) revealed a considerably enlarged liver with irregular borders. The liver parenchyma, with a density of 40 HU, was almost completely infiltrated with numerous round areas of normal density and up to 70 mm in size, which showed smaller contrast enhancement (Fig. 1). At the same time, an ultrasound scan showed a hyperechoic, solid tumor of the left lobe and isthmus of the thyroid gland. Assessment of the bioptic material obtained from the liver and thyroid gland confirmed histologically proven DLBCL.

In patient No. 7, CT revealed an infiltrative lesion of the urinary bladder. Specimens were obtained from the trigone and neck of the bladder during cystoscopy.

Table 4. Clinical characteristics of patients with RS diagnosis

Patient	Histological type	Location	Symptoms/tests suggesting RS	Treatment of RS	Response to treatment	RS duration [months]	Status during last observation (alive: yes/no)
No. 1	DLBCL	skin	lumpy lesions on the skin, fever	BR	progression	2	no
No. 2	DLBCL	lymph nodes	progressive lymphadenopathy, fever	R-CHOP	PR	13	yes
No. 3	HL	lymph nodes, bone marrow	progressive lymphadenopathy, fever	without treatment	NA	2	no
No. 4	HL	lymph nodes	progressive lymphadenopathy, fever, night sweats	ABVD	progression	1	no
No. 5	DLBCL	lymph nodes, pleura	progressive lymphadenopathy, dyspnoea, cough/chest CT scan	B + Bleo intrapleural	PR	18	yes
No. 6	BLBCL	lymph nodes	progressive lymphadenopathy, night sweats	R-CHOP	SD	5	yes
No. 7	DLBCL	urinary bladder	fever, abdominal pain/abdominal CT scan	without treatment	NA	1	no
No. 8	DLBCL	central nervous system	disturbances of consciousness/ cranial CT scans	without treatment	NA	0.5	no
No. 9	DLBCL	lymph nodes, thyroid gland, liver	weight loss, abdominal pain/chest and abdominal CT scan	R-CHOP	CR	13	yes
No. 10	DLBCL	lymph nodes	progressive lymphadenopathy, night sweats	COP	SD	5	yes

RS – Richter's syndrome; DLBCL – diffuse large B cell lymphoma; HL – Hodgkin's lymphoma; CT – computed tomography; B – bendamustine; R – rituximab; C – cyclophosphamide; H – doxorubicin; O – vincristine; P – prednisone; A – adriamycin; V – vinblastine; D – dacarbazine; Bleo – bleomycin; CR – complete remission; PR – partial remission; SD – stable disease; NA – not applicable.

Fig. 1. Computed tomography (CT) scan of the liver of patient No. 9

Histopathological assessment of the obtained material confirmed the diagnosis of DLBCL. Patient No. 8 presented with a neurological deficit, so a head and skull CT scan was performed. The scan revealed an 18 × 16 mm lesion with evidence of contrast enhancement in the right cavernous sinus. The diagnosis of DLBCL was made on autopsy. In patient No. 1, physical examination revealed red, lumpy lesions on the skin of the eyelids (Fig. 2), forearms and abdomen (Fig. 3). Histology skin specimens were obtained, following assessment by a dermatology consultant. A histopathological examination of the biopsy specimen results showed RS disease transformation.

Discussion

Richter's syndrome is a rare complication which was first described by Maurice Richter in 1928.[8] The incidence of RS in patients with CLL has been estimated to be between 2% and 10%.[9] In our study, the incidence of the disease was 4.6%. This remarkable discrepancy of the data may be due to patient selection of different referral centers and to the high heterogeneity of the patient groups, which probably included both patients with histopathologically confirmed disease and patients with clinically suspected RS.[10]

Clinical studies, the source of information about RS, do not always deliver reliable data on the incidence of the disease, as they usually describe only selected patient groups (of a certain age, clinical status or history of chemotherapy). They usually include patients with progressive forms of the disease who require intensive treatment.[11–14]

Contrary to the opinion that RS usually starts after a few years of CLL, Parikh et al. showed in their study that the median time to transformation was only 1.8 years. The authors of the publication suggest that the predisposition to RS may be congenital.[15]

The *TP53* and *CDKN2A* mutations were found in about 50% of patients with RS, while the trisomy 12 and *NOTCH1* mutations were identified in 30% of patients.[16] The genetic

instability and loss of cell cycle control, related to c-MYC abnormalities, may explain the mechanisms of transformation. Infection with the Epstein-Barr virus is indicated as the factor dysregulating the immune system in patients with HvRS.[17]

There are numerous controversies over the impact of previous therapies on the clonal selection process. Some cytostatic agents may be considered triggers in the development of RS. Patients with CLL/SLL are usually administered many different types of chemotherapy, which means that it is difficult to identify which drug is of particular significance for the RS disease transformation. Treatment with a combination of purine analogues and alkylating agents has been reported to have an adverse effect on the development of the disease, whereas the risk of RS did not appear to be increased in patients exposed to only 1 of these drug classes.[15] On the other hand, Catovsky et al. and Solh et al. did not observe this effect in their studies.[11,14]

Little is known about the role of the small molecules, such as ibrutinib, idelalisib, BCL-2, and GDC-199 antagonists. In the study by Woyach et al., who investigated ibrutinib used in monotherapy and in combination with ofatumumab, RS developed in 6% of patients (in 2/3 of them, RS occurred within the 1st year of the treatment).[18]

In our study group, RS was found in 2 patients receiving ibrutinib and developed after 4–5 months of the therapy. It appears that it is not possible at the moment to suggest the impact of the drug on the development of RS. The mechanism of clonal evolution should also be taken into account. In cases where the duration of treatment was short, it is also possible that transformation started before the therapy was initiated. An increased risk of RS is associated with adverse prognostic factors, which include genetic aberrations such as del(11q), del(17p), unmutated immunoglobulin heavy chain variable region genes (*IGHV*), and a high expression of ZAP-70, CD38 and CD49d at the moment of CLL diagnosis.[15,19,20] Recent studies have also suggested the significance of the *NOTCH1* mutation, which considerably increases the risk of transformation (20–30% in patients with the mutation vs 5% in patients without the mutation). It has also been proven that it concerns only the cases of clonally related RS.[21,22]

In our study, del(11q) was found in 2 patients, whereas leukemic B-cells showed expression of ZAP-70 and CD38 in 9 patients. It appears that not all adverse prognostic factors correlate with the development of RS. Rossi et al. proved that biological and molecular pathways leading to RS transformation and to the aggressive course of CLL differ from one another. They showed in their study that the SF3B1 mutation, which is the latest marker of CLL progression, did not have any impact on RS transformation.[22]

An additional argument supporting this hypothesis is the fact that in 1 of our patients, RS developed at the moment of CLL diagnosis, when the disease was in the stable stage. The clinical course of RS is usually aggressive and extremely rapid. The clinical picture of DLBCL-RS is similar to that of HvRS. More than half of the patients (59%) present with fever, considerable weight loss and drenching night sweats. Progressive lymphadenopathy, usually of 1 region, is observed in 64% of patients, while elevated LDH levels and monoclonal gammopathy are observed in 82% and 44% of patients, respectively.[23,24] Hypercalcemia is also sometimes observed.[25] These symptoms are not specific to RS and they may be associated with CLL progression.

Fig. 2. Red, lumpy lesions on the skin of the eyelids of patient No. 1

Fig. 3. Changes on the skin of the forearms and abdomen of patient No. 1

One examination which helps to diagnose RS is positron emission tomography (PET). A maximum standard uptake value (SUV_{max}) >5 indicates the potential location of the transformation, but it still requires confirmation by a histopathological examination, due to the need to exclude prolymphocytic leukemia, a coexisting lymphoma of different histology, the lymph node involvement by inflammation, or an unrelated malignancy.[26,27]

Richter's syndrome most often affects lymph nodes and bone marrow. The disease is located extranodally in 41% of patients. The prognosis for patients with CLL/SLL who were diagnosed with RS is extremely poor. It concerns typical DLBCL transformation as well as HvRS.[24] At the same time, there are some differences in the clinical course of the disease depending on which risk group, defined by Tsimberidou et al., the patient belongs to.[10] The "Richter score" was based on the platelet levels, LDH levels, Eastern Cooperative Oncology Group (ECOG) performance status, a tumor size >5 cm, and more than 1 prior cycle of chemotherapy. However, it did not take into account genetic aberrations which often occur during the course of the disease or clonality, which are probably the most important factor. The prognosis of the less common clonally unrelated RS seems to be significantly better.[3] An extranodal location of the disease also appears to be an important factor in prognosis. In our study, the disease was found in the central nervous system – a particularly poor prognostic location. The evaluation of clonality requires precise testing methods. The examination of the rearranged IGVH VH-D-JH nucleotide sequence by polymerase chain reaction and sequencing is currently considered the best one. It is not possible, however, to perform these tests in every healthcare center.[19]

The studied group included 130 patients with CLL/SLL diagnosed within the 5-year period (2012–2016) in the Department of Hematooncology of the Oncology Center in Brzozów (Poland) and followed by one of the researchers from our team. Out of this group, 4 patients with CLL suffered transformation into RS.

A poor prognosis in RS mainly results from the resistance to chemotherapy, which is often caused by genetic aberrations, particularly those acquired during the course of the disease. There are no prospective studies of patients with RS and it considerably complicates the development of effective treatment regimens. The results of the molecular studies which provide an explanation of the transformation mechanisms are not sufficiently used for therapeutic purposes. The most commonly used treatment regimen for DLBCL-RS is R-CHOP (rituximab, cyclophosphamide, doxorubicin, vincristine, prednisone), whereas for HvRS it is ABVD (adriamycin, bleomycin, vinblastine, and dacarbazine) and less frequently MOPP (mechlorethamine, oncovin, procarbazine, and prednisone).[28,29]

Recently, more attention has been paid to new molecules. It is especially true in regard to ibrutinib, which could be used in transplant-eligible patients with RS who showed resistance to previous chemoimmunotherapy.[30] New antibodies are also promising. One clinical study (MC1485), which evaluated the efficacy of PD-1 antibodies in resistant and recurrent forms of CLL and low-grade B-NHL, showed good response to the treatment in patients with RS.[31] In patients with the location of the disease in the central nervous system or with other solitary lesions, radiotherapy should be taken into consideration. An autologous or allogeneic stem cell transplant may also be considered.

Summary

Richter's syndrome is an uncommon complication of CLL/SLL with an unfavorable prognosis. Richter's syndrome should be considered at any time of the disease presentation, even at diagnosis – particularly when the course of the disease is aggressive (severe general symptoms, massive lymphadenopathy and internal organ involvement). There is currently no clear therapeutic algorithm for the treatment of the disease. Richter's syndrome occurs most often in elderly patients suffering from comorbid conditions and it often develops after a few cycles of chemotherapy. Treatment of active and aggressive forms of the disease is particularly difficult and cumbersome. Targeted therapies, based on the knowledge of the mechanisms of transformation, seem to give hope for the future. The RS treatment process requires further intensive research.

References

1. Dighiero G, Hamblin TJ. Chronic lymphocytic leukaemia. *Lancet*. 2008;371(9617):1017–1029.
2. Campo E, Swerdlow SH, Harris NL, Pileri SA, Stein H, Jaffe ES. The 2008 WHO classification of lymphoid neoplasms and beyond: Evolving concepts and practical applications. *Blood*. 2011;117(19):5019–5032.
3. Rossi D, Spina V, Deambrogi C, et al. The genetics of Richter syndrome reveals disease heterogeneity and predicts survival after transformation. *Blood*. 2011;11(12):3391–3401.
4. Travis LB, Curtis RE, Hankey BF, Fraumeni JF Jr. Second cancers in patients with chronic lymphocytic leukemia. *J Natl Cancer Inst*. 1992;84(18):1422–1427.
5. Link BK, Maurer MJ, Nowakowski GS, et al. Rates and outcomes of follicular lymphoma transformation in the immunochemotherapy era: A report from the University of Iowa/Mayo Clinic specialized program of research excellence molecular epidemiology resource. *J Clin Oncol*. 2013;31(26):3272–3278.
6. Lin P, Mansoor A, Bueso-Ramos C, Hao S, Lai R, Medeiros LJ. Diffuse large B-cell lymphoma occurring in patients with lymphoplasmacytic lymphoma/Waldenström macroglobulinemia. Clinicopathologic features of 12 cases. *Am J Clin Pathol*. 2003;120(2):246–253.
7. Camacho FI, Mollejo M, Mateo MS, et al. Progression to large B-cell lymphoma in splenic marginal zone lymphoma: A description of a series of 12 cases. *Am J Surg Pathol*. 2001;25(10):1268–1276.
8. Richter MN. Generalized reticular cell sarcoma of lymph nodes associated with lymphatic leukemia. *Am J Pathol*. 1928;4(4):285–292.
9. Parikh SA, Kay NE, Shanafelt TD. How we treat Richter syndrome. *Blood*. 2014;123:1647–1657.
10. Tsimberidou AM, O'Brien S, Khouri I, et al. Clinical outcomes and prognostic factors in patients with Richter's syndrome treated with chemotherapy or chemoimmunotherapy with or without stem-cell transplantation. *J Clin Oncol*. 2006;24(15):2343–2351.

11. Catovsky D, Richards S, Matutes E, et al. Assessment of fludarabine plus cyclophosphamide for patients with chronic lymphocytic leukaemia (the LRF CLL4 Trial): A randomised controlled trial. *Lancet*. 2007;370(9583):230–239.
12. Flinn IW, Neuberg DS, Grever MR, et al. Phase III trial of fludarabine plus cyclophosphamide compared with fludarabine for patients with previously untreated chronic lymphocytic leukemia: US Intergroup Trial E2997. *J Clin Oncol.* 2007;25(7):793–798.
13. Keating MJ, O'Brien S, Lerner S, et al. Long-term follow-up of patients with chronic lymphocytic leukemia (CLL) receiving fludarabine regimens as initial therapy. *Blood.* 1998;92(4):1165–1171.
14. Solh M, Rai KR, Peterson BL, et al. The impact of initial fludarabine therapy on transformation to Richter syndrome or prolymphocytic leukemia in patients with chronic lymphocytic leukemia: Analysis of an intergroup trial (CALGB 9011). *Leuk Lymphoma.* 2013;54(2):252–254.
15. Parikh SA, Rabe KG, Call TG, et al. Diffuse large B-cell lymphoma (Richter syndrome) in patients with chronic lymphocytic leukaemia (CLL): A cohort study of newly diagnosed patients. *Br J Haematol.* 2013;162(6):774–782.
16. Chigrinova E, Rinaldi A, Kwee I, et al. Two main genetic pathways lead to the transformation of chronic lymphocytic leukemia to Richter syndrome. *Blood.* 2013;122(15):2673–2682.
17. Dolcetti R, Carbone A. Epstein-Barr virus infection and chronic lymphocytic leukemia: A possible progression factor? *Infect Agent Cancer.* 2010;5:22. doi: 10.1186/1750-9378-5-22
18. Woyach JA, Ruppert AS, Lozanski G, et al. Association of disease progression on ibrutinib therapy with the acquisition of resistance mutations: A single-center experience of 267 patients. *J Clin Oncol*. 2014;32:5s (suppl; abstract 7010).
19. Rossi D, Cerri M, Capello D, et al. Biological and clinical risk factors of chronic lymphocytic leukaemia transformation to Richter syndrome. *Br J Haematol.* 2008;142(2):202–215.
20. Jain N. New developments in Richter syndrome. *Clin Adv Hematol Oncol.* 2015;13(4):220–222.
21. Rossi D, Bruscaggin A, Spina V, et al. Mutations of the SF3B1 splicing factor in chronic lymphocytic leukemia: Association with progression and fludarabine-refractoriness. *Blood.* 2011;118(26):6904–6908.
22. Rossi D, Rasi S, Spina V, et al. Different impact of NOTCH1 and SF3B1 mutations on the risk of chronic lymphocytic leukemia transformation to Richter syndrome. *Br J Haematol*. 2012;158(3):426–429.
23. Swords R, Bruzzi J, Giles F. Recent advances in the diagnosis and therapy of Richter's syndrome. *Med Oncol.* 2007;24(1):17–32.
24. Tsimberidou AM, Keating MJ. Richter syndrome: Biology, incidence, and therapeutic strategies. *Cancer.* 2005;103(2):216–228.
25. Robertson LE, Pugh W, O'Brien S, et al. Richter's syndrome: A report on 39 patients. *J Oncol.* 1993;11(10):1985–1989.
26. Hallek M, Cheson BD, Catovsky D, et al. Guidelines for the diagnosis and treatment of chronic lymphocytic leukemia: A report from the International Workshop on Chronic Lymphocytic Leukemia updating the National Cancer Institute-Working Group 1996 guidelines. *Blood.* 2008;111(22):5446–5456.
27. Kuppers R, Duhrsen U, Hansmann ML. Pathogenesis, diagnosis, and treatment of composite lymphomas. *Lancet Oncol.* 2014;15(10):435–446.
28. Jenke P, Eichhorst B, Busch R, et al. Cyclophosphamide, adriamycin, vincristine and prednisone plus rituximab (CHOP-R) in fludarabine (F) refractory chronic lymphocytic leukemia (CLL) or CLL with autoimmune cytopenia (AIC) or Richter' s transformation (RT): Final analysis of a phase II study of the German CLL Study Group. *Blood*. 2011;118:abstract 2860.
29. Bockorny B, Codreanu I, Dasanu CA. Hodgkin lymphoma as Richter transformation in chronic lymphocytic leukaemia: A retrospective analysis of world literature. *Br J Haematol.* 2012;156(1):50–66.
30. Rossi D. Richter's syndrome: Novel and promising therapeutic alternatives. *Best Pract Res Clin Haematol.* 2016;29(1):30–39.
31. Ding W, Dong H, Call TG, et al. PD-1 blockade with pembrolizumab (MK-3475) in relapsed/refractory CLL including Richter transformation: An early efficacy report from a phase 2 trial (MC1485). *Blood*. 2015;126:843.

Carotid artery stenting versus endarterectomy for the treatment of both symptomatic and asymptomatic patients with carotid artery stenosis: 2 years' experience in a high-volume center

Dariusz Janczak[1,A,E], Maciej Malinowski[1,A,E], Agnieszka Ziomek[1,B,C], Jakub Kobecki[2,B,D], Michał Leśniak[1,B,D], Tadeusz Dorobisz[3,A,B], Karolina Dorobisz[4,B,D], Dawid Janczak[3,B,C], Mariusz Chabowski[1,2,C,D]

[1] Division of Surgical Procedures, Department of Clinical Nursing, Faculty of Health Sciences, Wroclaw Medical University, Poland
[2] Department of Surgery, 4th Military Teaching Hospital, Wrocław, Poland
[3] Division of Oncology and Palliative Care, Faculty of Health Sciences, Wroclaw Medical University, Poland
[4] Department of Otolaryngology, Head and Neck Surgery, Faculty of Postgraduate Medical Training, Wroclaw Medical University, Poland

A – research concept and design; B – collection and/or assembly of data; C – data analysis and interpretation; D – writing the article; E – critical revision of the article; F – final approval of the article

Advances in Clinical and Experimental Medicine, ISSN 1899-5276 (print), ISSN 2451-2680 (online) *Adv Clin Exp Med.* 2018;27(12):1691–1695

Address for correspondence
Mariusz Chabowski
E-mail: mailto:mariusz.chabowski@gmail.com

Funding sources
None declared

Conflict of interest
None declared

Received on March 23, 2017
Reviewed on May 16, 2017
Accepted on July 14, 2017

Abstract

Background. Carotid endarterectomy (CEA) and carotid artery stenting (CAS) are the 2 current standard treatments for carotid artery stenosis. There is still no well-defined consensus with regard to their superiority. However, the minimally invasive nature of endovascular treatment makes CAS increasingly popular among vascular surgeons.

Objectives. The aim of the study is to compare the safety and efficacy of CEA and CAS in patients with symptomatic and asymptomatic carotid artery stenosis.

Material and methods. A single-center, retrospective analysis of patients who were treated for carotid artery stenosis using CAS or CEA between January 2014 and December 2015 was carried out. There were 471 patients (266 CEA and 205 CAS) who were eligible for inclusion. The vast majority of the patients had significant (>70%) stenosis of the internal carotid artery (92.1% of CEA and 87.8% of CAS). The occlusion of the contralateral carotid artery was observed in 9.8% of all cases (2.6% of CEA vs 17.7% of CAS).

Results. The occurrence of complications, such as stroke, myocardial infarction (MI) and death, did not vary statistically between the groups. There were 9 events of stroke in the CEA group (3.4%) and 8 in the CAS group (3.9%), 3 of which were fatal. There were no significant differences between the 2 groups ($\chi^2 = 0.76$; $p > 0.05$). There was no higher risk of mortality in any group (Fisher's exact test; $p = 0.08$). Symptomatic patients had a higher incidence of stroke than asymptomatic patients across both groups ($\chi^2 = 6.36$; $p < 0.05$; hazard ratio 3.03 (1.26–7.33)).

Conclusions. Carotid endarterectomy is equally effective as CAS in stroke prevention, but is associated with a higher incidence of cranial nerve palsy, access site hematoma and other non-stroke complications. Symptomatic patients had a higher incidence of stroke, regardless of the treatment method.

Key words: carotid artery stenting, carotid endarterectomy, carotid artery stenosis

DOI
10.17219/acem/75902

Introduction

Stroke is a major cause of disability in elderly patients and is the 3rd most common cause of death in developed countries. Approximately 75–80% of all strokes are of ischemic etiology, and 20% of ischemic strokes are secondary to extracranial cerebrovascular disease.[1] Atherosclerosis is responsible for carotid artery stenosis in more than 90% of patients. Endarterectomy of the carotid artery (CEA) was the gold standard for treatment of carotid artery stenosis until the introduction of carotid artery stenting (CAS) in the 1980s. Despite numerous multicenter, randomized clinical trials, it still remains unclear which of the 2 methods is superior. The aim of this study was to assess the efficacy and safety of CAS vs CEA in patients with symptomatic and asymptomatic carotid artery stenosis.

Material and methods

This is a single-center, retrospective study of patients treated for carotid artery stenosis in the Department of Vascular Surgery, 4th Military Teaching Hospital in Wrocław (Poland) between January 2014 and December 2015. Symptomatic patients were eligible for inclusion if there was 50–99% carotid artery stenosis, while asymptomatic patients were eligible if there was 70–99% carotid artery stenosis. Carotid stenosis is considered symptomatic when patients experienced a stroke, a transient ischemic attack (TIA) or amaurosis fugax in the last 6 months. Patients with a carotid artery aneurysm or carotid artery dissection were excluded from this study. For the assessment of carotid artery stenosis, each patient underwent duplex ultrasound examination prior to CAS or CEA. Patients were allocated to the study groups by the surgeon. There was no randomization since it was a case-control study. Directly before the procedure (both CAS and CEA), each patient was administered intravenously 16 mg of dexamethason, 40 mg of pantoprazol, 12 g of piracetam, and 10 mg of vinpocetine. Each patient was provided with 24-hour medical supervision after the procedure.

All patients provided written informed consent to having their data included in this study. This study was approved by the Medical University of Lodz Ethics Committee (No. 204/2015). All procedures performed in studies involving human participants were in accordance with the ethical standards of the institutional and/or national research committee and with the 1964 Helsinki declaration and its later amendments or comparable ethical standards.

Carotid artery stenting

Every CAS procedure was performed by an experienced vascular surgeon, i.e., one who performs approx. 100 such procedures yearly. Each patient was given dual antiplatelet therapy the day before the procedure (clopidogrel and aspirin, except for patients with contraindications). Additionally, an intravenous injection of 5,000 UI of unfractionated heparin was performed several minutes before stent implantation and low-molecular-weight heparin was administered in therapeutic doses for at least 24 h postoperatively. The common femoral artery access was used in all the procedures. Abbot Xact® (Abbott Laboratories, Lake Bluff, USA) and Boston Scientific Carotid Wallstent® (Boston Scientific, Marlborough, USA) were the stents used. Abbott Emboshield NAVA® (Abbott Vascular, Lake Bluff, USA) and Boston Scientific Filter Wire® (Boston Scientific, Marlborough, USA) were the distal neuroprotection devices used. Pre- and post-dilatation were performed when needed. In the case of bradycardia, atropine was given intravenously. Dual antiplatelet therapy was continued for 3 months unless contraindicated.

Carotid endarterectomy

The surgeries were performed under local anesthesia. The surgical technique (patch, shunt or suture) was chosen by the operating surgeon. Directly before carotid artery clamping, a 5,000 UI infusion of unfractionated heparin was administered.

Statistical analysis

Data analysis was performed using IBM SPSS v. 23.00 for Macintosh (IBM, Armonk, USA). Quantitative data, presented as mean values and standard deviations, was compared using a t-test. A χ^2 test was used to analyze nominal variables. The strength of the relationship between variables was calculated with the mean square contingency coefficient and the assessment of relative risk. Pearson's product – moment correlation coefficient was used to analyze correlations. Statistical test results were recognized as significant when the p-value was <0.05.

Endpoints

Patients were evaluated for perioperative stroke, death and myocardial infarction (MI) during 7 days of postoperative follow-up. Stroke was defined as a sudden deterioration in neurological condition, lasting for at least 24 h and confirmed by a cranial computer tomography (CT) scan. Severe stroke was defined as a stroke that led to death within 72 h of occurrence, or when the score in the modified Rankin scale was 3 points or more. Myocardial infarction diagnosis was based on clinical symptoms, the dynamic elevation of troponin levels and electrocardiography (ECG) changes.

Results

Four hundred seventy-one patients with internal carotid artery (ICA) stenosis were eligible for analysis. Two hundred sixty-six of them underwent classic CEA and 205 of them underwent CAS. Age was similar in both

groups (69.9 ±8.8 years in the CEA group vs 68.7 ±9.6 years in the CAS group; p > 0.05). There were slightly more male patients in the CAS group (52.2% males in CEA vs 61.4% males in CAS; p < 0.05). Elderly patients (>80 years old) constituted 16.9% of the CEA group and 17.1% of the CAS group. The vast majority of patients had significant (>70%) stenosis of the internal carotid artery (92.1% of CEA and 87.8% of CAS). The occlusion of the contralateral carotid artery was observed in 9.8% of all cases (2.6% of CEA vs 17.7% of CAS). Diabetes was more prevalent in the endovascular stenting group (29.3% of CAS vs 23.3% of CEA), while dyslipidemia was more frequent in the endarterectomy group. Other risk factors for cardiovascular diseases were distributed similarly in both groups (Table 1). A distal neuroprotective device was used in 96.6% of patients in the CAS group. Table 2 shows the number of complications during 7 days of postoperative follow-up. The occurrence of complications, such as stroke, MI and death, did not vary statistically between the groups. We observed such complications in 8 patients (3.9%) after CAS and in 9 patients (3.4%) after CEA (Fisher's exact test; p = 0.08). Nine strokes were observed in the CEA group, 8 of which were of ischemic etiology and 1 was caused by a intracerebral hematoma. In the CAS group, 3 out of 8 strokes that occurred were fatal. Myocardial infarction did not occur in any patient. This data did not lead to the conclusion that there was a higher risk of mortality in any group (Fisher's exact test; p = 0.08).

Table 1. Baseline characteristics of the study population

Characteristic	CEA (n = 266)	CAS (n = 205)
Age [years]	69.9 ±8.8	68.7 ±9.6
Male sex [%]	52.2	61.4
Diabetes mellitus [%]	23.3	29.3
Dyslipidemia [%]	18.2	19.1
ICA stenosis <70% ≥70% kinking	 5.6 92.1 2.3	 12.2 87.8
Occlusion of the contralateral ICA [%]	2.6	17.7
Symptomatic patients [%]	39.5	29.3
Treatment technique [%] continuous stitch vascular patch eversion shunt	 86.1 13.9 6.0 3.8	 – – – –
Distal neuroprotection during procedure [%]	–	96.6

CEA – carotid endarterectomy; CAS – carotid artery stenting; ICA – internal carotid stenosis.

Table 2. Complications during 7 days of postoperative follow-up

Perioperative complications	CEA		CAS	
	total CEA (n = 266)	symptomatic patients (n = 105)	total CAS (n = 205)	symptomatic patients (n = 60)
Death	0	0	3 (1.5%)	0
Stroke	9 (3.4%)	5 (4.8%)	5 (2.4%)	2 (3.3%)
MI	0	0	0	0
Total	9 (3.4%)	5 (4.8%)	8 (3.9%)	2 (3.3%)

CEA – carotid endarterectomy; CAS – carotid artery stenting; MI – myocardial infarction.

Symptomatic vs asymptomatic patients

The study showed a statistically significantly higher incidence of perioperative complications in symptomatic patients ($\chi^2 = 6.36$; p < 0.05). The evaluation of the relative risk (symptomatic patients vs asymptomatic ones) of stroke during the perioperative period was 3.03 (1.26–7.33). The occurrence of other complications, such as death or MI, did not differ between the 2 groups. The study did not reveal a correlation between age and the carotid artery stenosis percentage (r = –0.79; p > 0.05) or between age and the incidence of endpoint.

Table 3 shows additional adverse events. They occurred more frequently in the CEA group than in the CAS group (14.6% vs 4.39%; p < 0.05). In the CEA group, 12 patients (4.5%) required reoperation because of a hematoma at the site of the incision. One case of hematoma turned out to be a pseudoaneurysm due to the unsealing of the arteriotomy suture, which led to ischemic stroke. Wound infections, pulmonary edema and the inferior branch retinal artery embolism were complications observed exclusively in CEA patients.

The small number of additional complications among patients that underwent endovascular treatment is noteworthy. Only 3 (1.4%) out of 205 patients in the CAS group required surgery due to a pseudoaneurysm after puncturing the common femoral artery (AFC).

Perioperative transient central nervous system ischemia symptoms occurred in both groups with a comparable frequency during the procedure (4.1% CEA vs 5.4% CAS) and in the first 24 h after the surgery (3.0% CEA vs 2.4% CAS).

Discussion

Stroke prevention is the main purpose of the treatment of carotid artery stenosis. Despite numerous papers from recent randomized studies comparing CAS and CEA, including the International Carotid Stenting Study (ICSS), Carotid Revascularization Endarterectomy vs Stenting Trial (CREST) and Carotid and Vertebral Artery Transluminal Angioplasty Study (CAVATAS), it still remains unclear which of the 2 methods is superior.

One of the first major clinical trials comparing CAS and CEA was the Endarterectomy vs Angioplasty in Patients with Symptomatic Severe Carotid Stenosis (EVA-3S) trial. They found that the cumulative 4-year risk

Table 3. Additional adverse events

Perioperative complications (continued)	CAS	CEA
Laryngeal nerve palsy	0	3 (1.13%)
Pharyngeal and laryngeal hematoma	0	3 (1.13%)
Arytenoid cartilage edema	0	1 (0.38%)
Paralysis of the marginal mandibular branch of the facial nerve	0	2 (0.75%)
Reinke's edema	0	1 (0.38%)
Reoperations due to hematoma in the site of incision pseudoaneurysm ICA intravascular thrombosis	 0 3 (1.47%) 0	 12 (4.5%) 0 3 (1.13%)
Wound infection	0	1 (0.38%)
Pulmonary edema	0	1 (0.38%)
Epilepsy after local anesthetic	0	1 (0.38%)
Postoperative TIA	5 (2.44%)	8 (3%)
Postoperative psychotic symptoms requiring drug administration	1 (0.49%)	3 (1.13%)
Total	9 (4.39%)	39 (14.6%)

CAS – carotid artery stenting; CEA – carotid endarterectomy; ICA – internal carotid stenosis; TIA – transient ischemic attack.

of fatal or disabling stroke did not differ significantly between the CAS and CEA groups (6.3% vs 4%).[1] The CREST showed that the safety and efficacy of CAS and CEA were similar among patients with symptomatic and asymptomatic carotid artery stenosis. The CREST indicated that the risk of stroke, MI and death is similar in these 2 groups (5.2% CEA vs 4.5% CAS). However, it demonstrated a higher periprocedural risk of stroke and death after a CAS procedure.[2–4] The ICSS results published in "Lancet" in February 2015 did not provide a definitive answer to the question of superiority, either. The primary endpoint was fatal or disabling stroke in any territory. According to the ICSS, stenting is as effective as endarterectomy in the prevention of fatal or disabling stroke (6.4% vs 6.5%, respectively). In the ICSS and in the CREST, carotid artery stenting was associated with a higher procedure-related and long-term risk of non-disabling stroke, but the neurological outcomes were not different.[5,6]

Our study does not prove the superiority of CAS over CEA, either, though the number of complications is lower. We might relate this to the high number of procedures performed, the frequent application of neuroprotection devices (96.6%) and the extensive experience of the surgeons.[6]

Due to constant technological progress, the results of the trials published may not be accurate today. In these studies, some of the patients in the endovascular group were treated without stent placement, and embolic protection devices were not available.[7] These factors might have a significant impact on the number of procedure-related complications. The availability of new, improved proximal and distal neuroprotection devices and new mesh-covered stents may reduce the number of disabling strokes.[8]

However, a substudy of the ICSS showed that patients who underwent CAS had new ischemic brain lesions about 3 times more often than patients after CEA and, surprisingly, they were more frequent when cerebral protection devices were used.[9]

The incidence of neurological complications in our department is within the target of <6% for symptomatic artery sclerosis set by the American Heart Association/American Stroke Association guidelines and <3% for asymptomatic patients set by the Therapeutics and Technology Assessment Subcommittee of the American Academy of Neurology.[10]

Our study failed to show a correlation between patients' age and the risk of post-procedural neurological complications. On the contrary, the ICSS, the CREST and the Stent-Protected Angioplasty vs Carotid Endarterectomy (SPACE) trial proved that CAS is associated with better outcomes when performed on younger patients, while CEA is better in older patients. The cut-off point was the age of 70 years.[2,4,11] This is thought to be caused by increased vasa tortuosity and more calcified atherosclerotic plaques in elderly patients.[12,13]

Limitations of the study

The patients should preferably be observed for 30 days, but in our study they were followed-up for only 7 days after surgery, so restenosis and delayed neurological events were omitted. Our study is retrospective and represents only a single institution's experience with a small number of patients. There was no randomization, so the results may be influenced by the tendency of operators to surgically treat more sick patients.

Conclusions

Our analysis showed that CEA is as effective as CAS in stroke prevention, but is associated with a higher incidence of cranial nerve palsy, access site hematoma and other non-stroke complications. Symptomatic patients had a higher incidence of stroke, regardless of the treatment method. A new multi-center, randomized trial with methodology carefully determined by advocates of both CAS and CEA should be conducted in order to provide a final conclusion for this long-lasting dispute on which method is better.

References

1. Mas JL, Trinquart L, Leys D, et al. Endarterectomy Versus Angioplasty in Patients with Symptomatic Severe Carotid Stenosis (EVA-3S) trial: Results up to 4 years from a randomised, multicentre trial. *Lancet Neurol*. 2008;7(10):885–892.
2. Brott TG, Hobson RW, Howard G, et al. Stenting vs endarterectomy for treatment of carotid-artery stenosis. *N Engl J Med*. 2010;363(1):11–23.
3. Mantese VA, Timaran CH, Chiu D, Begg RJ, Brott TG. The Carotid Revascularization Endarterectomy vs Stenting Trial (CREST): Stenting versus carotid endarterectomy for carotid disease. *Stroke*. 2010;41(Suppl 10):31–34.
4. Voeks JH, Howard G, Roubin GS, et al. Age and outcomes after carotid stenting and endarterectomy: The carotid revascularization endarterectomy vs stenting trial. *Stroke*. 2011;42(12):3484–3490.
5. Timaran CH, Mantese VA, Malas M, et al. Differential outcomes of carotid stenting and endarterectomy performed exclusively by vascular surgeons in the Carotid Revascularization Endarterectomy versus Stenting Trial (CREST). *J Vasc Surg*. 2013;57(2):303–308.
6. Bonati LH, Dobson J, Featherstone RL, et al. Long-term outcomes after stenting versus endarterectomy for treatment of symptomatic carotid stenosis: The International Carotid Stenting Study (ICSS) randomised trial. *Lancet*. 2015;385(9967):529–538.
7. Endovascular versus surgical treatment in patients with carotid stenosis in the Carotid and Vertebral Artery Transluminal Angioplasty Study (CAVATAS): A randomised trial. *Lancet*. 2001;357(9270):1729–1737.
8. Schofer J, Musiałek P, Bijuklic K, et al. A prospective, multicenter study of a novel mesh-covered carotid stent: The CGuard CARENET Trial (Carotid Embolic Protection Using MicroNet). *JACC Cardiovasc Interv*. 2015;8(9):1229–1234.
9. Bonati LH, Jongen LM, Haller S, et al. New ischaemic brain lesions on MRI after stenting or endarterectomy for symptomatic carotid stenosis: A substudy of the International Carotid Stenting Study (ICSS). *Lancet Neurol*. 2010;9(4):353–362.
10. Kernan WN, Ovbiagele B, Black HR, et al. Guidelines for the prevention of stroke in patients with stroke and transient ischemic attack: A guideline for healthcare professionals from the American Heart Association/American Stroke Association. *Stroke*. 2014;45(7):2160–2236.
11. Ederle J, Dobson J, Featherstone RL, et al. Carotid artery stenting compared with endarterectomy in patients with symptomatic carotid stenosis (International Carotid Stenting Study): An interim analysis of a randomised controlled trial. *Lancet*. 2010;375(9719):985–997.
12. Chaturvedi S, Bruno A, Feasby T, et al. Carotid endarterectomy – an evidence-based review: Report of the Therapeutics and Technology Assessment Subcommittee of the American Academy of Neurology. *Neurology*. 2005;65(6):794–801.
13. Bradac O, Mohapl M, Kramar F, et al. Carotid endarterectomy and carotid artery stenting: Changing paradigm during ten years in a high-volume centre. *Acta Neurochir (Wien)*. 2014;156(9):1705–1712.

When should gallbladder polyps be treated surgically?

İbrahim T. Şahiner[A–F], Mete Dolapçı[A,C–E]

Department of General Surgery, Hitit University School of Medicine, Çorum, Turkey

A – research concept and design; B – collection and/or assembly of data; C – data analysis and interpretation;
D – writing the article; E – critical revision of the article; F – final approval of the article

Advances in Clinical and Experimental Medicine, ISSN 1899-5276 (print), ISSN 2451-2680 (online) *Adv Clin Exp Med.* 2018;27(12):1697–1700

Address for correspondence
İbrahim T. Şahiner
E-mail: tayfunsahiner@gmail.com

Funding sources
None declared

Conflict of interest
None declared

Received on December 18, 2016
Reviewed on February 23, 2017
Accepted on July 4, 2017

Abstract

Background. This study was performed to better understand the best surgery timing for gallbladder polyps (GP).

Objectives. The objective was to determine the potential for malignant transformation and the best timing for surgery in GP, based on an assessment of the clinical symptomatology and on the results of the imaging and histopathological examinations.

Material and methods. Age, gender, clinical symptoms, preoperative ultrasound findings, and the results of the postoperative histopathological examination were retrospectively assessed in a total of 2,656 patients undergoing cholecystectomy in Department of General Surgery, Hitit University School of Medicine, Çorum, Turkey, between 2008 and 2013.

Results. From a total of 2,656 patients undergoing cholecystectomy in our unit between 2008 and 2013, 96 subjects were found to have the following types of GP: 66.6% (n = 64) had cholesterol polyps, 13.54% (n = 13) had adenomyomatous polyps, 8.33% (n = 8) had adenocarcinoma, 7.2% (n = 7) had inflammatory polyps, and 4.16% (n = 4) had hyperplastic polyps. Also, 85.4% of these patients (n = 82) had a single polyp only, while 14.6% (n = 14) had 2 polyps. The polyp size in patients with adenocarcinoma was 9 mm, 10 mm and 12 mm in 2, 4 and 2 patients, respectively. The mean age of patients with adenocarcinoma was 60 years (55–74), all of whom had solitary polyps.

Conclusions. In patients over 50 years of age with co-existent cholelithiasis and GP exceeding 10 mm, surgical treatment should be undertaken due to the risk of malignancy. Other patients with polyps less than 10 mm in size should be followed up in 6-month intervals using ultrasound examination.

Key words: gallbladder polyp, malignancy potential, surgery timing, ultrasonographic finding, gallbladder adenocarcinoma

DOI
10.17219/acem/75678

Introduction

Gallbladder polyps (GP), occurring in 0.3–12% of healthy individuals, arise from the mucosal layer and disrupt the integrity of the mucosa.[1,2] Although their exact prevalence is currently unknown, an increase has been observed in the number of patients diagnosed with this condition, mainly due to the advances in diagnostic methods, to the increase in the proportion of individuals with access to healthcare facilities, and to the more widespread availability of ultrasound imaging. The majority of GP are asymptomatic and are diagnosed coincidentally during an abdominal ultrasound examination performed for other reasons. Gallbladder polyps may either be pseudo-polyps or true polyps. True polyps are further subdivided into benign (adenoma), pre-malignant (dysplastic) or malignant (adenocarcinoma) polyps. On the other hand, all types of pseudo-polyps are benign and are classified as inflammatory, hyperplastic, adenomatous, adenomyomatous, cholesterolotic, and cholesterol polyps.[3] Cholesterol polyps are the most common. Although the prevalence of gallbladder cancer may reach up to 27% in individuals over 50 years of age, these lesions may be readily confused with benign polyps in ultrasound examination, especially in the early stages. Previous studies have suggested that polyps greater than 10 mm in size in patients over 50 years of age may pose an increased risk of malignancy.[4–6] Ultrasound represents the most frequently used diagnostic imaging modality in the diagnosis of GP. However, since ultrasound does not always enable the examiner to differentiate between benign and malignant lesions, further imaging with advanced modalities, such as computed tomography (CT), endoscopic ultrasound (EUS) or magnetic resonance imaging (MRI), may be necessary.[7]

In this study, patients who had undergone cholecystectomy in the Department of General Surgery, Hitit University School of Medicine, Çorum, Turkey, were retrospectively examined with respect to the incidence of GP, polyp type and the occurrence of malignancy, as documented by the histology report.

Material and methods

Patients who had undergone cholecystectomy in our unit between 2008 and 2013 were retrospectively assessed with regard to the frequency of GP, polyp type, the frequency of malignancy, and the histopathological examination results. The study protocol was approved by the Institutional Review Board of Hitit University School of Medicine, Çorum, Turkey.

The structure, dimensions and number of polyps were evaluated using histopathological examination, and the polyps were sub-classified as pseudo-polyps (hyperplastic, inflammatory, adenomatous, adenomyomatous, cholesterolosis,, and cholesterol polyps) or true polyps (adenomas and adenocarcinomas). Also, the malignancy potential was examined on the basis of pathological examination. All clinical and demographic data was statistically evaluated using the SPSS software package v. 22 (IBM Corp., Armonk, USA). Frequency, minimum–maximum and mean values were recorded.

Results

A total of 2,656 cholecystectomies were performed in the Department of General Surgery, Hitit University School of Medicine, Çorum, Turkey, between 2008 and 2013. The mean age of the patients was 52 years (12–90); 79.3% (n = 2,106) were female and 20.7% (n = 550) were male. Laparoscopic or open cholecystectomy was performed in 88% (n = 2,338) and in 12% (n = 318) of the patients, respectively.

All patients underwent ultrasound examination prior to surgery and the results are shown in Table 1.

Clinical symptoms included food intolerance in 10.6% of the patients (n = 282), nausea and vomiting in 11.9% (n = 318), right upper quadrant pain in 18.2% (n = 480), and dyspepsia in 59.3% (n = 1,576).

Table 1. Results of pre-operative ultrasound examination

Result of pre-operative hepatobiliary ultrasound examination	n	[%]
Acute calculous cholecystitis	345	13
Acute cholecystitis	66	2.5
Chronic cholecystitis	40	1.5
Chronic calculous cholecystitis	164	6.2
Cholelithiasis	1,859	70
Gallbladder polyp	159	6
Gallbladder sludge	23	0.8

n – number of patients.

Table 2. Results of pathological examination

Results of postoperative pathological examination	n	[%]
Acute cholecystitis	66	2.5
Acute calculous cholecystitis	180	6.82
Chronic cholecystitis	536	20.2
Chronic calculous cholecystitis	1,726	65
Cholesterol polyp	64	2.4
Adenomyomatous	13	0.4
Xanthogranulomatous cholecystitis	34	1.3
Hyperplastic polyp	4	0.15
Adenomatous polyp	8	0.30
Inflammatory polyp	7	0.26
Adenocarcinoma	18	0.67

n – number of patients.

Table 3. Pathological results of postoperative pathological examination of the polyps

Results of postoperative pathological examination of the polyps	n	[%]
Cholesterol polyp	64	66.6
Hyperplastic polyp	4	4.16
Adenomatous polyp	13	13.54
Inflammatory polyp	7	7.29
Adenocarcinoma	8	8.33

n – number of patients.

The results of postoperative pathological examination of all subjects are shown in Table 2. A total of 96 subjects were found to have the following type of GP: cholesterol polyps in 66.6% of the patients (n = 64), adenomyomatous polyps in 13.54% (n = 13), adenocarcinoma in 8.33% (n = 8), inflammatory polyps in 7.29% (n = 7), and hyperplastic polyps in 4.16% (n = 4) (Table 3). Also, 85.4% of these patients (n = 82) had solitary single polyp only, while 14.6% (n = 14) had 2 polyps.

Table 4 shows the polyp size as determined by the pathological examination. The size of the polyp was 9 mm, 10 mm and 12 mm among 2, 4 and 2 patients diagnosed with adenocarcinoma, respectively. All adenocarcinoma patients had solitary polyps and their mean age was 60 years (range: 55–74 years).

Table 4. Polyp size as stated in the pathology report

Polyp size [mm]	4	5	7	9	10	12
Number of patients (n)	14	63	11	2	4	2
[%]	14.58	65.62	11.45	2.08	4.16	2.08

Discussion

Polyps commonly occur in the gallbladder and their clinical significance arises from their potential for malignant conversion. The reported incidence of GP varies between 0.3% and 12%.[8] A retrospective examination of the 2,656 patients undergoing cholecystectomy between 2008 and 2013 in the Department of General Surgery, Hitit University School of Medicine, Çorum, Turkey, showed the presence of GP in 96 individuals (3.6%), which is consistent with literature data.

Some previous reports suggested that certain demographic characteristics, such as age or gender, may have an impact on the incidence of GP.[8–10] Although gender was not found to have a significant effect on the occurrence of polyps in certain studies, others have generally reported a higher incidence among men. Notably, of the 96 patients with GP among the 2,656 individuals undergoing cholecystectomy, 73 (76.04%) were female. While this observation may be due to the higher occurrence of GP among women, it may also be due to the fact that more women (n = 2,016, 79.3%) in our unit underwent cholecystectomy, which confirms the fact that gallbladder diseases are more common among women. A total of 52 patients (54%) with GP were over 50 years of age, which is in line with data from previous publications.

Ultrasound is the most commonly used diagnostic modality in the diagnosis of GP. In the current study, all individuals (n = 2,656) had preoperative ultrasound examination, but only 159 (6%) were sonographically diagnosed with GP. However, histopathology confirmed GP in only 96 individuals (3.6%). This difference may be due to the level of expertise of the sonographer or to the small size of the polyps. Although polyps greater than 5 mm in size are more likely to be diagnosed by ultrasound, a size exceeding 10 mm greatly increases the chance of identification. Also, an accumulation of cholesterol and triglycerides on the gallbladder wall or the lamina propria by macrophages may give a false impression of polyps on the ultrasound. Table 3 shows the data from 96 patients with polyps assessed in our study. As the results suggest, there is a false positivity rate associated with the use of ultrasound in the detection of polyps.[11]

Another important criterion used when assessing GP is the size of the polyp. Literature data suggest an increased risk of malignancy in polyps larger than 10 mm, with an even more marked increase in those over 12 mm, though Kim et al. reported that a polyp size ≥15 mm is the strongest predictor of a neoplastic polyp with ultrasound and that the rate of malignancy is low even in polyps 10 mm or larger (15.1%).[4,9,12] Consistent with previous publications, only 2 of our patients with adenocarcinoma had polyps 9 mm in size, while the remaining patients had a polyp size ranging between 10 and 12 mm. Similarly to the current study, Dorobisz et al. researched incidental gallbladder cancer after cholecystectomy. They performed 7,314 cholecystectomies (1990–2014) and found among them 84 cases (0.87%) of incidental gallbladder carcinoma.[13]

Conclusions

In conclusion, we recommend surgery for all asymptomatic patients over 50 years of age who have GP greater than 10 mm in size, with or without cholelithiasis, because of the increased risk of malignancy. Other asymptomatic patients with polyps smaller than 10 mm should be followed up by ultrasound in 6-month intervals. An increase in the size or number of polyps or the emergence of symptoms during this period should prompt the consideration of surgery.

References

1. Hayashi Y, Liu JH, Moriguchi H, et al. Prevalence of polypoid lesions of the gallbladder in urban and rural areas of Japan: Comparison between 1988 and 1993. *J Clin Gastroenterol*. 1996;23(2):158–159.
2. Pandey M, Khatri AK, Sood BP, Shukla RC, Shukla VK. Cholecystosonographic evaluation of the prevalence of gallbladder diseases. A university hospital experience. *Clin Imaging*. 1996;20(4):269–272.

3. Babu BI, Dennison AR, Garcea G. Management and diagnosis of gallbladder polyps: A systematic review. *Langenbecks Arch Surg*. 2015; 400(4):455–462.
4. Inui K, Yoshino J, Miyoshi H, Yamamoto S. Epidemiology of gallbladder carcinoma [in Japanese]. *Nihon Rinsho*. 2015;73(Suppl 3):541–544.
5. Jessurun J, Mendez-Sanchez N, Lopez-Acuna MP, Hernandez-Avila M, Uribe M. Epidemiology and various etiologic considerations in relation to carcinoma of the gallbladder [in Spanish]. *Rev Gastroenterol Mex*. 1991;56(3):197–200.
6. Wang JH, Liu BJ, Xu HX, et al. Clinical, pathological and sonographic characteristics of unexpected gallbladder carcinoma. *Int J Clin Exp Med*. 2015;8(7):11109–11116.
7. Vijayakumar A, Vijayakumar A, Patil V, Mallikarjuna MN, Shivaswamy BS. Early diagnosis of gallbladder carcinoma: An algorithm approach. *ISRN Radiol*. 2013;2013:239424.
8. Jo HB, Lee JK, Choi MY, et al. Is the prevalence of gallbladder polyp different between vegetarians and general population? *Korean J Gastroenterol*. 2015;66(5):268–273.
9. Sarkut P, Kilicturgay S, Ozer A, Ozturk E, Yilmazlar T. Gallbladder polyps: Factors affecting surgical decision. *World J Gastroenterol*. 2013; 19(28):4526–4530.
10. Ito H, Hann LE, D'Angelica M, et al. Polypoid lesions of the gallbladder: Diagnosis and follow-up. *J Am Coll Surg*. 2009;208(4):570–575.
11. Fultz PJ, Skucas J, Weiss SL. Comparative imaging of gallbladder cancer. *J Clin Gastroenterol*. 1988;10(6):683–692.
12. Kim JS, Lee JK, Kim Y, Lee SM. US characteristics for the prediction of neoplasm in gallbladder polyps 10 mm or larger. *Eur Radiol*. 2016; 26(4):1134–1140.
13. Dorobisz T, Dorobisz K, Chabowski M, et al. Incidental gallbladder cancer after cholecystectomy: 1990 to 2014. *Onco Targets Ther*. 2016;9:4913–4916. doi: 10.2147/OTT.S106580

The relationship between *IFN-γ* and *TNF-α* gene polymorphisms and brucellosis: A meta-analysis

Ebrahim Eskandari-Nasab[1,A–C,E], Mehdi Moghadampour[2,A–F]

[1] Department of Clinical Biochemistry, School of Medicine, Zahedan University of Medical Sciences, Iran
[2] Department of Microbiology, School of Medicine, Isfahan University of Medical Sciences, Iran

A – research concept and design; B – collection and/or assembly of data; C – data analysis and interpretation;
D – writing the article; E – critical revision of the article; F – final approval of the article

Advances in Clinical and Experimental Medicine, ISSN 1899-5276 (print), ISSN 2451-2680 (online) *Adv Clin Exp Med.* 2018;27(12):1701–1709

Address for correspondence
Mehdi Moghadampour
E-mail: mehdimoghadampoor@yahoo.com

Funding sources
None declared

Conflict of interest
None declared

Received on October 9, 2016
Reviewed on December 4, 2016
Accepted on July 12, 2017

Abstract

Background. Brucellosis is an infectious disease and one of the major public health problems worldwide. Several current studies have provided data that polymorphisms in the interferon-gamma gene (*IFN-γ*) and tumor necrosis factor-alpha gene (*TNF-α*) are related to brucellosis.

Objectives. The aim of this study was to investigate the relationship between IFN-γ +874 A/T, IFN-γ UTR5644 A/T, TNF-α –308 G/A, and TNF-α –238 G/A single nucleotide polymorphisms (SNPs) and brucellosis risk by meta-analysis.

Material and methods. We performed a comprehensive search of the PubMed, MEDLINE, EMBASE, Web of Science, and Elsevier Science Direct databases. Crude odds ratios (ORs) with 95% confidence intervals (CIs) were used to measure the strength of association between IFN-γ and TNF-α polymorphisms and brucellosis risk.

Results. A total of 17 studies including 1,904 cases and 2,233 controls fulfilled the inclusion criteria. Our pooled analysis demonstrated that the IFN-γ +874 AT vs AA genotype in a codominant model may confer an increased risk of brucellosis in the overall population ($p = 0.001$; $OR = 0.51$). Regarding TNF-α –308 G/A, our pooled analysis revealed that the AA vs GG + GA (recessive) genotype increased the risk of brucellosis ($p = 0.02$; $OR = 2.00$).

Conclusions. In summary, our pooled analysis suggested that the IFN-γ +874 AT vs AA as well as the TNF-α –308 AA vs GG + GA genotypes demonstrated a trend for the association with a higher risk of brucellosis.

Key words: *IFN-γ*, *TNF-α*, gene polymorphism, brucellosis, meta-analysis

DOI
10.17219/acem/75869

Introduction

Brucellosis is a chronic granulomatous infection and the most frequent bacterial zoonotic disease worldwide.[1,2] The causative agent of brucellosis, *Brucella* spp., is a strain of facultative intracellular bacteria that infect over half a million humans annually.[3] Patients with active brucellosis have symptoms such as fever, headache, sweating, weakness, weight loss, persistent joint pain, endocarditis, neurological complications, and testicular or bone abscess formation.[4,5] *Brucella* spp. invade reticuloendothelial system cells and can reproduce in these cells, and escape from the host's immune system.[6–8]

Cytokines are key mediators responsible for the regulation of immune and inflammatory responses.[9,10] *Brucella* spp. can stimulate the secretion of inflammatory cytokines, e.g., interleukins (ILs), interferon-gamma (IFN-γ) and tumor necrosis factor-alpha (TNF-α).[2,10,11] IFN-γ is a crucial cytokine for the control of *Brucella* infection in hosts and is also a significant mediator in conferring protection against *Brucella* infection. The ultimate result of the activation of macrophages with IFN-γ, which is secreted by T helper-1 cells, is suppressing the reproduction of intracellular *Brucella* organisms and restoring the patient to health.[2] Tumor necrosis factor-alpha is a proinflammatory and immunoregulatory cytokine that is produced by a variety of cells including neutrophils (polymorphonuclear leukocytes – PMN cells), natural killer (NK) cells, macrophages, lymphocytes, and fibroblasts. Like IFN-γ, TNF-α also is a vital mediator for the clearance of brucellosis infection from a host.[11]

Genetic polymorphisms in cytokine genes can potentially modify the expression and/or biological activity of cytokines. Studies conducted to date have confirmed the connection between cytokine gene polymorphisms and brucellosis disease status in various populations.[2,11–16] The IFN-γ +874 A/T (rs2430561) and UTR5644 A/T polymorphisms, as well as the TNF-α –308 G/A (rs1800629) and –238 G/A (rs361525), are 4 SNP loci which affect the transcriptional regulation of IFN-γ and TNF-α. These 4 SNPs have been investigated for their association with the occurrence of brucellosis in different populations.[2,11–14,16] However, due to the relatively small sample size of individual studies, the results have been incoherent and contradictory. A wide retrieval of the pertinent literature is required to reach a more precise estimation of the association with disease susceptibility. Therefore, in the current study, we performed a meta-analysis to collect the available data and to examine whether these 4 polymorphisms of *IFN-γ* (+874 A/T (rs2430561) and UTR5644 A/T) and *TNF-α* (–308 G/A (rs1800629) and –238 G/A (rs361525)) genes are associated with susceptibility to brucellosis.

Material and methods

Literature search

We performed a comprehensive literature search using the electronic databases PubMed, EMBASE and MEDLINE. The comprehensive search strategies included the mesh term and keywords ("interferon gamma" or "interferon-gamma" or "interferon γ" or "interferon-γ" or "IFN gamma" or "IFN-gamma" or "IFN γ" or "IFN-γ"), ("tumor necrosis factor alpha" or "tumor necrosis factor-alpha" or "tumor necrosis factor α" or "tumor necrosis factor-α" or "TNF alpha" or "TNF-alpha" or "TNF α" or "TNF-α"),

Table 1. Main characteristics of studies included in a meta-analysis of *IFN-γ* gene polymorphisms and brucellosis

SNP	Author	Year	Country	Ethnicity	Sample size	Allele frequency		Genotype frequency			HWE (p-value)
						A	T	AA	AT	TT	
IFN-γ +874 A/T	Bravo[12]	2003	Spain	Caucasian	P 83 C 100	P 99 C 100	P 67 C 100	P 28 C 19	P 43 C 62	P 12 C 19	P 0.48 C 0.01
	Budak[16]	2007	Turkey	Caucasian	P 39 C 50	P 43 C 63	P 35 C 37	P 18 C 21	P 7 C 21	P 14 C 8	P 0.00 C 0.48
	Rasouli[9]	2007	Iran	Asian	P 195 C 91	P 176 C 71	P 214 C 111	P 40 C 9	P 96 C 53	P 59 C 29	P 0.93 C 0.03
	Karaoglan[13]	2009	Turkey	Caucasian	P 85 C 85	P 92 C 109	P 78 C 61	P 27 C 32	P 38 C 45	P 20 C 8	P 0.35 C 0.16
	Eskandari-Nasab[2]	2013	Iran	Asian	P 153 C 128	P 145 C 93	P 161 C 163	P 44 C 17	P 57 C 59	P 52 C 52	P 0.00 C 0.96
IFN-γ UTR5644 A/T	Davoudi[15]	2006	Iran	Asian	P 42 C 161	P 48 C 179	P 36 C 143	P 14 C 60	P 20 C 59	P 8 C 42	P 0.85 C 0.00
	Hedayatizadeh-Omran[17]	2010	Iran	Asian	P 259 C 238	P 341 C 285	P 177 C 191	P 125 C 91	P 91 C 103	P 43 C 44	P 0.00 C 0.12
	Eskandari-Nasab[2]	2013	Iran	Asian	P 153 C 128	P 191 C 157	P 115 C 99	P 67 C 53	P 57 C 51	P 29 C 24	P 0.01 C 0.07

IFN-γ – interferon-gamma; SNP – single nucleotide polymorphism; HWE – Hardy-Weinberg equilibrium.

("polymorphism" or "variant" or "genotype" or "SNP" or "mutations"), and (brucellosis). The search was conducted through July 2, 2016. Eligible studies were retrieved and examined carefully. Review articles and bibliographies of other relevant studies identified were manually searched to find additional eligible studies.

Data collection

The articles were screened by 2 separate reviewers (Mehdi Moghadampour and Ebrahim Eskandari-Nasab) to appraise the fitness of the articles selected by using a standardized protocol and data collection form. The inclusion criteria were: original data; a study which assessed the association of IFN-γ +874 A/T, IFN-γ UTR5644 A/T, TNF-α –308 G/A, and TNF-α –238 G/A and the risk of brucellosis; and a comparison between brucellosis patients and controls. The exclusion criteria were: non-human studies, abstracts only, comments, reviews, editorials or letters, mechanism studies, and studies that lacked controls; family-based design or sibling pair studies; studies with insufficient information for data extraction; and unpublished data.

The following information was extracted from each study: authors, year of publication, country, ethnicity, sample size, allele and genotype frequency distribution, and Hardy-Weinberg equilibrium (HWE). Discrepancies about the inclusion of studies and the interpretation of data were solved by discussion.

Statistical analyses

A quantitative meta-analysis was executed using Review Manager Software, v. 5.3 (the Cochrane Collaboration, Oxford, UK). Crude ORs with 95% CIs were used to measure the strength of association between the IFN-γ +874 A/T, IFN-γ UTR5644 A/T, TNF-α –308 G/A, and TNF-α –238 G/A polymorphisms and brucellosis risk. The significance of the pooled ORs was defined by the Z-test, and $p < 0.05$ was considered statistically significant.

The pooled ORs for IFN-γ polymorphisms (+874 A/T and UTR5644 A/T) and brucellosis risk were assessed for the codominant (AT vs AA and TT vs AA), dominant (AT+TT vs AA) and recessive model (TT vs TA+AA), and for the allele comparison (T vs A). The integrated ORs for TNF-α polymorphisms (–308 G/A and –238 G/A) and brucellosis risk were calculated for the codominant (AA vs GG and GA vs GG), dominant (GA+AA vs GG) and recessive model (AA vs GG+GA), and for the allelic contrast (A vs G). Forest-plot graphs were produced in order to estimate the combined association between the IFN-γ +874 A/T, IFN-γ UTR5644 A/T, TNF-α –308 G/A, and TNF-α –238 G/A polymorphisms and brucellosis risk. Heterogeneity among the studies was assessed by Cochran's Q test and I^2 measurement, which was interpreted as the proportion of total discrepancy among study variants. A p-value <0.05 and an I^2 value >50% showed significant heterogeneity. A random-effect model was used in cases of significant heterogeneity; otherwise, a fixed-effect model was applied. Sensitivity analysis was conducted to evaluate the validity and reliability of the primary meta-analysis, and to determine the effects attributed to any particular study.

Results

Study characteristics

In this meta-analysis, a total of 17 studies involving 1,904 cases and 2,233 controls met the inclusion criteria for both IFN-γ and TNF-α SNPs in brucellosis. Five studies assessed the association between the IFN-γ +874 A/T polymorphism and the risk for brucellosis; 3 studies assessed the association between the IFN-γ UTR5644 A/T polymorphism and the risk for brucellosis; 6 studies examined the association between the TNF-α –308 G/A variation and the risk for brucellosis; and 3 studies examined the association between the TNF-α –238 G/A variation and the risk for brucellosis. Baseline characteristics of the included studies on IFN-γ and TNF-α SNPs on brucellosis are presented in Tables 1 and 2, respectively.

IFN-γ +874 A/T polymorphism and susceptibility to brucellosis

Five studies including 555 brucellosis patients and 454 controls assessed the association between the IFN-γ +874 A/T polymorphism and susceptibility to brucellosis. In all studies, the distributions of genotypes in the control subjects were in HWE (Table 1). Figure 1 demonstrates the forest plot and results of the meta-analysis of associations between the IFN-γ +874 A/T polymorphism and the risk for brucellosis, using the codominant, dominant and recessive models. The results showed that the T allele vs A was not associated with the risk of brucellosis with an overall OR of 0.90 ($p = 0.55$; 95% CI = 0.64–1.27). In the codominant model, the pooled evidence suggested that the distribution of the AT vs AA genotypes between the groups was different and that the association was statistically significant ($p = 0.001$; OR = 0.51; 95% CI = 0.37–0.71). In contrast, the general difference between the groups for the TT genotype compared to the AA one did not reach the level of statistical significance, using the codominant model with an overall OR of 0.82 ($p = 0.63$; 95% CI = 0.36–1.87). In the dominant model, the AT+TT genotype vs the AA genotype was not associated with an increased risk of brucellosis with an overall OR of 0.82 ($p = 0.47$; 95% CI = 0.47–1.42). Likewise, in the recessive model, the TT genotype vs the TA+AA one was not associated with an increased risk of brucellosis with an overall OR of 1.22 ($p = 0.47$; 95% CI = 0.71–2.11).

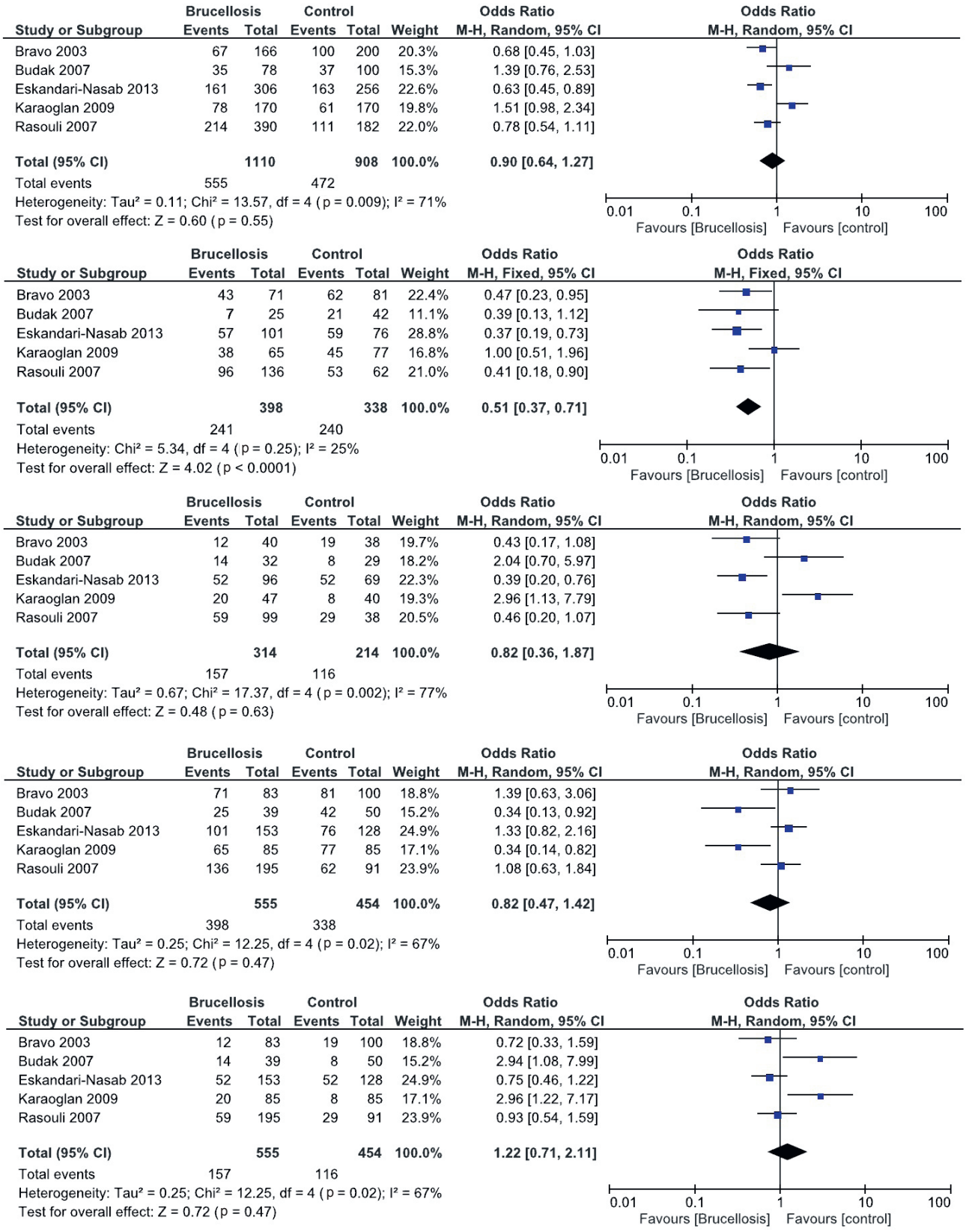

Fig. 1. Forest plot for the association of the IFN-γ +874 A/T polymorphism and brucellosis (T allele vs A allele, AT vs AA, TT vs AA, AT+TT vs AA, and TT vs TA+AA)

IFN-γ UTR5644 A/T polymorphism and susceptibility to brucellosis

Three studies including 454 brucellosis patients and 527 controls evaluated the association between the IFN-γ UTR5644 A/T polymorphism and susceptibility to brucellosis. In all studies, the distributions of genotypes in the control subjects were in HWE (Table 1). Figure 2 presents the forest plot and results of the meta-analysis of associations between the IFN-γ UTR5644 A/T polymorphism and the risk for brucellosis using codominant, dominant and recessive models. The results indicated that the T allele vs the A allele was not associated with the risk of brucellosis with an overall OR of 0.85 (p = 0.09; 95% CI = 0.70–1.03). None of the codominant (p = 0.12 and 0.22), dominant (p = 0.09) or recessive (p = 0.44) models showed a significant association between genotype distribution and an increased risk of brucellosis.

TNF-α –308 G/A variation and the risk for brucellosis

Six studies including 640 patients and 802 controls assessed the association between the TNF-α –308 G/A variation and brucellosis. In all studies, the distributions of genotypes in the control subjects were in HWE (Table 2). The pooled analysis revealed that the A allele vs the G allele was not associated with the risk of brucellosis with an overall OR of 1.02 (p = 0.94; 95% CI = 0.59–1.77). In the codominant model, the pooled evidence suggested that the AA genotype vs the GG genotype distribution between the groups was not different and that there was no statistically significant association (p = 0.06; OR = 1.74; 95% CI = 0.98–3.11). Additionally, the general difference between the groups for the GA genotype compared to the GG one did not reach the level of statistical significance, using the codominant model with an overall OR of 0.98 (p = 0.96; 95% CI = 0.48–1.99). In the dominant model, the GA+AA genotype vs the GG genotype was not associated with an increased risk of brucellosis with an overall OR of 0.99 (p = 0.98; 95% CI = 0.52–1.91). However, the recessive model suggested that the AA genotype compared to the GG+GA genotype increases the risk of brucellosis with an overall OR of 2.00 (p = 0.02; 95% CI = 1.14–3.50). Figure 3 presents the forest plot and results of the meta-analysis of associations between the TNF-α –308 G/A polymorphism and the risk of brucellosis, using codominant, dominant and recessive models.

TNF-α –238 G/A polymorphism and susceptibility to brucellosis

Three studies including 255 brucellosis patients and 450 controls evaluated the association between the TNF-α –238 G/A polymorphism and susceptibility to brucellosis. In all studies, the distributions of genotypes in the control subjects were in HWE (Table 2). Figure 4 demonstrates the forest plot and results of the meta-analysis of associations between the TNF-α –238 G/A polymorphism and the risk of brucellosis, using codominant, dominant and recessive models. The results showed that the A allele vs the G allele was not associated with the risk of brucellosis with an overall OR of 0.66 (p = 0.36; 95% CI = 0.27–1.60). In none of the models included – codominant (p = 0.34), dominant (p = 0.34) or recessive – was there a significant association between genotype distribution and the risk of brucellosis.

Table 2. Main characteristics of studies included in a meta-analysis of *TNF-α* gene polymorphisms and brucellosis

SNP	Author	Year	Country	Ethnicity	Sample size	Allele frequency		Genotype frequency			HWE (p-value)
						G	A	GG	GA	AA	
TNF-α –308 G/A	Caballero[14]	2000	Spain	Caucasian	P 59 C 160	P 100 C 292	P 18 C 28	P 41 C 134	P 18 C 24	P 0 C 2	P 0.16 C 0.44
	Davoudi[15]	2006	Iran	Asian	P 43 C 162	P 82 C 272	P 4 C 52	P 39 C 110	P 4 C 52	P 0 C 0	P 0.74 C 0.01
	Budak[16]	2007	Turkey	Caucasian	P 40 C 50	P 69 C 80	P 11 C 20	P 29 C 33	P 11 C 14	P 0 C 3	P 0.31 C 0.37
	Karaoglan[13]	2009	Turkey	Caucasian	P 85 C 85	P 159 C 154	P 11 C 16	P 75 C 71	P 9 C 12	P 1 C 2	P 0.24 C 0.11
	Reza[22]	2009	Iran	Asian	P 260 C 217	P 361 C 311	P 159 C 123	P 138 C 106	P 85 C 99	P 37 C 12	P 0.00 C 0.06
	Eskandari-Nasab[11]	2016	Iran	Asian	P 153 C 128	P 266 C 244	P 40 C 12	P 115 C 116	P 36 C 12	P 2 C 0	P 0.66 C 0.57
TNF-α –238 G/A	Caballero[14]	2000	Spain	Caucasian	P 59 C 160	P 106 C 292	P 12 C 28	P 47 C 132	P 12 C 28	P 0 C 0	P 0.38 C 0.22
	Davoudi[15]	2006	Iran	Asian	P 43 C 162	P 80 C 243	P 6 C 81	P 37 C 81	P 6 C 81	P 0 C 0	P 0.62 C 0.00
	Eskandari-Nasab[11]	2016	Iran	Asian	P 153 C 128	P 271 C 225	P 35 C 31	P 118 C 97	P 35 C 31	P 0 C 0	P 0.11 C 0.11

TNF-α – tumor necrosis factor-alpha; SNP – single nucleotide polymorphism; HWE – Hardy-Weinberg equilibrium.

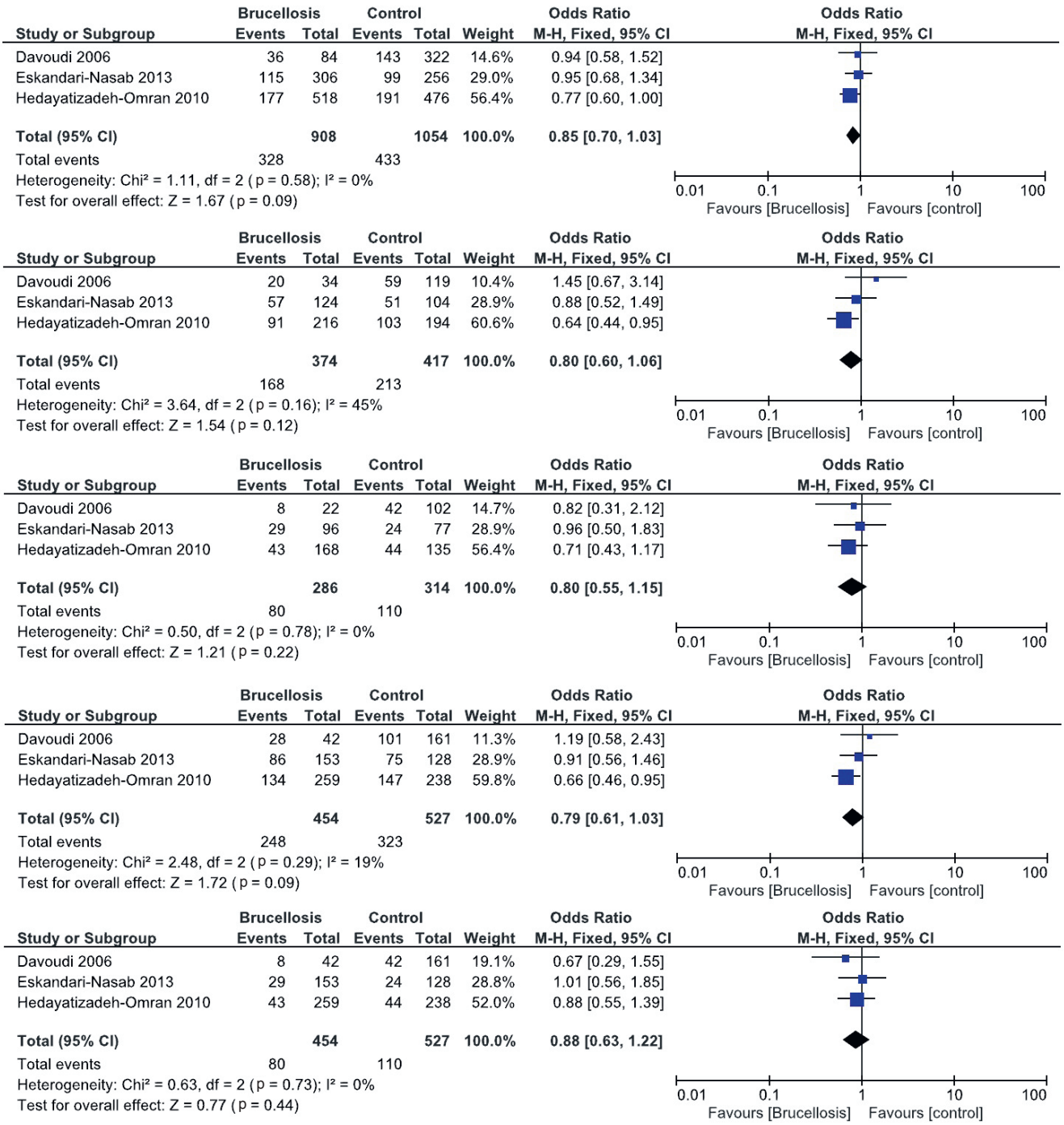

Fig. 2. Forest plot for the association of the IFN-γ UTR5644 A/T polymorphism and brucellosis (T allele vs A allele, TA vs AA, TT vs AA, AT+TT vs AA, and TT vs TA+AA)

Sensitivity analysis and the test for heterogeneity

Our pooled data showed the occurrence of heterogeneity in some genetic models ($I^2 > 50\%$). Sensitivity analyses for both IFN-γ and TNF-α were performed to estimate the stability of the results; specifically, a single study in the meta-analysis was removed each time to observe the impact of the individual data set on the overall OR. Sensitivity analysis indicated that no single study influenced the pooled OR qualitatively, suggesting that the results of this meta-analysis are stable.

Discussion

Seventeen studies were included in the present meta-analysis. Five studies in this meta-analysis were processed for the association between the IFN-γ +874 A/T polymorphism and brucellosis. Our pooled evidence suggests that the AT genotype vs AA genotype was associated with an increased risk of brucellosis overall. Similarly to our findings, Karaoglan et al. suggested that the TT genotype of IFN-γ +874 was associated with an increased risk of brucellosis.[13] However, Bravo et al.,[12] Rasouli and Kiany,[9]

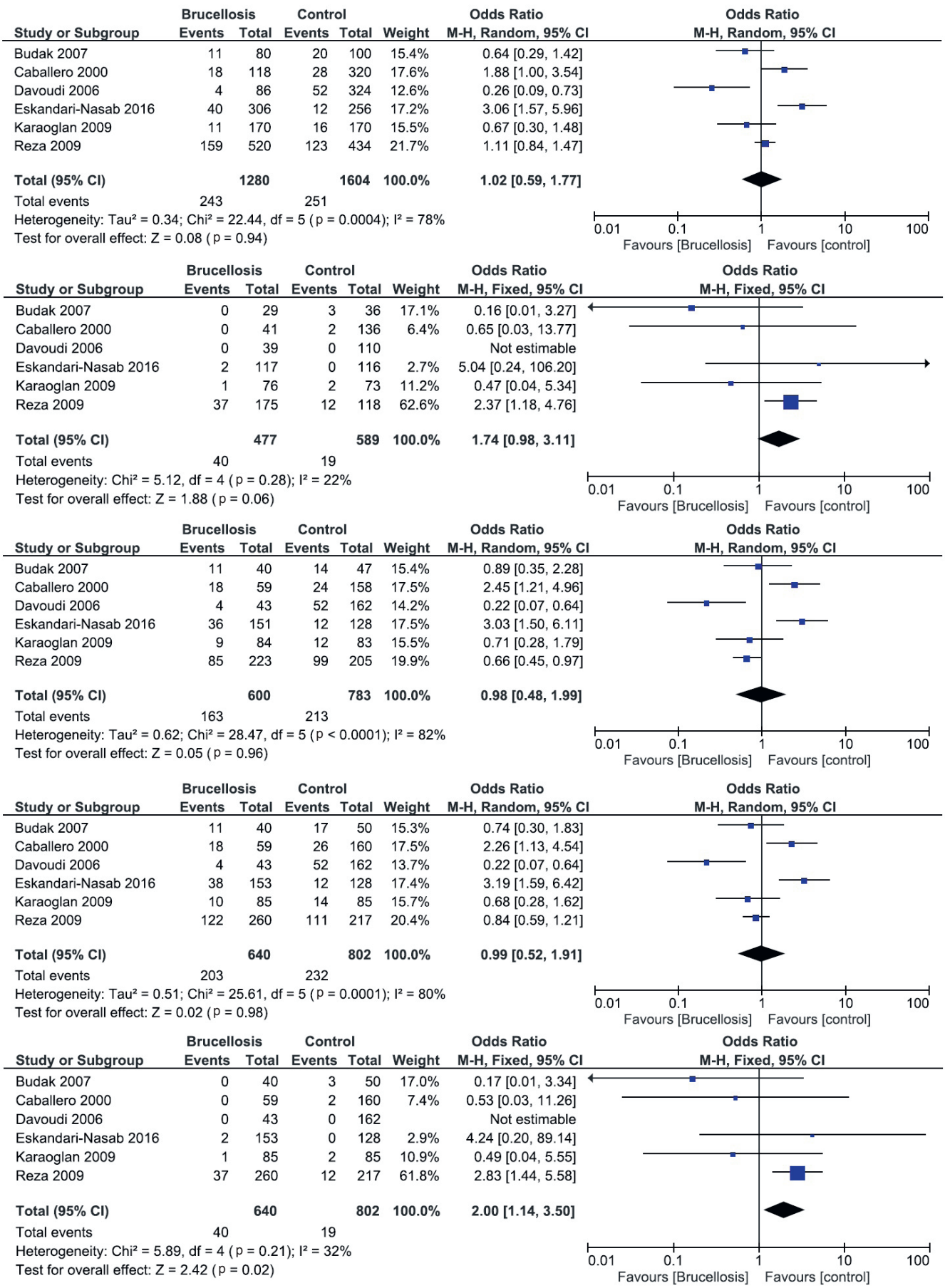

Fig. 3. Forest plot for the association of the TNF-α –308 G/A polymorphism and brucellosis (A allele vs G allele, AA vs GG, GA vs GG, GA+AA vs GG, and AA vs GG+GA)

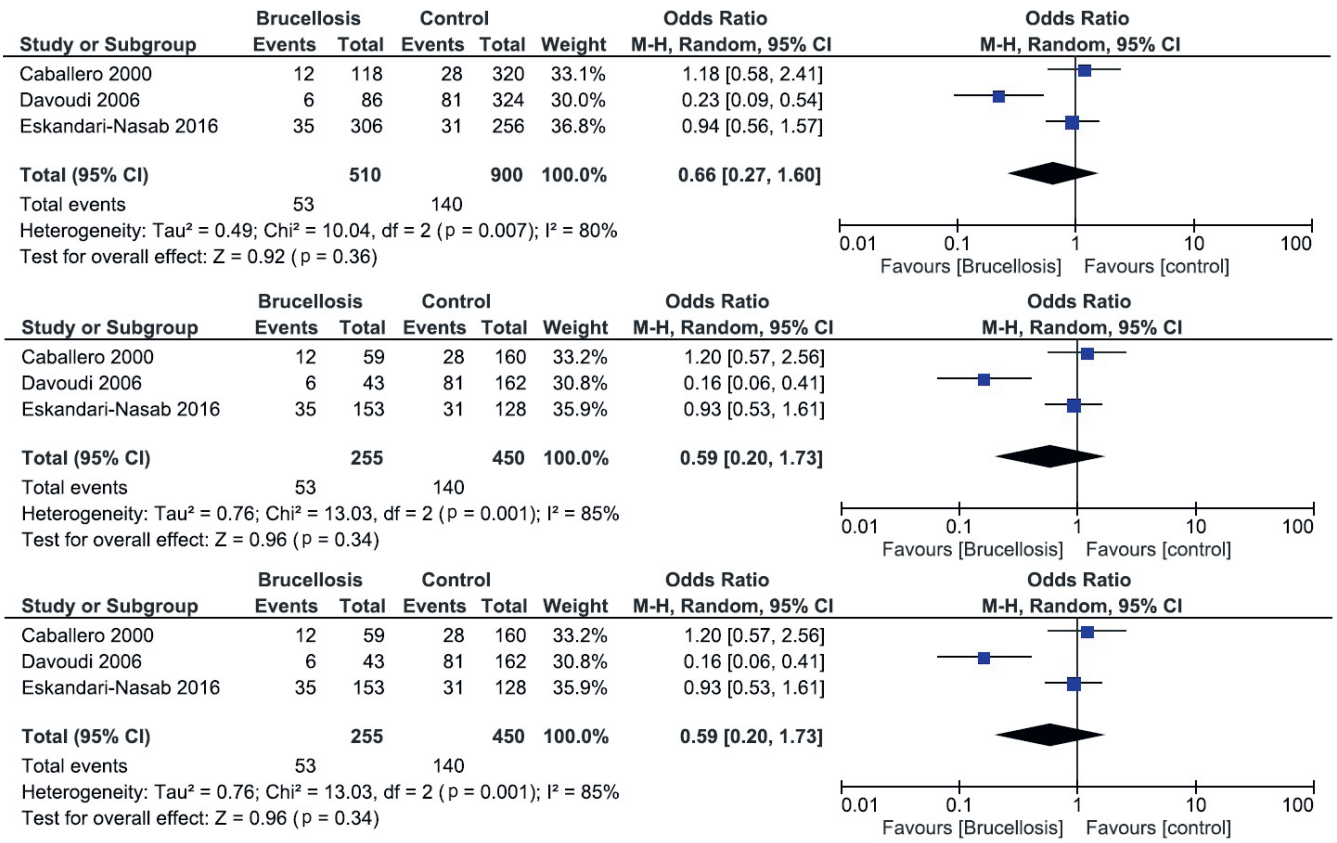

Fig. 4. Forest plot for the association of the TNF-α –238 G/A polymorphism and brucellosis (A allele vs G allele, GA vs GG and GA+AA vs GG)

and Eskandari-Nasab et al.[2] reported that individuals with the wild-type (AA) genotype of IFN-γ +874 A/T compared with the mutant (TT) genotype were susceptible to an increased risk of brucellosis.

Concerning the IFN-γ UTR5644 A/T polymorphism and susceptibility to brucellosis, 3 studies were processed in this meta-analysis. Our results showed that the UTR5644 polymorphism was not associated with the risk of brucellosis overall, using any models. In agreement with our findings, Davoudi et al.,[15] Hedayatizadeh-Omran et al.,[17] and Eskandari-Nasab et al.[2] also found no association between this polymorphism and the risk for brucellosis.[2,15,17]

IFN-γ is an essential cytokine for host control of intracellular pathogens, such as *Brucella* spp. This cytokine increases macrophage activation, promotes cellular immunity responses and contributes to the clearance of brucellosis infection.[18] One of the risk factors that may increase the host's vulnerability to brucellosis is genetic polymorphisms in the form of SNPs in the components of the immune system. Several SNPs, including +874 A/T and UTR5644 A/T in the coding region of the *IFN-γ* gene, have been shown to affect the expression of this cytokine.[12,19] Previous evidence has indicated that the +874 (A/T) AA genotype correlates with low production, the AT genotype with intermediate production, and the TT genotype with high production of IFN-γ.[19] With respect to the IFN-γ UTR5644 A/T polymorphism, it has been revealed that homozygosity for the T allele is associated with increased production of IFN-γ compared to other genotypes (AT or AA).[15] Our pooled evidence concurs with several reports demonstrating that TNF-α and IFN-γ induce cell-mediated resistance against *Brucella* spp. infection.[20] TNF-α exerts its antibacterial activity against *Brucella* spp. through the stimulation of IFN-γ production.[21]

Six studies were analyzed in this meta-analysis of the association between the TNF-α –308 G/A variation and susceptibility to brucellosis. Our pooled evidence indicated that in the recessive model, the AA genotype compared to the GG+GA genotype increased the risk of brucellosis overall. However, the A allele, AA or GA vs GG genotype in a codominant model and the GA+AA vs GG genotype in a dominant model were not associated with the risk of brucellosis overall. Our findings regarding the TNF-α –308 G/A polymorphism supports those of Reza et al., who found a relationship between –308 AA homozygosity and increased risk of brucellosis.[22] In contrast, Davoudi et al. reported that individuals carrying the GG genotype were associated with a higher risk of brucellosis.[15]

Three of the studies processed in this meta-analysis concerned the TNF-α –238 G/A polymorphism and susceptibility to brucellosis. Our results demonstrated that the TNF-α –238 G/A variation was not associated with the risk of brucellosis at both the genotype and allele level, which supports the findings of Caballero et al.,[14] Davoudi et al.[15] and Eskandari-Nasab et al.,[11] who reported that this polymorphism was not associated with an increased risk of brucellosis.

Our pooled survey suffers from a few limitations. The first is high genetic heterogeneity among the included studies, which may have resulted from the relatively small sample size of the studies included or from the insufficient amount of data. Our meta-analysis only included published studies, excluding some important relevant abstracts or unpublished studies. Thus, we were aware that these factors might result in high heterogeneity. Further large-scale studies are warranted to confirm the effect of *IFN-γ* and *TNF-α* gene polymorphisms on the risk of brucellosis.

Conclusions

Our meta-analysis demonstrated a significant association between the IFN-γ +874 AT and TNF-α –308 GG + GA genotypes and a higher risk for brucellosis. However, we found no relationship between the IFN-γ UTR5644 A/T and TNF-α –238 G/A SNPs and brucellosis.

References

1. Pappas G, Akritidis N, Bosilkovski M, Tsianos E. Brucellosis. *N Engl J Med*. 2005;352:2325–2336.
2. Eskandari-Nasab E, Moghadampour M, Hasani SS, et al. Relationship between gamma-interferon gene polymorphisms and susceptibility to brucellosis infection. *Microbiol Immunol*. 2013;57:785–791.
3. Pappas G, Memish ZA. Brucellosis in the middle East: A persistent medical, socioeconomic and political issue. *J Chemother*. 2007;19:243–248.
4. Moghadampour M, Eskandari-Nasab E, Shabani F. Relationship between CD14-159C/T gene polymorphism and acute brucellosis risk. *Asian Pac J Trop Med*. 2016;9:247–251.
5. Eskandari-Nasab E, Moghadampour M, Najibi H, Hadadi-Fishani M. Investigation of CTLA-4 and CD86 gene polymorphisms in Iranian patients with brucellosis infection. *Microbiol Immunol*. 2014;58:135–141.
6. Akhvlediani T, Clark DV, Chubabria G, Zenaishvili O, Hepburn MJ. The changing pattern of human brucellosis: Clinical manifestations, epidemiology and treatment outcomes over three decades in Georgia. *BMC Infect Dis*. 2010;10:346.
7. Moreno E. Retrospective and prospective perspectives on zoonotic brucellosis. *Front Microbiol*. 2014;5:213.
8. Christopher S, Umapathy BL, Ravikumar KL. Brucellosis: Review on the recent trends in pathogenicity and laboratory diagnosis. *J Lab Physicians*. 2010;2:55–60.
9. Rasouli M, Kiany S. Association of interferon-gamma and interleukin-4 gene polymorphisms with susceptibility to brucellosis in Iranian patients. *Cytokine*. 2007;38:49–53.
10. Eskandari-Nasab E, Moghadampour M, Asadi-Saghandi A, Kharazi-Nejad E, Rezaeifar A, Pourmasoumi H. Levels of interleukin-(IL)-12p40 are markedly increased in brucellosis among patients with specific IL-12B genotypes. *Scand J Immunol*. 2013;78:85–91.
11. Eskandari-Nasab E, Moghadampour M, Sepanj-Nia A. TNF-alpha –238, –308, –863 polymorphisms and brucellosis infection. *Hum Immunol*. 2016;77:121–125.
12. Bravo MJ, de Dios Colmenero J, Alonso A, Caballero A. Polymorphisms of the interferon gamma and interleukin 10 genes in human brucellosis. *Eur J Immunogenet*. 2003;30:433–435.
13. Karaoglan I, Pehlivan S, Namiduru M, et al. TNF-alpha, TGF-beta, IL-10, IL-6, and IFN-gamma gene polymorphisms as risk factors for brucellosis. *New Microbiol*. 2009;32:173–178.
14. Caballero A, Bravo MJ, Nieto A, Colmenero JD, Alonso A, Martin J. TNFA promoter polymorphism and susceptibility to brucellosis. *Clin Exp Immunol*. 2000;121:480–483.
15. Davoudi S, Amirzargar AA, Hajiabdolbaghi M, et al. Th-1 cytokines gene polymorphism in human brucellosis. *Int J Immunogenet*. 2006; 33:355–359.
16. Budak F, Goral G, Heper Y, et al. IL-10 and IL-6 gene polymorphisms as potential host susceptibility factors in brucellosis. *Cytokine*. 2007; 38:32–36.
17. Hedayatizadeh-Omran A, Rafiei A, Hajilooi M, Haghshenas M. Interferon-gamma low producer genotype +5644 over presented in patients with focal brucellosis. *Pak J Biol Sci*. 2010;13:1036–1041.
18. Chen X, Xu J, Chen Z, et al. Interferon-gamma +874A/T and interleukin-4 intron3 VNTR gene polymorphisms in Chinese patients with idiopathic thrombocytopenic purpura. *Eur J Haematol*. 2007;79: 191–197.
19. Ansari A, Hasan Z, Dawood G, Hussain R. Differential combination of cytokine and interferon-gamma +874 T/A polymorphisms determines disease severity in pulmonary tuberculosis. *PLoS One*. 2011;6:e27848.
20. Zhan Y, Liu Z, Cheers C. Tumor necrosis factor alpha and interleukin-12 contribute to resistance to the intracellular bacterium *Brucella abortus* by different mechanisms. *Infect Immun*. 1996;64:2782–2786.
21. Feldman KE, Loriaux PM, Saito M, et al. Ex vivo innate immune cytokine signature of enhanced risk of relapsing brucellosis. *PLoS Negl Trop Dis*. 2013;7:e2424.
22. Reza JS, Alireza R, Mostafa A, Alireza K, Mehrdad H. Association of tumor necrosis factor-alpha-308 (G-->A) polymorphism and susceptibility to brucellosis. *J Microbiol Immunol Infect*. 2009;42:22–26.

The use of direct immunofluorescence and nested polymerase chain reaction in diagnosing perinatal infections of *Chlamydia trachomatis*

Magdalena Frej-Mądrzak[1,A–D], Dorota Teryks-Wołyniec[1,B,C], Piotr Jankowski[2,A,B], Paulina Krochmal[1,C,D], Jolanta Sarowska[1,E], Agnieszka Jama-Kmiecik[1,E], Irena Choroszy-Król[1,A,E,F]

[1] Department of Basic Sciences, Faculty of Health Sciences, Wroclaw Medical University, Poland
[2] 1st Department and Clinic of Gynecology and Obstetrics, Faculty of Medicine, Wroclaw Medical University, Poland

A – research concept and design; B – collection and/or assembly of data; C – data analysis and interpretation; D – writing the article; E – critical revision of the article; F – final approval of the article

Advances in Clinical and Experimental Medicine, ISSN 1899-5276 (print), ISSN 2451-2680 (online) *Adv Clin Exp Med*. 2018;27(12):1711–1716

Address for correspondence
Magdalena Frej-Mądrzak
E-mail: magdalena.frej-madrzak@umed.wroc.pl

Funding sources
None declared

Conflict of interest
None declared

Received on February 7, 2016
Reviewed on September 19, 2016
Accepted on July 6, 2017

Abstract

Background. *Chlamydia* infection is the most frequently reported infectious, sexually transmitted disease (STD). Generally, *Chlamydia trachomatis* (*C. trachomatis*) infection of neonates is the result of perinatal exposure to the mother's infected cervix.

Objectives. The aim of the study was to estimate the frequency of infection caused by *C. trachomatis* in newborn infants. In this study of *C. trachomatis* perinatal infection, 107 infants born at the Wroclaw Medical University Clinic of Gynecology and Obstetrics (Poland) were tested to investigate whether *C. trachomatis* was present in swabs taken from the eyes and throats of children.

Material and methods. Each specimen was tested using the direct immunofluorescence test (DIF) and the nested polymerase chain reaction (PCR) method.

Results. The presence of *C. trachomatis*, irrespective of the origin of the swabs (ocular or from the throat), was confirmed in 62 newborns, amounting to 57.6% of the tested population. The occurrence of *C. trachomatis* in ocular swabs was confirmed in 35 children (32.7%). In the material taken from the throat, there were 48 newborns considered chlamydia-positive (44.9%). In the specimens taken from both the ocular and pharyngeal locations, there was a higher proportion of positive results while using the nested-PCR method in comparison to the DIF test. The specificity of the DIF method with reference to the nested-PCR was 67.9% for ocular swabs. In the material taken from the throat, the sensitivity of the DIF method with reference to the nested-PCR was 75.0% and the specificity was 62.1%.

Conclusions. Because of the importance of perinatal infections, it is recommended to perform a study among a larger group of patients in order to gain more reliable results.

Key words: *Chlamydia trachomatis*, infection, newborn

DOI
10.17219/acem/75724

Introduction

Infections of *Chlamydia trachomatis* (*C. trachomatis*), caused by oculogenital serotypes D-K, are among the most common sexually transmitted diseases (STDs). It is estimated that there are approx. 100 million new cases of *C. trachomatis* infection every year worldwide.[1] As long as chlamydia is the most commonly reported STD in the United States, it is recommended that annual screening examinations are carried out there in sexually active women under the age of 25 years, or in older women who are at an increased risk of infection.[2–4] Moreover, it is suggested that pregnant women in this age group undergo testing for *C. trachomatis* during their 3rd trimester of pregnancy.[4]

The oculogenital serovars (D-K) of *C. trachomatis* in newborn infants may be responsible for developing conjunctivitis and interstitial pneumonia, with conjunctivitis occurring more frequently. These include perinatal infections that take place during the passage of the newborn infant through the infected mother's cervix.[5,6] However, 1 case of *C. trachomatis* conjunctivitis was reported in a newborn infant delivered by cesarean section, which argues in favor of intrauterine infection by the continuity of tissues.[6] The risk of *C. trachomatis* perinatal infection in newborn infants is estimated at approx. 30%.[5]

A chlamydial etiology should be considered if the mother was infected in the past. Neonatal conjunctivitis occurs in 18–50% of children of infected mothers, with frequent occurrence in preterm infants, who are at risk, since chlamydia infections may cause premature labor.[7] The infection develops up to 3 weeks after birth and may become chronic. Its characteristic symptoms include mucopurulent discharge from the conjunctival sac with accompanying swelling and redness, but the infection can also be asymptomatic. Conjunctivitis, if left untreated, may lead to blindness.[8]

Chlamydia trachomatis conjunctivitis and pneumonia coexist in up to 1/2 of ill newborn infants. Interstitial pneumonia develops between the 3rd and the 12th week of age, and can vary in intensity. In most cases, the disease is mild, but breathing disorders may at times require oxygen therapy. High levels of eosinophils can be reported in the blood. A large number of B lymphocytes and plasma cells in the blood, which is characteristic for *C. trachomatis* pneumonia, results in high levels of immunoglobulin M (IgM) antibodies in the blood. The changes can be seen in spirometry and in radiological examination. The symptoms include a dry cough, a low-grade fever and rapid breathing.[6,7,9] It is suspected that *C. trachomatis* infection may be related to sudden infant death syndrome (SIDS).[7,10]

Infrequently, *C. trachomatis* in newborn infants can cause infections of the vagina, rectum, nasopharynx, or middle ear.

Aim of the study

The aim of the study was to estimate the frequency of infection caused by *C. trachomatis* in newborn infants.

Material and methods

The experimental material consisted of swabs collected from newborn infants at the 1st Department and Clinic of Gynecology and Obstetrics (Wroclaw Medical University, Poland). A total of 109 children were tested. Four swabs were collected from every newborn infant: 2 from the eye and 2 from the throat. We used a direct immunofluorescence test (DIF) – Chlamydia Pathfinder (Bio-Rad Laboratories, Marnes-la-Coquette, France) and the nested polymerase chain reaction technique (nested-PCR) – PCR-*Chlamydia trachomatis* test (DNA Gdańsk, Poland) in order to detect chlamydia infection. Two hundred and eighteen tests were conducted by DIF (109 eye swabs and 109 throat swabs), and the same number of tests was done by nested-PCR. All tests were performed in the Chlamydia Research Laboratory, Department of Basic Sciences, Wroclaw Medical University, Poland.

The quality of the tested material is of great diagnostic importance in the case of *C. trachomatis*. Due to the fact that chlamydiae are obligate intracellular parasites, the obtained material must contain epithelial cells. Detecting bacteria in the absence of epithelial cells provides unreliable results. Neither eye fluid nor saliva constitute suitable test material.

Since epithelium was not detected in the swabs taken from 2 patients, we did not take into account the results from these samples. Altogether, we analyzed 428 results.

The swabs were collected by authorized personnel in accordance with the appropriate procedures.

The analysis of results was performed using the statistical package PQStat v. 1.6.0.428 (PQStat Software, Poznań, Poland).

Comparing the results of the eye swabs to those of the throat swabs, the measure of compliance was applied. Comparing the results of the DIF method in reference to the gold standard – the PCR method – the results of compliance, sensitivity, specificity, and positive and negative predictive value were specified, and 95% confidence intervals (CI) were estimated for these results. Compliance measurements were also analyzed with McNemar's test.

A probability of $p < 0.05$ was determined to be significant and a level of $p < 0.01$ was determined to be highly significant.

Results

We found chlamydia in both the eye and throat in 19.6% of all newborn infants (21 patients). Chlamydia was not detected at all in 42.1% of newborn infants (45 patients).

In the material taken from both the eye and throat, there was a significantly higher percentage of positive results obtained by nested-PCR (34/107 for the eye, 45/107 for the throat) than by DIF (1/107 for the eye; 12/107 for the throat) (Table 1).

Table 1. Test results for the presence of *Chlamydia trachomatis* by the method used and the source location of the sample

Sample type	Number of samples	Positive results
		n
DIF – eye	107	1
DIF – throat	107	12
Nested-PCR – eye	107	34
Nested-PCR – throat	107	45

DIF – direct immunofluorescence test; PCR – polymerase chain reaction.

The presence of *C. trachomatis* in eye swabs was reported in 35 newborns, i.e., in 32.7% of patients. There was only 1 positive result in DIF. In this sample, the nested-PCR results were negative, which is equivalent to the lack of consistently positive results in eye swabs. We reported 72 consistently negative results (68.2%) and 35 inconsistently negative results (32.7%) (Table 2).

Table 2. Consistency of results obtained by nested-PCR and DIF

Sample type	Number of samples	Consistent positive results		Consistent negative results		Inconsistent results
		n	%	n	%	n
Eye	107	0	0.0	72	67.3	35
Throat	107	9	8.4	59	55.1	39

DIF – direct immunofluorescence test; PCR – polymerase chain reaction.

We detected *C. trachomatis* in throat swabs of 48 newborns (44.9%). Consistently positive results were obtained from 9 patients (8.4%), whereas consistently negative results were found in 59 patients (55.1%). There were 36.4% of inconsistent results (39 patients) (Table 2).

In the medical interview, the respondents reported the occurrence of additional factors that could increase the likelihood of neonatal chlamydia. Newborn infants without such additional factors accounted for 57.0% of all patients (61 patients). We isolated several groups on the basis of a history of diabetes in the mother or the occurrence of specific symptoms accompanying chlamydia infection in the child (or even previously confirmed *C. trachomatis* infection). Among participants with no family history, chlamydia was reported in 36 patients (33.6%).

In the medical interview, 17 mothers of newborn infants (15.9%) who were tested during pregnancy or before pregnancy reported previous *C. trachomatis* infection. Chlamydia was detected in newborns in 23.5% of cases, whereas in 3 out of 4 cases, positive results were obtained from both the eye and throat, but only by nested-PCR (Table 3).

We reported symptoms of respiratory tract infections in 7 newborn infants, including 42.9% (3 newborns) with positive nested-PCR results taken from the throat, and – in 1 case – from the eye. In 3 newborns, we did not report *C. trachomatis* in either the eye or throat.

Table 3. The presence of the risk factors of *Chlamydia trachomatis* infection in the tested material and the incidence of positive results

Risk factor	Number of samples	Positive results
	n	n
Presence of *C. trachomatis* infection in the mother	17	4
Symptoms of the respiratory system	7	4
Symptoms of the eye	6	4
Check tests	16	9
Lack of load	61	36

In 6 newborn infants, we reported symptoms related to eye infection, whereas in 3 newborns (50.0%), we reported positive results from the eye, and in 1 case from the throat alone. In 2 patients, we found negative results despite the occurrence of symptoms.

In patients with eye or respiratory symptoms, we obtained positive results mainly by nested-PCR. In most of these cases, in both the throat and eye, DIF testing gave negative results (in all 6 newborns with ocular symptoms and in 6 out of 7 newborns with respiratory symptoms).

We carried out a follow-up examination in 16 newborn infants (15.0%). *Chlamydia trachomatis* was confirmed in 9 cases (56.3%) by nested-PCR, while there were no positive DIF results.

The compatibility (accuracy) of diagnosis for both methods equaled 87.85% (95% CI = 80.12–93.37%), which refers only to the "negative" results. However, in any case, the "positive" results were not consistent in both measurements. This is mainly due to the fact that the DIF method for eye swabs showed only 1 positive result. Among the results obtained by the DIF method for the throat, 12 positive results were reported. The results of McNemar's compliance test indicated a significantly high level of inconsistency of the results for both measurements (χ^2 = 7.69; degree of freedom (df) = 1; p = 0.0055) (Table 4).

The compatibility (accuracy) of diagnosis for both methods equaled 65.42% (95% CI = 55.61–74.35%), and this result is the sum of consistent negative results (45.79%) and consistent positive results (19.63%). The results of McNemar's compliance test indicated an insignificant level of differences in both measurements (χ^2 = 2.70; df = 1; p = 0.1002), so both measurements can be considered compatible (Table 5).

The compatibility (accuracy) of diagnosis for both methods equaled 67.29% (95% CI = 57.54–76.05%), which refers only to the "negative" results. However, in any case, the "positive" results were not consistent in both measurements. This is mainly due to the fact that the DIF method for the eye swabs showed only 1 positive result. Among the results obtained by the PCR method for the eye, there were 34 positive results. Accordingly, the sensitivity of the DIF method for the eye compared to the PCR method for the eye equaled 0%; the specificity equaled 98.63%

Table 4. Summary of the results of DIF – eye and DIF – throat

Results of DIF – eye and DIF – throat			DIF – throat		Total
			1	0	
DIF – eye	1	quantity (n)	0	1	1
		% of line	0	100	–
		% of column	0	1.05	–
		% of total	0	0.93	0.935
	0	quantity (n)	12	94	106
		% of line	11.32	88.68	–
		% of column	100	98.95	–
		% of total	11.21	87.85	99.065
Total		quantity (n)	12	95	107
		% of total	11.215	88.785	100

DIF – direct immunofluorescence test.

Table 5. Summary of the results of PCR – eye and PCR – throat

Results of PCR – eye and PCR – throat			PCR – throat		Total
			1	0	
PCR – eye	1	quantity (n)	21	13	34
		% of line	61.76	38.24	–
		% of column	46.67	20.97	–
		% of total	19.63	12.15	31.776
	0	quantity (n)	24	49	73
		% of line	32.88	67.12	–
		% of column	53.33	79.03	–
		% of total	22.43	45.79	68.224
Total		quantity (n)	45	62	107
		% of total	42.056	57.944	100

PCR – polymerase chain reaction.

Table 6. Summary of the results of DIF – eye and PCR – eye

Results of DIF – eye and PCR – eye			PCR – eye		Total
			1	0	
DIF – eye	1	quantity (n)	0	1	1
		% of line	0	100	–
		% of column	0	1.37	–
		% of total	0	0.93	0.935
	0	quantity (n)	34	72	106
		% of line	32.08	67.92	–
		% of column	100	98.63	–
		% of total	31.78	67.29	99.065
Total		quantity (n)	34	73	107
		% of total	31.776	68.224	100

DIF – direct immunofluorescence test; PCR – polymerase chain reaction.

Table 7. Summary of the results of DIF – throat and PCR – throat

Results of DIF – eye and PCR – throat			PCR – throat		Total
			1	0	
DIF – throat	1	quantity (n)	9	3	12
		% of line	75	25	–
		% of column	20	4.84	–
		% of total	8.41	2.8	11.215
	0	quantity (n)	36	59	95
		% of line	37.89	62.11	–
		% of column	80	95.16	–
		% of total	33.64	55.14	88.785
Total		quantity (n)	45	62	107
		% of total	42.056	57.944	100

DIF – direct immunofluorescence test; PCR – polymerase chain reaction.

(95% CI = 92.60–99.96%). The positive predictive value was 0% and the negative predictive value was 67.92% (95% CI = 58.16–76.66%). The results of McNemar's compliance test indicated a significantly high lack of consistency of results for both measurements ($\chi^2 = 29.26$; df = 1; $p < 0.0001$).

The compatibility (accuracy) of diagnosis for both methods equaled 63.55% (95% CI = 53.69–72.64%), and this result is the sum of consistent negative results (55.14%) and consistent positive results (8.41%). The sensitivity of the DIF method for throat swabs comparing to the reference method (PCR) was 20% (95% CI = 9.58–34.60%) and the specificity was 95.16% (95% CI = 86.50–98.99%). The positive predictive value was 75% (95% CI = 42.81–94.51%) and the negative predictive value was 62.10% (95% CI = 51.57–71.86%). The results of McNemar's compliance test indicated a significantly high lack of consistency of results for both measurements ($\chi^2 = 26.26$; df = 1; $p < 0.0001$) (Table 7). When testing the sensitivity and specificity, PCR and DIF methods were compared, the compliance of positive and negative results obtained with these methods in the same patients.

Discussion

Researchers rarely raise the subject of the occurrence of *C. trachomatis* in newborn infants, but studies carried out on newborn infants born to healthy mothers are even less frequent. This may result from the fact that conjunctivitis, the most common form of chlamydia in newborn infants, usually presents mild symptoms and can resolve spontaneously. Another reason may be associated with the reluctance of some parents to take material from their children if there is no such need. Swabs, washes or aspirates from the nasopharynx and eyes are commonly used in diagnosing *C. trachomatis* infections in children. Competent eye or throat swabbing, even if it causes the child's discomfort, is necessary to achieve research reliability.

In 2012 and 2013, in order to diagnose perinatal infections, Frej-Mądrzak et al. examined the material collected from 55 children.[11] The authors chose DIF as the research technique. The material included 33 eye swabs, 19 throat swabs and 11 urethra swabs. The authors reported 1 positive result in the throat swab (1.8%).

In Buenos Aires, between July 1995 and December 1998, Di Bartolomeo et al. examined 332 newborns diagnosed with conjunctivitis.[12] The chosen method of research was the enzyme-linked immunosorbent assay (ELISA) technique. Positive results were confirmed by nested-PCR. The authors detected *C. trachomatis* in 7.8% of cases, which was the only pathogen detected in 22 out of 26 children. The authors detected other bacteria in 4 cases, but they did not have any significance as to the type of infection. The authors reported decreased occurrence of chlamydial conjunctivitis throughout the study period; in 1995, this number amounted to 4.4 cases per 1,000 live births, and in 1998 to only 0.8 cases per 1,000 live births.

In studies carried out in Iran from 2007 to 2008 in a group of 223 newborn infants with symptoms of conjunctivitis, the authors confirmed positive results with the ELISA study method and by the indirect immunofluorescence test.[13] There were 22 newborn infants, representing 13.6% of the whole study group, who tested positive for IgM against *C. trachomatis*. The authors reported bacteria in 8.0% of patients (18 of 223 newborns) in the confirmation test.

Bekler et al. conducted a study in a group of 56 newborns, including 35 premature and 21 term-born infants.[14] The authors applied the DIF method and cultured the cell samples shortly after birth. Additionally, in the 2nd and 6th week of age, the authors examined the sera for immunoglobulin A (IgA) and IgM class antibodies with ELISA. Neither method revealed the presence of *C. trachomatis* in term-born children. In premature infants, the bacteria were reported in the throat of 10 out of 35 children (28.6%).

In a group infected with *C. trachomatis*, a higher prevalence of conjunctivitis (60.0% compared to 24.0% in healthy subjects) was reported. Similarly, a lower prevalence of conjunctivitis was observed in the children of healthy mothers (14–18.3% compared to 45–47% in infected mothers). Neonatal pneumonia did not develop in the study groups. The DIF sensitivity amounted to 40.0%, i.e., much lower than the sensitivity of the cell culture method (70.0%).

Yu et al. examined 300 pregnant women and 305 newborns using the nested-PCR method.[15] The test material taken from the women consisted of cervical swabs, and nasopharyngeal swabs were taken from the newborn infants. In the group of pregnant women, the authors reported positive test results in 11.0% of cases. In 24.2% of children of infected mothers (8 out of 33 newborns), the authors detected the presence of *C. trachomatis* in nasopharyngeal swabs. It should be noted, however, that 2 newborns with positive test results were born by cesarean section.

In our own research, which studied newborn infants at the 1st Department and Clinic of Gynecology and Obstetrics of Wroclaw Medical University, we reported a very high percentage of patients (57.9%) with positive laboratory test results for *C. trachomatis*.

When analyzing the test results from throat and eye swabs, we noted that chlamydiae were slightly more frequently detected in the throat. We reported that *C. trachomatis* was found more frequently by nested-PCR than by DIF.

At the time of carrying out this review, we did not find any new data on the subject regarding simultaneous examination of throat and eye swabs with the same research techniques. Therefore, we found it difficult to refer to individual authors.

Considering the importance of this subject, we suggest conducting studies on a larger group of patients in order to draw statistically relevant conclusions.

Conclusions

The detection of 48 cases of *C. trachomatis* infection in swabs from the throat and 35 cases in swabs from the eye by the PCR method suggests that tests detecting *C. trachomatis* in pregnant women should be included in routine diagnosis before giving birth. These examinations should be applied also to newborns whose mothers were diagnosed with chlamydia in the past in order to avoid the complications of perinatal infection by this pathogen.

In summary, the results obtained by the DIF method are not compatible with the reference results obtained by the PCR method. The DIF method is not diagnostically reliable.

References

1. World Health Organization. Baseline report on global sexually transmitted infection surveillance. WHO; 2012. http://www.who.int/reproductivehealth/publications/rtis/9789241505895/en/.
2. Centers for Disease Control and Prevention. Sexually Transmitted Disease Surveillance 2013. Atlanta, GA: Department of Health and Human Services; 2014.
3. Centers for Disease Control and Prevention. Recommendations for the laboratory-based detection of *Chlamydia trachomatis* and *Neisseria gonorrhoeae* – 2014. *MMWR Recomm Rep*. 2014;63 (RR-02):1–19.
4. Workowski KA, Berman S; Centers for Disease Control and Prevention. Sexually transmitted diseases treatment guidelines, 2010. *MMWR Recomm Rep*. 2010;59(RR-12):1–110.
5. Choroszy-Król I, Frej-Mądrzak M, Jama-Kmiecik A, Bober T, Sarowska J. Characteristics of the *Chlamydia trachomatis* species: Immunopathology and infections. *Adv Clin Exp Med*. 2012;21(6):799–808.
6. Frej -Mądrzak M, Krzemińska I, Choroszy-Król I. Zakażenia chlamydialne u dzieci. *Forum Zakażeń*. 2011;2(3):41–44.
7. Wilkowska-Trojniel M. Udział zakażenia *Chlamydia trachomatis* w niepowodzeniach ciążowych u kobiet w regionie północno-wschodniej Polski. Akademia Medyczna w Białymstoku, Poland; 2007.
8. World Health Organization. Global Strategy for the Prevention and Control of Sexually Transmitted Infections: 2006–2015. WHO; 2007. http://www.who.int/hiv/pub/toolkits/stis_strategy%5B1%5Den.pdf.
9. Nitsch-Osuch A, Wardyn KA, Choroszy-Król I. *Zakażenia wywołane patogenami atypowymi w praktyce lekarskiej*. Wrocław, Poland: Górnicki Wydawnictwo Medyczne; 2007:11–22.
10. Pawlikowska M, Deptuła W. Choroby u ludzi spowodowane chlamydiami i chlamydofilami. *Postepy Hig Med Dosw*. 2007;61:708–717.
11. Frej -Mądrzak M, Teryks-Wołyniec D, Jama-Kmiecik A, Sarowska J, Gosciniak G, Choroszy-Król I. Zakażenia układu moczowo-płciowego oraz spojówek *Chlamydia trachomatis* u dorosłych i dzieci w latach 2012–2013. *Family Medicine & Primary Care Review*. 2014;16(3):225–227.
12. Di Bartolomeo S, Mirta DH, Janer M, et al. Incidence of *Chlamydia trachomatis* and other potential pathogens in neonatal conjunctivitis. *Int J Infect Dis*. 2001;5(3):139–143.

13. Khoshdel A, Taheri S, Khadivi R, et al. Incidence and bacteriological profile of neonatal conjunctivitis in Hajar Hospital, Shahrekord, Iran. *Iran J Pathol*. 2012;7(2):86–91.
14. Bekler C, Kultursay N, Ozacar T, Sayiner A, Yalaz M, Akisu M. Chlamydial infections in term and preterm neonates. *Jpn J Infect Dis*. 2012;65:1–6.
15. Yu J, Wu S, Li F, Hu L. Vertical transmission of *Chlamydia trachomatis* in Chongqing, China. *Curr Microbiol*. 2009;58(4):315–320.

ALOX12 gene polymorphisms and serum selenium status in elderly osteoporotic patients

Atiyeh Al-e-Ahmad[1,2,A–D,F], Hadi Parsian[3,A–F], Mojtaba Fathi[2,A–F], Soghrat Faghihzadeh[4,A,C,E,F], Seyed Reza Hosseini[5,A,B,F], Haji Ghorban Nooreddini[6,A,B,F], Abbas Mosapour[7,B,F]

[1] Mobility Impairment Research Center, Health Research Institute, Babol University of Medical Sciences, Iran
[2] Department of Biochemistry and Nutrition, Faculty of Medicine, Zanjan University of Medical Sciences, Iran
[3] Cellular and Molecular Biology Research Center, Health Research Institute, Babol University of Medical Sciences, Iran
[4] Department of Biostatistics and Epidemiology, Faculty of Medicine, Zanjan University of Medical Sciences, Iran
[5] Social Determinants of Health Research Center, Health Research Institute, Babol University of Medical Sciences, Iran
[6] Department of Internal Medicine, Ayatollah Rouhani Hospital, Babol University of Medical Sciences, Iran
[7] Department of Biochemistry, School of Medicine, Babol University of Medical Sciences, Iran

A – research concept and design; B – collection and/or assembly of data; C – data analysis and interpretation; D – writing the article; E – critical revision of the article; F – final approval of the article

Advances in Clinical and Experimental Medicine, ISSN 1899-5276 (print), ISSN 2451-2680 (online) *Adv Clin Exp Med*. 2018;27(12):1717–1722

Address for correspondence
Hadi Parsian
E-mail: hadiparsian@yahoo.com

Funding sources
This work was financially supported in a large part by research grant No. A-12-802-3 from the Department of Biochemistry and Nutrition, Zanjan University of Medical Sciences, Iran.

Conflict of interest
None declared

Acknowledgements
We would like to thank Babol University of Medical Sciences, Iran, for their professional assistance and consultation. We are greatly indebted to the families who participated in this study, without whom this work would not have been possible.

Received on October 15, 2016
Reviewed on January 24, 2017
Accepted on July 5, 2017

DOI
10.17219/acem/75689

Abstract

Background. Osteoporosis is a systemic bone disease which leads to a reduction in bone mass. Many studies have shown that up to 80% of bone mineral density (BMD) variations are attributed to genetic factors. Arachidonate 12-lipoxygenase enzyme, encoded by the *ALOX12* gene, produces lipid peroxides as reactive oxygen species (ROS), leading to oxidative stress and the development of osteoporosis. Selenium (Se) is incorporated into selenoproteins, which may reduce the risk of osteoporosis.

Objectives. We aimed to investigate the association of 2 *ALOX12* single nucleotide polymorphisms (SNPs) and serum Se level with lumbar spine and femoral neck BMD among elderly individuals living in Amirkola, Iran.

Material and methods. The study consisted of 180 individuals aged ≥60 years (90 healthy and 90 osteoporotic patients). We examined the effect of 2 *ALOX12* SNPs (rs2292350 and rs9897850), using the polymerase chain reaction – restriction fragment length polymorphism (PCR–RFLP) on both BMD regions measured by dual energy X-ray absorptiometry (DXA). Serum Se level was measured using an atomic absorption spectrophotometer PGG990 AAS (PG Instruments Ltd., Lutterworth, USA).

Results. The rs2292350 SNP showed a significant association with femoral neck BMD ($p = 0.04$). Moreover, in terms of serum Se level, a significant difference was found between the patient group (57.58 ±25.54 µg/L) and the control group (81.09 ±25.58 µg/L) ($p < 0.001$). In addition, individuals with higher serum Se levels also had higher BMD of the lumbar spine ($r^2 = 0.392$; $p < 0.001$) and the femoral neck ($r^2 = 0.478$; $p < 0.001$).

Conclusions. The results suggested that genetic variation in *ALOX12* might influence BMD variations in our recruited participants. As for the patients with lower serum Se levels, it was observed that serum Se deficiency was accompanied by some *ALOX12* variation, contributing to the development of osteoporosis.

Key words: osteoporosis, single nucleotide polymorphism, bone mineral density, *ALOX12*, selenium

Introduction

Osteoporosis is a systemic bone disease mostly occurring in elderly individuals. In this disease, disturbance in bone remodeling (bone resorption and formation) leads to a bone mass reduction, bone fragility, and eventually, to fracture. Osteoporotic fracture may cause disability, decreased quality of life, and ultimately, mortality – it affects all aspects of the patient's life.[1] It has been estimated that over 200 million people suffer from osteoporosis worldwide.[2] There have also been studies reporting the rate of this disease in a local region; for example, in 2009, an Iranian multi-center study indicated that 70% of women and 50% of men aged ≥50 years suffered from osteoporosis or osteopenia.[3]

Peak bone mineral density (BMD) as a major determinant of bone strength achieved in early adulthood plays an important role in the prediction of osteoporotic fracture in later life.[1] In addition to many confirmed factors, such as race, sex, age, nutrition, hormonal status, menopausal state, smoking, alcohol intake, and physical activity, there are many studies that support the remarkable influence of genetic factors on bone strength. Studies show that up to 80% of BMD variation is attributable to genetic factors.[4–7]

A link between hip, spine and wrist BMD and the arachidonate 12-lipoxygenase (*ALOX12*) gene has been reported, and some researchers have suggested that *ALOX12* is a susceptible gene for BMD variation. *ALOX12* belongs to the arachidonate lipoxygenase enzyme super-family, which catalyzes the insertion of molecular oxygen into polyunsaturated fatty acids, such as arachidonic acid.[8,9]

The product of *ALOX12* activity, i.e., 12-hydroperoxyeicosatetraenoic acid (12-HPETE), serves as an endogenous ligand for the peroxisome proliferator-activated receptors (PPARs), which inhibit osteoblastogenesis and increase adipogenesis from a common progenitor – the mesenchymal stem cells (MSCs) of bone marrow.[10–12] Therefore, *ALOX12* activation could result in the upregulation of the pathway of PPARs, subsequently decreasing osteoblastogenesis and BMD.[13,14] Accordingly, several single nucleotide polymorphisms (SNPs) in *ALOX12* have been suggested as being associated with BMD variations in humans, but the results are controversial.[1,4,5,7,15]

Selenium (Se) is an essential trace element that incorporates into selenoproteins as selenocysteine – the 21st amino acid. Various members of the glutathione peroxidase (GPx) family (including phospholipid hydroperoxide glutathione peroxidase – PHGPx) are well-known selenoproteins with antioxidant capacity that play an important role in the scavenging of lipid peroxide products.[16,17] Therefore, 12-HPETE serves as a reactive oxygen species (ROS), quickly converting to 12-hydroxyeicosatetraenoic acid (12-HETE) by peroxidase 2, 4. Therefore, a decrease of Se can interfere with the turnover of lipid peroxidation, resulting in ROS accumulation that leads to cellular and extracellular damage in bone turnover, such as inhibition of osteoblastic differentiation, which is a major contributor to the development of osteoporosis.[18,19]

Although there is no clear mechanism indicating a relationship between the Se status and osteoporosis development, reports show that antioxidant supplementation reduces the risk of osteoporosis via an improvement in antioxidant capacity.[16,18,20,21] Furthermore, Se intake would reduce the risk of osteoporotic hip fracture in a population-based case-control study and Se deficiency also resulted in a reduction in femur and tibia BMD in rats. Therefore, Se deficiency can be considered a putative risk factor of osteoporosis.[22,23]

To the best of our knowledge, there have been no reports on the status of *ALOX12* polymorphisms and Se in osteoporotic individuals in our area. Therefore, we aimed to investigate the association of 2 *ALOX12* polymorphisms (rs2292350 and rs9897850) and serum Se with lumbar spine and femoral neck BMD in this population.

Material and methods

Participants

From among 1,616 elderly participants in the Amirkola Health and Aging Project (AHAP), we randomly selected 90 out of 558 osteoporotic individuals (45 males and 45 females) as the study group and 90 out of 326 age- and gender-matched individuals (45 males and 45 females) as control subjects.[24] The remaining participants had osteopenia. Informed consent was obtained from each participant and the study was approved by the Zanjan University of Medical Sciences (Iran) Ethics Committee. The osteoporosis status was determined by BMD measurement. All selected participants were ≥60 years old and they had never taken any medication related to BMD or bone turnover, or Se supplementary drugs, and they were all non-smokers. None of the participants had renal or metabolic bone disease.

Bone mineral density measurement

Bone mineral density [g/cm^2] of the lumbar spine (L1–L4) and proximal femur were measured by a dual energy X-ray absorptiometry (DXA) densitometer, using a Lexxos densitometer (DMS, Montpellier, France). According to the World Health Organization (WHO) criteria, the participants were categorized into 2 separate groups, osteoporotic and normal. Subjects with a BMD of 2.5 standard deviations (SD) or below the average value for young healthy adults (i.e., a T-score of <–2.5 SD) were considered osteoporotic patients, and subjects with a T-score of >–1.0 SD were considered normal subjects.[25]

Serum selenium measurement

Serum Se levels were measured by an atomic absorption spectrophotometer PG990 AAS (PG Instruments Ltd., Lutterworth, USA) equipped with a graphite furnace. Each serum sample was first diluted with deionized water (1:1); then, 10 µL of each diluted sample was injected into the graphite

furnace. The working standard solution was prepared from stock standards of Se, according to Standard Reference Material (SRM) from National Institutes of Standards and Technology (NIST); 1000 mg/L for AAS (selenium dioxide in nitric acid 0.5 mol/L (Merch KGaA, Darmstadt, Germany)). The operating parameters for measuring serum Se levels were set as recommended by the manufacturer (wavelength: 196 nm; bandwidth: 0.4 nm; and lamp current: 5 mA).

Genotyping

Polymorphism selection

Using extensive literature searches, among all known polymorphisms of *ALOX12*, 2 SNPs (rs9897850 and rs2292350) were selected on the basis of other researchers' findings.[1,4,5,7] Both SNPs were listed in the National Center for Biotechnology Information (NCBI) SNP database and happened to be very common (minor allele frequencies >0.35).

Polymerase chain reaction

Genomic DNA was extracted from whole blood using a QIAamp DNA Blood Mini Kit (QIAGEN Korea Ltd., Seoul, Korea) and stored at –20°C. The polymerase chain reaction (PCR) was performed using 2 pairs of forward and reverse primers (CinnaGen, Tehran, Iran) as follows: forward – 5'AGTGTTCTCATCTATGTTCGC3', reverse – 5'CCCAGACTAGCCCAAACC3' for rs9897850 targeting the promoter region, and forward – 5'AGTAGGTGTAGGTGTATAGGTGAC3', reverse – 5'TGTGGTTAGCCGTATTCC3' for rs2292350 targeting the intron 2 region of the *ALOX12* gene.

The PCR was carried out using a PCR Master Mix 2X (CinnaGen) according to the manufacturer's protocol, adjusted to a total reaction mixture of 25 µL, containing 50 ng of total DNA template. Amplification was performed using a DNA thermal cycler (Analytik Jena AG, Jena, Germany) for 35 cycles (93°C, 60 s; 57°C, 60 s; 72°C, 60 s) with an initial heating at 95°C for 5 min and a final extension for 5 min at 72°C. The PCR products were analyzed by 1% agarose gel electrophoresis and visualized with a gel documentation and analysis system (Gel Doc™ EZ System; Bio-Rad Laboratories, Hercules, USA) after staining by DNA safe stain (CinnaGen). The PCR product size was 215 bp for rs9897850 and 300 bp for rs2292350.

Restriction Fragment Length Polymorphism (RFLP)

Each PCR product in a dose of 10 µL was digested using 5 U of HinfI (BIORON GmbH, Ludwigshafen, Germany) and PscI (PciI) (Thermo Scientific, Waltham, USA) restriction enzyme per 20 µL of reaction mixture at 37°C for 3 h. The digestion products were analyzed by 1.5% agarose gel electrophoresis after staining by DNA safe stain, and were then visualized using UVdoc.

Statistical analysis

Statistical analysis was performed using SPSS 16.0 (SPSS Inc., Chicago, USA). The genotype frequencies of both SNPs were estimated by allele counting for all participants, and the Hardy-Weinberg equilibrium (HWE) was assessed using the χ^2 test.[26] The linkage disequilibrium (LD) and haplotyping were analyzed using CubeX online software (www.oege.org/software/cubex) (Gaunt et al.; licensee BioMed Central Ltd., London, UK).[27] Values of $p \leq 0.05$ were considered statistically significant.

Differences in the frequency of genotypes between the osteoporotic patients and the gender-matched normal controls were tested using χ^2 tests. The correlation of the genotypes and lumbar spine or femoral neck BMD adjusted for age and gender was analyzed using a one-way analysis of variance (ANOVA) followed by Tukey's test.

In the next step, differences in serum Se level between the patients and the controls were tested using an independent sample t-test. In addition, the correlation between Se level and lumbar spine or femoral neck BMD was evaluated using Pearson's bivariate correlation.

Results

Clinical characteristics

A total of 90 individuals with osteoporosis (45 males and 45 females) were recruited as the study group and 90 aged-

Table 1. The general characteristics of participants

Participants	Normal controls			Osteoporotic patients		
Gender	male	female	total	male	female	total
Number of patients	45	45	90	45	45	90
Age [years]	68.11 ±6.36#	64.93 ±4.69	66.52 ±5.78	69.73 ±6.83#	66.04 ±4.88	67.89 ±6.19
Height [cm]	164.93 ±5.30*	154.04 ±5.82*	159.49 ±7.78*	158.52 ±7.08	150.41 ±6.07	154.47 ±7.72
Weight [kg]	77.58 ±10.88*	76.30 ±9.89*	76.94 ±10.36*	58.41 ±10.58	63.56 ±11.84	60.98 ±11.46
BMI [kg/m^2]	28.50 ±3.62*	32.18 ±3.96*	30.34 ±4.20*	23.20 ±3.71	28.02 ±4.60	25.61 ±4.81
Lumbar spine BMD [g/cm^2]	1.12 ±0.12#*	1.04 ±0.09*	1.08 ±0.11*	0.70 ±0.13	0.67 ±0.12	0.69 ±0.12
Femoral neck BMD [g/cm^2]	1.05 ±0.11#*	0.98 ±0.07*	1.02 ±0.10*	0.69 ±0.11	0.73 ±0.12	0.71 ±0.12
Serum Se [µg/L]	87.15 ±26.08#*	73.68 ±23.19*	81.09 ±25.58*	62.14 ±28.66#	54.91 ±23.55	57.58 ±25.54

Data is presented as mean ± standard deviation (SD); BMI – body mass index; BMD – bone mineral density; * statistical significance between normal controls and osteoporotic patients; # statistical significance between males and females of each group.

-matched normal participants (45 males and 45 females) were selected to be the control group. Table 1 represents the demographic and morphometric characteristics and the BMD values of all participants.

Allelic frequencies and haplotype structure

Two SNPs (rs9897850 and rs2292350) in the *ALOX12* gene were genotyped using the polymerase chain reaction – restriction fragment length polymorphism (PCR–RFLP). Neither SNP was found to be in HWE due to high p-values of the χ^2 test. The genotype characteristics of the participants are outlined in Table 2. The 2 SNPs analyzed in *ALOX12* – rs9897850 and rs2292350 – are located in the promoter region and in the intron 2 region of chromosome 17p13, respectively. The LD was calculated for the *ALOX12* gene polymorphisms (rs9897850 and rs2292350) for the whole population (D' = 0.305; r^2 = 0.0628). There was no significant correlation between any of the 4 possible haplotypes and the risk of disease.

Association between single nucleotide polymorphisms and bone mineral density variations

The effect of each SNP genotype on the lumbar spine and femoral neck BMD parameters was examined using ANOVA. For rs9897850, there was no significant difference in either lumbar spine or femoral neck BMD, but a marginal trend was observed involving rs2292350.

The rs2292350 SNP showed the most significant association for femoral neck BMD (p = 0.04), as individuals homozygous for the G allele at rs2292350 had 0.17 ±0.7 g/cm^2 higher mean femoral neck BMD than those homozygous for the A allele (p = 0.037) (Table 3).

Serum selenium concentration

A significant difference was found between the osteoporotic patients (57.58 ±25.54 µg/L) and the controls (81.09 ±25.58 µg/L) in terms of serum Se levels (p < 0.001). However, the mean Se concentration in male subjects happened to be significantly higher compared to females (p = 0.002). Individuals with higher Se levels also had higher BMD of the lumbar spine (r^2 = 0.392; p < 0.001) and the femoral neck (r^2 = 0.478; p < 0.001), but no association was found for genotype frequency of either SNP.

Discussion

Previous studies have shown a linkage between hip, spine and wrist BMD and the 17p13 chromosomal region where the *ALOX12* gene has been mapped to.[8,9] 12-hydroperoxyeicosatetraenoic acid, i.e., the product of *ALOX12* activity, serves as an endogenous ligand for PPARs, which inhibits osteoblastogenesis.[11,12] Therefore, *ALOX12* has been considered a candidate gene for the development of osteoporosis and several SNPs in the human *ALOX12* gene have been suggested as being associated with BMD in humans.[1,4,5,7,15]

In the present study, 2 polymorphisms (rs9897850 and rs2292350) of *ALOX12* were investigated for a probable association with BMD in the elderly population of Amirkola, Iran. None of the mentioned polymorphisms were found to be in HWE. Deviations from HWE may have happened as a result of a new mutation, inbreeding, selective mating, or a genotyping error.[28,29]

The rs2292350 polymorphism was significantly associated with reduced femoral neck BMD in both genders.

Table 2. The genotype properties of *ALOX12* gene SNPs

Variable	Common Hz n (% within the group)	Het n (% within the group)	Rare Hz n (% within the group)	Overall p-value for χ^2 test	OR rare Hz vs common Hz (CI), p-value
rs9897850	C/C	C/T	T/T	0.784	0.85 (0.33–2.15), 0.728
normal controls	24 (26.7)	50 (55.6)	16 (17.8)		
osteoporotic patients	23 (25.6)	54 (60)	13 (14.4)		
rs2292350	G/G	G/A	A/A	0.054	9.15 (1.06–79.11), 0.044
normal controls	34 (37.8)	55 (61.1)	1 (1.1)		
osteoporotic patients	26 (28.9)	57 (63.3)	7 (7.8)		

SNPs – single nucleotide polymorphisms; Hz – homozygote; Het – heterozygote; N – number of patients; OR – odds ratio; CI – confidence interval.

Table 3. The association of *ALOX12* genotypes with BMD

BMD [g/cm^2]	Genotype							
	rs9897850				rs2292350			
	CC	CT	TT	p-value	GG	GA	AA	p-value
Lumbar spine	0.88 ±0.23	0.88 ±0.23	0.91 ±0.23	0.84	0.90 ±0.23	0.88 ±0.23	0.74 ±0.18	0.19
Femoral neck	0.87 ±0.19	0.85 ±0.18	0.9 ±0.22	0.44	0.90 ±0.18	0.86 ±0.19	0.72 ±0.13	0.04

Data is presented as mean ± standard deviation (SD); BMD – bone mineral density.

Our results showed that individuals homozygous for the A allele of this polymorphism had the lowest BMD values.

Similarly to our findings, it was found by Mullin et al. that rs2292350 was significantly associated with spine and various hip BMD parameters in postmenopausal women; however, they report that homozygotes for the A allele of rs2292350 had significantly higher spine BMD compared with the heterozygous group, as opposed to our results.[7]

Harsløf et al. reported that heterozygous individuals for both polymorphisms (rs9897850 and rs2292350) had lower lumbar spine BMD and an increased risk of vertebral fractures compared with homozygous individuals for either allele.[4] In addition, Xiao reported the rs2292350 polymorphism to be significantly associated with BMD in the lumbar spine, the femoral neck and the total hip in Chinese families.[5]

In another study, Ichikawa et al. investigated the relationship between 12 SNPs in *ALOX12* and BMD variations in the hip and the spine in a healthy American population. They observed that up to 3% of the spine BMD variation in men and 0.8% of that in women is due to genetic variations in *ALOX12*. Both rs9897850 and rs2292350 were associated with lumbar spine BMD in both genders, but the most significant association was found with rs9897850 in men.[1]

Neither SNP in our study was in a haplotype block due to a weak LD with each other. Therefore, we did not observe any association of the abovementioned SNPs with lumbar spine or femoral neck BMD in the haplotype analysis, but Ichikawa et al. reported that a common haplotype containing both rs9897850 and rs2292350 was associated with high lumbar spine BMD in women and low lumbar spine BMD in men.[1]

The inhibition of osteoblastic differentiation of bone MSCs due to oxidative stress is a major contributor to the development of osteoporosis.[19,30–33] Basu et al. found that the levels of 8-iso-PGF2a (a major F2-isoprostane) as a biomarker of oxidative stress negatively correlated with BMD. They concluded that an increase in oxidative stress was related to a reduction in BMD values.[34]

Experimental evidence suggests that Se might decrease the risk of osteoporosis via incorporating into selenoproteins, such as GPx, and can act as an antioxidant against oxidative damage.[23,35] Chen et al. in their study on human epidermoid carcinoma cells observed that GPx and PHGPx activity decreased with a lowering of the glutathione (GSH) content.[36] In another study, this team observed that an overexpression of the Se-dependent PHGPx enzyme could reduce *ALOX12* activity, and in this manner it was possible to decrease the risk of developing osteoporosis.[37,38] Besides, Liu et al. showed that selenite (Na_2SeO_3), as a selenium supplement, could increase the activity and gene expression of GPx. This Se supplementation is able to reverse the reduced antioxidant capacity and GSH, in addition to its ability to suppress the ROS production in H_2O_2-treated MSCs.[18]

Odabasi et al. measured the Se concentration in plasma and red blood cells in postmenopausal women with osteoporosis in comparison with BMI-matched healthy postmenopausal women. They did not observe any significant difference between the 2 groups.[39] In another study, Arikan et al. investigated serum Se levels in postmenopausal women with osteoporosis or osteopenia and healthy controls, and did not find any correlation between Se and lumbar spine BMD.[40] In contrast, in this study we observed higher serum Se levels in the controls than in the osteoporotic patients ($p < 0.001$), and individuals that had higher Se levels had higher BMD in the femoral neck and the lumbar spine.

Conclusions

The effect of 2 SNPs in *ALOX12* on the BMD of both the lumbar spine and the femoral neck was investigated in the present study. Our findings suggest the significance of *ALOX12* in both BMD variations and in the development of osteoporosis. In addition, the antioxidant effect of PHGPX, which is due to Se as an essential trace element acting as a cofactor, may be able to reduce *ALOX12* activity. The results of this study can open the door to a better understanding of the mechanism of Se action in osteoporosis. Surely, further investigation into this area would be needed in order to improve our knowledge of osteoporosis development.

References

1. Ichikawa S, Koller DL, Johnson ML, et al. Human *ALOX12*, but not *ALOX15*, is associated with BMD in white men and women. *J Bone Miner Res*. 2006;21:556–564.
2. Cooper C, Campion G, Melton III LJ. Hip fractures in the elderly: A worldwide projection. *Osteoporos Int*. 1992;2:285–289.
3. Rahnavard Z, Zolfaghari M, Hossein-Nezad A, Vahid Dastgerdi M. The incidence of osteoporotic Hip fracture: Iranian Multicenter Osteoporosis Study (IMOS). *Res J Biol Sci*. 2009;4:171–173.
4. Harsløf T, Husted LB, Nyegaard M, et al. Polymorphisms in the *ALOX12* gene and osteoporosis. *Osteoporos Int*. 2011;22:2249–2259.
5. Xiao WJ, Ke YH, He JW, et al. Polymorphisms in the human *ALOX12* and *ALOX15* genes are associated with peak bone mineral density in Chinese nuclear families. *Osteoporos Int*. 2012;23:1889–1897.
6. Brown LB, Streeten EA, Shapiro JR, et al. Genetic and environmental influences on bone mineral density in pre-and post-menopausal women. *Osteoporos Int*. 2005;16:1849–1856.
7. Mullin B, Spector T, Curtis C, et al. Polymorphisms in *ALOX12*, but not *ALOX15*, are significantly associated with BMD in postmenopausal women. *Calcif Tissue Int*. 2007;81:10–17.
8. Devoto M, Shimoya K, Caminis J, et al. First-stage autosomal genome screen in extended pedigrees suggests genes predisposing to low bone mineral density on chromosomes 1p, 2p and 4q. *Eur J Hum Genet*. 1998;6:151–157.
9. Deng HW, Xu FH, Huang QY, et al. A whole-genome linkage scan suggests several genomic regions potentially containing quantitative trait loci for osteoporosis. *J Clin Endocrinol Metab*. 2002;87:5151–5159.
10. Gimble JM, Zvonic S, Floyd ZE, Kassem M, Nuttall ME. Playing with bone and fat. *J Cell Biochem*. 2006;98:251–266.
11. Lecka-Czernik B, Moerman EJ, Grant DF, Lehmann JM, Manolagas SC, Jilka RL. Divergent effects of selective peroxisome proliferator-activated receptor-γ 2 ligands on adipocyte versus osteoblast differentiation. *Endocrinology*. 2002;143:2376–2384.
12. Khan E, Abu-Amer Y. Activation of peroxisome proliferator–activated receptor-γ inhibits differentiation of preosteoblasts. *J Lab Clin Med*. 2003;142:29–34.

13. Akune T, Ohba S, Kamekura S, et al. PPAR-γ insufficiency enhances osteogenesis through osteoblast formation from bone marrow progenitors. *J Clin Invest*. 2004;113:846.
14. Kawaguchi H, Akune T, Yamaguchi M, et al. Distinct effects of PPAR-γ insufficiency on bone marrow cells, osteoblasts, and osteoclastic cells. *J Bone Miner Metab*. 2005;23:275–279.
15. Xiong DH, Shen H, Zhao LJ, et al. Robust and comprehensive analysis of 20 osteoporosis candidate genes by very high-density single-nucleotide polymorphism screen among 405 white nuclear families identified significant association and gene–gene interaction. *J Bone Miner Res*. 2006;21:1678–1695.
16. Ebert R, Jakob F. Selenium deficiency as a putative risk factor for osteoporosis. *Int Congr Ser*. 2007;1297:158–164.
17. Müller C, Wingler K, Brigelius-Flohe R. 3'UTRs of glutathione peroxidases differentially affect selenium-dependent mRNA stability and selenocysteine incorporation efficiency. *Biol Chem*. 2003;384:11–18.
18. Liu H, Bian W, Liu S, Huang K. Selenium protects bone marrow stromal cells against hydrogen peroxide-induced inhibition of osteoblastic differentiation by suppressing oxidative stress and ERK signaling pathway. *Biol Trace Elem Res*. 2012;150:441–450.
19. Manolagas SC. From estrogen-centric to aging and oxidative stress: A revised perspective of the pathogenesis of osteoporosis. *Endocr Rev*. 2010;31:266–300.
20. Mackinnon E, Rao A, Josse R, Rao L. Supplementation with the antioxidant lycopene significantly decreases oxidative stress parameters and the bone resorption marker N-telopeptide of type I collagen in postmenopausal women. *Osteoporos Int*. 2011;22:1091–1101.
21. Ruiz-Ramos M, Vargas LA, Van der Goes TF, Cervantes-Sandoval A, Mendoza-Nunez V. Supplementation of ascorbic acid and alpha--tocopherol is useful to preventing bone loss linked to oxidative stress in elderly. *J Nutr*. 2010;14:467–472.
22. Zhang J, Munger RG, West NA, Cutler DR, Wengreen HJ, Corcoran CD. Antioxidant intake and risk of osteoporotic hip fracture in Utah: An effect modified by smoking status. *Am J Epidemiol*. 2006;163:9–17.
23. Moreno-Reyes R, Egrise D, Neve J, Pasteels JL, Schoutens A. Selenium deficiency-induced growth retardation is associated with an impaired bone metabolism and osteopenia. *J Bone Miner Res*. 2001;16:1556–1563.
24. Hosseini SR, Cumming RG, Kheirkhah F, et al. Cohort profile: The Amirkola Health and Ageing Project (AHAP). *Int J Epidemiol*. 2014;43:1393–1400.
25. WHO. Assessment of fracture risk and its application to screening for postmenopausal osteoporosis. Report of a WHO study group. *World Health Organ Tech Rep Ser*. 1994;843:1–129.
26. Rodriguez S, Gaunt TR, Day IN. Hardy-Weinberg equilibrium testing of biological ascertainment for Mendelian randomization studies. *Am J Epidemiol*. 2009;169:505–514.
27. Gaunt TR, Rodríguez S, Day IN. Cubic exact solutions for the estimation of pairwise haplotype frequencies: Implications for linkage disequilibrium analyses and a web tool 'CubeX'. *BMC Bioinformatics*. 2007;8:428.
28. Khoury MJ, Beaty TH, Cohen BH. *Fundamentals of Genetic Epidemiology*. New York, NY: Oxford University Press; 1993.
29. Hosking L, Lumsden S, Lewis K, et al. Detection of genotyping errors by Hardy-Weinberg equilibrium testing. *Eur J Hum Genet*. 2004;12: 395–399.
30. Bai XC, Lu D, Bai J, et al. Oxidative stress inhibits osteoblastic differentiation of bone cells by ERK and NF-κB. *Biochem Biophys Res Commun*. 2004;314:197–207.
31. Mody N, Parhami F, Sarafian TA, Demer LL. Oxidative stress modulates osteoblastic differentiation of vascular and bone cells. *Free Radic Biol Med*. 2001;31:509–519.
32. Almeida M, Ambrogini E, Han L, Manolagas SC, Jilka RL. Increased lipid oxidation causes oxidative stress, increased peroxisome proliferator-activated receptor-γ expression, and diminished pro-osteogenic Wnt signaling in the skeleton. *J Biol Chem*. 2009;284:27438–27448.
33. Kim WK, Meliton V, Bourquard N, Hahn TJ, Parhami F. Hedgehog signaling and osteogenic differentiation in multipotent bone marrow stromal cells are inhibited by oxidative stress. *J Cell Biochem*. 2010;111:1199–1209.
34. Basu S, Michaëlsson K, Olofsson H, Johansson S, Melhus H. Association between oxidative stress and bone mineral density. *Biochem Biophys Res Commun*. 2001;288:275–279.
35. Zeng H, Cao JJ, Combs GF. Selenium in bone health: Roles in antioxidant protection and cell proliferation. *Nutrients*. 2013;5:97–110.
36. Chen CJ, Huang HS, Lin SB, Chang WC. Regulation of cyclooxygenase and 12-lipoxygenase catalysis by phospholipid hydroperoxide glutathione peroxidase in A431 cells. *Prostaglandins Leukot Essent Fatty Acids*. 2000;62:261–268.
37. Chen CJ, Huang HS, Chang WC. Inhibition of arachidonate metabolism in human epidermoid carcinoma a431 cells overexpressing phospholipid hydroperoxide glutathione peroxidase. *J Biomed Sci*. 2002;9:453–459.
38. Chen CJ, Huang HS, Chang WC. Depletion of phospholipid hydroperoxide glutathione peroxidase up-regulates arachidonate metabolism by 12 (S)-lipoxygenase and cyclooxygenase 1 in human epidermoid carcinoma A431 cells. *FASEB*. 2003;17:1694–1696.
39. Odabasi E, Turan M, Aydin A, Akay C, Kutlu M. Magnesium, zinc, copper, manganese, and selenium levels in postmenopausal women with osteoporosis. Can magnesium play a key role in osteoporosis? *Ann Acad Med Singapore*. 2008;37:564–567.
40. Arikan DC, Coskun A, Ozer A, Kilinc M, Atalay F, Arikan T. Plasma selenium, zinc, copper and lipid levels in postmenopausal Turkish women and their relation with osteoporosis. *Biol Trace Elem Res*. 2011; 144:407–417.

Clinical applicability of monitoring pulmonary artery blood flow acceleration time variations in monitoring fetal pulmonary artery pressure

Hong-Yan Zhan[1,B–F], Feng-Qin Xu[1,B,C,E,F], Chuan-Xi Liu[2,B,C,F], Gang Zhao[3,A,D–F]

[1] Department of B-Ultrasound, Fourth People's Hospital of Jinan, China
[2] Department of B-Ultrasound, Shandong Provincial Hospital Affiliated to Shandong University, Jinan, China
[3] Department of Emergency Surgery, Shandong Province Qianfoshan Hospital, Shandong University, Jinan, China

A – research concept and design; B – collection and/or assembly of data; C – data analysis and interpretation; D – writing the article; E – critical revision of the article; F – final approval of the article

Advances in Clinical and Experimental Medicine, ISSN 1899-5276 (print), ISSN 2451-2680 (online) *Adv Clin Exp Med.* 2018;27(12):1723–1727

Address for correspondence
Gang Zhao
E-mail: zhaogang198s@sina.cn

Funding sources
Science and Technology Star Program of Jinan Science and Technology Bureau of Shandong Province (grant No. 201406017).

Conflict of interest
None declared

Received on February 7, 2017
Reviewed on April 14, 2017
Accepted on July 5, 2017

Abstract

Background. In recent years, pulmonary artery blood flow acceleration time (AT) has been believed to be applicable in the examination of fetal lung development.

Objectives. This study aims to evaluate the clinical significance of pulmonary artery blood flow AT as a parameter in monitoring of fetal pulmonary artery pressure.

Material and methods. A total of 31 fetuses in mid- or late-term pregnancy with tricuspid regurgitation were set as the study group (congenital heart disease with a tricuspid regurgitation pressure difference of more than 20 mm Hg was excluded). A total of 68 normal fetuses in mid- or late-term pregnancy were selected as the control group (strictly screened for tricuspid regurgitation, congenital heart disease and other congenital diseases before inclusion). The average ATs of both groups were calculated. Correlations of pulmonary artery systolic pressure (PASP) and AT, as well as the ratio of AT to right ventricular ejection time (ET) (AT/ET ratio) of both groups were investigated by 1-way analysis of variance (ANOVA).

Results. The average AT of the study group was significantly lower than that of the control group ($p < 0.0001$). In the study group, AT negatively correlated with PASP ($r = -0.52$; $p < 0.01$), AT/ET ratio negatively correlated with PASP ($r = -0.52$; $p < 0.01$) and both showed statistical significance.

Conclusions. The results indicated that fetuses in the study group showed lower ATs and AT/ET ratios than the control group. Acceleration times and AT/ET ratios decreased as PASP increased. Thus, AT and AT/ET ratio can be used clinically as new parameters for the qualitative and – to some extent – quantitative evaluation of fetal pulmonary artery pressure.

Key words: pulmonary artery systolic pressure, fetal ultrasonic cardiogram, pulmonary artery blood flow acceleration time

DOI
10.17219/acem/75686

Introduction

In recent years, Schenone et al. have introduced the determination of pulmonary artery blood flow acceleration time (AT) into the research on the development of fetal pulmonary tissues for the first time.[1] Acceleration time is believed to be applicable to the examination of fetal lung development. Kim et al. have managed to examine neonatal respiratory distress syndrome.[2] Previous studies have reported an association of AT and AT/ejection time (ET) ratio with the Doppler flow curve of the fetal pulmonary artery.[3–5] Till now, no report has been published on the association between AT and pulmonary artery pressure. The present study is an investigation on using AT and AT/ET ratio as new parameters for monitoring fetal pulmonary artery pressure, based on the study of the AT of fetuses in mid- or late-term pregnancy with simple high pulmonary pressure.

Material and methods

Patients

Information and ultrasonic cardiograms from the regular fetal ultrasonic cardiogram examinations of over 26,000 pregnant women, carried out between June 2011 and December 2013, were collected from the Ultrasonography Department of Provincial Hospital, the Maternal and Child Health Center of Jinan, the Ultrasonography Department of the Fourth People's Hospital of Jinan, and Maternity and Child Healthcare Hospital of Shizhong District, Jining (China) (Table 1).

Trial grouping

Study group consisted of 31 subjects and included 8 mid-term pregnant women aged 28 ±4 years (gestational age: 26 ±1 weeks) and 23 late-term pregnant women aged 28 ±4 years (gestational age: 33 ±5 weeks). The inclusion criteria were: 1. enlarged right atrium or ventricle; 2. medium or severe tricuspid regurgitation; 3. tricuspid regurgitation pressure difference <20 mm Hg; and 4. no tricuspid regurgitation induced by vascular deformity in congenital heart disease.

The control group consisted of 68 subjects, including 33 mid-term pregnant women aged 27 ±5 years (gestational age: 26 ±1 weeks) and 35 late-term pregnant women aged 29 ±6 years (gestational age: 33 ±5 weeks). None of the pregnant women habitually used tobacco or alcohol, and none of them had a history of chronic diseases, including pulmonary tuberculosis or rheumatic heart diseases. Their fetuses were normal according to physical examination; fetal deformity screening was strictly conducted to exclude heart deformity. The inclusion criteria were: 1. normal cardiac cavity sizes; 2. no tricuspid regurgitation; and 3. no vascular malformation caused by congenital heart diseases.

Methods of ultrasonographic examination

"Fetal heart" mode was selected. The standard sections of fetal ultrasonic cardiograms recommended by the American Society of Echocardiography were employed, and a regular fetal examination was conducted by a cranial side-deviated 4-chamber view.[6] The pregnant women assumed a supine or lateral position. At first, the position of the fetal heart was detected, then the angles of examination and other parameters (depth, gain, focus, etc.) were optimized based on the conditions of the mother and the baby in order to obtain a standard and clear long-axis view of the pulmonary artery.[7] The pulsed-waved Doppler (PW) sampling spot was set at 3 mm over the pulmonary valve. A recording rate of 100 cm/s was selected for better accuracy and blood spectrum performance. Acceleration time (Fig. 1A) and ET were recorded, and AT/ET ratio was calculated. Acceleration time is the time interval from the start of blood flow spectrum of the right ventricle contraction phase to the time-point of max contraction velocity. Ejection time is the time interval from the start of right ventricular contraction to the end of right ventricular contraction. In a standard 4-chamber view, the max velocity of tricuspid regurgitation and the pressure difference were determined by continuous-wave Doppler (CW) (Fig. 1B). All data was presented as the average value of 3 measurements. The angle between the directions of blood flow and the acoustic beam was kept within 20° to assure the accuracy of blood flow velocity and the pressure difference.

Calculation of pulmonary artery systolic pressure

Pulmonary artery systolic pressure (PASP) is the right ventricular pressure (Fig. 1A) + the tricuspid regurgitation

Table 1. Subjects' characteristics

Group	Pregnancy type	n	Average age [years]	Range of gestational age [weeks]	Average gestational age [weeks]
Study group	Mid-term pregnancy	8	28 ±4	24–27	26 ±1
	Late-term pregnancy	23	28 ±4	28–39	33 ±5
Control group	Mid-term pregnancy	33	27 ±5	26–27	26 ±1
	Late-term pregnancy	35	29 ±6	28–38	33 ±5

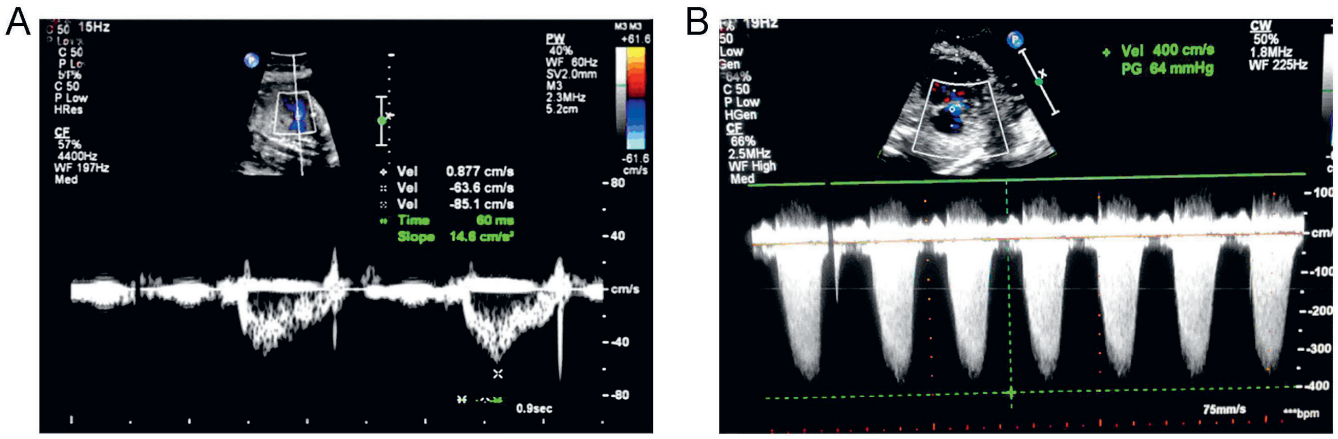

Fig. 1. Blood flow spectrum and tricuspid regurgitation

A – blood flow spectrum of the fetus (AT was from the start to the peak); B – determination of the max velocity of tricuspid regurgitation and the pressure difference; AT – acceleration time

pressure difference (Fig. 1B). The right ventricular pressure of the fetuses was calculated based on the right ventricular pressure of an adult (5 mm Hg in mild tricuspid regurgitation, 10 mm Hg in moderate tricuspid regurgitation and 15 mm Hg in severe tricuspid regurgitation) and was set as follows: 3 mm Hg in mild tricuspid regurgitation, 6 mm Hg in moderate tricuspid regurgitation and 11 mm Hg in severe tricuspid regurgitation. Further, the tricuspid regurgitation pressure difference was considered to be 2 mm Hg in mild tricuspid regurgitation, 3 mm Hg in moderate tricuspid regurgitation and 5 mm Hg in severe tricuspid regurgitation.

The severity of tricuspid regurgitation was graded as follows: none (grade 0), no regurgitant jet; mild (grade 1+), a jet area <20% in the right atrial area; moderate (grade 2+), a jet area of 20–33% in the right atrial area; and severe (grade 3+), a jet area >33% in the right atrial area.

Statistical analysis

SPSS v. 17.0 (SPSS Inc., Chicago, USA) was employed in the statistical analysis; all values were presented as mean ± standard deviation (SD). Student's t-test was used in intergroup comparison. Multiple factors of the observation group were analyzed with bivariate correlation. Pearson's correlation coefficient was verified by t-statistics. A p-value <0.05 was considered statistically significant.

Results

The average AT of the study group was 47.6 ±5.0 ms, whereas the average AT of the control group was 54.3 ±9.8 ms, and the difference was very significant ($p < 0.0001$). The average AT/ET ratio of the study group was 0.24 ±0.02, the average AT/ET ratio of the control group was 0.27 ±0.04 and the difference was statistically significant ($p < 0.01$) (Table 2).

The results indicated that AT negatively correlated with PASP ($r = -0.52$; $p < 0.01$) (Fig. 2); AT/ET ratio negatively correlated with PASP ($r = -0.52$; $p < 0.01$) (Fig. 3).

The results indicated that the AT values of the fetuses with increased pulmonary artery pressure were significantly lower than those of normal fetuses. Meanwhile, AT decreased as pulmonary artery pressure increased.

Discussion

In 1987, the negative relationship between pulmonary artery pressure and pulmonary artery blood flow AT was discovered in the correlative analysis on the pulmonary artery blood flow AT of adults and the average pulmonary artery pressure determined by cardiac catheter, conducted by Dabestani et al., where an increase in pulmonary artery pressure resulted in shortened pulmonary artery blood flow AT.[6] Average pulmonary artery pressure was 0.79 – (0.45 × AT) mm Hg, based on the reported data.[7] As reported by Chaoui et al., pulmonary hypertension in adults can lead to increased pulmonary vascular resistance, showing an abnormal blood flow spectrum similar to the aorta; in their study, AT was shortened and the peak appeared earlier, and the extent of increase correlated to the severity of pulmonary hypertension.[8] Kitabatake et al. revealed that when average pulmonary artery pressure was <20 mm Hg in an adult, AT was 137 ±24 ms, and when average pulmonary artery

Table 2. Comparison of ATs and AT/ET ratios of the study group and the control group of mid- and late-term pregnancy fetuses

Index	Study group	Control group	p-value
Pulmonary artery blood flow AT [ms]	47.6 ±5.0	54.3 ±9.8	<0.01
Ratio of AT and right ventricular blood ET (AT/ET)	0.24 ±0.02	0.27 ±0.04	<0.01

AT – acceleration time; ET – ejection time.

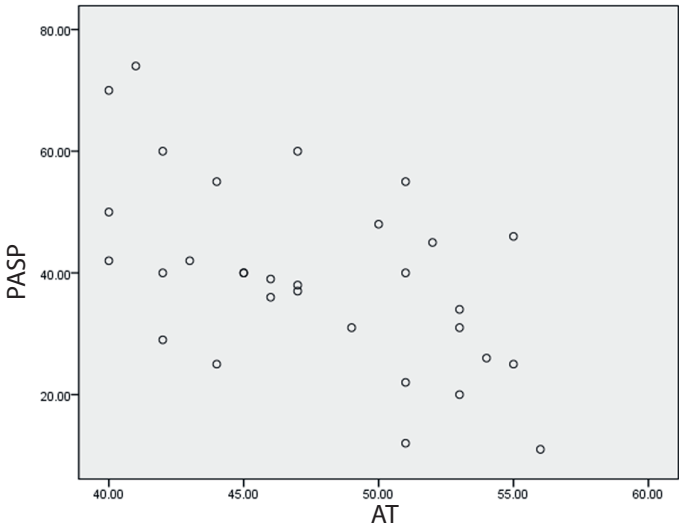

Fig. 2. A negative correlation was shown in the correlation analysis of AT and PASP (r = –0.52; p < 0.01)

AT – acceleration time; PASP – pulmonary artery systolic pressure.

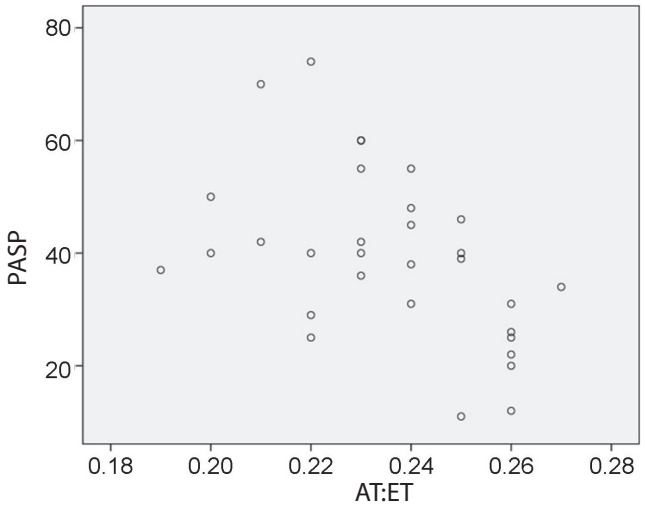

Fig. 3. A negative correlation was shown in the correlation analysis of AT/ET ratio and PASP (r = –0.52; p < 0.01)

AT – acceleration time; ET – ejection time; PASP – pulmonary artery systolic pressure.

pressure was >20 mm Hg, AT was 97 ±20 ms.[9] Nevertheless, the accuracy of pulmonary artery pressure determination can be affected by the operator's expertise, the selection of sections, and the angle between the sonic beam and blood flow. Granstam et al. have elucidated the clinical significance of the determination of blood AT in the systolic phase at the pulmonary valve in the classification of pulmonary hypertension.[10] Acceleration times of 70–90 ms, 50–70 ms and <50 ms corresponded to mild, medium and severe pulmonary hypertension, respectively. Kim et al. prognosed neonatal respiratory distress syndrome using pulmonary artery AT and AT/ET ratio as parameters, and their research proved that AT was a prospectively useful index in the prognosis of neonatal respiratory distress syndrome, but no correlative study was included on pulmonary artery pressure.[2] Pavankumar et al. reported the significance of mid- to late-term functional pulmonary hypertension; they revealed that a pressure difference in severe tricuspid regurgitation in fetuses >70 mm Hg indicated that PASP of the fetus can be >70 mm Hg, in which case right ventricular failure may occur, leaving the fetus with a potentially fatal outcome if elective premature delivery is not conducted.[11] All the abovementioned reports have shown that studies on pulmonary artery pressure from different points of view are drawing more and more attention in clinical practice.

As discovered through years of clinical practice, tricuspid regurgitation is very common among fetuses in mid- or late-term pregnancy; mostly this is physiological regurgitation, and the incidence is approx. 6.0%.[12,13] Pathological or high-speed regurgitation accounts for about 0.12%. The possible explanations for this condition are likely to be the increased resistance along with the growth of the fetus and the compressed vascular cavity, strengthened by the contractility of the artery or resistance in pulmonary arteries. Increased pulmonary artery pressure can lead to increased systolic pressure of the right ventricle, and eventually to tricuspid regurgitation. The higher pulmonary artery pressure, the greater regurgitation volume. Severe pulmonary hypertension and tricuspid regurgitation can result in right ventricular failure manifested by an increased ventricular rate, a significantly enlarged right heart, or signs such as pericardium, peritoneal or pleural effusion. Therefore, it is critical to monitor the pulmonary artery pressure in the etiological analysis of right heart enlargement and tricuspid regurgitation in fetuses. In the fetal period, the only determination method for pulmonary artery pressure is non-invasive Doppler ultrasonography.[14] Currently, the commonly used method is to calculate the right ventricular systolic pressure by adding the right ventricular pressure to the measured value of tricuspid regurgitation pressure difference; the right ventricular systolic pressure is equal to PASP when no pulmonary stenosis is present. By the same method, pulmonary artery diastolic pressure (PADP) can be calculated from the pulmonary valve regurgitation.

However, in some cases, tricuspid or pulmonary valve regurgitation was too mild to be detected, or difficult to detect due to the position of the fetus.[15] Determination of the ratio of pulmonary artery blood flow AT and ET is a novel approach for monitoring pulmonary artery pressure. The results of this study indicated that AT was negatively correlated with PASP, and that increased PASP could lead to a decrease in AT. Thus, AT can be used as a more accessible parameter in measuring pulmonary artery pressure. Especially when pulmonary artery pressure increases, and no tricuspid or pulmonary valve regurgitation is detected, AT and AT/ET ratio are more convincing in signifying pulmonary artery pressure.

Acceleration time and AT/ET ratio are semi-quantitative parameters in pulmonary artery pressure determination

that can be used in the approximate evaluation of pulmonary hypertension; whether "average pulmonary artery pressure = 0.79 – (0.45 × AT) mm Hg" – a rule for calculating adult pulmonary pressure – is applicable in the quantitative determination of fetal pulmonary artery pressure, still needs more clinical evidence and more specific research.[16]

Although this study produced some interesting findings, there were also a few limitations. Firstly, the foramina ovale (FO), which has a significant influence on the diameters of right ventricle and right atrium, will finally result in changes in PASP. Therefore, the FO is important for evaluating cardiac function, which should be investigated in further studies. Secondly, the numbers of patients involved in the study group and the control group were relatively small, though over 26,000 pregnant women were examined through regular ultrasound in this study. In future studies, we would involve a larger number of patients.

In conclusion, for fetuses of mid- or late-term pregnancy, AT and AT/ET ratio are closely related to PASP, especially for those showing no signs of tricuspid regurgitation; thus, AT and AT/ET ratio can be used as qualitative and semi-quantitative parameters in the determination of fetal pulmonary artery pressure, based on which a new method for pulmonary artery pressure determination has been proposed for clinical diagnosis.

References

1. Schenone MH, Samson JE, Jenkins L, Suhag A, Mari G. Predicting fetal lung maturity using the fetal pulmonary artery Doppler wave acceleration/ejection time ratio. *Fetal Diagn Ther*. 2014;36(3):208–214. doi: 10.1159/000358299
2. Kim SM, Park JS, Norwitz ER, et al. Acceleration time-to-ejection time ratio in fetal pulmonary artery predicts the development of neonatal respiratory distress syndrome: A prospective cohort study. *Am J Perinatol*. 2013;30(10):805–812. doi: 10.1055/s-0032-1333132
3. Guan Y, Li S, Luo G, et al. The role of Doppler waveforms in the fetal main pulmonary artery in the prediction of neonatal respiratory distress syndrome. *J Clin Ultrasound*. 2015;43(6):375–383. doi: 10.1002/jcu.22219
4. Rychik J, Ayres N, Cuneo B, et al. American Society of Echocardiography guidelines and standards for performance of the fetal echocardiogram. *J Am Soc Echocardiogr*. 2004;17(7):803–810.
5. Lindeley W, Hale R, Spear A, et al. Does corticosteroid impact fetal pulmonary artery blood flow in women at risk for preterm birth? *Med Ultrason*. 2015;17(3):280–283. doi: 10.11152/mu.2013.2066.173.wly
6. Dabestani A, Mahan G, Gardin JM, et al. Evaluation of pulmonary artery pressure and resistance by pulsed Doppler echocardiography. *Am J Cardiol*. 1987;59(6):662–668.
7. Chuanxi L, Chuiping L. *Screening and Diagnosis of Fetal Heart Malformation by Color Doppler Ultrasound*. Beijing, China: Scientific and Technical Documents Publishing House; 2003.
8. Chaoui R, Taddei F, Rizzo G, Bast C, Lenz F, Bollmann R. Doppler echocardiography of the main stem of the pulmonary arteries in the normal human fetus. *Ultrasound Obstet Gynecol*. 1998;11(3):173–179.
9. Kitabatake A, Inoue M, Asao M, et al. Noninvasive evaluation of pulmonary hypertension by a pulsed Doppler technique. *Circulation*. 1983;68(2):302–309.
10. Granstam SD, Björklund E, Wikström G, Roos MW. Use of echocardiographic pulmonary acceleration time and estimated vascular resistance for the evaluation of possible pulmonary hypertension. *Cardiovasc Ultrasound*. 2013;11(1):7. doi: 10.1186/1476-7120-11-7
11. Pavankumar P, Venugopal P, Kaul U, et al. Closed mitral valvotomy during pregnancy: A 20-year experience. *Scand J Thorac Cardiovasc Surg*. 1988;22(1):11–15.
12. Pawelec M, Dżugalik M, Pietras J, Bełza Ł, Latkowski Ł. Medical and ethical considerations related to viable fetuses with trisomy 13 in the 36th week of pregnancy: A review of the literature. *Adv Clin Exp Med*. 2015;24(5): 911–921. doi: 10.17219/acem/26324
13. DiBardino DJ, Jacobs JP. Current readings: Long-term management of patients undergoing successful pediatric cardiac surgery. *Semin Thorac Cardiovasc Surg*. 2014;26(2):132–144. doi: 10.1053/j.semtcvs.2014.08.002
14. Barczykowska E, Szwed-Kolińska M, Wróbel-Bania A, Ślusarz R. The use of central venous lines in the treatment of chronically ill children. *Adv Clin Exp Med*. 2014;23(6):1001–1009. doi: 10.17219/acem/37359
15. Chiappa E, Micheletti A, Sciarrone A, Botta G, Abbruzzese P. The prenatal diagnosis of and short-term outcome for patients with congenitally corrected transposition. *Cardiol Young*. 2004;14(3):265–276.
16. Hansel J, Burgstahler C, Medler S, Axmann D, Niess AM, Tetzlaff K. Effect of simulated diving trips on pulmonary artery pressure in healthy men. *Clin Res Cardiol*. 2012;101(12):947–953. doi: 10.1007/s00392-012-0482-9

Application of fractal dimension analysis and photodynamic diagnosis in the case of differentiation between lichen planus and leukoplakia: A preliminary study

Kamil Jurczyszyn[1,A,C,D], Klaudia Kazubowska[1,B], Paweł Kubasiewicz-Ross[1,D], Piotr Ziółkowski[2,E], Marzena Dominiak[1,F]

[1] Department of Oral Surgery, Faculty of Dentistry, Wroclaw Medical University, Poland
[2] Department of Pathology, Faculty of Medicine, Wroclaw Medical University, Poland

A – research concept and design; B – collection and/or assembly of data; C – data analysis and interpretation;
D – writing the article; E – critical revision of the article; F – final approval of the article

Advances in Clinical and Experimental Medicine, ISSN 1899-5276 (print), ISSN 2451-2680 (online) *Adv Clin Exp Med*. 2018;27(12):1729–1736

Address for correspondence
Kamil Jurczyszyn
E-mail: kjurczysz@interia.pl

Funding sources
Grant for young scientists PBMN152

Conflict of interest
None declared

Received on April 19, 2017
Reviewed on October 5, 2017
Accepted on November 27, 2017

Abstract

Background. Photodynamic therapy (PDT) is a noninvasive method for the treatment of premalignant lesions, such as leukoplakia and lichen planus (LP). These lesions are very irregular. In the case of such irregular lesions, fractal dimension analysis (FDA) is very helpful. Photodynamic diagnosis (PDD) enables the visualization of irregular lesion shapes more precisely than a classical white-light examination.

Objectives. In our study, we tried to distinguish oral leukoplakia and LP, using FDA in a classical examination with white light and PDD. Lesions treated using PDT were histopathologically verified.

Material and methods. We enrolled 35 patients in our study. Fractalyse software v. 2.4 (University of Franche-Comté, Besançon, France) was used to count fractal dimensions (FDs). Photodynamic therapy and PDD were mediated with 20% delta-aminolevulinic acid (5-ALA).

Results. Fractal dimensions of leukoplakia foci of the tongue in a white-light examination were significantly lower than in PDD. In the case of LP, a significant difference of FDs was observed between lesions in the cheek and in the alveolar ridge region. Differences in FDs were observed between leukoplakia foci of the alveolar ridge, tongue and palate. A complete response of leukoplakia foci to PDT was observed in 10 out of 34 lesions, partial remission occurred in 20 lesions and a total lack of response was noted in 4 lesions. Generally, LP was completely treated in 7 out of 14 cases, a partial response was observed in 5 lesions and a failure of PDT treatment was noted in 2 cases.

Conclusions. Fractal dimension analysis may be a useful method in the comparison of complicated shapes of such lesions as LP or leukoplakia, but our study did not confirm that this method may be used to distinguish LP and leukoplakia without a histopathological examination. Photodynamic therapy is an effective treatment method in the case of LP and leukoplakia of the oral cavity.

Key words: photodynamic therapy, lichen planus, leukoplakia, fractal dimension analysis, photodynamic diagnosis

DOI
10.17219/acem/80831

Introduction

Photodynamic therapy (PDT) is a noninvasive treatment method for premalignant and malignant lesions. This therapy is commonly used in dermatology for the treatment of solar keratosis, actinic keratosis, Bowen's disease, and basal cell carcinoma.[1–4] Photodynamic therapy is composed of 2 main agents: light and a photosensitizer (PS). It has to be emphasized that the doses of light and PS are too weak to manage the clinical effect separately; only the combination of these 2 agents is responsible for the effect of the treatment. One of the most important features of PS is an affinity for cells with higher metabolism. After penetrating the cell membrane, PS accumulates in the target cells. Delta-aminolevulinic acid (5-ALA) is one of the most commonly used precursors of PS in PDT. After penetrating the cells, 5-ALA passes into the biochemical pathways of heme. Protoporphyrin IX (PPIX) is the effect of these reactions; it is also a proper photosensitizer. Protoporphyrin IX has few peaks in the spectrum of absorption. The first and the highest peak of absorption – at the 405 nm wavelength – is called Sorret's band. It is used during the procedure of photodynamic diagnosis (PDD). The irradiation of PPIX in Sorret's band leads to red fluorescence and phosphorescence inside the cells. This phenomenon is used during PDD. Unmetabolized 5-ALA is unable to fluoresce after 405 nm excitation. It prevents false-positive trials during PDD. Higher wavelengths are used in the case of PDT, because skin and mucous membrane penetration by light increases along with the longer waves of light in the visible and near infrared (vis–NIR) electromagnetic spectrum. Because of this function, red light (635–650 nm) is used during PDT.

Photodynamic diagnosis very often enables the visualization of irregular lesion shapes more precisely than a classical white-light examination.[5,6] In the case of hyperkeratotic lesions, during PDD, the fluorescence of healthy background tissue is higher than the fluorescence of pathological lesions due to the thicker layer of the epithelium; thus, in these cases a negative image of the examined lesion is observed.

Leukoplakia and lichen planus (LP) are mucous membrane lesions which are very difficult to treat when they are large or multifocal; these 2 lesions are also precancerous stages. The classic World Health Organization (WHO) definition of leukoplakia from 1978 characterizes it as "a white patch or plaque that cannot be characterized clinically or pathologically as any other disease".[7] The etiology of leukoplakia is multifactorial. The most important factors are cigarette smoking, alcohol consumption, poor oral hygiene, sharp edges of the teeth, defective fillings, electrogalvanic currents (due to various metals in the oral cavity, i.e., amalgam, gold or nickel), food irritation, or the oral mucosa.

Since 2002, it has been recommended to make a distinction between a provisional clinical diagnosis of oral leukoplakia and a definitive one. A provisional clinical diagnosis is made when a lesion at the initial clinical examination cannot be clearly diagnosed as either leukoplakia or any other disease.[8]

The etiology of LP is still not fully known. According to the most common theories, it is a chronic, probably autoimmune, mucocutaneous, psychosocial disease that usually presents in middle-aged females and primarily affects the oral mucosa, skin, genital mucosa, scalp, and nails. Oral LP can clinically present in various forms, including reticular, papular, plaque-like, atrophic, erosive, and bullous types.[9]

The characteristic feature of both abovementioned lesions is a very irregular shape, therefore it is very hard to measure the area of these lesions. In the case of such irregular lesions, fractal dimension analysis (FDA) is very helpful. Fractal dimension analysis is a very promising method which is widely used to describe complicated shapes when the classical methods fail.

The term "fractal" refers to a shape which is described by potentially simple mathematic formulas. If these formulas are iterated into infinity, they may create shapes which we are able to magnify indefinitely and each time we can see infinite numbers of details of the shape – it has the feature of self-similarity. In classical Euclidean geometry, dimension is an integer – it is a number of coordinates which we need to describe the point inside the shape. For example, a point has no dimension, so it equals 0; to describe a straight line we need only 1 dimension (length); the main features of a rectangle are its length and width; a 3-dimensional shape needs to have width, length and height. Classic examples of fractals are Cantor set, Koch snowflake and Sierpinski triangle (Fig. 1).

The fractal dimension (FD) of Cantor set equals approx.

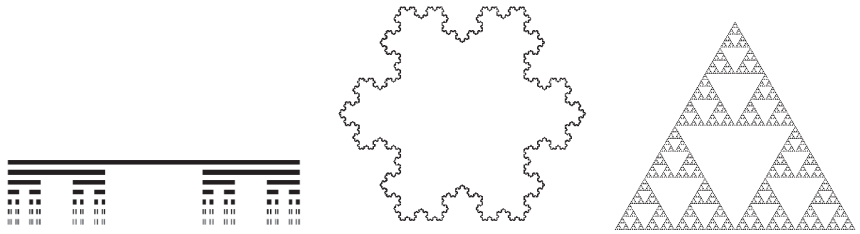

Cantor set Koch snowflake Sierpinski triangle

Fig. 1. Examples of fractals

0.631. This means that this shape is something between a point and a line. Koch snowflake, with a FD ≈ 1.262, is a shape which is closer to a line than to a flat figure, in contrast to Sierpinski triangle, with a FD ≈ 1.585, which is nearly halfway between a line and a flat figure.

Some natural shapes may be considered fractals, e.g., coast lines, trees, clouds, and mountains. Examples of fractals in living organisms include nerves and branches of blood vessels, the structure of brain neurons and the structure of bone. These shapes are too complicated to measure or compare between each other using traditional methods based on Euclidean geometry. In such cases, FDA is non-substitutable.

It is important to mention that FDA offers the ability to compare complicated shapes. The value of FD describes only the distribution of points (on a surface or in space) which create these shapes, as opposed to traditional ways of physically describing the dimension of a shape.

Fractal dimension analysis can be very useful in medicine; examples of FDA usage in medicine are mammographic image analysis, or estimation of tumor neoangiogenesis or of the pattern of coronary vessels.[10–12] Fractal dimension analysis of jaw bone cone beam computed tomography (CBCT) images is useful in the diagnosis of osteoporosis.[13]

In our study, we tried to distinguish oral leukoplakia and LP using FDA with a classical white-light examination and PDD. Lesions treated using PDF were histopathologically verified.

Material and methods

Patients

We enrolled patients (20 females and 15 males) in our study. The mean age of the study group was 58 years (range: 32–81 years). The total number of patients suffering from leukoplakia was 26, while 9 patients suffered from LP. Each lesion was histopathologically examined after taking the specimen from pathologically changed oral mucosa under local anesthesia (a classical examination with hematoxylin and eosin (H&E) staining). Leukoplakia foci occurred at the same rate in females and males. In the case of LP, females suffered from lesions more frequently than males (77.8% vs 22.2%, respectively). All procedures were conducted after obtaining the approval of the Ethics Committee of Wroclaw Medical University, Poland (approval No. KB-367/2014).

Leukoplakia foci were estimated using van der Waal classification. This classification is based on 3 parameters: L, C and P. The L parameter describes the size of the lesion: 1 – focus ≤2 cm; 2 – a lesion size 2–4 cm; and 3 – a lesion size >4 cm. L_X refers to an unspecified size. C is the clinical appearance of the lesion: 1 – homogenic; 2 – non-homogenic. P describes the occurrence of dysplasia (P_1) in a histopathological examination or a non-dysplastic lesion (P_0). P_X is the absence or presence of epithelial dysplasia not specified in the pathology report. According to these properties, van der Waal distinguishes 4 stages of leukoplakia: stage I (L_1P_0); stage II (L_2P_0); stage III (L_3P_0 or $L_1L_2P_1$); or stage IV (L_3P_1). In our study, we admitted only patients with homogenic leukoplakia without dysplasia (L_1P_0, L_2P_0, or L_3P_0). Other patients were treated by surgery. In the case of erosive LP, the patients were excluded from the study. All LP lesions were classified as reticular.

Photodynamic therapy and photodynamic diagnosis procedure

A solution of 20% 5-ALA (Sigma-Aldrich, St. Louis, USA) was dissolved in an eucerin base directly before each procedure. Delta-aminolevulinic acid was applied to lesions and covered by an occlusive dressing (gelatinous sponge flakes). After 2 h, PDD was performed. A Viofor-PDT lamp (Med & Life, Komorów, Poland) was used as the source of light. To excite the photoensitizer, we used a 405-nanometer wavelength with 250 mW of power. Photos were taken using the same parameters: Canon EOS 500D (Canon Inc., Tokyo, Japan), a 13-millimeter intermediate ring, a 50-millimeter lens, orange and UV-cut filters, an ISO of 1600, f-stop of 1/9, and exposure time of 1/50 s. Photo resolution was 4752 × 3168 pixels. After the PDD procedure, the 5-ALA ointment was applied again with an occlusive dressing for 2 h. Next, PDT was performed using red light (635 nm, a Viofor PDT lamp) in a total dose of 120 J per lesion. All PDT procedures were repeated every 3 weeks for each patient. Patients were observed 3, 6 and 12 months after their last photodynamic procedure.

Image preparation

All graphical operations were performed in GIMP v. 2.8.0 (GNU Image Manipulation Program; www.gimp.org). In the center of the lesion, a square with 300 pixels per side was selected. Prepared image selection was cropped from the original photo. A high pass filter was applied and the Levels tools were used to equalize the histogram of the image. Next, the images were converted into a grayscale and then converted into bitmap images (with a 50% threshold). The file was saved in TIFF format without any compression algorithms. All graphical operations for white-light photos are shown in Fig. 2. The PDD photos were prepared in the same way, but after the last bitmap transformation, color inversion was applied (Fig. 3). During PPD, hyperkeratotic lesions are darker than healthy mucosa, so color inversion was necessary to obtain pictures analogous to the white-light ones. These prepared files were the basis for FDA.

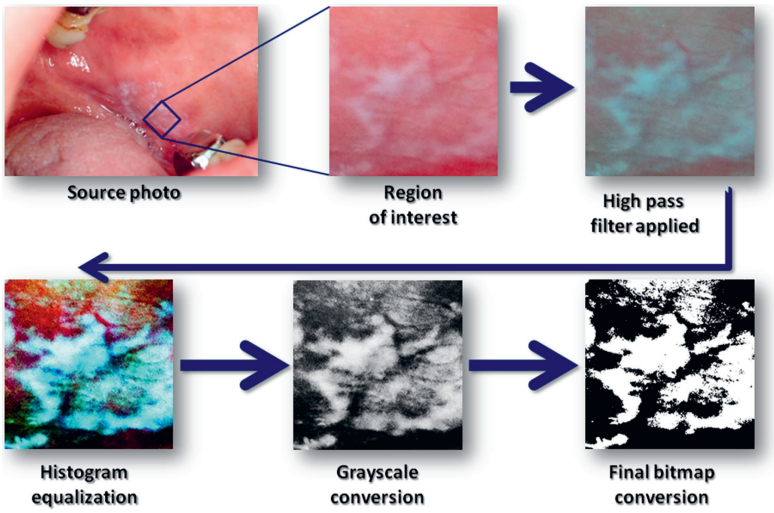

Fig. 2. Preparation of images during a white-light examination

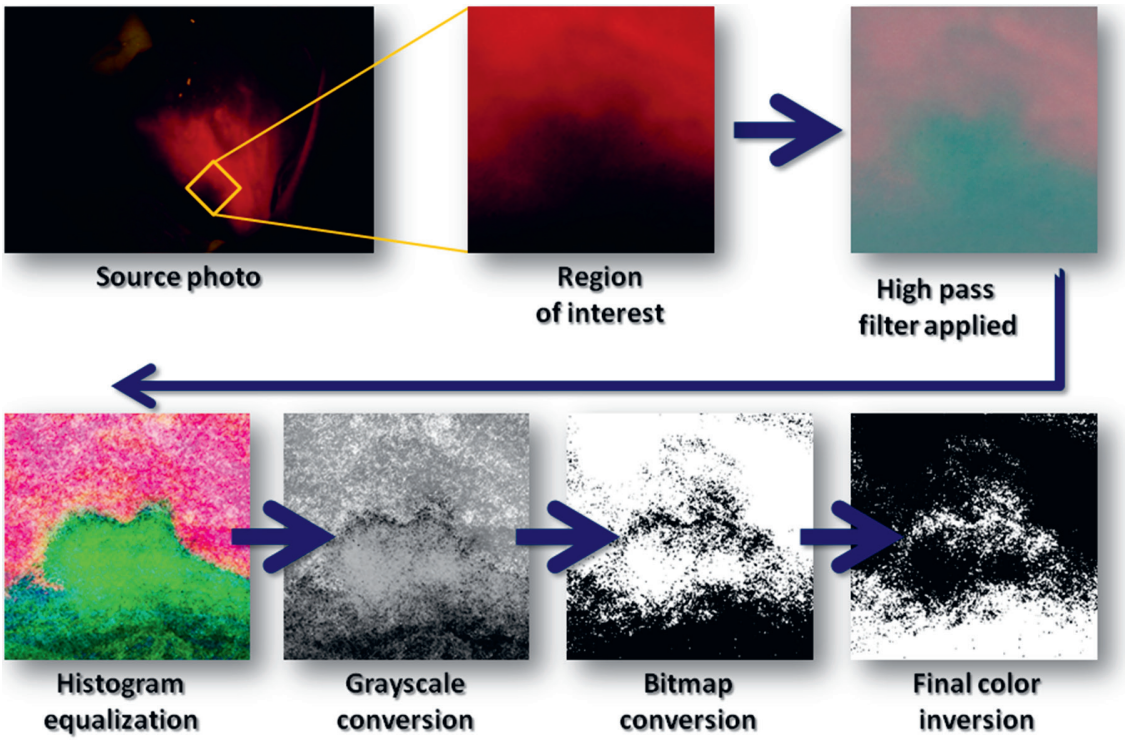

Fig. 3. Preparation of PDD images

PDD – photodynamic diagnosis.

Fractal dimension analysis

We used the computer program Fractalyse v. 2.4 (University of Franche-Comté, Besançon, France). Fractalyse enables the user to measure FDs using the box-counting method. The fractal dimension (D_s) is counted using the formula below[14]:

$$D_S = \lim_{\varepsilon \to 0} \frac{\log N(\varepsilon)}{\log\left(\frac{1}{\varepsilon}\right)},$$

where D_s – the fractal dimension; ε – the length of the box which creates a mesh covering the surface with the examined pattern; $N(\varepsilon)$ – the minimal number of boxes required to cover the examined pattern.

Statistical analysis

GraphPad Prism v. 6.01 (GraphPad Software, La Jolla, USA) was used for the statistical analysis. The Shapiro-Wilk test was applied to check for normality. Due to the lack of normal distribution in the examined samples, we used a non-parametric test. The Mann-Whitney test was applied to compare 2 values of FD. In the cases of more than 2 FD values, we used the Kruskal-Wallis test with Dunn's multiple comparisons test. The significance level was set at 0.05.

Results

The most frequent location of lesions was the mucous membrane of the cheeks: for leukoplakia, 15 lesions were

located there and for LP there were 6 lesions. Another 5 lesions of LP occurred in the alveolar ridge. The floor of the oral cavity was affected by LP in 2 cases. Lichen planus very rarely occurred on the tongue – only 1 lesion – and was not observed in the region of the lips or the hard palate. Leukoplakia lesions occurred in the tongue area in 7 cases and in 5 cases, in the alveolar ridge. Leukoplakia was very rarely observed in the region of the hard palate (3 lesions), the floor of the oral cavity (2 lesions) or the lips (2 lesions).

Stage L2 was most commonly observed (41.2%), L1 lesions occurred in 35.3% of cases and L3 occurred least often (23.5%).

The differences between the FDs of leukoplakia and LP in a white-light examination and the PDD procedure are shown in Tables 1 and 2. It is important to note that in the case of leukoplakia, the FD of lesions in the tongue in a white-light examination was significantly lower than during PDD. This means that lesions in PDD seem to be larger in both dimensions. No other FDs show statistically significant differences.

There were no significant differences observed between the FDs of leukoplakia and LP in the case of a white-light, classical examination or PDD. These results are shown in Tables 3 and 4.

Table 1. Fractal dimension values of leukoplakia in a white-light examination and the PDD procedure (Mann-Whitney test)

Site	Leukoplakia						p-value
	white light			PDD			
	median	mean	SD	median	mean	SD	
Cheek	1.780	1.793	0.029	1.808	1.795	0.049	0.271
Alveolar ridge	1.805	1.811	0.027	1.857	1.854	0.011	0.057
Palate	1.746	1.718	0.049	1.634	1.640	0.144	0.600
Tongue	1.744	1.744	0.009	1.773	1.769	0.014	0.026
All locations	1.773	1.774	0.042	1.782	1.780	0.084	0.162

PDD – photodynamic diagnosis; SD – standard deviation.

Table 2. Fractal dimension values of lichen planus in a white-light examination and the PDD procedure (Mann-Whitney test)

Site	Lichen planus						p-value
	white light			PDD			
	median	mean	SD	median	mean	SD	
Cheek	1.760	1.766	0.029	1.783	1.778	0.008	0.195
Alveolar ridge	1.823	1.819	0.023	1.806	1.803	0.005	0.314
All locations	1.780	1.787	0.038	1.787	1.787	0.016	0.914

PDD – photodynamic diagnosis; SD – standard deviation.

Table 3. Values of fractal dimension of leukoplakia and lichen planus during a white-light examination (Mann-Whitney test)

Site	White light						p-value
	leukoplakia			lichen planus			
	median	mean	SD	median	mean	SD	
Cheek	1.780	1.793	0.029	1.760	1.766	0.029	0.068
Alveolar ridge	1.805	1.811	0.027	1.823	1.819	0.023	0.629
All locations	1.773	1.774	0.042	1.780	1.787	0.038	0.452

SD – standard deviation.

Table 4. Values of fractal dimension of leukoplakia and lichen planus during PDD (Mann-Whitney test)

Site	PDD						p-value
	leukoplakia			lichen planus			
	median	mean	SD	median	mean	SD	
Cheek	1.808	1.795	0.049	1.783	1.778	0.008	0.196
Alveolar ridge	1.857	1.854	0.011	1.806	1.803	0.005	0.057
All locations	1.782	1.780	0.084	1.787	1.787	0.016	0.899

PDD – photodynamic diagnosis; SD – standard deviation.

Table 5. Differences in fractal dimension of lichen planus between the cheek and the alveolar ridge during a white-light examination and PDD (Mann-Whitney test)

Diagnostic method	Lichen planus						p-value
	cheek			alveolar ridge			
	median	mean	SD	median	mean	SD	
White light	1.760	1.766	0.029	1.823	1.819	0.023	0.019
PDD	1.783	1.778	0.008	1.806	1.803	0.005	0.036

PDD – photodynamic diagnosis; SD – standard deviation.

Table 6. Statistical differences between foci of leukoplakia in various locations according to the examination method (Dunn's multiple comparisons test)

Dunn's multiple comparisons test	Leukoplakia			
	White light		PDD	
	mean rank diff.	significant: yes or no	mean rank diff.	significant: yes or no
Cheek vs alveolar ridge	–2.95	no	–7.80	no
Cheek vs palate	10.88	no	7.87	no
Cheek vs tongue	10.13	yes	5.87	no
Alveolar ridge vs palate	13.83	yes	15.67	yes
Alveolar ridge vs tongue	13.08	yes	13.67	yes
Palate vs tongue	–0.75	no	–2.00	no

In the case of LP, a significant difference in FD was observed between lesions in the cheek and the alveolar ridge region. The values of FD were greater in the region of the alveolar ridge in both white-light and PDD examination. These results are shown in Table 5.

Differences in the FD were observed between the leukoplakia foci of the alveolar ridge, the tongue and the palate. These differences occurred in both white-light and PDD. Different values of FD were observed between cheek and tongue lesions in a white-light examination, in contrast to PDD, where the values were similar. The results of the Kruskal-Wallis and Dunn's multiple comparisons tests are shown in Table 6.

In all leukoplakia foci, in the region of the palate and the floor of the mouth, we observed a complete response. In the region of the tongue, a complete response was observed in 4 lesions and a partial response in 3 lesions. Leukoplakia of the alveolar ridge was completely treated in the case of 2 lesions, a partial response was achieved in 2 lesions and a lack of therapeutic effect was observed in the case of 1 lesion. Lesions in the region of the cheeks were the most resistant to PDT. Only in the case of 2 lesions we observed a complete response, a partial response was observed in the case of 11 lesions and a lack of therapeutic results occurred in the case of 2 lesions. Overall, a complete response of leukoplakia foci to PDT observed in 29.4% cases, a partial remission occurred in 58.8% cases and a total lack of treatment was noted in 11.8% cases.

Complete treatment was achieved in the case of 1 LP lesion in the tongue area. In the alveolar ridge, 4 out of 5 lesions were completely treated and 1 was partially treated. In the region of the floor of the mouth, a complete response was noted in the case of 1 lesion and a partial response occurred in 1 lesion. The most resistant areas to PDT treatment were the cheeks, where complete response was seen in 1 lesion, a partial response was observed in 4 lesions and a lack of treatment effects was seen in 1 lesion. Generally, LP was completely treated in 50% of all cases (7 lesions), a partial response was observed in 35.7% of cases (5 lesions) and failed PDT treatment was noted in 14.3% of cases (2 lesions). After PDT application, symptoms of LP, such as a burning pain, sensitivity to spicy foods and discomfort during speaking, disappeared in all of our patients, even if the lesion did not respond or only partially responded to the treatment.

Discussion

The diagnosis and treatment of leukoplakia and LP as premalignant lesions are important therapeutic problems. Photodynamic diagnosis allows the visualization of lesions in much more detail than a normal white-light examination. In many cases, the actual size and range of lesions are larger during a PDD session. This is particularly important in neoplasm lesions, where a margin of healthy tissue should be preserved. Due to the complicated shapes of leukoplakia and LP, FDA appears to be the most efficient method for estimating the size of these lesions. Fractal dimension analysis may be useful to check the microvascular pattern of LP in various locations of the oral cavity. Lucchese et al. showed that the FD of LP microvascular pattern is higher in buccal mucosa (1.167) and in the tongue mucosa (1.196) in comparison to healthy mucosa (1.123).[15]

No statistical differences were found in our study between the FDs of leukoplakia and LP. However, statistical

differences within the groups were observed. The value of FD in a white-light examination and in PDD was lower in the cheek region than in the alveolar ridge. This means that lesions in the cheek region were smaller in 1 dimension (width or height) than in the alveolar ridge. Differences in the FD of leukoplakia were mainly observed in the tongue region during both white-light examination (1.744) and PDD examination (1.773). This suggests that tongue lesions during PDD are larger and that the shape is more complicated than during a classical examination. Fractal dimension analysis may be a useful method for comparing complicated shapes, such as those of LP or leukoplakia, though our study did not confirm the usefulness of this method for distinguishing LP and leukoplakia without a histopathological examination.

The clinical detection of leukoplakia facilitates autofluorescence, chemiluminescence or vital staining with toluidine blue, though these methods have relatively low specificity and are not recommended for distinguishing leukoplakia from other lesions.[16] Another option is optical coherence tomography (OCT), which detects dysplasia by the fluctuation of light scattering due to random cellular changes in dysplastic tissues in comparison to normal mucosa.[17] Another study proved that narrow-band imaging (NBI) demonstrating an intraepithelial papillary capillary loop (IPCL) pattern destruction or a twisted elongation are indicative of histological changes in oral leukoplakia.[18] Application of 5% Lugol's solution aids in the featuring of suspicious lesions. Normal mucosa stains brown because of the high glycogen content, whereas leukoplakia appears pale compared to the surrounding normal tissue.[19]

Biopsy of the lesion and a histopathological examination still remains the standard diagnostic procedure for suspicious lesions. One of the possible features of leukoplakia is dysplasia, which manifests as architectural changes within the epithelial strata, combined with cellular atypia due to inappropriate differentiation.

The diagnostic process of LP is similar to the previously described diagnostic process of leukoplakia; it involves a provisional clinical diagnosis and histopathological confirmation. Lichen planus clinically presents mostly as one of 2 forms: reticular or erosive.[20] The reticular form occurs more frequently and is usually asymptomatic. The erosive form is less common, but is more symptomatic. Symptoms may range from a slight discomfort to an intense pain that interferes with chewing.[20,21] Our study revealed that after PDT application, these symptoms disappeared in all patients, even when the lesion did not respond or only partially responded to treatment.

Lichen planus and leukoplakia very frequently occur on a large area of the mucous membrane, which leads to complicated surgical treatment and requires reconstruction of the mucosa after complete excision. Surgical excision creates contracted scars, which may decrease patients' comfort. Photodynamic therapy as a noninvasive procedure is more frequently used for the treatment of leukoplakia and LP.[22–27]

Maloth et al. revealed that in their study, in the leukoplakia group, 17% of cases showed a complete response, 66% showed a partial response and 17% of the lesions did not respond to the treatment. In the LP group, 80% of the lesions showed a partial response and 20% did not respond.[28] Those results are similar to our study in the case of leukoplakia, in contrast to the lower effectiveness of PDT in LP found in our study. Pietruska et al. used chlorin-e6-mediated PDT, and their results were similar to 5-ALA-mediated PDT.[29] In the case of leukoplakia, the results were as follows: 27.3% of cases with a total response, 50% of cases with a partial response and 22.7% with no effect.[29] A study by Semkin et al. demonstrated that laser ablation may be another treatment method; successful results were seen in 42% of cases, but a recurrence of lesions was observed in 58% of cases.[30]

Photodynamic therapy and cryotherapy appear to be comparative treatment methods that may both serve as alternatives for the traditional surgical treatment of oral leukoplakia. The advantages of PDT are its minimal invasiveness and localized character, which prevents damage of collagenous tissue structures. Photodynamic therapy is more convenient for patients, less painful and more esthetically pleasing.[31]

Conclusions

Fractal dimension analysis may be a useful method for the comparison of complicated shapes, such as those of LP or leukoplakia, but our study did not confirm that this method may be used to distinguish LP and leukoplakia without a histopathological examination.

Photodynamic therapy is a promising, noninvasive treatment method of leukoplakia and LP in the region of the oral cavity.

After PDT application, symptoms of LP, such as a burning pain, sensitivity to spicy foods and discomfort during speaking, disappeared in all of our patients, even when the lesion did not respond or only partially responded to treatment.

References

1. Canavan TN, de la Feld SF, Huang C, Sami N. Photodynamic therapy effective for the treatment of actinic keratosis and basal cell carcinoma in bullous pemphigoid patients. *Photodiagnosis Photodyn Ther*. 2017;18:257–259. doi: 10.1016/j.pdpdt.2017.03.019
2. Vignion-Dewalle AS, Baert G, Devos L, et al. Red light photodynamic therapy for actinic keratosis using 37 J/cm^2: Fractionated irradiation with 12.3 mW/cm^2 after 30 minutes incubation time compared to standard continuous irradiation with 75 mW/cm^2 after 3 hours incubation time using a mathematical modeling. *Lasers Surg Med*. 2017;49(7):686–697. doi: 10.1002/lsm.22665
3. Megna M, Fabbrocini G, Marasca C, Monfrecola G. Photodynamic therapy and skin appendage disorders: A review. *Skin Appendage Disord*. 2017;2(3–4):166–176. doi: 10.1159/000453273

4. Griffin LL, Lear JT. Photodynamic therapy and non-melanoma skin cancer. *Cancers (Basel)*. 2016;8(10). pii: E98.
5. Hillemanns P, Wimberger P, Reif J, Stepp H, Klapdor R. Photodynamic diagnosis with 5-aminolevulinic acid for intraoperative detection of peritoneal metastases of ovarian cancer: A feasibility and dose finding study. *Lasers Surg Med*. 2017;49(2):169–176. doi: 10.1002/lsm.22613
6. Kata SG, Zreik A, Ahmad S, Chłosta P, Aboumarzouk O. Concurrent bladder cancer in patients undergoing photodynamic diagnostic ureterorenoscopy: How many lesions do we miss under white light cystoscopy? *Cent European J Urol*. 2016;69(4):334–340.
7. World Health Organization. *Collaborative Reference Centre for Oral Precancerous Lesions Application of the International Classification Of Diseases to Dentistry and Stomatology*. Geneva, Switzerland: WHO; 1978.
8. Awan KH, Morgan PR, Warnakulasuriya S. Utility of chemiluminescence (ViziLite™) in the detection of oral potentially malignant disorders and benign keratoses. *J Oral Pathol Med*. 2011;40(7):541–544.
9. Gupta A, Mohan RP, Gupta S, Malik SS, Goel S, Kamarthi N. Roles of serum uric acid, prolactin levels, and psychosocial factors in oral lichen planus. *J Oral Sci*. 2017;59(1):139–146. doi: 10.2334/josnusd.16-0219
10. Zyout I, Togneri R. A new approach for the detection of architectural distortions using textural analysis of surrounding tissue. *Conf Proc IEEE Eng Med Biol Soc*. 2016;2016:3965–3968. doi: 10.1109/EMBC.2016.7591595
11. Saidov T, Heneweer C, Kuenen M, et al. Fractal dimension of tumor microvasculature by DCE-US: Preliminary study in mice. *Ultrasound Med Biol*. 2016;42(12):2852–2863. doi: 10.1016/j.ultrasmedbio.2016.08.001
12. Yipintsoi T, Kroll K, Bassingthwaighte JB. Fractal regional myocardial blood flows pattern according to metabolism, not vascular anatomy. *Am J Physiol Heart Circ Physiol*. 2016;310(3):351–364. doi: 10.1152/ajpheart.00632.2015
13. Güngör E, Yildirim D, Çevik R. Evaluation of osteoporosis in jaw bones using cone beam CT and dual-energy X-ray absorptiometry. *J Oral Sci*. 2016;58(2):185–194. doi: 10.2334/josnusd.15-0609
14. Grizzi F, Russo C, Colombo P, et al. Quantitative evaluation and modeling of two-dimensional neovascular network complexity: The surface fractal dimension. *BMC Cancer*. 2005;8:14.
15. Lucchese A, Gentile E, Capone G, De Vico G, Serpico R, Landini G. Fractal analysis of mucosal microvascular patterns in oral lichen planus: A preliminary study. *Oral Surg Oral Med Oral Pathol Oral Radiol*. 2015;120(5):609–615. doi: 10.1016/j.oooo.2015.06.029
16. Awan K, Yang Y, Morgan P, Warnakulasuriya S. Utility of toluidine blue as a diagnostic adjunct in the detection of potentially malignant disorders of the oral cavity – a clinical and histological assessment. *Oral Dis*. 2012;18(8):728–733.
17. Lee CK, Chi TT, Wu CT, Tsai MT, Chiang CP, Yang CC. Diagnosis of oral precancer with optical coherence tomography. *Biomed Opt Express*. 2012;3(7):1632–1646.
18. Yang SW, Lee YS, Chang LC, Hwang CC, Chen TA. Diagnostic significance of narrow-band imaging for detecting high-grade dysplasia, carcinoma in situ, and carcinoma in oral leukoplakia. *Laryngoscope*. 2012;122(12):2754–2761.
19. Petruzzi M, Lucchese A, Baldoni E, Grassi FR, Serpico R. Use of Lugol's iodine in oral cancer diagnosis: An overview. *Oral Oncol*. 2010;46(11):811–813.
20. Edwards PC, Kelsch R. Oral lichen planus: Clinical presentation and management. *J Can Dent Assoc*. 2002;68(8):494–499.
21. Ismail SB, Kumar SK, Zain RB. Oral lichen planus and lichenoid reactions: Etiopathogenesis, diagnosis, management and malignant transformation. *J Oral Sci*. 2007;49(2):89–106.
22. Rabinovich OF, Rabinovich IM, Guseva AV. Photodynamic therapy in treatment of severe oral lichen planus [in Russian]. *Stomatologiia (Mosk)*. 2016;95(4):27–30.
23. Prażmo EJ, Kwaśny M, Łapiński M, Mielczarek A. Photodynamic therapy as a promising method used in the treatment of oral diseases. *Adv Clin Exp Med*. 2016;25(4):799–807
24. Vohra F, Al-Kheraif AA, Qadri T, et al. Efficacy of photodynamic therapy in the management of oral premalignant lesions. A systematic review. *Photodiagnosis Photodyn Ther*. 2015;12(1):150–159. doi: 10.1016/j.pdpdt.2014.10.001
25. Romeo U, Russo N, Palaia G, Tenore G, Del Vecchio A. Oral proliferative verrucous leukoplakia treated with the photodynamic therapy: A case report. *Ann Stomatol (Roma)*. 2014;5(2):77–80.
26. Wong SJ, Campbell B, Massey B, et al. A phase I trial of aminolevulinic acid-photodynamic therapy for treatment of oral leukoplakia. *Oral Oncol*. 2013;49(9):970–976. doi: 10.1016/j.oraloncology.2013.05.011
27. Jerjes W, Upile T, Hamdoon Z, Mosse CA, Akram S, Hopper C. Photodynamic therapy outcome for oral dysplasia. *Lasers Surg Med*. 2011;43(3):192–199. doi: 10.1002/lsm.21036
28. Maloth KN, Velpula N, Kodangal S, et al. Photodynamic therapy – a non-invasive treatment modality for precancerous lesions. *J Lasers Med Sci*. 2016;7(1):30–36. doi: 10.15171/jlms.2016.07
29. Pietruska M, Sobaniec S, Bernaczyk P, et al. Clinical evaluation of photodynamic therapy efficacy in the treatment of oral leukoplakia. *Photodiagnosis Photodyn Ther*. 2014;11(1):34–40. doi: 10.1016/j.pdpdt. 2013.10.003
30. Semkin VA, Rabinovich OF, Kasparov AS, Agapitova LP, Bezrukov AA. Analysis of comprehensive treatment of oral leukoplakia by laser ablation [in Russian]. *Stomatologiia (Mosk)*. 2016;95(6):33–35.
31. Kawczyk-Krupka A, Waśkowska J, Raczkowska-Siostrzonek A, et al. Comparison of cryotherapy and photodynamic therapy in treatment of oral leukoplakia. *Photodiagnosis Photodyn Ther*. 2012;9(2):148–155. doi: 10.1016/j.pdpdt.2011.12.007

The diagnostic usefulness of the basophil activation test (BAT) with annexin V in an allergy to *Alternaria alternata*

Emilia Królewicz[1,B–D], Krzysztof Gomułka[2,B], Anna Wolańczyk-Mędrala[2,B], Wojciech Mędrala[2,A,C], Wojciech Barg[3,B], Irena Kustrzeba-Wójcicka[1,E,F]

[1] Department of Medical Biochemistry, Wroclaw Medical University, Poland
[2] Department of Internal Diseases and Allergology, Wroclaw Medical University, Poland
[3] Department of Physiology, Wroclaw Medical University, Poland

A – research concept and design; B – collection and/or assembly of data; C – data analysis and interpretation; D – writing the article; E – critical revision of the article; F – final approval of the article

Advances in Clinical and Experimental Medicine, ISSN 1899-5276 (print), ISSN 2451-2680 (online) *Adv Clin Exp Med.* 2018;27(12):1737–1744

Address for correspondence
Emilia Królewicz
E-mail: emilia_krolewicz@wp.pl

Funding sources
None declared

Conflict of interest
None declared

Received on July 3, 2017
Reviewed on October 8, 2017
Accepted on October 12, 2017

Abstract

Background. The basophil activation test (BAT) is an effective diagnostic tool in mold allergy, which is still not sufficiently known.

Objectives. The aim of our study was to assess the degree of annexin V binding to the surface of the basophil cell membrane after stimulation with anti-immunoglobulin E (anti-IgE) and *Alternaria alternata* allergenic extract.

Material and methods. *Alternaria alternata* allergic patients (n = 32) and healthy volunteers (n = 33) were evaluated using skin prick tests (SPT), quantification of specific IgE (sIgE) and the BAT. Basophil activation was detected as a percentage degree of annexin V binding to the surface of the basophil cell membrane.

Results. Receiver operating characteristic (ROC) curve analysis yielded a threshold value of 4.95% of activated basophils when the tested group and control group were studied, with a sensitivity and specificity of 100% (area under curve (AUC) = 1; p = 0.00000) for 100 SBU/mL *Alternaria alternata* allergen extract. The threshold value was 10.28% with a sensitivity of 93.8% and specificity of 100% (AUC = 0.98958; p = 0.00000) for 10 SBU/mL mold extract, and 9.37% with a sensitivity of 90.3% and specificity of 100% (AUC = 0.96307; p = 0.00000) for 1 SBU/mL *Alternaria alternata* allergen extract. The method was least efficacious in anti-IgE stimulation, where the threshold value was 5.48% with a sensitivity of 90.6% and specificity of 30.3% (AUC = 0.46780; p = 0.67039).

Conclusions. The BAT with annexin V and sIgE measurement against *Alternaria alternata* increase the capability of a diagnostic laboratory for detecting mold sensitization. Both methods may certainly replace SPT, which are currently routinely used in allergy diagnosis. Annexin V may be considered a new basophil activation marker with an efficacy comparable to that of CD63 or CD203c.

Key words: *Alternaria alternata* allergy, basophil activation test, specific immunoglobulins E, flow cytometry, receiver operating characteristic curve

DOI
10.17219/acem/78563

Introduction

The basophil activation test (BAT) is a modern and promising research tool in the field of medical immunology. It was introduced to flow cytometry in 1994 by Sainte-Laudy et al.[1] The assessment of basophil activity during stimulation with an allergen or other causative agent is an in vitro method that raises special interest among scientists. The BAT uses various markers for the identification and activation of basophils. Currently, the gold standard in this field is the evaluation of CD63 expression as a de novo molecule after antigen activation.[2,3] The CD63 antigen was used in studies with various inhalant allergens: mites, grasses,animal dander,in allergy to insect venom and to drugs.[4–14] CD203c is the second antigen used in scientific research as a double marker of both identification and activation of basophils, occurring constantly on its surface.[15–17] Other antigens, such as CD13, CD45, CD107a, and CD164, are also well-known and used in scientific experiments.[18,19] However, no objective studies have so far compared the properties and diagnostic efficacy of most of these markers. Although the BAT has been used in allergology for over 20 years, work continues on improving the protocols for basophil identification. The lack of standardization of experiments using various antigens remains the main problem, causing discrepancies and fundamental differences in test results. In the area of laboratory research, a constant search continues for new and effective markers which could improve modern allergy diagnostics. Cytometry studies may provide an opportunity to develop mold allergy detection, including *Alternaria alternata* hypersensitivity. Although *Alternaria* allergies are fairly frequent, with an occurrence of 3–20% in Europe and 47% in the Polish population, knowledge about molecular mold allergy detection is still insufficient.[20]

In this paper, we investigated if annexin V may be considered a new basophil activation marker, useful in *Alternaria alternata* allergy detection.

Basophil activation was demonstrated by using the phenomenon of basophil membrane reorganization under the influence of applied stimuli. In this process, phosphatidylserine, as the main constitutive phospholipid, is displaced from the cytosolic to the basophil external membrane site. Using annexin V bound to fluorochrome, which is the ligand for phosphatidylserine, it was proven that a colored complex forms, which may be depicted in a flow cytometer. The only fluorescent cells were those bounded to annexin V, i.e., activated basophils.

Our studies are a reference to the experiments conducted by Sainte-Laudy and Ouk, who demonstrated changes in the conformation of the basophil membrane after activation with specific and nonspecific stimuli.[21]

Material and methods

Patients and controls

A total of 32 patients (17 males and 15 females) aged from 17 to 42 years (median: 25 years) with seasonal allergic rhinitis and positive skin prick tests (SPT) to the *Alternaria alternata* allergen mix (Allergopharma, Joachim Ganzer KG, Reinbek, Germany) were included in the study. Control group consisted of 33 healthy volunteers (9 males and 24 females) aged from 19 to 54 years (median: 23 years) with no allergic symptoms and with negative SPT results. All the procedures were performed in accordance with the ethical standards of the Helsinki Declaration. The study was approved by the Ethics Committee of Wroclaw Medical University, Poland. Informed consent was obtained from all the enrolled individuals.

Skin prick tests

Skin prick tests were performed according to the standard procedure, using the panel of inhalant allergen extracts (Allergopharma, Joachim Ganzer KG). The kit of reagents contained *Alternaria alternata*, *Cladosporium herbarum*, *Aspergillus fumigatus*, and *Penicilium notatum* extracts at a concentration of 10,000 SBU/mL, histamine hydrochloride 1.7 mg/mL and sodium chloride 9 mg/mL were used as a positive and negative control. The SPT results were read after 15 min and considered positive if the wheal diameter was >3 mm.

Specific immunoglobulins E measurement

Specific immunoglobulins E (sIgE) against the *Alternaria alternata* allergen mix m6 were determined by the ImmunoCAP FEIA system measurements (Thermo Fisher Scientific Inc., Uppsala, Sweden) according to the manufacturer's instruction. The detection range was 0.35–100 kU/L. Values ≥0.35 kU/L were considered positive.

Basophil activation test protocol

Blood specimens were collected into K-EDTA venipuncture tubes (Sarstedt AG & Co, Nümbrecht, Germany) and used for cell stimulation in BD Falcon Round Bottom Tubes (BD Biosciences, San Diego, USA). Testing samples were performed for each patient as the patient background (Pb), positive (stimulation) control (Pc) with Polyclonal Rabbit anti-Human IgE antibody at a final concentration of 10 µg/mL (Dako Denmark A/S, Glostrup, Denmark) and with the *Alternaria alternata* allergen mix used in SPT at the 3 final concentrations of 100, 10 and 1 SBU/mL, identified as C_1, C_2 and C_3.

Sample preparation and analysis

At the beginning of the experiment, 50 µL of stimulation control anti-Human IgE and 50 µL of corresponding *Alternaria alternata* allergen solution was added to 100 µL of stimulation buffer and marked as Pc, C_1, C_2, and C_3 probe. Only 150 µL stimulation buffer was added to the background probe Pb. In the next step, 50 µL of the patient's whole blood was added to each tube and gently mixed. To analyze basophil activation, cells were stained with 5 µL of annexin V-FITC (BD Biosciences) and 5 µL of anti-CCR3-PE (R&D Systems, Minneapolis, USA), and the samples were incubated for 15 min at 37°C. Then, stimulation was terminated by adding 2 mL of Lysing Solution (BD Biosciences) after which the mixing tubes were incubated at room temperature for 10 min. After centrifugation (5 min, 500 g), supernatants were decanted and cell pellets were resuspended in 300 µL of Cell Wash (BD Biosciences) and gently mixed. A total amount of 100,000 cells were acquired per sample using the FACScan flow cytometer (BD Biosciences).

The data was analyzed using CellQuest flow cytometry analysis software (BD Biosciences) according to the manufacturer's instructions. Basophils were identified following the $CCR3^{high}/SSC^{low}$ BAT protocol (Fig. 1).

The percentage degree of annexin V binding to the surface of the basophil cell membrane after stimulation with anti-Human IgE and *Alternaria alternata* allergenic extract was defined as basophil activation. The calculation of the percentage of annexin V binding expression was detected as brightly fluorescent fluorescein isothiocyanate (FITC) (Fig. 2). The activated cells were identified by comparison of their number to the total amount of basophil population gated (Fig. 1). The results were presented after subtracting patient background values.

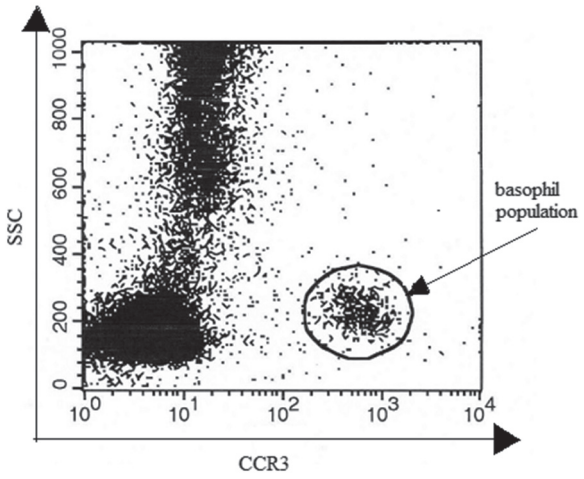

Fig. 1. Basophil population gating

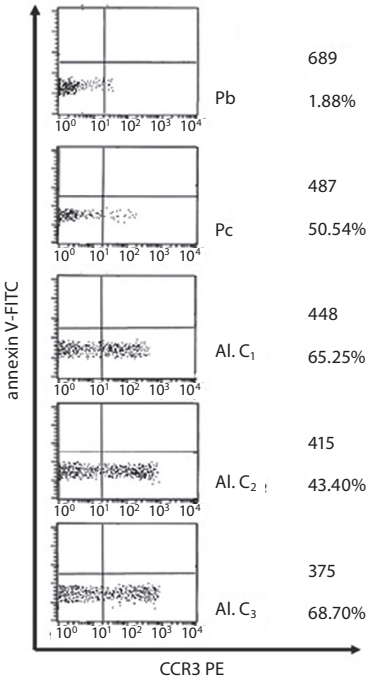

Fig. 2. The number and percentage of activated basophils in each probe in selected individuals in the study group

FITC – fluorescein isothiocyanate; Pb – patient background; Pc – positive control; Al. – allergen; C_1, C_2, C_3 – the concentrations of the *Alternaria alternata* allergen mix (100, 10 and 1 SBU/mL, respectively).

Statistical analysis

Statistical analysis was performed with the use of STATISTICA v. 12.5 software (StatSoft, Kraków, Poland). The distribution of data was performed using the Shapiro-Wilk test. Due to the lack of a normal distribution, the nonparametric Mann-Whitney test was used for the comparison of 2 independent samples. Probability values $p < 0.05$ were considered significant. The optimal cut-off values for allergen stimulation, sensitivity and specificity were determined using receiver operating characteristic (ROC) curve analysis.[22]

Results

Skin prick tests

The results of the SPT with histamine hydrochloride in the study group (n = 32) ranged from a 3 mm to a 6 mm wheal diameter (median: 4 mm). In the control group (n = 33), the results were within the 3–5.5 mm range (median: 3.5 mm). There were no statistically significant differences in SPT with histamine hydrochloride between the groups (p = 0.12721).

The results of SPT with *Alternaria alternata* extract in the control group were completely negative and reached 0 mm for each volunteer, while in the study group the results ranged from 3.5 mm to 11 mm (median: 6.5 mm).

Specific immunoglobulins E

Specific immunoglobulins E concentration to the *Alternaria alternata* allergen mix m6 in the control group (n = 33) were within the range of 0–0.06 kU/L (median: 0.01 kU/L). In the case of patients with mold allergy (n = 32), the results obtained were in the range of 0.002–28.2 kU/L (median: 5.47 kU/L).

Specific IgE concentrations acquired in kU/L were qualified for assigned classes from 0 to 6 according to the manufacturer's instruction. A result was considered positive if the concentration of sIgE was ≥0.35 kU/L, which was interpreted as a low result in class 1.

In the study group (n = 32), 27 positive and 5 negative results of sIgE to *Alternaria alternata* were obtained (Table 1).

Table 1. Specific immunoglobulins E (IgE) concentration to *Alternaria alternata* in the study group (n = 32) by grade of CAP classes

sIgE concentration [kU/L]	CAP class	Study group (n = 32)
>100	6	0
From 50 to <100	5	0
From 17.5 to <50	4	3 (9.38%)
From 3.5 to <17.5	3	15 (46.88%)
From 0.7 to <3.5	2	7 (21.88%)
From 0.35 to <0.7	1	2 (6.25%)
<0.35	0	5 (15.63%)

sIgE – specific immunoglobulin E.

Flow cytometry studies

Basophil number

The number of basophils identified in the whole tested population (n = 65) ranged from 108 to 872 cells (median: 488).

Basophil activity

The activity of basophils in each probe was determined as the percentage of active cells of the whole identified basophil population.

Patient background

The median of Pb in the tested population (n = 65) was 1.75% (min 1.33%, max 1.98%; standard deviation (SD): 0.14%). The mean value of Pb increased by a value of 2 SD (X + 2 × SD) was adopted as the cut-off point and reached 2.04%.

Positive control

In the study group (n = 32), the percentage degree of annexin V binding to the surface of the basophil cell membrane after stimulation with anti-Human IgE was 14.26% (min 2.95%, max 76.01%). The results of Pc in the healthy volunteers were slightly higher than in the patients. After anti-Human IgE stimulation, the median of basophil activation reached 21.69% (min 2.08%, max 83.68%), but the difference was not statistically significant (p = 0.66025).

Stimulation using *Alternaria alternata* extract

In the group of *Alternaria alternata* allergic patients (n = 32), the median percentage of basophil activation at the highest concentration, C_1 = 100 SBU/mL, was 20.42% (min 6.73%, max 74.70%). At the intermediate concentration of mold allergen extract, C_2 = 10 SBU/mL, the median expression of annexin V binding reached 21.89% (min 3.14%, max 85.92%). Stimulation at the lowest concentration of *Alternaria* extract, C_3 = 1 SBU/mL, gave the highest median of basophil activation, 29.41% (min 2.31%, max 88.55%). In the control group, the results of the BAT were considerably lower. The highest *Alternaria alternata* extract concentration (C_1) resulted in a median at the level of 2.31% (min 1.04%, max 5.48%). Stimulation by the C_2 concentration resulted in a median of basophil activation equal to 2.46% (min 1.51%, max 4.83%). In the case of mold allergen extract at the C_3 concentration, the median of annexin V binding to the basophil surface reached 2.54% (min 1.06%, max 5.96%). There were statistically significant differences in basophil activity between the 2 tested groups in C_1, C_2 and C_3 probes ($p < 0.05$). The cut-off value for anti-IgE, and allergen stimulation positivity and specificity was determined on the basis of ROC curves and reached 5.45% for anti-IgE, 4.95% at the C_1 concentration, 10.28% at the C_2 concentration, and 9.37% at the C_3 concentration (Fig. 3).

Sensitivity and specificity

Based on ROC curves, it was demonstrated that the method achieved its lowest effectiveness for the Pc sample. The sensitivity and specificity evaluated together were 120.9%.

The highest sensitivity and specificity of the BAT was achieved for the highest concentration of *Alternaria alternata* extract, C_1 = 100 SBU/mL. In this case, the sensitivity and specificity evaluated together were 200%.

The analysis of ROC curves for the allergen stimulated probes was carried out on the basis of the calculated significance level (p) and area under ROC curve (AUC). A comparison of the results is demonstrated in Table 2.

The dependence of activated basophil percentage on the concentration of *Alternaria alternata* allergen extract

It has been shown that in both tested groups and in the control group, the highest mean value and median of activated basophils was achieved by stimulation with the lowest concentration of *Alternaria alternata* extract, C_3 = 1 SBU/mL (Fig. 4).

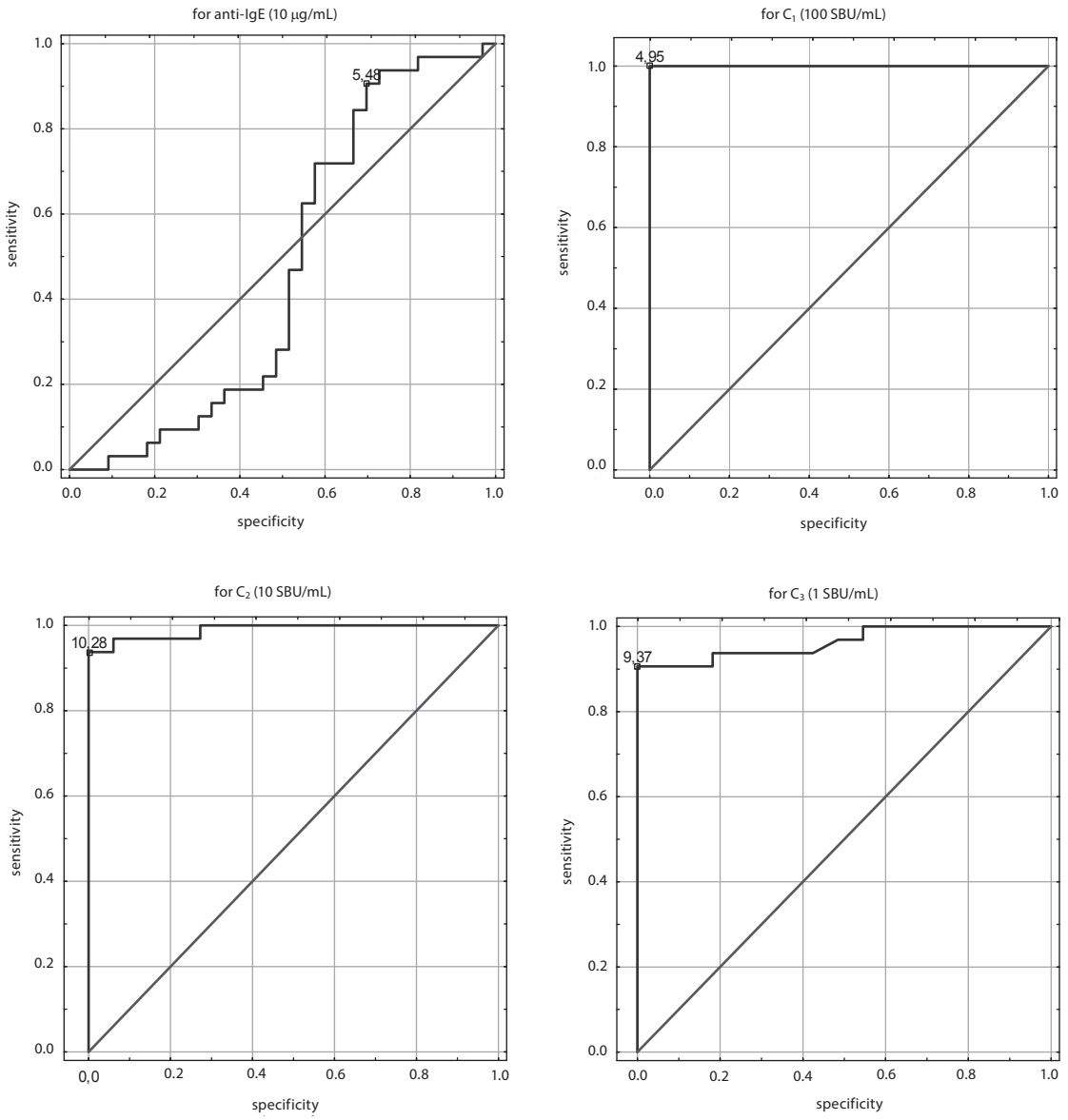

Fig. 3. Receiver operating characteristic (ROC) curves with cut-off value for basophil stimulation with anti-immunoglobulin E (anti-IgE) and *Alternaria alternata* allergen extract

C_1, C_2, C_3 – the concentrations of the *Alternaria alternata* allergen mix (100, 10 and 1 SBU/mL, respectively).

Table 2. The comparison of sensitivity, specificity, p-value, and AUC for the allergen-stimulated probes

Probe	Sensitivity [%]	Specificity [%]	The sum of sensitivity and specificity [%]	p-value	AUC
Pc	90.6	30.3	120.9	0.67039	0.46780
C_1	100	100	200	0.00000	1
C_2	93.8	100	193.8	0.00000	0.98958
C_3	90.6	100	190.6	0.00000	0.96307

Pc – positive control; C_1, C_2, C_3 – the concentrations of the *Alternaria alternata* allergen mix (100, 10 and 1 SBU/mL, respectively); AUC – area under receiver operating characteristic curve.

Discussion

The aim of this study was to evaluate and optimize the diagnostic usefulness of the BAT in *Alternaria alternata* allergies. We also investigated if annexin V could be considered a new basophil activation marker and if it might replace the antigens commonly used in cell tests, such as CD63 or CD203c.

The studies were performed in a group of 65 people, of whom 32 patients were sensitized to *Alternaria alternata*; they had positive results of SPT and presented clinical symptoms. The remaining 33 healthy volunteers

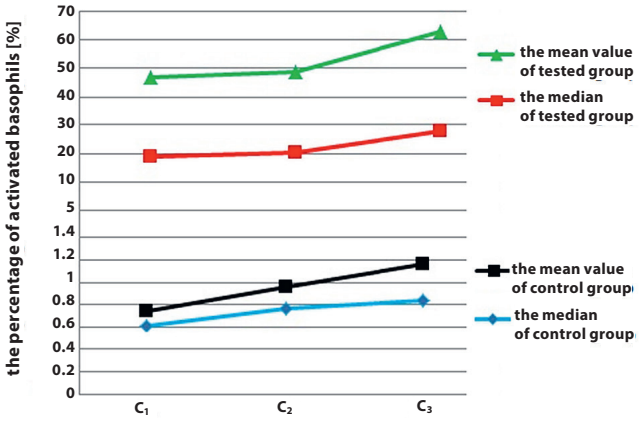

Fig. 4. The distribution of the mean value and median of basophil activity in the tested and control groups (n = 65)

C_1, C_2, C_3 – the concentrations of the *Alternaria alternata* allergen mix (100, 10 and 1 SBU/mL, respectively).

had totally negative results of the SPT and did not present symptoms of allergy-based diseases.

The results of specific IgE measurement directed against the *Alternaria alternata* allergen extract m6 were interesting. Out of 32 patients allergic to *Alternaria* mold with positive SPT results, as many as 5 persons had a sIgE anti-m6 result <0.35 kU/L, i.e., below the lower limit of concentration at which the result is considered positive and qualified as class 1 sIgE. In the tested group, in more than 15% of allergic patients, the concentration of sIgE was in class 0 and the remaining more than 84% of patients were in classes 1–4. The highest percentage of patients sensitized to *Alternaria* had a high level of IgE, qualified as class 3, and they accounted for over 46% of the studied group. After a comparison between the results of SPT and sIgE values, it was observed that the sIgE class is not correlated to the size of the wheal, the diameter of which is interpreted in SPT. In some respondents, the SPT result with the *Alternaria alternata* extract was 12 × 10 mm, in others it was 6 × 7 mm or 5 × 5 mm, but in each case, the sIgE value was qualified as class 3. Moreover, there were allergic patients in the tested group for whom the results of the SPT reached 8 × 7 mm, while the sIgE value was qualified as class 0. In the whole control group, the result was negative, as the concentration of sIgE against *Alternaria alternata* was <0.35 kU/L. It was proven that the concentration of sIgE anti-m6 in the studied group was significantly higher than in the control group, where the min, max and median were equal to 0 mm (p = 0.00000). The results of *Alternaria alternata* sIgE quantification demonstrated a sensitivity of 90.6% and a specificity of 100%. Currently, in order to increase the sensitivity and specificity of IgE measurement, shifting of the lower concentration of sIgE from 0.35 kU/L to 0.1 kU/L is contemplated. However, according to the instructions for interpreting the results of the ImmunoCAP FEIA system (Thermo Fisher Scientific Inc.), the value of 0.35 kU/L is still regarded as the threshold.

The first parameter analyzed in the cytometry studies conducted was the number of cells identified as basophils. Bühlmann Laboratories AG (Schönenbuch, Switzerland) notes that in cell tests, the number of gated basophils should be within the range of 200–600. In the experiment, the median of identified basophils (median: 488) in each sample in the tested and control group (n = 65) was contained in the range specified by the manufacturer, but in some unstimulated and stimulated samples, less than 200 or more than 600 of basophils were collected.

The main objective of the cytometry study was to demonstrate that the binding of annexin V depends on the activation of basophils after stimulation with anti-IgE and the *Alternaria alternata* allergen extract. The displacement of phosphatidyl serine as a ligand for annexin V from the cytosolic to the basophil external membrane site occurs only under the influence of applied stimuli.

The median of basophil activity in unstimulated samples, Pb, was similar in the tested group (1.77%) and in healthy volunteers (1.75%). These results are comparable to the values obtained by De Weck et al., who indicated that the basophil activity at rest is generally below 5%.[16]

No statistically significant differences between the groups studied were observed after anti-Human IgE stimulation (p = 0.66025). The positive control stimulation gave median results equal to 14.26% in the tested group vs 21.69% in the control group.

Receiver operating characteristic curve analysis was performed to determine the cut-off value of the percentage of activated basophils between *Alternaria alternata*-sensitized patients and controls. The positive control stimulation with anti-IgE gave unsatisfactory results, because the specificity reached only 30.3% and the sensitivity was 90.6% (AUC = 0.46780; p = 0.67039). Among the participants there were 6 persons with a negative reaction to anti-IgE below the cut-off value of 5.48%. The threshold was established at 4.95% for C_1 = 100 SBU/mL mold extract concentration with a sensitivity and specificity of 100% (AUC = 1; p = 0.00000). The analysis of the data obtained with C_2 = 10 SBU/mL allergen extract defined a cut-off value of 10.28% activated basophils with a sensitivity of 93.8% and a specificity of 100% (AUC = 0.98958; p = 0.00000). Sensitivity reached 90.3% with a specificity of 100% concerning C_3 = 1 SBU/mL *Alternaria alternata* allergen extract with a threshold of 9.37% (AUC = 0.96307; p = 0.00000). In all healthy volunteers (n = 33), the results of stimulation with the mold allergen extract were negative.

In the BAT, the dependence between the degree of IgE-dependent activation and the value of the concentration of a specific stimulus was variable between individuals. It was assumed that each allergen is characterized by the curve of the dependence of its concentration on the degree of basophil activation. Kleine-Tebbe et al. demonstrated that in the initial phase of the experiment, an increase in the concentration of the allergen causes an increase of basophil activation. Then there is a plateau on the curve,

after which a further increase in the concentration of the allergen causes a decrease of basophil activation.[23] It has been proven that in the tested and control group, the highest percentage of activated basophils was observed at the lowest concentration of the mold allergen extract C_3 = 1 SBU/mL (Fig. 4). In the tested group, the basophil activation in each of the 3 concentrations of the *Alternaria alternata* extract was in the range from a dozen to several dozen percent, while in the control group it extended slightly above or below 1%. The mold allergen extract caused basophil activation only in people allergic to *Alternaria*.

Currently, only a few works describe the BAT performed with mold allergens. Not all researchers have utilized standardized and calibrated allergens in cell tests. Although they are free from preservatives and other cytotoxic additives, their use is expensive. In our studies, we used the *Alternaria alternata* allergen extract intended for SPT. Therefore, a comparison of the results of our studies with the effects of the experiments presented in the literature is possible only to a limited extent. In the paper presented by Mirković et al., a CD203c marker was used for *Aspergillus fumigatus* allergy detection and for allergic bronchopulmonary aspergillosis diagnosis in cystic fibrosis patients.[24] However in this study, the sensitivity and specificity of the BAT were not appointed. It has been proven that the combination of BAT with CD203c and routine measurement of total and specific IgE increases the correct classification of patients into subgroups of unsensitized persons, allergic to *Aspergillus* and aspergillosis-affected.

The results obtained may be compared to the results of experiments with other allergens and basophil activation markers. Sanz et al., in a protocol of BAT using anti-IgE/anti-CD63, mite allergen *Dermatophagoides pteronyssinus* and grass fodder *Lolium perenne* obtained a sensitivity equal to 93.3% and a specificity of 98.7%.[25] González-Muñoz et al. also conducted research in the direction of flow cytometry to detect mite allergy, using anti-CD123/anti-CD63. For allergens at a higher concentration (16 µg/mL) they received sensitivity and specificity of 100%, and in the case of a lower concentration (1.6 µg/mL), sensitivity reached 83% and specificity did not change.[26]

The BAT with annexin V, anti-CCR3 and the *Alternaria alternata* allergen extract presented in this paper has a sensitivity and efficiency comparable to CD63, which is considered the gold standard in the in vitro cell tests used in allergology. It also has a higher diagnostic value than CD203c. Undoubtedly, the advantage of the flow cytometry study with annexin V is the cost, which is much lower than in the case of other markers used in research work. Developing experiments using this protein is therefore encouraging. Further work using the BAT with different markers and mold allergens is necessary in order to validate the method.

References

1. Sainte-Laudy J, Vallon C, Guérin JC. Analysis of membrane expression of the CD63 human basophil activation marker. Applications to allergologic diagnosis [in French]. *Allerg Immunol (Paris)*. 1994;26(6):211–214.
2. Netchiporouk E, Moreau L, Rahme E, Maurer M, Lejtenyi D, Ben-Shoshan M. Positive CD63 basophil activation tests are common in children with chronic spontaneous urticaria and linked to high disease activity. *Int Arch Allergy Immunol*. 2016;171(2):81–88.
3. Masilamani M, Kamalakannan M, Sampson HA. Basophil degranulation assay. *Methods Mol Biol*. 2017;1592:139–146.
4. Leśniak M, Czarnobilska E. Usefulness of basophil activation test for the diagnosis of inhaled allergies [in Polish]. *Przegl Lek*. 2015;72(12):773–778.
5. An S, Shen C, Liu X, et al. Alpha-actinin is a new type of house dust mite allergen. *PloS ONE*. 2013;8(12):e81377.
6. Korošec P, Silar M, Kopač P, Eržen R, Zidarn M, Košnik M. Distinct contributory factors determine basophil-allergen sensitivity in grass pollen rhinitis and in anaphylactic wasp venom allergy. *Int Arch Allergy Immunol*. 2016;171(2):89–101.
7. Wolańczyk-Mędrala A, Gogolewski G, Liebhart J, et al. A new variant of the basophil activation test for allergen-induced basophil CD63 upregulation. The effect of cetirizine. *J Investig Allergol Clin Immunol*. 2009;19(6):465–473.
8. Crockard AD, Ennis M. Laboratory-based allergy diagnosis: Should we go with the flow? *Clin Exp Allergy*. 2001;31(7):975–977.
9. Ocmant A, Peignois Y, Mulier S, Hanssens L, Michilis A, Schandené L. Flow cytometry for basophil activation markers: The measurement of CD203c up-regulation is as reliable as CD63 expression in the diagnosis of cat allergy. *J Immunol Methods*. 2007;320(1–2):40–48.
10. Herzinger T, Scharrer E, Placzek M, Przybilla B. Contact urticaria to giraffe hair. *Int Arch Allergy Immunol*. 2005;138(4):324–327.
11. Bidad K, Navijn MC, van Oosterhout AJ, van der Heide S, Elberink JN. Basophil activation test in the diagnosis and monitoring of mastocytosis patients with wasp venom allergy on immunotherapy. *Cytometry B Clin Cytom*. 2014;86(3):183–190.
12. Eberlein-König B, Rakoski J, Behrendt H, Ring J. Use of CD63 expression as marker of in vitro basophil activation in identifying the culprit in insect venom allergy. *J Investig Allergol Clin Immunol*. 2004;14(1):10–16.
13. Ariza A, Fernandez TD, Doña I, et al. Basophil activation after nonsteroidal anti-inflammatory drugs stimulation in patients with immediate hypersensitivity reactions to these drugs. *Cytometry A*. 2014;85(5):400–407.
14. Sudheer PS, Hall JE, Read GF, Rowbottom AW, Williams PE. Flow cytometric investigation of per-anaesthetic anaphylaxis using CD63 and CD203c. *Anaesthesia*. 2005;60:251–256.
15. Harada N, Hiragun M, Mizuno M, et al. A case of erythritol allergy studied by basophil histamine release and CD203c expression in vitro in addition to a challenge test in vivo. *J Investig Allergol Clin Immunol*. 2016;26(2):135–136.
16. De Weck A, Sanz ML, Gamboa PM, et al. Diagnostic tests based on human basophils: More potentials and perspectives than pitfalls. II. Technical issues. *J Investig Allergol Clin Immunol*. 2008;18(3):143–155.
17. Boumiza R, Debard AL, Monneret G. The basophil activation test by flow cytometry: Recent developments in clinical studies, standardization and emerging perspectives. *Clin Mol Allergy*. 2005;3:9.
18. Wolańczyk-Mędrala A, Barg W, Mędrala W. CD 164 as a basophil activation marker. *Curr Pharm Des*. 2011;17(34):3786–3796.
19. Hennersdorf F, Florian S, Jakob A, et al. Identification of CD13, CD107a, and CD164 as novel basophil-activation markers and dissection of two response patterns in time kinetics of IgE-dependent upregulation. *Cell Res*. 2005;15(5):325–335.
20. Kustrzeba-Wójcicka I, Siwak E, Terlecki G, Wolańczyk-Mędrala A, Mędrala W. Alternaria alternata and its allergens: A comprehensive review. *Clin Rev Allergy Immunol*. 2014;47(3):354–365.
21. Sainte-Laudy J, Ouk C. Use of lipid rafting for the analysis of human basophil activation by flow cytometry. *Inflamm Res*. 2010;59(Suppl 2):S193–S195.
22. Pencina MJ, D'Agostino RB Sr, D'Agostino RB Jr, Vasan RS. Evaluating the added predictive ability of a new marker: From area under the ROC curve to reclassification and beyond. *Stat Med*. 2008;27(2):157–172.

23. Kleine-Tebbe J, Erdmann S, Knol EF, MacGlashan DW, Poulsen LK, Gibbs BF. Diagnostic tests based on human basophils: Potentials, pitfalls and perspectives. *Int Arch Allergy Immunol*. 2006,141(1):79–90.
24. Mirković B, Lavelle GM, Azim AA, et al. The basophil surface marker CD203c identifies *Aspergillus* species sensitization in patients with cystic fibrosis. *J Allergy Clin Immunol*. 2016;137(2):436–443.
25. Sanz ML, Sánchez G, Gamboa PM, et al. Allergen-induced basophil activation: CD63 cell expression detected by flow cytometry in patients allergic to *Dermatophagoides pteronyssinu*s and Lolium perenne. *Clin Exp Allergy*. 2001;31(7):1007–1013.
26. González-Muñoz M, Villota J, Moneo I. Analysis of basophil activation by flow cytometry in pediatric house dust mite allergy. *Pediatr Allergy Immunol*. 2008;19(4):342–347.

The phospholipid fraction obtained from egg yolk reduces blood pressure increase induced by acute stress in spontaneously hypertensive rats

*Helena Martynowicz[1,C,D], *Dorian Nowacki[1,A–C], Grzegorz Mazur[1,E,F], Tadeusz Trziszka[2,A,F], Andrzej Szuba[3,A,E,F]

[1] Department and Clinic of Internal and Occupational Diseases and Hypertension, Faculty of Medicine, Wroclaw Medical University, Poland
[2] Department of Animal Products Technology and Quality Management, Wrocław University of Environmental and Life Sciences, Poland
[3] Division of Angiology, Faculty of Health Sciences, Wroclaw Medical University, Poland

A – research concept and design; B – collection and/or assembly of data; C – data analysis and interpretation;
D – writing the article; E – critical revision of the article; F – final approval of the article

Advances in Clinical and Experimental Medicine, ISSN 1899-5276 (print), ISSN 2451-2680 (online) *Adv Clin Exp Med*. 2018;27(12):1745–1749

Address for correspondence
Dorian Nowacki
E-mail: dorian.nowacki@wp.pl

Funding sources
The study was conducted within the project "Innovative Technologies of Production of Biopreparations Based on New Generation Eggs", Innovative Economy Operational Program Priority 1.3.1, thematic area "Bio". The project was co-financed by the European Union through the European Regional Development Fund within the Innovative Economy Operational Program, 2007–2013.

Conflict of interest
None declared

* Helena Martynowicz and Dorian Nowacki contributed equally to this work.

Received on October 24, 2016
Reviewed on February 3, 2017
Accepted on October 8, 2018

Abstract

Background. Despite continuous research, an improved understanding of the pathophysiology of hypertension and the development of new antihypertensive therapies, hypertension is still the most prevalent chronic cardiovascular disease (CVD) among adults in Western societies. Stress is a common factor related to cardiovascular morbidity. An increase in blood pressure is one of the most common reactions to stress. Chronic and acute stress have also been related to cardiovascular disorders. Polyunsaturated fatty acids (PUFAs) have attracted considerable interest as potential complementary therapy for the treatment of CVD, including hypertension. Egg yolk, rich in PUFAs and phospholipids, might be a good source of phospholipids and PUFAs.

Objectives. The current study was aimed at investigating the potential effect of the phospholipid fraction of eggs on blood pressure changes in spontaneously hypertensive rats (SHRs) as a response to acute stress.

Material and methods. Male, 7-week-old SHRs received dietary phospholipid fraction for 12 weeks. The control animals received standard feed. At the end of the treatment, they were exposed to 40 min of white noise in order to induce acute stress. Then, blood pressure measurements were carried out under normal conditions for 12 h before and during the acute stress procedure. Blood pressure was measured using telemetry.

Results. Diastolic, systolic and mean blood pressure were significantly lower in the SHRs treated with phospholipid fraction than in the control group. The acute stressor caused a significant increase in diastolic, systolic and mean blood pressure in both the treated and untreated animals, but the increase in blood pressure as a response to the stressor was significantly less pronounced in the rats treated with phospholipid fraction than in control rats. These results show that egg phospholipids can limit a stress-induced rise in blood pressure.

Conclusions. The results of this research show that phospholipid fraction derived from egg yolk reduces stress-induced increases in blood pressure.

Key words: stress, hypertension, phospholipid fraction, hen eggs

DOI
10.17219/acem/97377

Introduction

Eggs are an inexpensive and low-calorie food source which contains many substances indispensable for the development of a young organism, including minerals, proteins, n-3 polyunsaturated fatty acids (PUFAs), and phospholipids. However, eggs are also a source of cholesterol; therefore, the relationship between egg consumption and the risk of cardiovascular disease (CVD) remains controversial. Recently, the remarkable role of PUFAs in the prevention and treatment of CVD, including hypertension, has been described. The consumption of n-3 PUFAs reduces heart rate and systolic and diastolic blood pressure.[1,2] The consumption of freshwater fish (300–600 g daily) is associated with increased plasma concentrations of n-3 PUFAs, lower blood pressure and lower plasma lipid concentrations.[3] A meta-analysis of the effect of n-3 PUFAs in fish oil on blood pressure concluded that a higher consumption of n-3 PUFAs was associated with a higher reduction in blood pressure, particularly in hypertensive subjects and those with lipid disorders and atherosclerosis.[4] Also, n-3 PUFA consumption improves endothelial function.[5] The reduction in blood pressure may result from increased nitric oxide production, a reduced vasoconstrictive response to catecholamines and angiotensin I, improved vasodilatory responses, arterial compliance,[6,7] and reduced oxidative stress.

Hypertension is the most common chronic CVD in adults[8,9] and according to the WHO, it is the leading cause of death worldwide.[10,11] Known hypertension risk factors include age, gender, obesity, lifestyle (diet and physical activity),[12,13] and additional cardiovascular risk factors (e.g., diabetes, dyslipidemia or insulin resistance).[14,15] Chronic stress is linked to all cardiovascular disorders, including hypertension. Through the repeated occurrence of acute stressors and the activation of physiological stress-mediating systems, including the autonomic system, hypothalamic–pituitary–adrenal axis and immune system, chronic stress causes an elevation in circulating catecholamine and cortisol levels. Circulating catecholamines acutely elevate blood pressure and contribute to vascular stiffening and cardiac hypertrophy.[16] A stimulation of adrenergic activity increases sodium resorption, promoting blood pressure elevation.[17] Elevated levels of cortisol additionally activate the renin–angiotensin–aldosterone system, contribute to insulin resistance and hyperinsulinemia, and suppress nitric oxide, kallikrein and prostacyclin production.

Despite the progress in pharmacotherapy, hypertension treatment is still insufficient and the majority of patients worldwide have inadequately controlled blood pressure.[18] Although antihypertensive drugs play a fundamental role in blood pressure management, they may cause side effects; therefore, a number of studies have searched for food substances that can help reduce or prevent hypertension. In recent years, functional foods have attracted considerable interest as potential complementary therapies for the treatment of hypertension. The aim of this study was to evaluate the impact of a diet enriched with phospholipid fraction obtained from hen egg yolk on blood pressure in spontaneously hypertensive rats (SHRs) exposed to acute stress.

The study was conducted within the project "Innovative Production Technologies of Biopreparation Based on New Generation Eggs (OVOCURA)". We report here the primary findings of OVOCURA.

Material and methods

Male SHRs were purchased from Charles River Laboratories (Hamburg, Germany) and maintained under specific pathogen-free conditions in a temperature-controlled room (22 ±2°C) with a 12-hour light/dark cycle. All rats had ad libitum access to food and drinking water throughout the experiments. The experiments on animals were performed in accordance with relevant guidelines and regulations, and were conducted with the approval of the Local Ethical Commission at the Institute of Immunology and Experimental Therapy of the Polish Academy of Sciences in Wrocław, Poland (approval No. 48/2012). Male, 7-week-old SHRs were divided into 2 groups: a study group on a supplemented diet (SHR/E group; n = 8) and a control group on a standard Labofeed B diet (SHR/C group; n = 8). The rats from the SHR/E group were given the supplemented diet for 12 weeks.

In our study, we used phospholipid fraction obtained from hen eggs and enriched naturally through feeding the hens substances such as PUFAs (DHA, for example); in this way, the yolk phospholipids were improved. The composition of the fraction was analyzed by gas chromatography/mass spectrometry (GC/MS). The egg phospholipid fraction is a mixture of phosphatidylcholine and phosphatidylethanolamine (the composition is detailed in Table 1). The diet of the study group after enrichment with phospholipid formulation contained 5% phosphatidylcholine, 0.65% omega-3 fatty acid and 0.95% omega-6 fatty acid, calculated globally.

Table 1. Composition [%] of fatty acids in the phospholipid fraction of egg yolk

Composition of supplement	[%]
PC	81.72
PE	18.27
Fatty acid profile	**[%]**
ω-3	10.82
ω-6	15.79
ω6/ω3	1.46
Saturated	41.05
Unsaturated	58.95
MUFA	32.34
PUFA	26.61

PC – phosphatidylcholine; PE – phosphatidylethanolamine; MUFA – monounsaturated fatty acid; PUFA – polyunsaturated fatty acid.

Spontaneously hypertensive rats (age of 15 week) were fitted with DSI telemetry devices (PA11P-C40, Data Sciences International, St. Paul, USA) at the 8th week of diet supplementation. The animals were anesthetized with isoflurane (2–3%) through inhalation with a flow rate of 1.5 L/min. For all animals, the isoflurane concentration was adjusted by decreasing the dose to the minimum which would provide analgesia. An aseptic laparotomy was performed to expose the abdominal aorta. A catheter tip was inserted into the aorta and secured with medical glue. The body of the telemetry device was left inside the abdominal cavity and secured to the abdominal wall during suture closure of the incision. The system was programmed to collect data on systolic, mean and diastolic pressure.

Following the 12th week of study, blood pressure was measured. The blood pressure measurements were taken before the stress procedure under normal conditions in each animal for 12 h. Subsequently, a model of acute stress with white noise was used. Blood pressure measurement was carried out during the exposure to stress. One 40-minute cycle of blood pressure monitoring in the presence of a stressor was carried out in each subject.

White noise was emitted at 100 dB through speakers located 30 cm above the cage. Blood pressure was measured simultaneously. The volume of sound was monitored by a decibel meter. After pressure measurement, the rats were anesthetized with isoflurane and sacrificed by cervical dislocation. Differences between the parameters under stress and before the procedure of acute stress (Δ) were calculated. Changes in the cardiovascular parameters (Δ) caused by acute stress were used as an indicator factor of stress level.

Statistical analysis

The data is expressed as mean ± standard error of the mean (SEM) for each parameter and group. The difference between means for independent variables was analyzed using the Student's t-test or Mann–Whitney U test, while differences within one group (dependent variables) were analyzed using the dependent Student's t-test or Wilcoxon test. A p-value <0.05 was considered statistically significant. The statistical analysis was performed with STATISTICA v. 10.0 software (StatSoft Inc., Tulsa, USA).

Results

Twelve-hour measurement intervals under normal conditions showed that the mean pressure, systolic pressure and diastolic pressure were significantly lower in the SHRs fed an enriched diet than in the control group (159/106 mm Hg vs 174/117 mm Hg). In all groups, the acute stress exposure evoked a significant increase in mean pressure, systolic pressure, diastolic pressure, and heart rate, whereas pulse pressure significantly increased only in the control group (Table 2). Moreover, a stress-induced increase in mean pressure (ΔP) and systolic pressure (ΔSP) was significantly lower in the study group than in the control group (ΔP: 23.42 mm Hg vs 36.86 mm Hg; ΔSP: 24.95 mm Hg vs 40.02 mm Hg). The increase in these parameters caused by stress was less pronounced in rats fed a diet enriched with PUFAs. However, the difference in stress-induced diastolic pressure changes (ΔDP) between groups did not reach statistical significance (p = 0.07) due to the small number of animals (Table 3).

Table 2. The mean pressure, systolic pressure, diastolic pressure, pulse pressure, and heart rate under normal conditions and under acute stress in both groups: the control group (SHR/C) and the study group (SHR/E)

Measured parameters	SHR/C		SHR/E	
	12 h, normal conditions	acute stress conditions	12 h, normal conditions	acute stress conditions
Pressure [mm Hg]	145.10 ±1.19	181.96 ±3.69*	132.05 ±1.66	155.47 ±5.49**
Systolic pressure [mm Hg]	173.75 ±1.95	213.77 ±3.96*	158.96 ±2.19	183.91 ±6.16**
Diastolic pressure [mm Hg]	117.40 ±1.10	151.83 ±3.73*	106.41 ±1.78	128.41 ±4.70**
Pulse pressure [mm Hg]	56.35 ±1.68	61.94 ±1.36*	52.55 ±2.06	55.50 ±2.29
Heart rate [bpm]	278.45 ±4.21	378.16 ±19.17*	274.41 ±4.95	367.90 ±13.63**

* p < 0.05; statistically significant difference in comparison to normal conditions for SHR/C.
** p < 0.05; statistically significant difference in comparison to normal conditions for SHR/E.

Discussion

There has been an increased focus on identifying the natural components of foods which could be used in the prevention and treatment of hypertension. Grains, vegetables, fruits, dairy products, meat, chicken, eggs, fish, soybean, tea, wine, mushrooms, and lactic acid bacteria are various natural food sources with potential antihypertensive effects.[19] Blood pressure is regulated through complex mechanisms, including the modification of angiotensin-converting enzyme (ACE) activity and changes in oxidative

Table 3. Stress-induced increase of mean pressure (ΔP), systolic pressure (ΔSP), diastolic pressure (ΔDP), pulse pressure (ΔPP), and heart rate (ΔHR) in the control group (SHR/C) and study group (SHR/E)

Calculated parameters	SHR/C	SHR/E
ΔP [mm Hg]	36.86 ±3.73	23.42 ±4.27*
ΔSP [mm Hg]	40.02 ±4.02	24.95 ±4.23*
ΔDP [mm Hg]	34.43 ±3.72	22.00 ±4.10**
ΔPP [mm Hg]	5.58 ±1.16	2.96 ±0.97
ΔHR [bpm]	99.71 ±20.10	93.49 ±13.37

* p < 0.05; statistically significant difference in comparison to SHR/C.
** p = 0.07 in comparison to SHR/C. Δ – difference between parameter under stress and parameter before acute stress procedure.

status. Antioxidants may decrease arterial blood pressure by decreasing oxidative stress, thus preserving the activity of nitric oxide synthase (NOS) and increasing nitric oxide bioavailability. It was previously demonstrated that egg consumption may decrease oxidative stress levels; thus, our results are in agreement with those reported by Jahandideh et al.[20] Peptides obtained from egg white, such as novokinin, may act as a potent hypotensive factor through the AT(2) receptor.[21] Fatty acids from fish oil are known to decrease blood pressure.[22] It has been shown in clinical trials that n-3 PUFAs reduce the incidence of CVD and sudden cardiac death, and they decrease blood pressure.[23] It has been demonstrated that dietary compounds rich in PUFAs reduce pressor responses of the mesenteric artery to norepinephrine.[24] It is well-established that egg yolk contains peptides that demonstrate antioxidant, ACE-inhibitory and antidiabetic (α-glucosidase and DPP-IV inhibitory) activities.[25]

However, there has not been any clinical experience with the use of phospholipid fraction obtained from hen egg yolk as a mean to control blood pressure. Hen eggs are a relatively inexpensive source of not only fatty acids but also of amino acids and arginine, a precursor to nitric oxide.[26] In our study, rats fed a diet enriched with phospholipid fraction obtained from egg yolk had decreased blood pressure compared to the control group. The decrease in blood pressure was even more significant in rats exposed to acute stress.

Stress has become a prevalent part of people's lifestyle; therefore, the effect of stress on blood pressure is of increasing relevance and importance. We used noise as a stressor because it is a constant component of modern life and is considered to be a hypertensive factor. For what is likely the first time, advanced cardiovascular telemetry devices were utilized to evaluate the response to stress. The use of a modern experimental model which allows blood pressure monitoring in conscious rats via telemetry seems to be an important step in identifying the effects of phospholipid fraction on stress and blood pressure. It is well-known that acute stress causes a rise in blood pressure and heart rate. This new method of stress level evaluation might be used in the pre-clinical selection of bioactive products with the highest anti-stress potential.

Our results showing the influence of PUFAs on blood pressure are in agreement with the data of Jayasooriya et al., who showed that PUFA supplementation reduces hypertension in rats (animals with high ANG II activity).[27] Thus, our findings in this study expand on existing evidence that PUFAs decrease blood pressure.[28] Moreover, we observed that a diet enriched with PUFAs reduces the increase in blood pressure evoked by acute stress. We observed that phospholipid fraction obtained from hen egg yolk rich in PUFAs acts as a hypotensive agent and that it could be used in the prevention or treatment of hypertension evoked or exacerbated by acute stress. This finding suggests that egg phospholipid fraction could play an important role in the prevention of blood pressure rise related to stress.

Moreover, if we suppose that blood pressure change is an indicator of stress level, this study would suggest that phospholipids demonstrate anti-stress activity. The use of a hypertensive animal model probably enhances this effect. However, further studies with different stressors and stress models are needed in order to confirm these early results. In the last decade, there has been increasing interest in foods that promote health and could prevent hypertension and CVD. Chicken eggs have been demonstrated to decrease blood pressure; therefore, they can be considered hypotensive agents because they may become a part of a daily diet as functional food.

Conclusions

The results of this study indicate that the phospholipid fraction rich in fatty acids which is obtained from egg yolk reduces the negative response of the cardiovascular system to acute stress in SHRs. Since the study demonstrated the beneficial effects of phospholipid fraction on blood pressure in rats exposed to stress, the implications for patients need to be tested in further studies.

References

1. Geleijnse JM, Giltay EJ, Grobbee DE, Donders ART, Kok FJ. Blood pressure response to fish oil supplementation: Metaregression analysis of randomized trials. *J Hypertens*. 2002;20(8):1493–1499.
2. Mozaffarian D, Geelen A, Brouwer IA, Geleijnse JM, Zock PL, Katan MB. Effect of fish oil on heart rate in humans: A meta-analysis of randomized controlled trials. *Circulation*. 2005;112(13):1945–1952.
3. Pauletto P, Puato M, Caroli MG, et al. Blood pressure and atherogenic lipoprotein profiles of fish-diet and vegetarian villagers in Tanzania: The Lugalawa study. *Lancet*. 1996;348(9030):784–788.
4. Morris MC, Sacks F, Rosner B. Does fish oil lower blood pressure? A meta-analysis of controlled trials. *Circulation*. 1993;88(2):523–533.
5. Schiano V, Laurenzano E, Brevetti G, et al. Omega-3 polyunsaturated fatty acid in peripheral arterial disease: Effect on lipid pattern, disease severity, inflammation profile, and endothelial function. *Clin Nutr*. 2008;27(2):241–247.
6. Kenny D, Warltier DC, Pleuss JA, Hoffmann RG, Goodfriend TL, Egan BM. Effect of omega-3 fatty acids on the vascular response to angiotensin in normotensive men. *Am J Cardiol*. 1992;70(15):1347–1352.
7. Nestel P, Shige H, Pomeroy S, Cehun M, Abbey M, Raederstorff D. The n-3 fatty acids eicosapentaenoic acid and docosahexaenoic acid increase systemic arterial compliance in humans. *Am J Clin Nutr*. 2002;76(2):326–330.
8. Kearney PM, Whelton M, Reynolds K, Muntner P, Whelton PK, He J. Global burden of hypertension: Analysis of worldwide data. *Lancet*. 2005;365(9455):217–223.
9. Wolf-Maier K, Cooper RS, Benegas JR, et al. Hypertension prevalence and blood pressure levels in 6 European countries, Canada and the United States. *JAMA*. 2003;289(18):2363–2369.
10. Castelli WP. Epidemiology of coronary heart disease: The Framingham Study. *Am J Med*. 1984;76(2A):4–12.
11. Lewington S, Clarke R, Qizilbash N, Peto R, Collins R; Prospective Studies Collaboration. Age-specific relevance of usual blood pressure to vascular mortality: A meta-analysis of individual data for one million adults in 61 prospective studies. *Lancet*. 2002;360(9349):1903–1913.
12. Whelton PK. Epidemiology of hypertension. *Lancet*. 1994;344(8915):101–106.
13. Wojtyla A, Bilinski P, Jaworska-Luczak B. Regulatory strategies to ensure food and feed safety in Poland: Update review. *Ann Agric Environ Med*. 20110;17:215–220.

14. Isomaa B, Almgren P, Tuomi T, et al. Cardiovascular morbidity and mortality associated with the metabolic syndrome. *Diabetes Care*. 2001;24(4):683–689.
15. Cuspidi C, Ambrosioni E, Mancia G, Pessina AC, Trimarco B, Zanchetti A; APROS Investigators. Role of echocardiography and carotid ultrasonography in stratifying risk in patient with essential hypertension: The Assessment of Prognostic Risk Observational Survey. *J Hypertens*. 2002;20(7):1307–1314.
16. Pauletto P, Sarzani R, Rappelli A, Pessina AC, Sartore S. Vascular smooth muscle cell differentiation and growth response in hypertension. In: Laragh JH, Brenner BM, eds. *Hypertension: Pathophysiology, Diagnosis and Management*. 2nd ed. New York, NY: Raven Press Publishers; 1995:697–709.
17. Grassi G, Mancia G. Hyperadrenergic and labile hypertension. In: Lip GH, Hall J, eds. *Comprehensive Hypertension*. Philadelphia, PA: Mosby Elsevier; 2007:719–726.
18. Grassi G, Cifkova R, Laurent S, et al. Blood pressure control and cardiovascular risk profile in hypertensive patient from Central and Eastern European countries: Results of BP-CARE study. *Eur Heart J*. 2011;32(2):218–225.
19. Huang WY, Davidge ST, Wu J. Bioactive natural constituents from food sources: Potential use in hypertension prevention and treatment. *Crit Rev Food Sci Nutr*. 2014;53(6):615–630.
20. Jahandideh F, Majumder K, Chakrabarti S, et al. Beneficial effects of simulated gastro-intestinal digests of fried egg and its fractions on blood pressure, plasma lipids and oxidative stress in spontaneously hypertensive rats. *PLOS ONE*. 2014;9(12):e115006.
21. Yamada Y, Yamauchi D, Yokoo M, Ohinata K, Usui H, Yoshikawa M. A potent hypotensive peptide, novokinin, induces relaxation by AT2- and IP-receptor-dependent mechanism in the mesenteric artery from SHRs. *Biosci Biotechnol Biochem*. 2008;72(1):257–259.
22. Appel LJ, Miller ER, Seidler AJ, Whelton, PK. Does supplementation of diet with "fish oil" reduce blood pressure? A meta-analysis of controlled clinical trials. *Arch Intern Med*. 1993;153(12):1429–1438.
23. Calder PC. n-3 fatty acids and cardiovascular disease: Evidence explained and mechanisms explored. *Clin Sci (Lond)*. 2004;107(1):1–11.
24. Skoczyńska A, Wojakowska A, Nowacki D, et al. Unsaturated fatty acids supplementation reduces blood lead level in rats. *Biomed Res Int*. 2015;2015:189190.
25. Zambrowicz A, Pokora M, Setner B, et al. Multifunctional peptides derived from an egg yolk protein hydrolysate: Isolation and characterization. *Amino Acids*. 2015;47(2):369–380.
26. Preli RB, Klein KP, Herrington DM. Vascular effects of dietary L-arginine supplementation. *Atherosclerosis*. 2002;162(1):1–15.
27. Jayasooriya AP, Begg DP, Chen N, et al. Omega-3 polyunsaturated fatty acid supplementation reduces hypertension in TGR(mRen-2)27 rats. *Prostaglandins Leukot Essent Fatty Acids*. 2008;78(1):67–72.
28. Nowacki D, Martynowicz H, Skoczyńska A, et. al. Lecithin derived from ω-3 PUFA fortified eggs decreases blood pressure in spontaneously hypertensive rats. *Sci Rep*. 2017;7(1):12373.

Annual Contents

No. 1 (January)

Original papers

Reviews

No. 2 (February)

Original papers

Reviews

No. 3 (March)

Original papers

Reviews

No. 4 (April)

Original papers

Reviews

No. 5 (May)

Original papers

Reviews

No. 6 (June)

Original papers

Reviews

No. 7 (July)

Original papers

Reviews

No. 8 (August)

Original papers

Reviews

No. 9 (September)

Original papers

Reviews

No. 10 (October)

Original papers

Reviews

No. 11 (November)

Original papers

No. 12 (December)

Original papers

Index of Authors